Baseline soundscape, sound sources and transmission (Final Report)

Theme: Noise

WAMSI Westport Marine Science Program

WESTERN AUSTRALIAN MARINE SCIENCE INSTITUTION

WESTPORT

Better science **Better decisions**

WAMSI WESTPORT MARINE SCIENCE PROGRAM

WESTERN AUSTRALIAN
MARINE SCIENCE INSTITUTION

WESTPORT

ABOUT THE MARINE SCIENCE PROGRAM

The WAMSI Westport Marine Science Program (WWMSP) is a $13.5 million body of marine research funded by the WA Government. The aims of the WWMSP are to increase knowledge of Cockburn Sound in areas that will inform the environmental impact assessment of the proposed Westport development and help to manage this important and heavily used marine area into the future. Westport is the State Government's program to move container trade from Fremantle to Kwinana, and includes a new container port and associated freight, road and rail, and logistics. The WWMSP comprises more than 30 research projects in the biological, physical and social sciences that are focused on the Cockburn Sound area. They are being delivered by more than 100 scientists from the WAMSI partnership and other organisations.

FUNDING SOURCES
The $13.5 million WAMSI Westport Marine Science Program was funded by the Western Australian Government, Department of Transport. WAMSI partners provided significant in-kind funding to the program to increase the value to >$22 million.

DATA
Finalised datasets will be released as open data, and data and/or metadata will be discoverable through Data WA and the Shared Land Information Platform (SLIP).

YEAR OF PUBLICATION
March 2025

This report is for the project: Baseline soundscape, sound sources and transmission.

CITATION
Parnum, I., Tollefsen, C., Duncan, A., Erbe, C. (2025)
Baseline soundscape, sound sources and transmission (Final report). Prepared for the WAMSI Westport Marine Science Program. Western Australian Marine Science Institution, Perth, Western Australia. 122pp.

FRONT COVER IMAGE

Theme: Noise

Contents

The WAMSI Westport Marine Science Program is a $13.5 million body of research that is designed to fill knowledge gaps relating to the Cockburn Sound region. It was developed with the objectives of improving the capacity to avoid, mitigate and offset environmental impacts of the proposed Westport container port development and increase the WA Government's ability to manage other pressures acting on Cockburn Sound into the future. Funding for the program has been provided by Westport (through the Department of Transport) and the science projects are being delivered by the Western Australian Marine Science Institution.

1 Project 7.1 Baseline Soundscape, Sound Sources, and Transmission Final report

Authors
Iain Parnum, Cristina Tollefsen, Alec Duncan, Christine Erbe

Centre for Marine Science and Technology
Curtin University
Bentley, WA, Australia

Project
Project 7.1 Baseline Soundscape, Sound Sources and Transmission

Executive Summary

The WAMSI Westport Marine Science Program (WWMSP) is designed to improve the capacity to avoid, mitigate, and offset environmental impacts of the proposed Westport container port development and increase the WA Government's ability to manage other pressures acting on Cockburn Sound into the future. The establishment of a container port in Cockburn Sound will result in an increase in ship traffic, which will increase underwater noise. To understand the potential impact an increase in noise levels from shipping and port activities might have, a comprehensive study of underwater noise in Cockburn Sound was undertaken with three main objectives:

1. To record and quantify the baseline marine soundscape over a 12-month period at multiple sites,
2. To fill the gap in noise data for port operations and ships under specific conditions, and
3. To develop validated models for sound propagation in Cockburn Sound.

The baseline marine soundscape was measured over a 12-month period at nine sites, seven within Cockburn Sound and two just outside of Cockburn Sound to the north. At each site, noise percentiles across a frequency range of 20-48000 Hz were calculated for narrowband, broadband, and one-third octave band levels. Seasonal variability, diurnal variability, and spatial and temporal correlations among sites were quantified using statistical methods including correlation analysis and principal component analysis. Observed noise was grouped into three categories: geophony, anthropophony, and biophony. The geophony was dominated by wind-generated noise. Anthropophony was dominated by vessel noise, with industrial noise contributing at the south end of Cockburn Sound and an unknown but strong 50-Hz noise source contributing to the noise measured on the Kwinana Shelf. Biophony was dominated by dolphins, fish, and snapping shrimp, which varied also by location, season, and time of day.

Noise source signatures were observed for large ships (tankers and bulk carriers) entering Cockburn Sound via the channel at its northern end. Due to the peculiarities of underwater acoustic propagation in Cockburn Sound, broadband ship noise at close range was higher from the bow aspect of the ship, dominated by frequencies higher than 1000 Hz, and varied considerably between ships of the same classes. Source signatures for a pilot boat and several tugs were measured at the southern end of the Sound. Broadband noise levels varied up to ±15 dB for both boat classes and did not show a significant dependence on vessel speed over the limited number of observations available. The combined noise from port operations was measured for ships arriving, loading, and departing the Kwinana Grain Terminal at the southern end of Cockburn Sound. Pilot boats and tugs were involved in the arrival and departure, contributing to higher noise levels for a short time, while the loading phase was quieter.

Sound propagation input model parameters, in particular, parameters describing propagation in the sediments, were explored by using a combination of airgun measurements and modelling. The accuracy of an "equivalent fluid layer" model for bottom parameters was compared with a more conventional two or three-layer structure and with *in situ* propagation measurements. Models were able to qualitatively reproduce the higher propagation losses observed at frequencies of 100-300 Hz, but the detailed pattern of high-loss and low-loss frequencies depends strongly on the assumed layer properties. In practice, the layering between any source and receiver will vary in a range-dependent manner and the high- and low-loss bands be smoothed out across multiple frequencies, resulting in a high-loss "notch" in which sound propagates more efficiently through the bottom than via the water column. Suggested model parameters derived from a combination of airgun experiments and modelling are summarised for future use.

Future work was identified that could be explored with the existing datasets. Additional finer-scale temporal analysis of biophony could include exploration of the behavioural and ecological implications of presence and absence of various species, and examination of the potential impact of masking by anthropophony. Sound exposure levels from geophysical surveys and other types of sonar noise could be measured in a relatively straightforward way by combining AIS tracks during known geophysical surveys with existing measurements of underwater noise. Analysis of port operations noise and noise from individual ships and boats could be expanded from the few dozens of occasions described in this document to the several hundred occasions theoretically available by exploiting the entire dataset, in order to increase the statistical validity of the conclusions.

2 Introduction

The WAMSI Westport Marine Science Program (WWMSP) has been designed to improve the capacity to avoid, mitigate, and offset environmental impacts of the proposed Westport container port development and increase the Western Australia (WA) Government's ability to manage other pressures acting on Cockburn Sound into the future (WAMSI 2022). The establishment of a container port in Cockburn Sound (Figure 1) will result in an increase in ship traffic, which will increase underwater noise levels.

A soundscape constitutes sounds from all sources that contribute to the total sound field in location. What differentiates "noise" from "sound" is the opinion of the observer: an unwanted or undesirable sound is considered noise. (In signal processing terms, the signal is the sound the user is trying to detect, and the noise is all the other sounds in the recording.) Underwater soundscapes vary in space and time and the underwater environment is naturally loud, even without the addition of anthropogenic sound. However, if anthropogenic sound interferes with animal communication and behaviour, animals may be negatively impacted; therefore, it is appropriate to refer to it as anthropogenic noise in this context. It is necessary to characterise the existing soundscape before considering the impact of an increase in anthropogenic noise. Acoustic characteristics of noise sources and other port activities must be quantified, and an understanding of acoustic propagation characteristics in Cockburn Sound is required. Knowledge of the existing soundscape can then be combined with noise source characteristics, acoustic characteristics specific to Cockburn Sound, and numerical models of sound propagation in order to quantify and mitigate (if required) potential impacts on marine fauna.

The project objectives were as follows:

1. Record and quantify the baseline marine soundscape in Cockburn Sound over a 12-month period at multiple sites.
    a. Quantify the marine soundscape in Cockburn Sound.
    b. Identify the dominant contributors (geophony, anthropophony, and biophony).
    c. Quantify noise budgets.
    d. Assess existing variability (in time and space) of the soundscape.
    e. Identify vocal marine fauna (dolphins, fish, crustaceans).
2. Determine noise characteristics for ships under a range of conditions and port operations.
    a. Conduct a literature review of ship source spectra and identify gaps in knowledge.
    b. Derive potential scaling laws to predict noise from larger ships.
    c. Measure ship noise signatures in Cockburn Sound and during berthing operations at existing marine facilities.
    d. Determine ship source levels by sound propagation modelling from the sources to the recorders in the field.
3. Develop validated models for sound propagation in Cockburn Sound.
    a. Collate physical and geoacoustic data for Cockburn Sound.
    b. Model sound propagation.
    c. Measure sound propagation in the field.
    d. Validate, and if necessary, improve the model for future applications in the Westport EIA and other industrial developments.

This report is the final report for this project summarising the work and findings associated with project objectives.

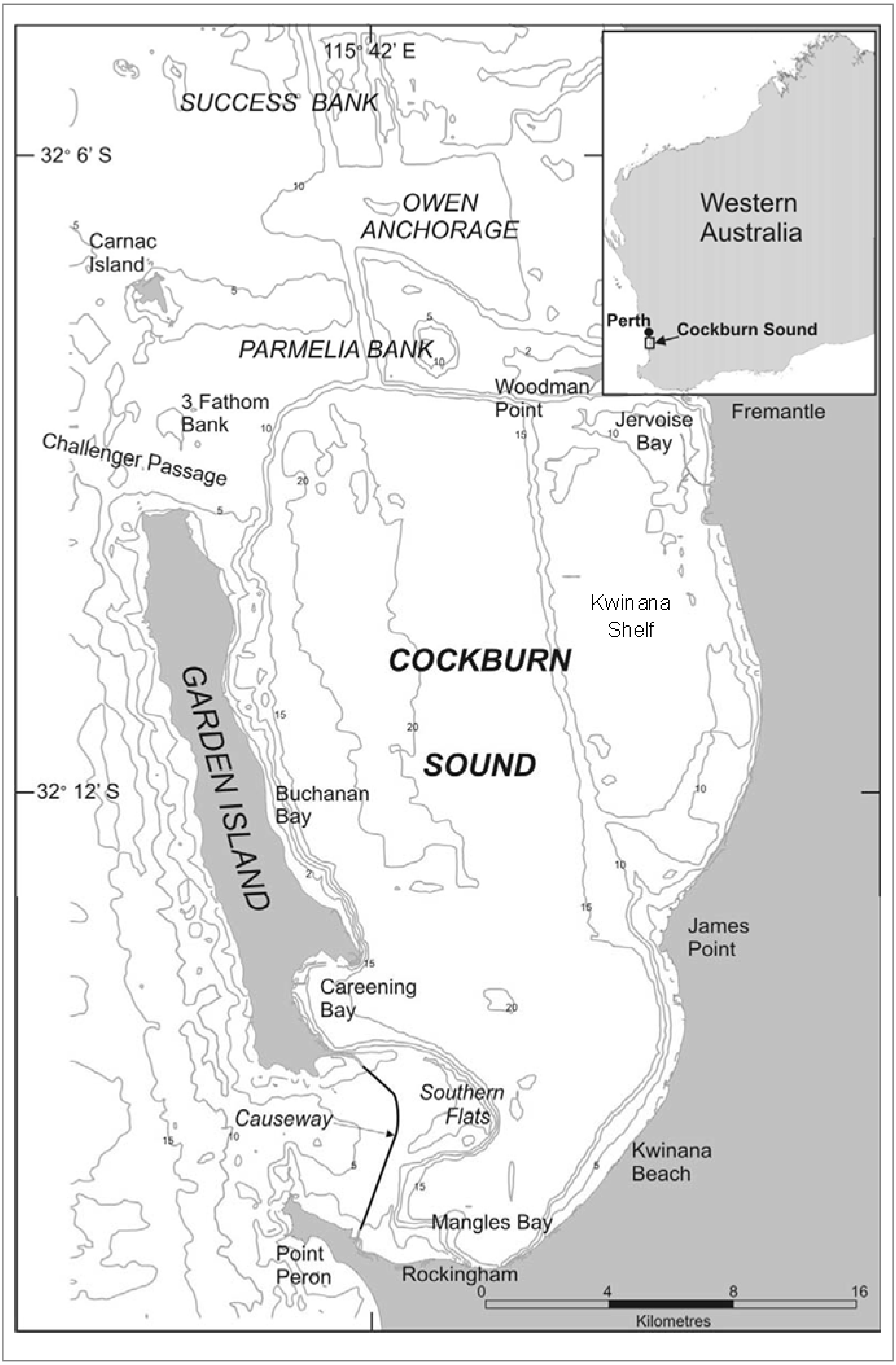

Figure 1. Map of Cockburn Sound, Western Australia (modified from Skene et al. 2005).

2.1 Description of Cockburn Sound and its importance

Cockburn Sound is a marine embayment off the west coast of WA, sheltered from ocean swell by Garden Island to its west, and delineated by Woodman Point and Carnac Island to the north, with the WA mainland between Fremantle and Rockingham to its west and south (Figure 1). It is 22 km long (north to south) and the width ranges from 9 km at the south end to 15 km at the north end, with a relatively flat bottom (17-22m in the central basin) and a lower gradient bank to the east, with steeper banks, shoals, and shoreline to the north, south, and west (Cockburn Sound Management Council 2018). Cockburn Sound has undergone extensive modification since European settlement began in the 1800s and is now used for a range of anthropogenic activities, including maritime trade (anchorage and material import/export), recreational and commercial fisheries (crab, octopus, and finfish), and tourism. It is an ecologically important area for numerous species including pink snapper (*Chrysophrys auratus*), little penguins (*Eudyptula minor*), and resident Indo-Pacific bottlenose dolphins (*Tursiops aduncus*). In addition, it is valued by the community for its ecological, recreational, and aesthetic attributes (Cockburn Sound Management Council 2018).

2.2 Review of existing literature on source spectra relevant to Cockburn Sound

Soundscape research is a holistic way of studying underwater sound that considers sounds originating from different places arriving at a given location. Underwater sound arises from both anthropogenic and natural sources, and for descriptive purposes it is helpful to categorise sounds by the type of process generating the sound. Sound categories include: geophony (sounds from wave and wind-generated bubbles, precipitation, earthquakes, volcanoes, and polar ice movement), biophony (sounds from crustaceans, fishes, and marine mammals), and anthropophony (shipping, seismic surveying, sonar imaging, and pile driving) (Pijanowski et al. 2011). Sounds from any of these categories are often referred to as “noise” in the literature as well as colloquially, for example, wind noise or snapping shrimp noise. Sound propagating under water undergoes frequency and timing changes due to frequency-dependent propagation over long distances and moving or intermittent sources, resulting in soundscapes that vary widely in time and space. Soundscape measurements necessarily include underwater sound recordings, but may also include auxiliary data required to explain the observations (e.g., water temperature, wind speed, light intensity and lunar phase, chlorophyll-A, as well as ship location and speed logs). By understanding the acoustic characteristics of the sources of sound within a soundscape, their variability, and dependencies, soundscape models can be developed to predict underwater soundscapes under specific conditions (van Geel et al. 2022).

Geophysical sources of underwater sound are part of the natural, physical environment, including the seafloor, the water, and the atmosphere above it, provided that the sound can propagate into the aquatic habitat. Any event that causes bubbles to be formed under water will generate noise, since bubbles oscillate at a resonant frequency that depends on their size (Minnaert 1933). Wind noise arises from the bubbles generated by breaking waves at the surface, and its spectrum has a broad peak between 300-500 Hz and overall level that rises as the wind speed increases (Wenz 1962). However, since the geoacoustic properties of seabed materials vary worldwide, sound levels due to wind also vary. For example, over the Northwest Shelf of Australia, spectral density levels are about 10 dB lower than those predicted by models based on open-ocean northern hemisphere measurements, due to the acoustically absorptive seabed found in the area (Gavrilov 2021).

Precipitation noise (raindrops, hail, and snow) arises from both the surface impact and the entrained bubbles and increases with the rate and size of precipitation, resulting in highly vertically directional noise that propagates downward very efficiently (Barclay & Buckingham 2013). Surf noise arises from long-period waves originating from distant storms, as they break in shallow water and produce bubbles (Deane 2000).

Though not able to generate underwater sound on their own, ocean currents can induce noise artefacts on underwater recordings through flow noise across instrument faces, resonant strumming in mooring cables, and banging or clanking of loose mooring parts (Erbe et al. 2015). Careful attention to mooring design and placement should limit the contribution of these types of noise. Finally, at frequencies above 30 kHz, the thermal agitation of water molecules sets a lower limit on observable underwater noise (Mellen 1952).

Biotic sound sources include marine invertebrates and fishes as well as marine mammals. Marine invertebrate sound is generally produced by stridulation of hard body parts, though it can also be created by gas bubble cavitation in the case of snapping shrimp (*Alpheidae* species). Invertebrate sounds may be described by onomatopoeic words like rasps, hisses, snaps, sizzling, rumbles, and clicks, most of which are actually broadband pulse trains at various repetition frequencies. These sounds can occur in choruses (multiple animals making the same sound at the same time), often synchronised with daylight or moonlight, that can be 20-30 dB higher than ambient levels at other times of day (Cato 1980, Radford et al. 2008, Staaterman et al. 2011). Over 800 species of fish from 109 families have been documented to emit sound (Slabbekoorn et al. 2010). Some fish have a swimbladder, which is an internal gas-filled organ used for buoyancy control that can also be used to generate sound. Other sounds are made by rasping hard body parts or banging fins on the fish body wall. Again, the onomatopoeic names are numerous and include click, cluck, croak, grunt, hoot, hum, knock, pop, purr, whistle, and others. Typically, most of the spectral power is below 1 kHz, occasionally extending above 4 kHz (Parsons et al. 2016b). Pulse duration and inter-pulse intervals are in the order of tens of milliseconds, with overall durations ranging from less than 1 s to 20 s. Source levels as high as 165 dB re 1 µPa m (SPL) and 158 dB re 1 $\mu Pa^2 m^2 s$ (SEL) have been reported (McCauley & Cato 2000, Locascio & Mann 2011, Parsons et al. 2016a).

Marine mammals produce a variety of sounds, which range from narrow- to broadband and from short to long duration, exhibiting different types and degrees of modulation, singly or in packages. Sounds may be described as constant-frequency or tonal, frequency-modulated (FM), amplitude-modulated (AM), or pulsed. Tonal sounds may be emitted with or without harmonics. Sounds of different types may be merged into one call; for example, starting as a constant-frequency sound, then introducing amplitude modulation, and eventually becoming pulsed. Pulses themselves may be of constant-frequency, frequency-modulated, or truly broadband type.

Mysticetes (baleen whales) produce all of these sound types, while odontocete (toothed whale) sounds are most commonly classified as whistles, burst-pulse sounds, and clicks. Across all species of mysticetes, fundamental tones range from 10 to 2000 Hz and last 0.1-10 s (Thompson et al. 1992, Rankin et al. 2005, Parks et al. 2007, Baumgartner et al. 2008, Stafford et al. 2012). Most of the mysticete species have been documented to arrange their sounds into songs, which can last many hours (Payne & McVay 1971, Croll et al. 2002). Odontocete whistles typically last from 0.1 to 1-2 s. Fundamental frequencies of odontocete whistles can be as low as 100 Hz, for example for orcas (*Orcinus orca*) (Samarra et al. 2016) and as high as 20-30 kHz, for example for common dolphins (*Delphinus delphis*) (Ansmann et al. 2007). The highest frequencies observed are 40 kHz from bottlenose dolphins (*Tursiops truncatus*) (Hiley et al. 2017) and 75 kHz from orcas (Samarra et al. 2010). Burst-pulse sounds range in frequency from 200 Hz to over 100 kHz (Lammers et al. 2003, Branstetter et al. 2012) and last from 0.1 to 1 or 2 s. Broadband clicks (1-200 kHz) are always emitted in series in which the inter-click interval (ICI) is greater than the inter-pulse interval in burst-pulse sounds. Clicks are typically tens to hundreds of microseconds long, with click trains lasting several seconds. The ICI for most odontocete echolocation is on the order of tens of milliseconds (Baumann-Pickering et al. 2010, Wahlberg et al. 2011, Neves 2013) but can be as long as a few seconds for the “slow clicks” of sperm whales (*Physeter macrocephalus*) (Madsen et al. 2002).

On land and under water, pinnipeds (eared seals, sea lions, walrus, and earless seals) mostly make amplitude-modulated or pulsed sounds, while sirenians mostly produce tonal, frequency-modulated sounds, although amplitude-modulated and pulse sounds have also been reported. When many animals of one species aggregate in one region, distinct choruses may be formed, such as those of sperm whales (Cato 1978), blue whales (*Balaenoptera musculus*) (McCauley et al. 2018) or fin whales (*Balaenoptera physalus*) (Leroy et al. 2016).

Anthropogenic sound sources can be categorised in a variety of ways, and include vessels, survey operations (marine seismic surveys, geotechnical drilling), construction activities (drilling, dredging, pile driving), windfarms in operation, explosions, and sonars (sub-bottom profilers, echosounders, military sonar, acoustic mitigation devices).

Vessels range in length from a few metres (small boats and personal watercraft) to over 300 m (supertankers). Noise from an individual vessel arises from three main physical sources: propeller-induced noise (propeller vibrations, hull resonance, and cavitation), noise generated on-board the ship which is often well-coupled to the hull and transmitted efficiently into the water (machinery, pumps, hydraulics, sonar), and hydrodynamic flow noise arising from the hull moving through the water. Vessel noise has been the subject of numerous empirical and theoretical studies since World War II, with some vessel classes subject to more detailed investigation than others.

Multiple studies have examined noise from merchant shipping (McKenna et al. 2013, Simard et al. 2016, Chion et al. 2019, MacGillivray et al. 2022). In particular, one group analysed measurements from 9,880 passes of 3,188 different merchant ships and found that speed through water and vessel draft were the strongest predictors of radiated noise (MacGillivray et al. 2022). They developed a functional regression analysis model that relates source spectrum to various vessel design and operational characteristics for six different vessel classes (container ships, vehicle carriers, tankers, bulk carriers, tugs, and cruise ships).

Small boats exist in a broad variety of configurations and lengths ranging from a few metres to tens of metres. They may have propellers or impellers; inboard or outboard motors; hulls made of steel, aluminium, fibreglass, or inflatable. Previous studies (Parsons et al. 2021, Lagrois et al. 2023) found a correspondingly large variation in source level, emphasizing the difficulty of generalising measurements of specific vessels in any of these classes. The few papers specifically mentioning pilot boats were non-peer reviewed studies (Barlett & Wilson 2002, Amron et al. 2021).

Most studies to date have focused on either isolating the sound from individual vessels, or measuring overall soundscape characteristics. However, port activities often consist of repeated events of limited duration involving multiple ships, for example, the arrival, docking, loading, and departure of bulk carrier ships at a grain processing terminal. The sound levels arising from such activities is a combination of sounds from an individual vessel undertaking reasonably repeatable manoeuvres in consistent locations. Therefore, the subsequent sound levels could be measured and an effective source level estimated for these combined activities which could be termed “port operations”.

Marine seismic survey operations involve transmitting pulses or bursts of low-frequency sound and then receiving the resulting reflected and/or refracted energy on an array of hydrophones. The resulting hydrophone signals can be analysed to provide images of Earth’s crust down to 10 km or more below the seafloor, which can be used for geophysical research, geotechnical investigations, and petroleum exploration. The requisite low-frequency sounds are produced by single or multiple airguns, cylindrical containers in which the volume of air (10-800 in^3/0.00016-0.013 m^3) is highly compressed (to about 2000 psi/14MPa). The rapid release of air when the air chamber is opened generates a giant bubble which oscillates and produces the desired low-frequency sound. Airguns are frequently operated in arrays with total volume of 2000-8000 m^3, towed 5-8 m below the water surface, and firing every 5-20 s. The result is a highly directional array, with vertically directed spectral levels peaking at lower frequencies (e.g., below 200 Hz). Horizontally-directed sound levels can be considerably lower than the vertical level, but they differ between along-track and across-track directions, with lower levels in the along-track (fore and aft) directions and higher levels in the across-track directions. Spectral characteristics of airgun signals that propagate long distances horizontally are then considerably modified by the frequency dispersion of the ocean medium and can change from brief, broadband pulses to longer-lasting, narrow-band, frequency-modulated sounds (Greene & Richardson 1988, Guerra et al. 2011). Numerical modelling of airgun signals consists of first, modelling the spectral characteristics and source levels produced by the airgun(s), and second, modelling its frequency-dependent propagation to the location of interest. By selecting appropriate models for the environment in question it is possible to generate a map of received sound levels at depths and locations of interest.

Ocean drilling may involve large and deep boreholes for oil and gas; multiple shallow holes for geotechnical site investigations; or fewer shallow holes for foundations. Drilling platforms may be fixed to the bottom, or floating and thus kept in place by dynamic positioning systems. Sound arises from the mechanical systems on the platform (generators, compressors, and pumps), dynamic positioning thrusters, the drill casing ("string") vibrating, and the underground drill bit creating vibrations in the rock that propagate into the water. In addition, oil and gas drilling platforms are serviced frequently by ships, leading to increased vessel noise in the area. It can be difficult to isolate the actual sound from drilling in the superposition of sound from all the other sources. Sounds from drill-rigs in quiet ambient noise conditions have been detected up to 40 km away, with radiated noise levels determined to be 184 and 190 dB re 1 µPa m during drilling and rig maintenance, respectively (Kyhn et al. 2014). The sound spectra recorded from operating drill-rigs exhibit distinct tones at frequencies of 5-40 Hz, likely from drill-string vibrations and tones from power generation, plus overtones up to 2000 Hz (Gales 1982, Nedwell & Edwards 2004, Kyhn et al. 2014, Todd et al. 2020). For drilling, the geometric arrangement of sound sources is complicated: the vibrating drill string is a line source spanning the water column, but there is also a point source underground where the drill bit grinds, and the drill platform is an extended source at the surface. Furthermore, drilling often happens in shallow water where predicting acoustic propagation is very complicated and depends on the specific environment surrounding the drilling platform.

Underwater sound from dredging is produced by the excavation, transfer, and deposition of material that ranges from soft sand and mud to gravel and rock, generating sound in myriad ways. Mechanical dredges, such as clamshell, bucket ladder, and backhoe dredges, remove material mechanically, which generates underwater noise (Clarke et al. 2003). Hydraulic dredges use water pumps to remove material and when in use, sound is generated throughout the water column. In deeper water, dredges may use thrusters, which generate cavitation noise. Dredges might transfer material to a dump site or a transportation barge, resulting in noise from reloading the material, ship noise, and sound from expelling, pumping, or dumping of material at the deposit site. In general, dredging sound is continuous and broadband, overlain with tones and occasionally pulses (e.g., from bottom impact of a backhoe or bucket), and computation of source levels for dredges during dredging is difficult due to the distributed nature of the noise sources.

Underwater piles come in different shapes and materials, and can be driven vertically or at an angle. The most common methods of pile driving are vibratory pile driving, used in soft substrates, and percussive (impact) pile driving for harder substrates. Vibratory pile drivers use counter-rotating eccentric weights to create vibrations in the vertical direction that drive the pile into the ground. Sound arises from a superposition of sources: sound generated in air enters the water close to the pile, and vibrations transmit through the pile into the ground, generating water- and ground-borne acoustic waves. The sound from vibratory pile driving is continuous with most energy below 1 kHz and the spectrum typically features tones related to the frequency of vibration of a few tens of Hz (Matuschek & Betke 2009). Percussive pile drivers consist of a hammer with a supporting casing, and a ram (weight) of a large mass dropping onto an anvil, which is placed on the top of the pile to be driven. In percussive marine pile driving, sound is generated in air by the impact of the hammer onto the top of the pile and the mechanism of raising the ram, in addition to a deformation (bulge) in the pile that results in a supersonic wave radiating directly into the water (Reinhall & Dahl 2011). The sound from percussive pile driving is pulsed and broadband with peak energy typically between 100 and 1000 Hz and received levels commonly increase while driving one pile as the resistance of the ground and the hammer energy increase (Robinson et al. 2012). The international standard ISO 18406 (International Organization for Standardization 2017) which sets pile driving recording, analysis, and reporting procedures does not define a source level but instead defines acoustic quantities to be reported: the peak sound pressure level (SPL_{pk}), the single-strike sound exposure level (SEL_{SS}), and the signal-to-noise ratio (at a specified range).

Active sonar systems use an acoustic source to emit sound into the ocean and then record and analyse the resulting echoes from objects in the water column, surface, and the seafloor. Active sonar systems may be used for geophysical studies, seafloor mapping, fisheries, acoustic deterrence, locating underwater mines and hazards, and tracking other vessels. The active source may be a transducer transmitting relatively narrow-band continuous wave (CW) or frequency-modulated (FM) pulses, or a source of broadband energy such as an airgun, sparker, or boomer. Sources may be omni-directional or directional, focusing energy either vertically (e.g., for geophysical or fisheries studies) or horizontally (e.g., for anti-submarine warfare). Geophysical sources can be divided into two broad categories: sub-bottom profiling systems, which are used to obtain cross-sections of the seabed; and seafloor mapping systems such as multibeam and sidescan sonars, which are used to obtain images of the seafloor surface (Crocker et al. 2019). Figure 2 is an overview of typical frequency ranges for the most common categories of sonar sources. The frequency limits in Figure 2 are representative – individual models of sonar may go slightly beyond these limits; furthermore, a particular make or model of sonar source operates in a narrower band within the frequency range shown in Figure 2.

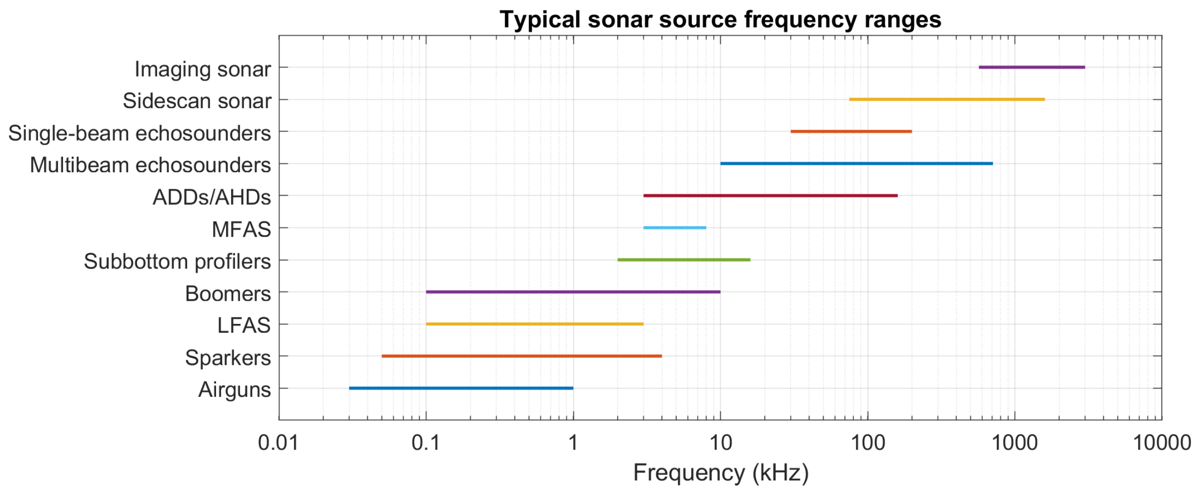

Figure 2. Typical frequency ranges for common sonar sources: imaging sonars, sidescan sonars, single-beam echosounders, multibeam echosounders, acoustic deterrent devices (ADDs) and acoustic harassment devices (AHDs), medium-frequency active [military] sonar (MFAS), subbottom profilers, boomers, low-frequency active [military] sonar (LFAS), sparkers, and airguns. Adapted from Erbe et al. (in press).

2.3 Report structure

The remainder of this report is structured as follows. Field measurements and data processing are described in Section 3. Results and discussion (Section 4 and 5, respectively) are grouped to address the three aims of this report: general characterisation of the entire soundscape (Sections 4.1 and 5.1), detailed measurements of sound arising from vessel traffic (Sections 4.2 and 5.2), and sound propagation model studies (Sections 4.3 and 5.3). Conclusions and recommendations are provided in Section 6, Section 8 contains a list of references, and Section 9 contains appendices with auxiliary information.

3 Materials and Methods

The field deployments and measurements carried out as part of this work are described in detail in Section 3.1, while the data analysis methods are underwater acoustic modelling software are described in Section 3.2.

3.1 Field deployments and measurements

Five field deployments of underwater sound recorders (Section 3.1.1) were used to collect underwater acoustic data for this project. The first deployment (Section 3.1.2) was designed to measure vessel signatures during their transit through the northern end of Cockburn Sound, west of Woodman Point (red diamonds in Figure 3 and Figure 4). Then three deployments (Section 3.1.3) were designed to measure the underwater soundscape at nine different locations in Cockburn Sound over a one-year period (blue circles in Figure 4) with recorders being recovered and redeployed every four months. The nine sites were chosen following consideration of the study area and consultation with other researchers in other themes of the WWMSP, particularly (Theme 4) Fisheries and aquatic resources, (Theme 8) Apex predators and iconic species, and (Theme 9) Coastal processes. An airgun survey described in Section 3.1.4 was used to determine seabed layering and estimate the sound speed in each layer. A further deployment of acoustic loggers to determine seabed layering and estimate the sound speed in each layer was undertaken to coincide with a geophysical survey test, using an airgun array (described in Section 3.1.4).

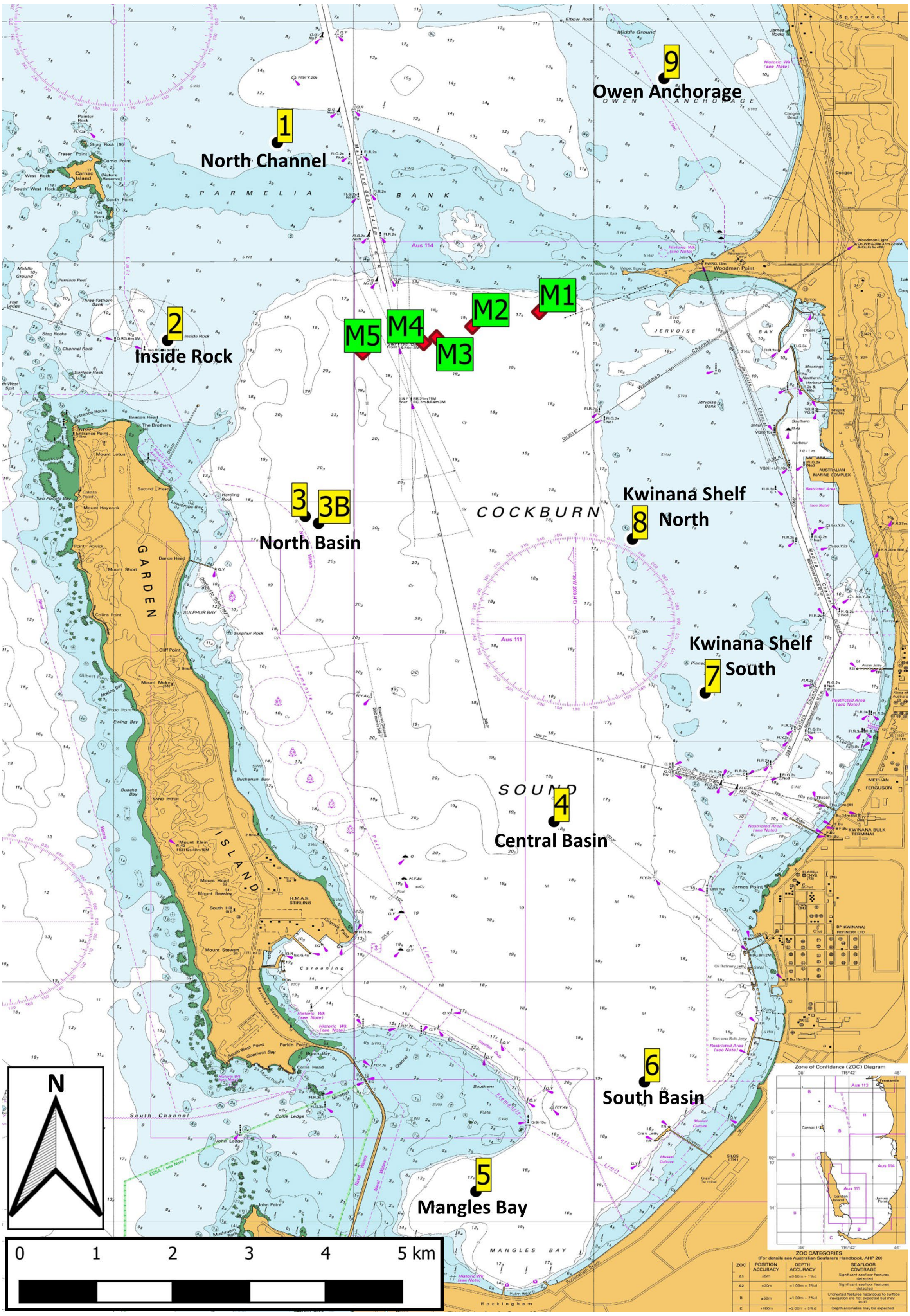

Figure 3. Locations within Cockburn Sound of the five sites for recording vessel transit noise (red diamonds with green labels) and the nine sites chosen to record the underwater soundscape (black circles with yellow labels).

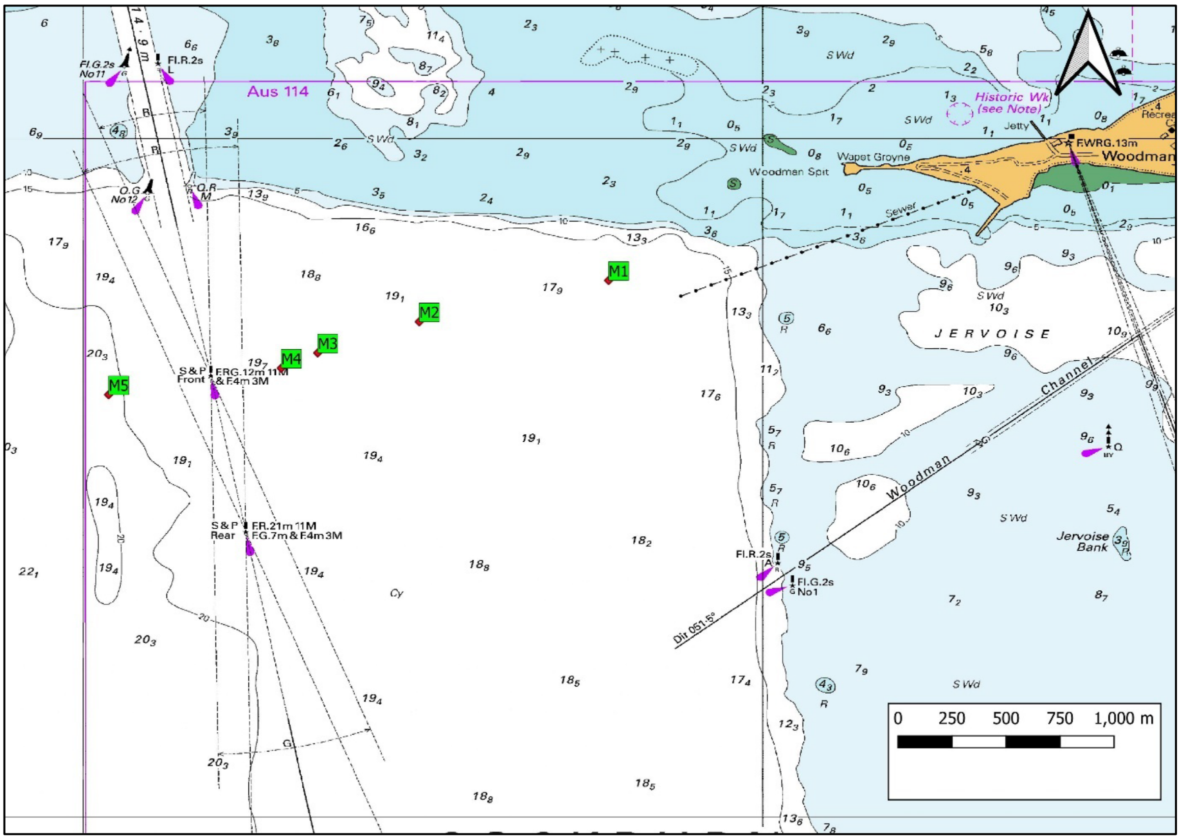

Figure 4. Close up of locations of the five sites for recording vessel transit noise (red diamonds with green labels).

3.1.1 Underwater sound recorders

The underwater sound recordings were made using several types of underwater sound recorder (USR): Ocean Instruments' SoundTrap ST500 STD and ST600 STD sound recorders, and one custom-built by the Centre for Marine Science and Technology (CMST) at Curtin University, known as the CMST HF (high-frequency) recorder. All the recorders are able to autonomously measure underwater sound for several months, with a bandwidth between 20 Hz and 60 kHz (Ocean Instruments 2020, 2023). Figure 5 is a photograph of a ST600 STD mounted on a frame. Each recorder has a hydrophone, batteries, internal electronics for communication and operation of the device, and memory for data storage. The CMST HF USR was calibrated as per the procedure described in McCauley et al. (2017), the sensitivity of the SoundTrap USRs was checked using the inbuilt calibration tones and/or the procedure described by Gavrilov et al. (2024) which also measures the low-frequency roll off.

Sound recorders were deployed on the seafloor at each site in Figure 3 using the mooring configuration detailed in Figure 5. The sound recorder was fixed to a "T" shaped weighted frame to provide a stable platform. A ground line of length greater than three times the water depth was attached to the end of the frame, with a weight at the other end of the line. A series of 2-kg weights were attached along the ground line to keep it close to the seafloor and away from ship propellers, resulting in moorings with no surface expression that could be straightforwardly recovered by grappling.

In consultation with the Royal Australian Navy (RAN), specific time periods at certain sites were identified and subsequently deleted from the datasets due to the proximity of the underwater sound recorders to the base HMAS Stirling on Garden Island on the west side of Cockburn Sound.

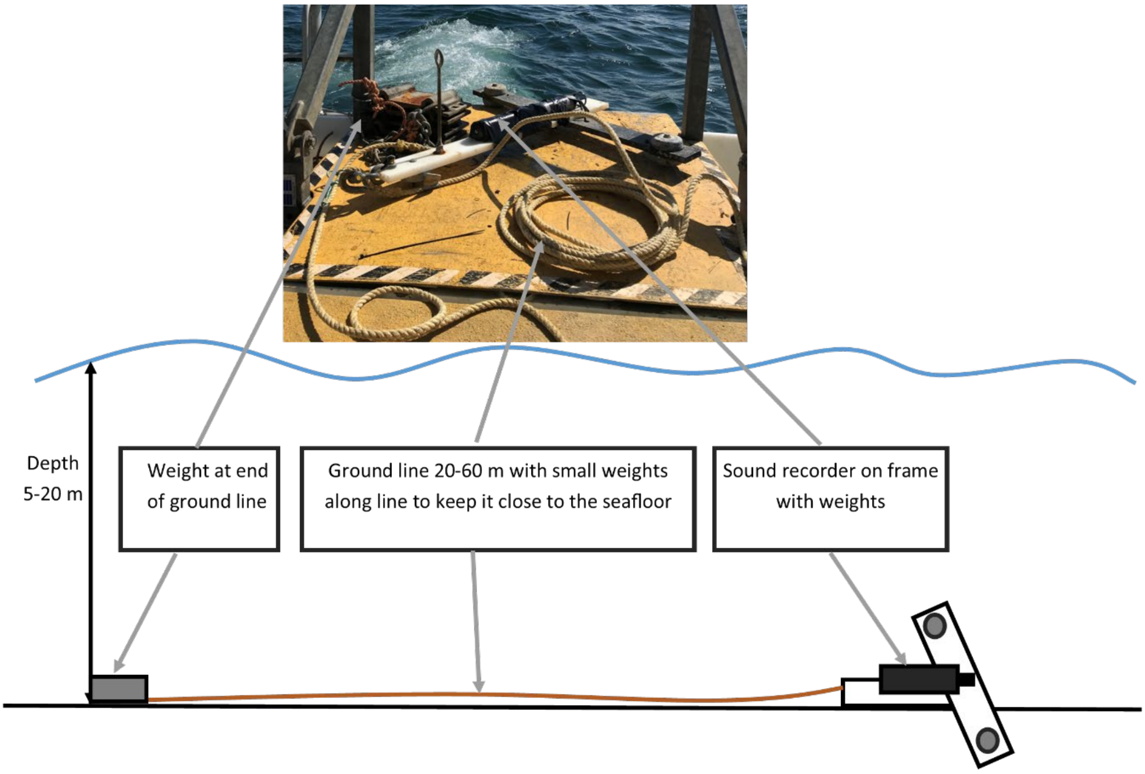

Figure 5. Photograph (top) and schematic (bottom) of mooring used to deploy sound recorders for underwater soundscape.

3.1.2 Vessel noise measurement and AIS data collection

For the vessel noise measurements, five underwater sound recorders were deployed on 22 July 2022, comprising four Ocean Instruments SoundTrap ST500 STD sound recorders and one custom CMST HF sound recorder (McCauley et al. 2017). One recorder was installed at each location M1 to M5 (Figure 4).

The recorders located at M1, M2, M4, and M5 were successfully recovered on 16 September 2022. The initial attempt to recover the M3 recorder was unsuccessful but it was subsequently recovered as part of a field trip on 14 October 2022. A hardware fault resulted in the M4 recorder failing to record any data, but the others all returned good quality data. Table 1 is a summary of the deployment and sampling details.

Table 1. Details of sound recorders for vessel noise deployments: site name, longitude (degrees East), latitude (degrees South), water depth (m), date deployed, date recovered, date of last recording, sample frequency fs, duty cycle (minutes/minutes), recorder model.

Site	Longitude (E)	Latitude (S)	Depth (m)	Deployed	Recovered	Recording end	f_s (kHz)	Duty cycle (min/ min)	Model
M1	115.72578	32.14032	17.9	22/07/2022	16/09/2022	29/08/2022	96	4/5	SM2
M2	115.71649	32.14235	19.1	22/07/2022	16/09/2022	16/09/2022	96	Cont.	ST500
M3	115.71151	32.14388	19.1	22/07/2022	14/10/2022	14/10/2022	96	Cont.	ST500
M4	115.70972	32.14463	19.1	22/07/2022	16/09/2022	N/A (failed)	96	Cont.	ST500
M5	115.70125	32.14593	20.0	22/07/2022	16/09/2022	16/09/2022	96	Cont.	ST500

A ship automatic identification system (AIS) receiver (GME, model AISR 120) and data logging computer were installed at the CMST facility south of Fremantle from 20 June 2022 to 21 February 2023. A second AIS receiver and logger were installed on Rottnest Island from 24 January 2023 to 02 Jan 2024. Between the two receivers, reasonably continuous AIS coverage was available from the first deployment until after the last recorders were recovered (Figure 6). The AIS logging stations provided frequent position updates (approximately every 10 s) for AIS-equipped vessels operating throughout Cockburn Sound.

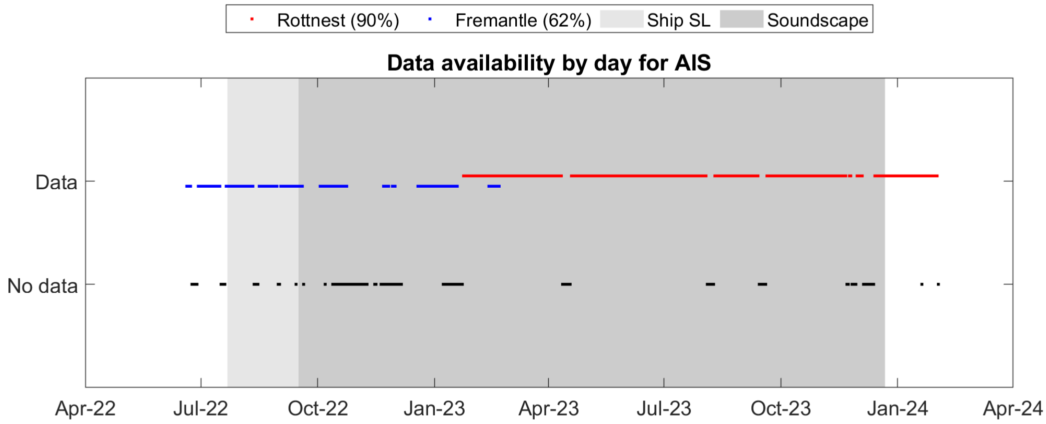

Figure 6. Plot of data availability for Fremantle and Rottnest AIS receivers.

Figure 7 shows the location of both AIS stations and some example vessel tracks for the four tugs operating in Cockburn Sound for the month of February 2023. All four tugs operated in different locations while being based out of Fremantle Harbour. SVITZER ALBATROSS and SVITZER HARRIER were involved in port operations at the various berthing sites along the east side of Cockburn Sound, whereas SVITZER EAGLE and SVITZER FALCON generally operated in and around Fremantle Harbour and in the Gage Roads area just outside Fremantle Harbour.

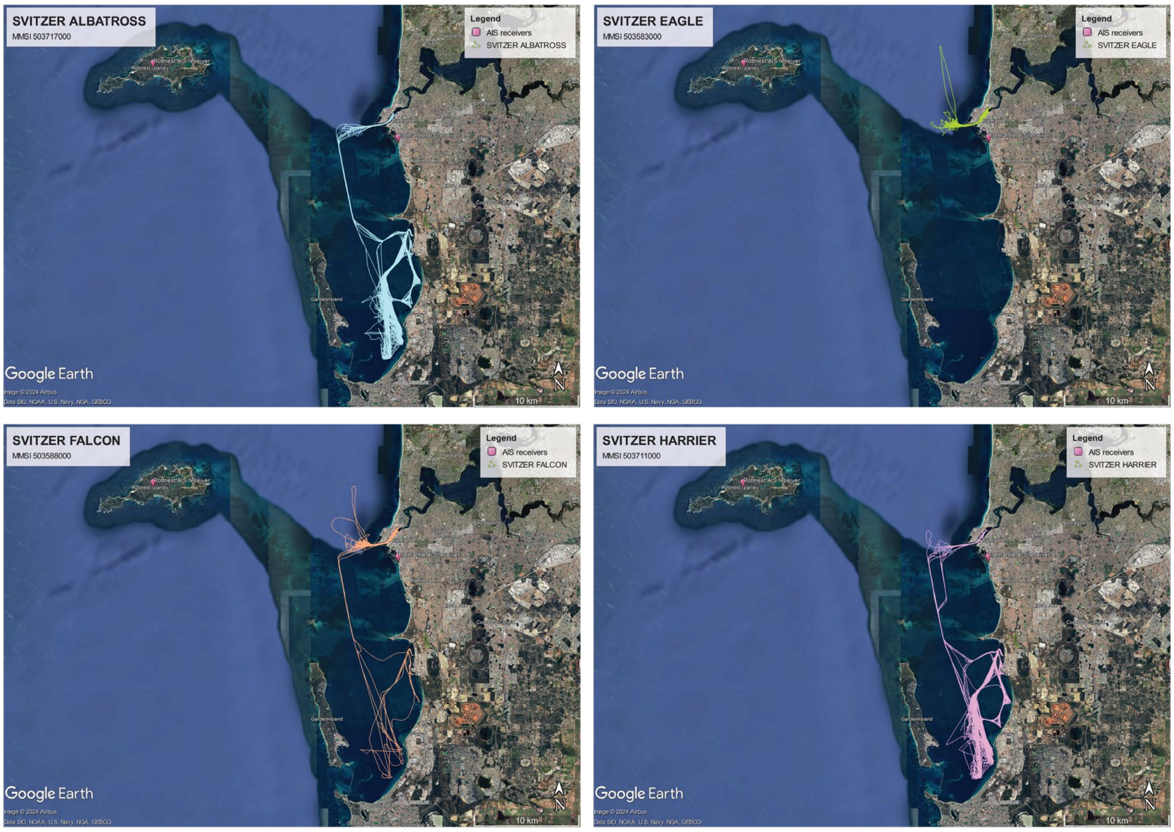

Figure 7. Map showing location of the Fremantle AIS VHF receiver and the Rottnest Island AIS receiver (yellow pins) and tug tracks for the month of February 2023 for SVITZER FALCON (red), SVITZER EAGLE (cyan), SVITZER HARRIER (yellow), and SVITZER ALBATROSS (orange).

3.1.3 Soundscape measurement

Underwater sound recorders were deployed at nine sites across three separate deployments, each lasting approximately four months (Figure 3):

- *Deployment 1*: Four of the sound recorders were deployed on 17 September 2022 (Sites 1, 2, 3 and 9), and the remaining five on 14 October 2022.
- *Recovery 1 and Deployment 2*: All nine recorders were recovered on 20 January 2023 and redeployed for a second deployment on 7 February 2023.
- *Recovery 2 and Deployment 3*: Eight of the nine recorders were recovered 20 July, and then redeployed for a third and final deployment on 7 August 2023. The recorder at Site 3 that was not recovered in July 2023 was replaced with another recorder located 235 m SE of the original Site 3 during the August 2023 deployment (referred to as Site 3A).
- *Recovery 3*: Eight of the nine recorders were recovered on 15 January 2024. Site 2 was recovered from Deployment 3 on 6 March 2023, but the recorder failed to store data.

Details of the recorder positions and settings are found in Table **2** for Deployment 1, Table 3 for Deployment 2, and Table 4 for Deployment 3. Duty cycles, which depended on sampling frequency, battery life, and recorder capacity, were chosen to maximise useful measurements over each four month deployment.

3.1.4 Airgun measurements

Surrich Hydrographics Pty. Ltd. provided CMST with the opportunity to temporarily deploy a mooring during tests of an airgun sound source in Cockburn Sound on 12 October 2023, and also offered to include some test lines that passed close to several of CMST's Deployment 3 recorders. The airgun had a volume of 0.33L (20 in^3) and a nominal chamber pressure of 6.9 MPa (1000 psi), and was towed at a depth of 3 m.

To maximise the dynamic range of the recordings, the temporary mooring included two independent sound recorders, both made by Ocean Instruments: a SoundTrap ST500 (high gain) and a SoundTrap ST300 set to low gain. Both instruments recorded at 48 kHz and they were mounted on the same frame, which was placed on the seafloor in approximately 7 m of water. Data from both instruments were analysed and gave very similar results with the exception that the ST500 data had more issues with saturation when the airgun was within a few hundred metres of the recorder. The results presented here are therefore based on data recorded with the ST300. The temporary mooring was deployed at Site MA in Figure 8, and after carrying out an initial series of airgun test transmissions the vessel proceeded clockwise around the track shown in red.

The actual source vessel track (Figure 9) followed the planned track closely apart from a gradual deviation to avoid another vessel about halfway along the leg from recorder 4 to WP1. This took the source vessel a maximum of 100 m to the west of the straight-line track.

The temporary recorder was recovered following some more test transmissions that were carried out after completing the track.

Table 2. Details of sound recorders for the first soundscape deployment: site name, longitude (degrees East), latitude (degrees South), water depth (m), date deployed, date recovered, date of last recording, sample frequency fs, duty cycle (minutes/minutes), recorder model.

Site	Longitude (E)	Latitude (S)	Depth (m)	Deployed	Recovered	Recording end	f_s (kHz)	Duty cycle (min/ min)	Model
1	115.68939	32.11678	6.7	16/09/2022	20/01/2023	19/01/2023	192	7/10	ST600
2	115.67415	32.14426	10.0	16/09/2022	20/01/2023	20/01/2023	192	7/10	ST600
3	115.69326	32.16871	21.5	16/09/2022	20/01/2023	20/01/2023	192	7/10	ST600
4	115.72782	32.21110	20.0	14/10/2022	20/01/2023	19/01/2023	96	4/5	ST500
5	115.71698	32.26248	19.0	14/10/2022	20/01/2023	23/12/2022	96	4/5	ST500
6	115.74040	32.24726	19.0	14/10/2022	20/01/2023	20/01/2023	96	4/5	ST500
7	115.74882	32.19321	8.0	14/10/2022	20/01/2023	21/01/2023	96	4/5	ST500
8	115.73872	32.17186	8.0	14/10/2022	20/01/2023	18/01/2023	96	4/5	ST500
9	115.74310	32.10787	9.0	16/09/2022	20/01/2023	08/01/2023	192	7/10	ST600

Table 3. Details of sound recorders for the second soundscape deployment: site name, longitude (degrees East), latitude (degrees South), water depth (m), date deployed, date recovered, date of last recording, sample frequency fs, duty cycle (minutes/minutes), recorder model.

Site	Longitude (E)	Latitude (S)	Depth (m)	Deployed	Recovered	Recording end	f_s (kHz)	Duty cycle (min/ min)	Model
1	115.68920	-32.11658	7.0	07/02/2023	20/07/2023	22/06/2023	96	4/5	ST600
2	115.67433	-32.14418	9.7	07/02/2023	20/07/2023	08/06/2023	96	4/5	ST600
3	115.69338	-32.16807	21.5	07/02/2023	Not yet	N/A	96	4/5	ST600
4	115.72818	-32.21088	19.8	07/02/2023	20/07/2023	06/07/2023	96	4/5	ST500
5	115.71738	-32.26240	18.7	07/02/2023	20/07/2023	08/06/2023	96	4/5	ST500
6	115.74042	-32.24707	19.0	07/02/2023	20/07/2023	02/07/2023	96	4/5	ST500
7	115.74902	-32.19315	8.9	07/02/2023	20/07/2023	01/07/2023	96	4/5	ST500
8	115.73883	-32.17183	8.9	07/02/2023	20/07/2023	06/06/2023	96	4/5	ST500
9	115.74312	-32.10788	9.0	07/02/2023	20/07/2023	08/06/2023	96	4/5	ST600

Table 4. Details of sound recorders for the third soundscape deployment: site name, longitude (degrees East), latitude (degrees South), water depth (m), date deployed, date recovered, date of last recording, sample frequency fs, duty cycle (minutes/minutes), recorder model.

Site	Longitude (E)	Latitude (S)	Depth (m)	Deployed	Recovered	Recording end	f_s (kHz)	Duty cycle (min/ min)	Model
1	115.68917	-32.11707	6.6	07/08/2023	15/01/2024	16/01/2024	96	4/5	ST600
2	115.67395	-32.14450	11.0	07/08/2023	06/03/2024	N/A	96	4/5	ST600
3A	115.69512	-32.16968	21.5	07/08/2023	15/01/2024	16/01/2024	96	4/5	ST600
4	115.72787	-32.21117	20.0	07/08/2023	15/01/2024	16/01/2024	96	4/5	ST500
5	115.71687	-32.26230	19.0	07/08/2023	15/01/2024	22/12/2023	96	4/5	ST500
6	115.74045	-32.24723	19.1	07/08/2023	15/01/2024	16/01/2024	96	4/5	ST500
7	115.74892	-32.19315	9.0	07/08/2023	15/01/2024	15/01/2024	96	4/5	ST500
8	115.73877	-32.17205	8.6	07/08/2023	15/01/2024	26/12/2023	96	4/5	ST500
9	115.74263	-32.10813	9.2	07/08/2023	15/01/2024	16/01/2024	96	4/5	ST600

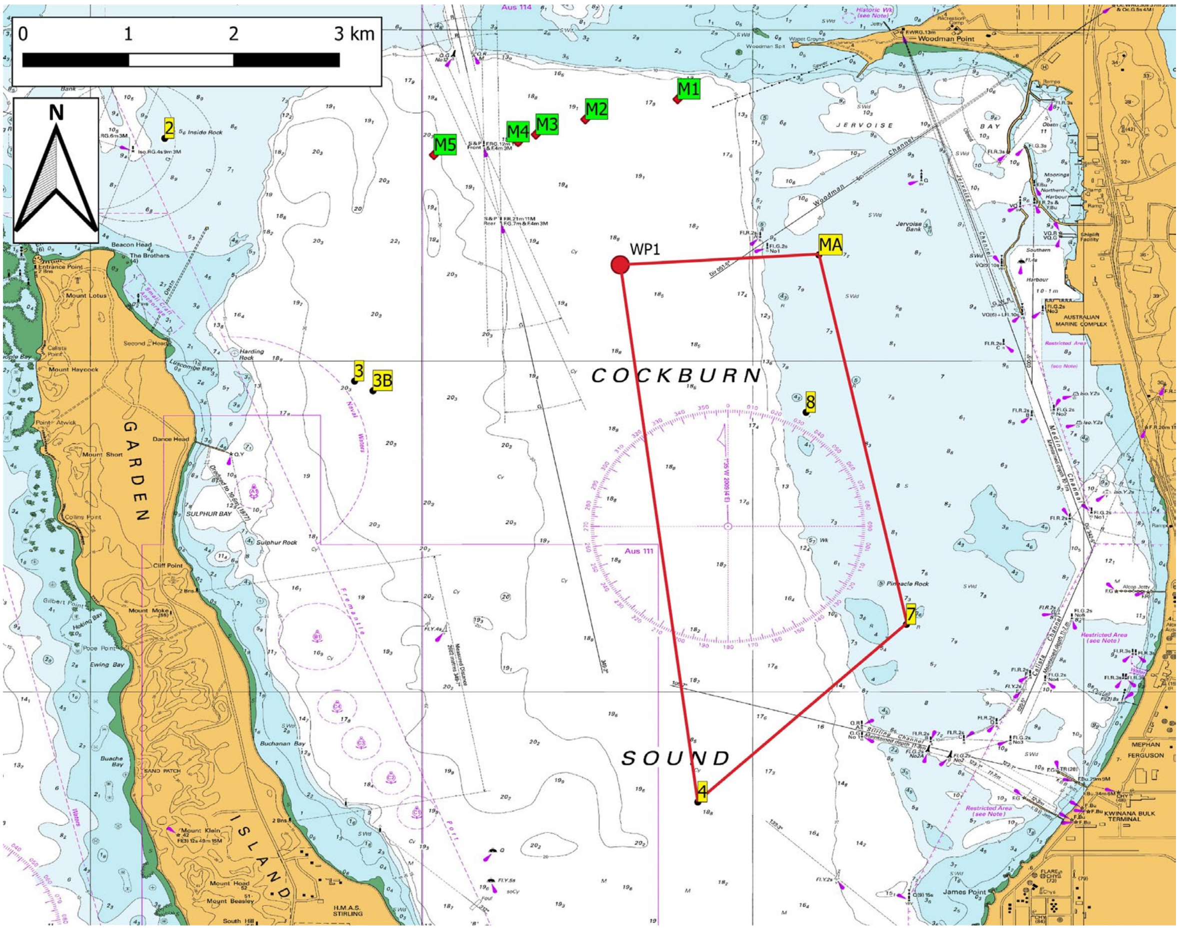

Figure 8. Map showing the planned airgun test lines. The temporary recorder was deployed at MA, and a number of test transmissions were made in that vicinity. After that, the vessel proceeded clockwise around the red track. Magenta dots are the positions of the CMST Deployment 3 recorders. WP1 was a track waypoint and does not represent the location of any physical object.

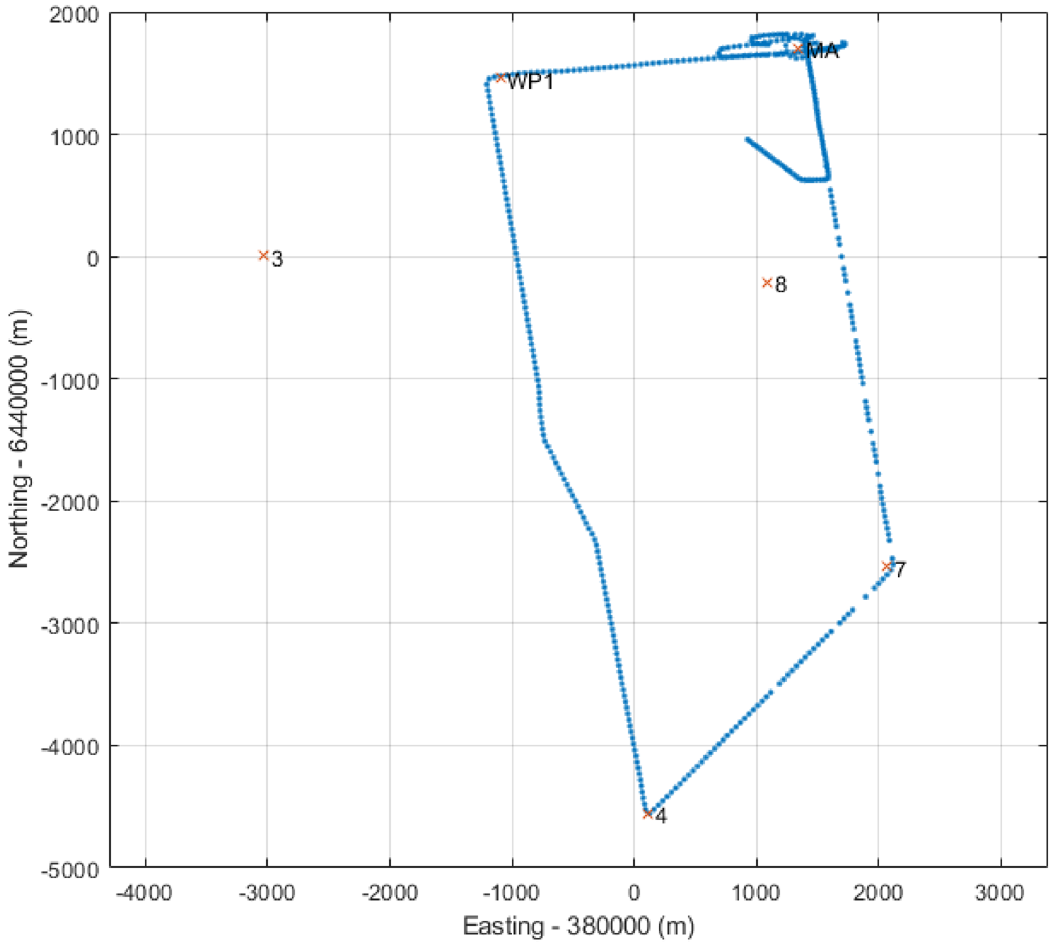

Figure 9. GPS positions of all logged airgun transmissions. Numbered red crosses are the positions of the CMST Deployment 3 recorders.

3.2 Data analysis

Vessel and port operations noise analysis, including clock synchronisation and data quality control measures, are described in Section 3.2.1. Signal processing for soundscape analysis is described in Section 0. Analysis of the airgun measurements is described in Section 3.2.3, while the use of the acoustic modelling software is described in Section 3.2.4.

3.2.1 Vessel noise analysis

Vessel noise was estimated for four vessel classes (tanker, bulk carrier, tug, and pilot boat) as well as for the combined noise arising from routine port operations near the Kwinana Grain Terminal (32.2548°S, 115.7432°E). Bulk carrier and tanker noise were measured using the vessel noise deployment at the northern end of Cockburn Sound from July to September 2022 (Figure 4). Tug, pilot boat, and port operations noise were measured using the recorder deployed 700 m from the grain terminal at Site 6 during Deployment 2 (Figure 3) during February and March 2023.

Clock synchronisation: Each recorder was synchronised by hand to a GPS clock upon deployment; however each recorder has a different clock drift of approximately 0.5s/day and an offset of up to 60s for each deployment. In order to synchronise the clocks, multiple times for the closest point of approach (CPA) calculated using AIS data for the relatively fast-moving pilot boat GENESIS were identified at each recorder. The maximum broadband noise in the recording due to each corresponding boat CPA could be identified and associated with a time on the recorder's internal clock for 18 passes at M3 and M5 and 4 passes at Site 6. A least-squares fit of recorder time t_{Rec} as a function of GPS time t_{GPS} for each CPA was performed for each recorder in order to calculate its clock drift and offset, so that all vessel positions could be correctly synchronised with the audio recordings.

Bulk carrier and tanker noise analysis: Recorders M3 and M5 were sampled continuously at a rate of 96 kHz with a 100% duty cycle. Ships were identified for analysis by filtering AIS data for ships passing northward or southward through an imaginary line separating M3 from M5 in a straight line. There are stationary berths 4.0-4.2 km away from M3 and M5. Ships moored at those locations show up on the AIS but have zero velocity and their noise does not reach the recorders, therefore a further requirement for isolating ship passes was that there be no other ships within 5000 m that were moving faster than 5 kn. A total of 28 ship passes (14 tankers and 14 bulk carriers) were identified as being suitable for further analysis. For each ship pass, the time at which the ship crossed the line between M3 and M5 was identified as the time of interest t_0, and acoustic data were analysed in 30s intervals for a 5-minute period centred on t_0. One-third octave (one-) band received levels at the recorder were computed for each 30-s interval, as well as the mean range and bearing between ship and recorder.

Tug and pilot boat noise analysis: X and Y passes of tugs and the pilot boat near Site 6 were identified. The time of interest t_0 for each boat pass was defined as the CPA to recorder 6, and the same analysis was performed as for the bulk carriers and tankers, resulting in one-third octave (OTO) band received levels at the recorder for a 5-minute period centred on t_0. However, recorder 6 was operating for 4 minutes out of every 5 minutes at a sample rate of 48 kHz, resulting in measurement gaps during boat approaches.

Port operations noise analysis: Review of AIS data revealed a repeatable pattern of activity surrounding the Kwinana Grain Terminal jetty. Bulk carriers would arrive at the terminal accompanied by one or two tugs and the pilot boat, all passing within a few hundred metres of Recorder 6 within a few minutes of each other. The tugs would assist the carrier in docking at the jetty (32.2545° S, 115.7434° E), generally one boat at the bow and one at the stern, and then they would leave the carrier at the jetty while it was being loaded. Tugs would then return to assist the ship during its departure from the terminal. A total of ten such events were identified for analysis. The arrival and departure procedures typically lasted from 0.3-1.0 hours, while loading time varied from 12 to 73 hours (Table 5). The bulk carrier ship for each event was termed the "focal ship" and times were defined relative to the focal ship and wharf location as follows:

- Arrival: begins when focal ship is less than 200m away from the jetty, ends when focal ship is alone at the jetty
- Loading: begins 30 minutes after the end of Arrival, ends 30 minutes before the start of Departure
- Departure: begins when the first assisting ship is within 200m of the jetty, ends when focal ship is greater than 200m away from the jetty

Background noise levels: At M3 and M5, background noise levels relevant to each ship pass were calculating by finding the 5-minute period of lowest broadband noise in a 2-hour time window centred on t_0, and calculating OTO band levels for that period. For the tug, pilot boat, and port operations measurements at Site 6, a 39-hour time period with no ships present at the grain terminal was identified from 14:11 on 26 February 2023 until 05:00 on 28 February 2023. Noise levels were calculated in 5-minute blocks during this period and the median noise level was used as a background noise level for all measurements at Site 6. Figure 10 is a plot of median background noise levels at all three receiver locations. All the background levels agree within ±2 dB between 315 Hz and 1587 Hz, and the noise levels at M3 and M5 agree to within ±6dB over the entire 10-10000 Hz frequency range. However, the levels are as much as 17 dB higher at Site 6 than at M3/M5 for frequencies less than 315 Hz, and 3-8 dB lower at Site 6 than M3/M5 for frequencies higher than 1587 Hz.

Table 5. Information on port operations events used for analysis: MMSI, ship name, start and end times of analysis, arrival, loading, and departure durations in hours.

MMSI	Ship Name	Start Time (UTC)	End Time (UTC)	Arrival (h)	Loading (h)	Departure (h)
354644000	MYRTO	2023-02-11 05:39:45	2023-02-14 05:01:15	0.5	69.1	0.8
636021707	NEW JOYFUL	2023-02-14 05:14:15	2023-02-14 23:17:25	4.9	11.7	0.5
212745000	EPICTETUS	2023-02-14 23:35:50	2023-02-18 02:24:50	0.4	73.0	0.4
419001768	MAHA YAYA	2023-02-18 02:40:05	2023-02-20 04:37:50	0.6	47.7	0.7
636017559	ROSALIA	2023-02-20 04:51:25	2023-02-21 07:30:40	0.5	24.1	1.0
209004000	GRAECIA AETERNA	2023-02-24 16:30:55	2023-02-26 14:11:45	0.5	43.9	0.3
538008489	SSI PRIVILEGE	2023-02-21 07:42:10	2023-02-22 16:29:50	0.6	30.6	0.6
538007422	MONDIAL COSMOS	2023-02-22 16:45:40	2023-02-24 16:13:35	5.0	41.2	0.3
538009110	MARINA I	2023-03-03 01:11:35	2023-03-03 15:51:55	0.5	12.8	0.4
538004774	GENEVA QUEEN	2023-03-03 16:13:30	2023-03-06 04:21:15	0.6	57.8	0.7

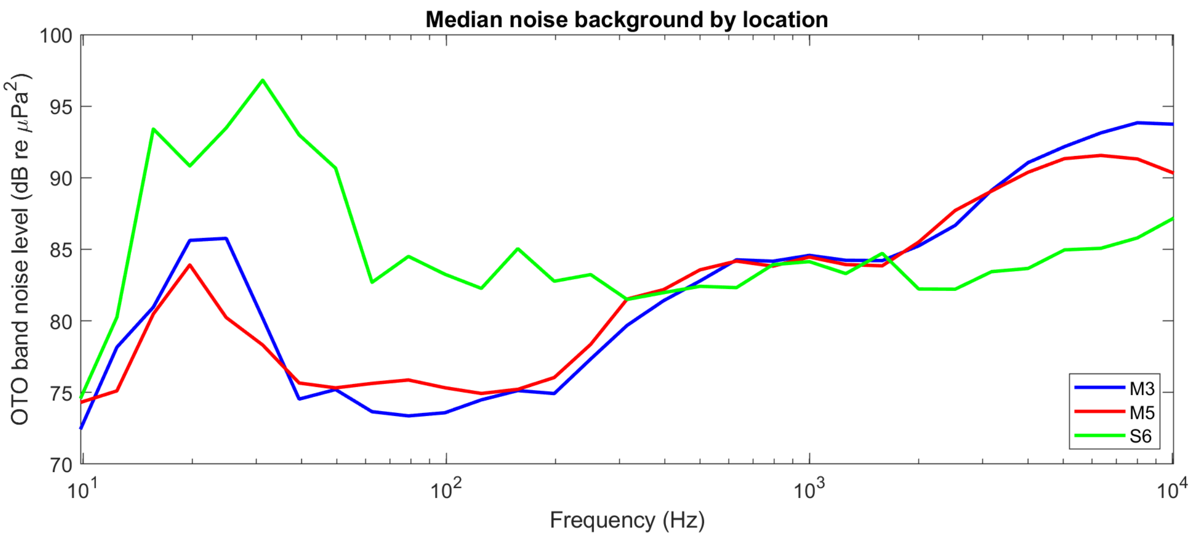

Figure 10. Median OTO band background noise level as function of frequency by location: M3 (blue line), M5 (red line), Site 6 (green line).

Quality control and conversion to source level: In order improve accuracy of source level estimates, measurements of OTO band received level (RL) were only used for further analysis if the signal-to-noise ratio (SNR) exceed 6 dB and the distance between source and receiver was less than 1000 m.

3.2.2 Soundscape analysis

Data recorded on the sound recorders were downloaded as *.wav* files using Ocean Instruments' SoundTrap software. CMST's CHORUS MATLAB toolbox was used to process the data (Gavrilov & Parsons 2014). For each downloaded dataset, the power spectral density (PSD) was calculated for each *.wav* file in the dataset using the default parameters of a time step of the file length and frequency resolution of 1 Hz. Using CHORUS, the datasets were reviewed using the long-term spectrograms (middle panel, Figure 11) to select individual files to listen to and inspect their spectrogram (top panel, Figure 11) to identify sound sources. Ambient noise was calculated for one-third and one-twelfth octave bands at 1st, 5th, 25th, 50th, 75th, and 95th percentiles, over the whole deployment period and monthly intervals, for the different locations (bottom right panel, Figure 9). Spectrograms were generated using the monthly 50th percentile data (bottom left panel, Figure 11). The broadband sound pressure level (40 to 48000 Hz) was calculated using the OTO band levels for each recording. Where appropriate, the Cato ambient noise model was used for comparison (Cato 1997). Tabulated values for the OTO band spectral levels by site and percentile are found in the Appendix (9.1)

To investigate spatial variation between the sites, the Pearson correlation coefficient was calculated between sites for the daily broadband and OTO band levels, for each deployment. To understand the contribution of the different frequencies to the temporal variation in the soundscape at each site, principal component analysis (PCA) was performed on the OTO band levels calculated from the power spectral density for each recording, for each deployment. In addition, diurnal variation in the PSD for each site was calculated by subtracting the nighttime from the daytime PSD for each site and deployment. In order to understand potential sound sources, comparison of OTO band levels was made with wind speed (from the Bureau of Meteorology's Garden Island weather station), rain rate, AIS, water temperature (from WA's Department of Water and Environmental Regulation Cockburn Sound mooring data), and sea level (from the Bureau of Meteorology's Fremantle station) data. Due to the high levels of vessel and snapping shrimp noise, bioacoustic detection of dolphins and fish was most effectively achieved through manual review of the data, as opposed to automatic detection routines. Reviewing data for temporal variation of dolphin sounds was concentrated on Sites 1, 5, 7, and 8, as they were identified as being of importance by Theme 8: Apex predators and iconic species. Based on fisheries mooring locations, effort for bioacoustics detection of fish was focused on 2, 3, 7, and 8, and expanded to include Site 6 after fish were observed there during preliminary analysis.

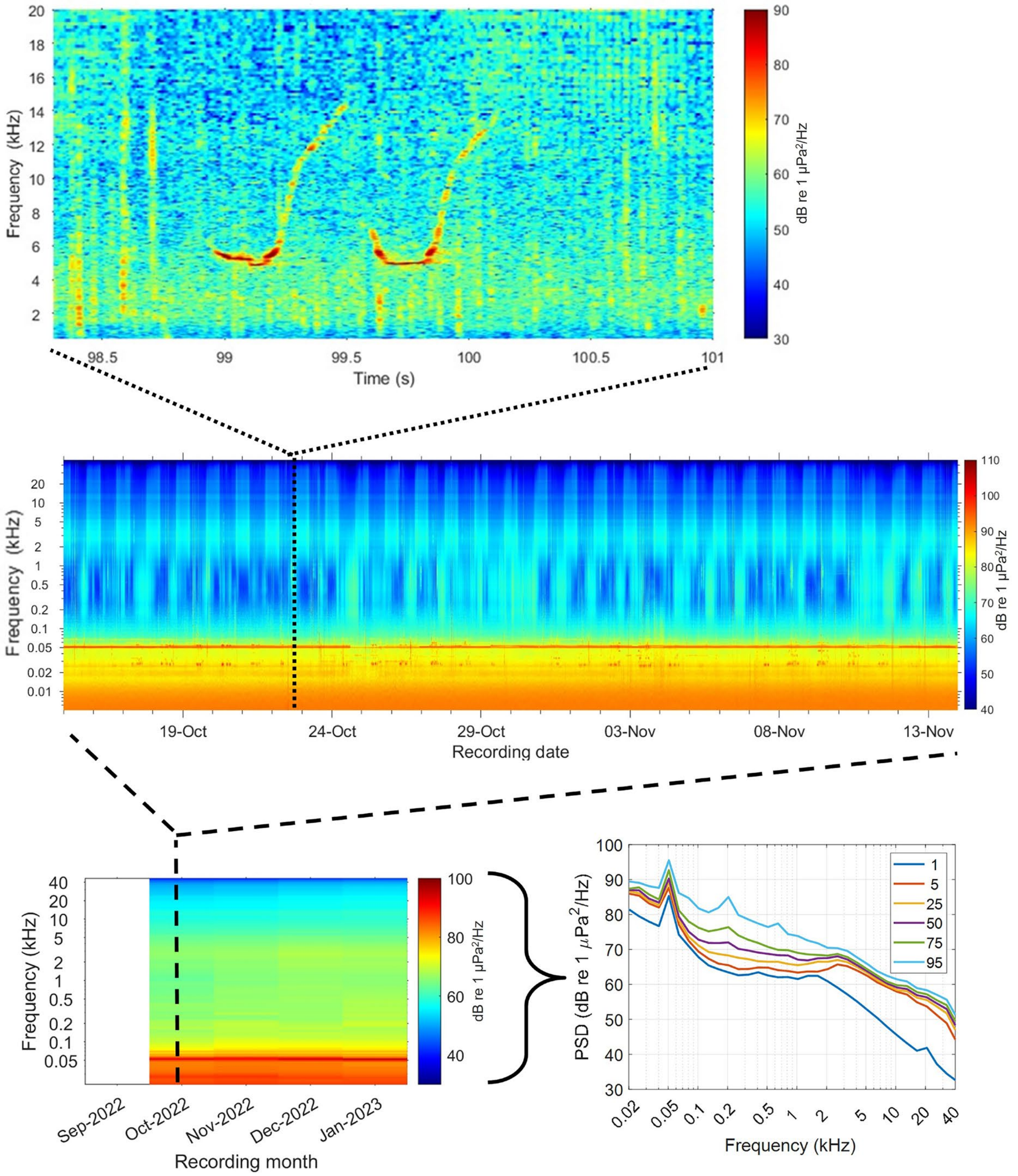

Figure 11. Spectrograms at different temporal scales from Site 7: seconds (top), days (middle) and months (bottom left), and the power spectral density at 1%, 5%, 25%, 50%, 75%, and 95% over the whole deployment (bottom right).

3.2.3 Airgun analysis

Recorded airgun signals contained head-waves, which are arrivals that precede the through-water signals and are a result of energy that has travelled via higher speed paths through the seabed. This made it possible to determine compressional sound speeds and depths of major layers within the seabed. This analysis was carried out by plotting the received signals relative to their transmission times, offset vertically in proportion to the source-receiver range, which was determined from GPS. Two versions of the signals were overlaid: one with the head-wave arrivals emphasised by low-pass filtering with a cut-off of 200 Hz, and the other with the through-water arrivals emphasised by band-pass filtering with a pass-band from 500 Hz to 800 Hz.

An example of the resulting plot is shown in Figure 12. Arrivals from each layer have a different linear relationship between arrival time and range, which allows them to be readily identified on this type of plot (straight lines overlaid on Figure 12). The slope of the linear relationship gives the compressional wave sound speed in the layer and the depth of the layer can be calculated from the zero range travel time (X intercept) (Hall 1996).

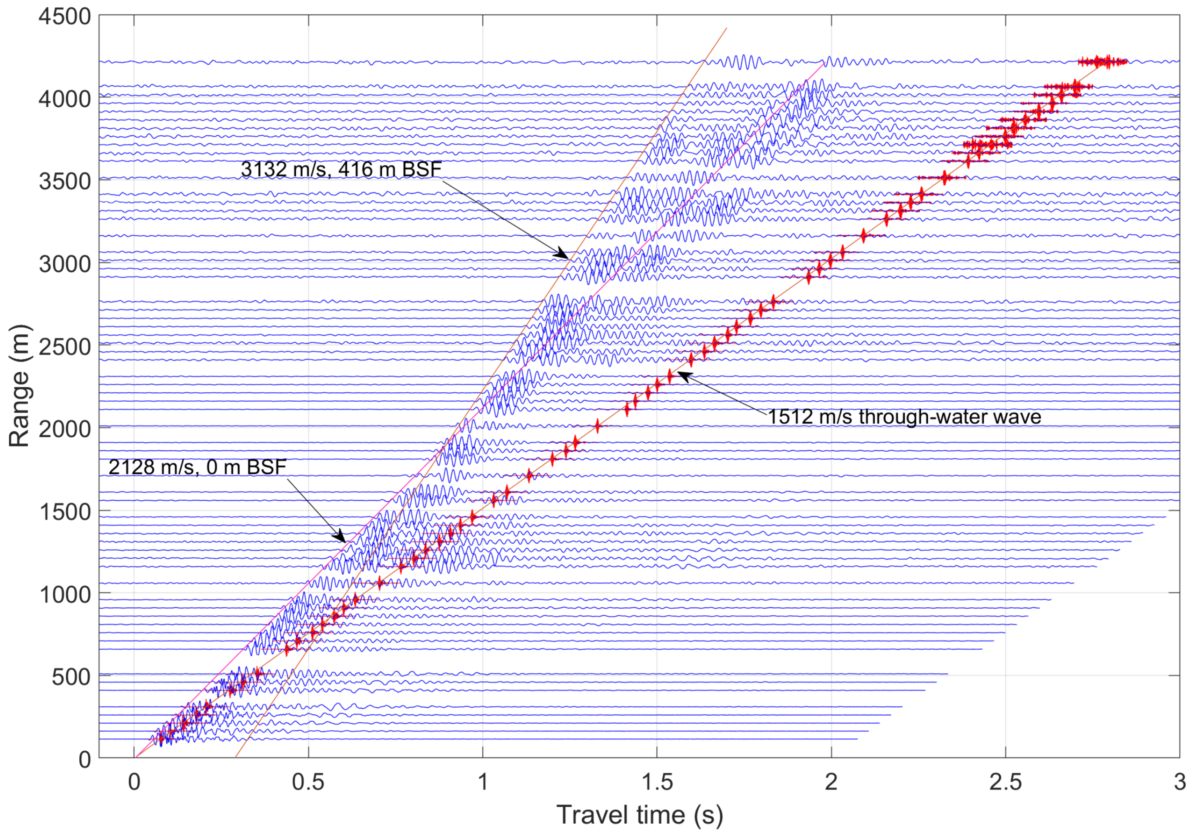

Figure 12. Stacked arrival plot for Leg 1 of the track shown in Figure 8 (MA to recorder 7) with the through-water arrival (red) and head-wave arrivals (blue) from two different seabed layers indicated. Data is from the ST300 recorder on the temporary mooring at MA.

The airgun's acoustic signature was not measured during the trial, however CMST has developed an airgun array model, Cagam, that has been verified against measurements and other models (Duncan & Gavrilov 2019). Cagam was used to model the airgun source signal which allowed the determination of propagation loss (PL) as a function of frequency and range by subtracting the measured received spectral level from the modelled source spectral level at each frequency for each transmission. These results were directly compared to those produced by numerical propagation models and, after averaging into OTO bands, were also fitted to functions of the form

$$PL = C + B_0 \log_{10}\left(\frac{r}{r_0}\right) + B_1 \log_{10}\left(1 + \frac{r}{R_1}\right) \quad (1)$$

where r is the horizontal separation between source and receiver, and r_0 is the standard reference distance (1 m), Here C, B_0, B_1 and $R_1$are unknown parameters that were obtained by a standard nonlinear least squares fit based on the Levenberg-Marquadt method (Press et al. 2007). This function transitions smoothly between a slope of B_0 dB per decade change in range for ranges much less than R_1 and $B_0 + B_1$ dB per decade change in range for ranges much greater than R_1.

3.2.4 Numerical acoustic propagation modelling

Cockburn Sound is a shallow embayment with a seabed consisting of a thin layer of unconsolidated sediment overlaying a soft limestone known as calcarenite, which is itself variable and layered (Skene et al. 2005). Calcarenite typically has a shear speed slightly less than the in-water sound speed resulting in strong coupling of the water-borne sound to shear waves in the seabed (Duncan et al. 2008, Duncan et al. 2013), which makes this a very challenging situation for acoustic propagation modelling, particularly at low frequencies where waveguide effects dominate the propagation and shear wave effects are important.

Wavenumber integration (WNI) models (Jensen et al. 2011, Etter 2018) are the only commonly available models that can accurately calculate low-frequency propagation loss in this type of environment out to the ranges typically required for environmental impact studies. However, these are only practical for situations where there are no significant changes in water depth, water column sound speed, or seabed properties along the propagation path, referred to as “range independent” acoustic propagation. Fortunately, in Cockburn Sound, there are large areas where the water depth is close to constant and WNI can be used. In these cases we have used the WNI modelling code SCOOTER (Porter 2020) to calculate PL.

At sufficiently high frequencies, waveguide effects become unimportant and it becomes feasible to deal with range dependent environments by calculating seabed reflectivity vs. grazing angle using a wavenumber integration based reflection code (Jensen et al. 2011), and using this as input to a beam tracing code (Jensen et al. 2011)which calculates the PL. For the purposes of this project, this situation was dealt with using Bounce (Porter 2020) for reflection coefficient calculation and Bellhop (Porter 2020) for PL calculation. When used in this mode Bellhop can deal with range dependent water depth, but not range dependent seabed reflectivity, however this is a good approximation for most modelling tasks in Cockburn Sound.

One approach to carrying out low-frequency range dependent modelling is to use a parabolic equation propagation model (Jensen et al. 2011, Etter 2018) together with an equivalent fluid geoacoustic model of the calcarenite layer. This approach is discussed more fully in the Appendix (9.4) and typically works well at frequencies high enough that shear wave effects are unimportant—usually above a few hundred Hertz. In this study, RAMGeo, a variant of the fluid parabolic equation model, RAM (Collins 1993) has been used for this type of modelling.

All of these codes require geoacoustic models of the seabed, which were determined from a variety of different types of data (Sections 3.1.4, 3.2.3), after which numerical experiments were carried out to establish the frequency ranges of validity of the various propagation model types in the Cockburn Sound environment (see Appendix, 9.4 and 9.5).

4 Results

In this Section, results are presented from the underwater soundscape (4.1), vessel noise signatures (4.2), and sound propagation studies (4.3).

4.1 Soundscape

The results of the underwater soundscape study begin with a description of baseline levels and statistics (4.1.1), followed by the soundscape spatial variation (4.1.2) and soundscape temporal variation (4.1.3), then, specific source categories are described: geophony (4.1.4), anthropophony (4.1.5), and biophony (4.1.6).

4.1.1 Baseline levels and statistics

The distribution of the broadband (40-48000 Hz) SPL for each file at each site and deployment is shown in Figure 13, and median levels in Table 6. The South Basin site (6) recorded the highest median broadband (BB) levels with a value of 97.3 dB re 1µPa across all deployments. The high BB SPLs recorded at Site 6 are most likely due to its proximity to the grain terminal, as detailed in Section 4.1.5. The variation in BB SPLs at each site was relatively consistent between deployments, except for North Basin (Site 3), Central Basin (Site 4), and Mangles Bay (Site 5). However, due to recovery problems, Site 3 consisted of two deployments that were more than 200 m apart, which is the likely reason for this difference at Site 3. Sites 3 (Deployment 3), 4 (Deployments 2 and 3), and Kwinana Shelf North (Site 8) (all deployments) recorded some of the lowest median BB SPLs.

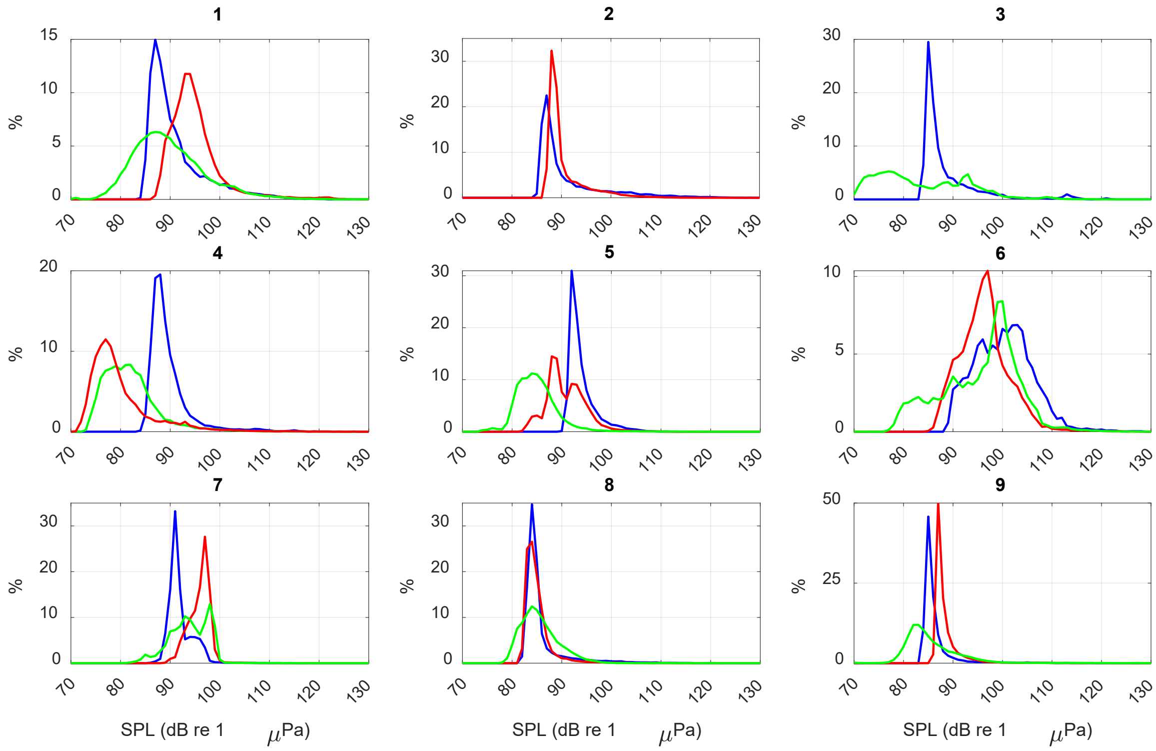

Figure 13. Histograms of broadband (40-48000 Hz) sound pressure levels (dB re 1µPa) at Sites 1-9 for deployments 1 (blue), 2 (red) and 3 (green).

Table 6. Median broadband (40-48000 Hz) sound pressure levels (dB re 1µPa) for each deployment for the nine sites. Highest (in red) and lowest (in blue) sites for each deployment and overall highlighted.

Site	Deployment			Overall
	1	2	3	
1	89.1	94	88.8	**91.6**
2	88.1	88.8	NS	**88.7**
3	86.2	NS	81.8	**85.2**
4	88.4	78.1	81.2	**83.69**
5	93	90.1	84.5	**88.9**
6	100.2	96.1	97.4	**97.3**
7	91.2	96.4	94	**94.4**
8	84.4	84.3	84.9	**84.5**
9	85.3	87.4	84.2	**86.9**

The power spectral density (PSD) percentiles (1, 5, 25, 50, 75, 95, and 99%) are shown over the probability density of PSD levels (shown in colour) for each site (Figure 14 to Figure 23). Note there are two plots for Site 3 as it was moved 200 m during Deployment 3.

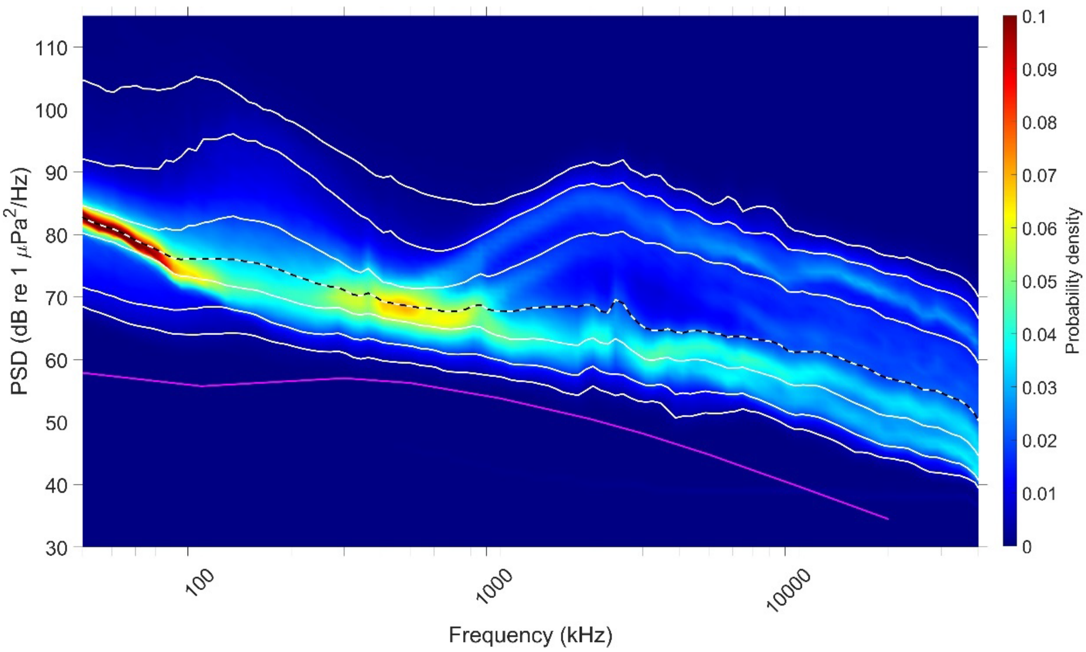

Figure 14. PSD percentiles (1, 5, 25, 75, 95, and 99% shown as white lines; 50% shown as a dashed white-black line) computed over and probability density of PSD levels (shown in colour) for Site 1 (North Channel). Pink line is the Cato model of underwater noise at a wind speed of 5 kn.

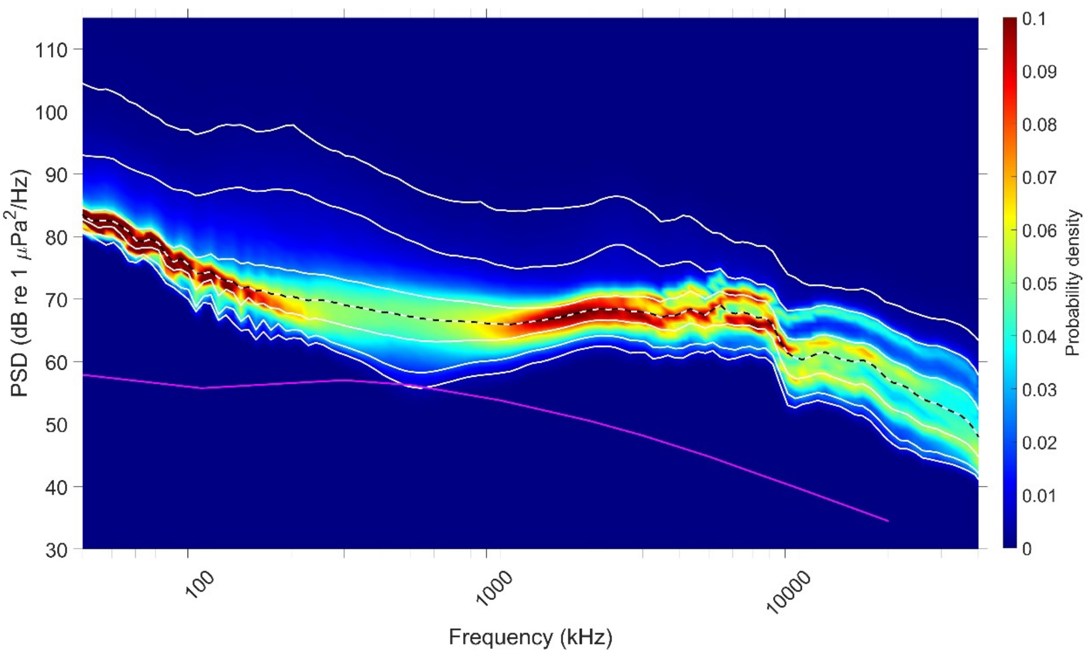

Figure 15. PSD percentiles (1, 5, 25, 75, 95, and 99% shown as white lines; 50% shown as a dashed white-black line) computed over and probability density of PSD levels (shown in colour) for Site 2 (Inside Rock). Pink line is the Cato model of underwater noise at a wind speed of 5 kn.

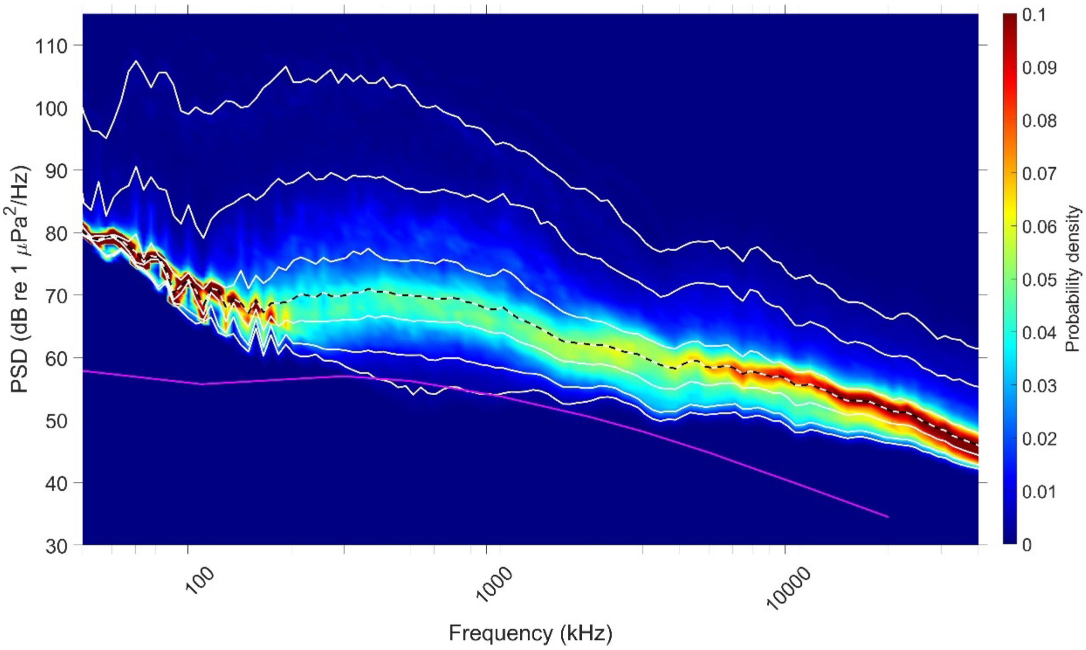

Figure 16. PSD percentiles (1, 5, 25, 75, 95, and 99% shown as white lines; 50% shown as a dashed white-black line) computed over and probability density of PSD levels (shown in colour) for Site 3 (North Basin) – Deployment 1. Pink line is the Cato model of underwater noise at a wind speed of 5 kn.

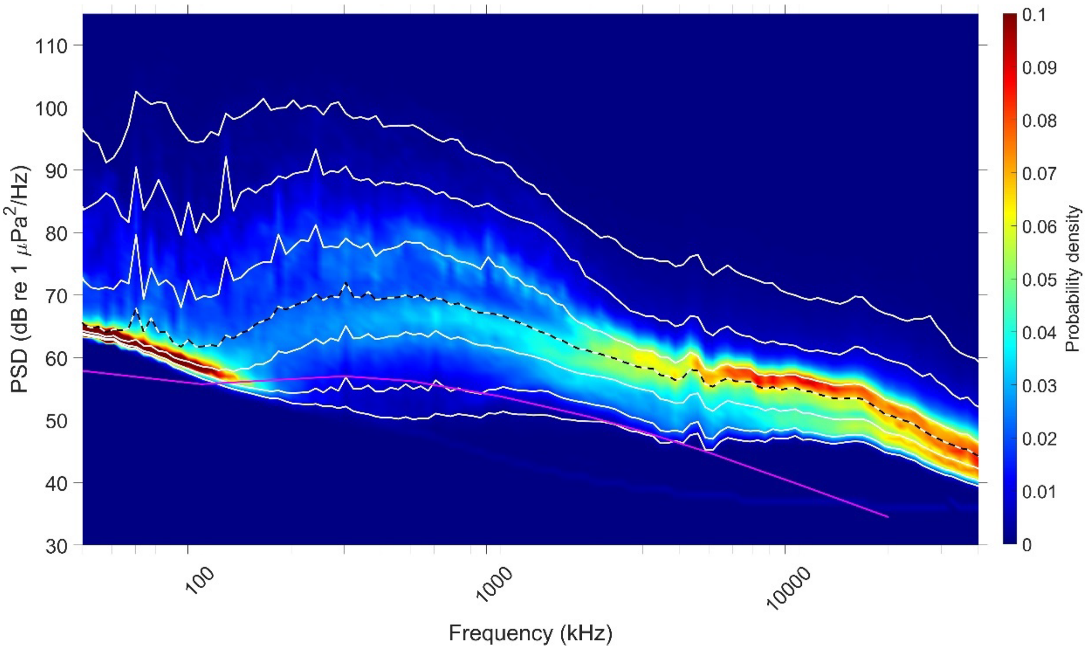

Figure 17. PSD percentiles (1, 5, 25, 75, 95, and 99% shown as white lines; 50% shown as a dashed white-black line) computed over and probability density of PSD levels (shown in colour) for Site 3 (North Basin) – Deployment 3. Pink line is the Cato model of underwater noise at a wind speed of 5 kn.

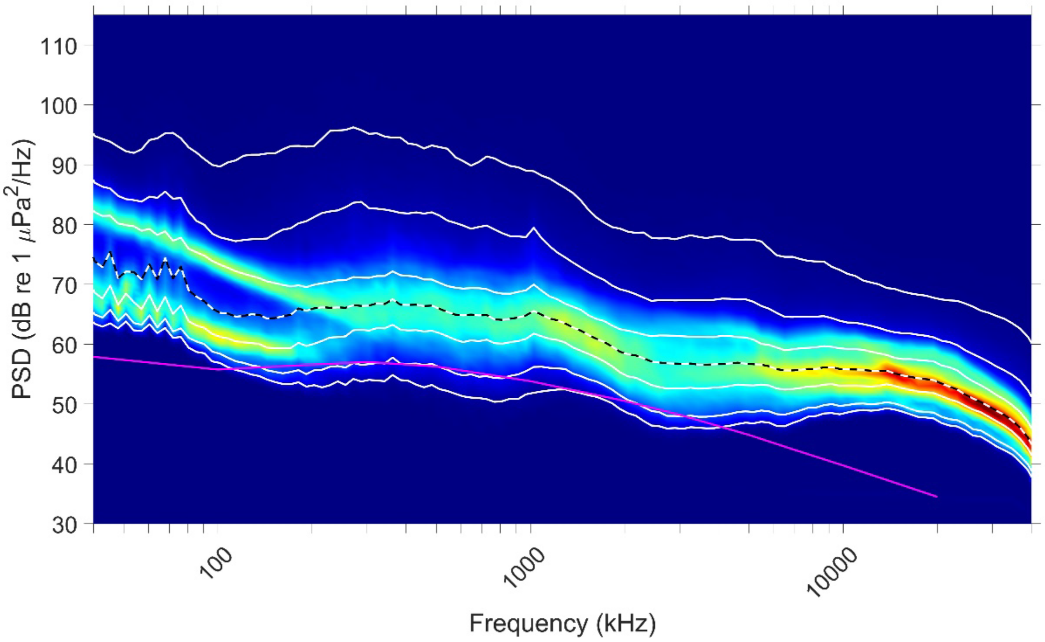

Figure 18. PSD percentiles (1, 5, 25, 75, 95, and 99% shown as white lines; 50% shown as a dashed white-black line) computed over and probability density of PSD levels (shown in colour) for Site 4 (Central Basin). Pink line is the Cato model of underwater noise at a wind speed of 5 kn.

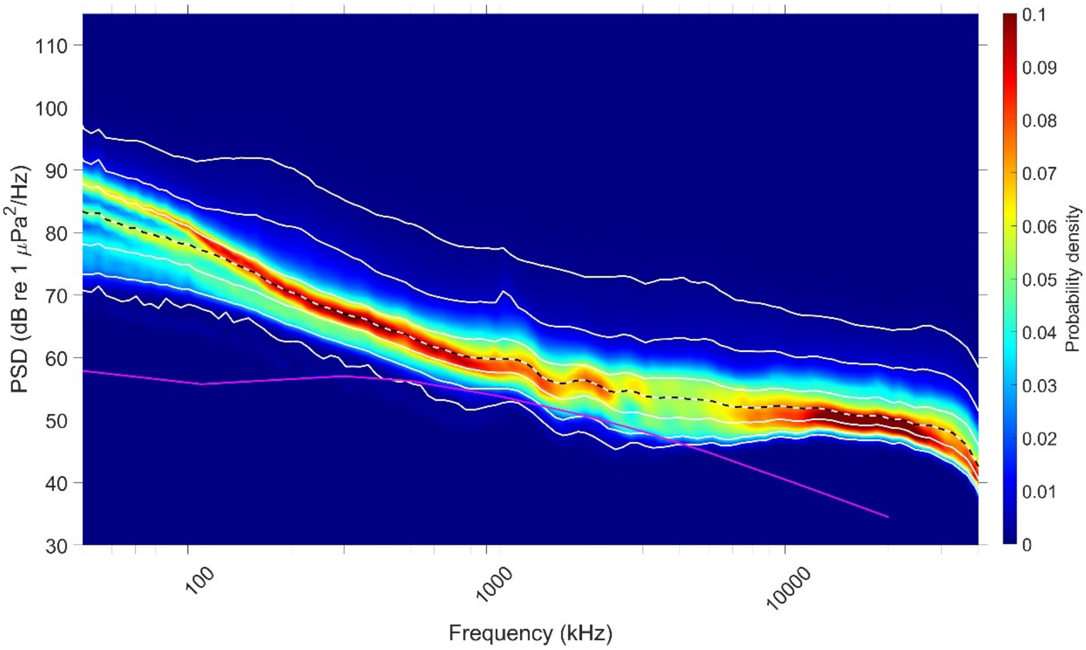

Figure 19. PSD percentiles (1, 5, 25, 75, 95, and 99% shown as white lines; 50% shown as a dashed white-black line) computed over and probability density of PSD levels (shown in colour) for Site 5 (Mangles Bay). Pink line is the Cato model of underwater noise at a wind speed of 5 kn.

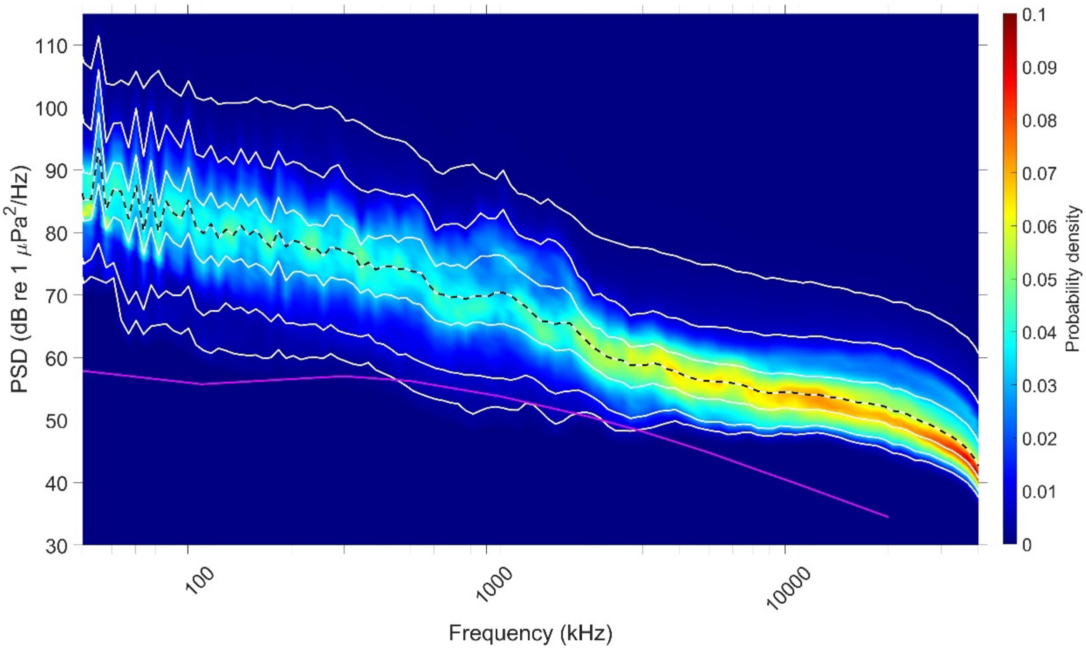

Figure 20. PSD percentiles (1, 5, 25, 75, 95, and 99% shown as white lines; 50% shown as a dashed white-black line) computed over and probability density of PSD levels (shown in colour) for Site 6 (South Basin). Pink line is the Cato model of underwater noise at a wind speed of 5 kn.

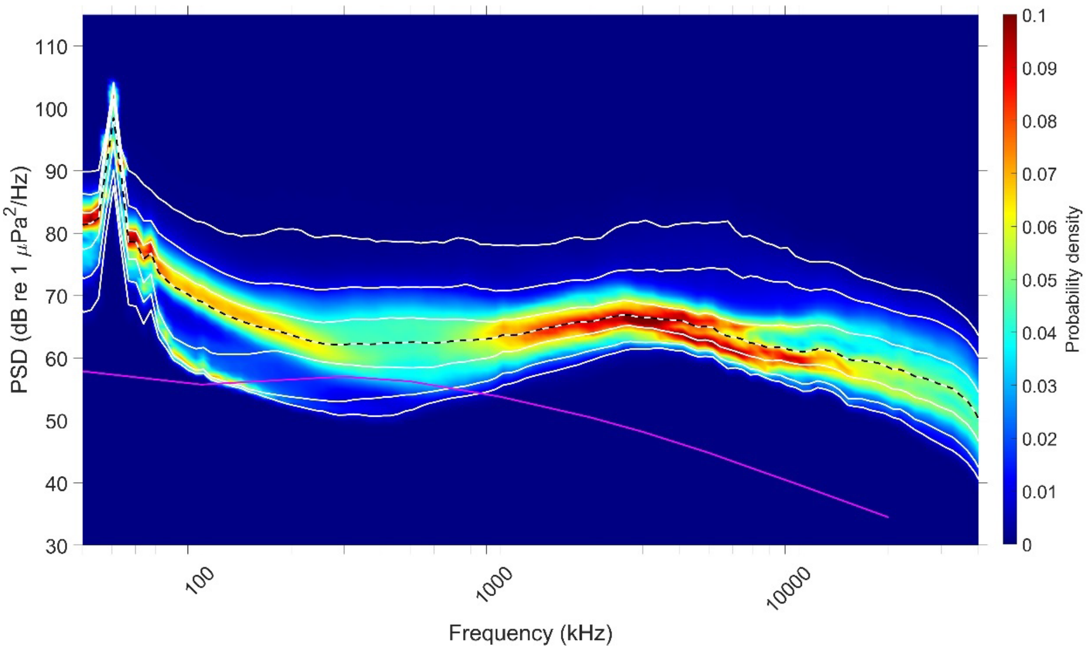

Figure 21. PSD percentiles (1, 5, 25, 75, 95, and 99% shown as white lines; 50% shown as a dashed white-black line) computed over and probability density of PSD levels (shown in colour) for Site 7 (Kwinana Shelf South). Pink line is the Cato model of underwater noise at a wind speed of 5 kn.

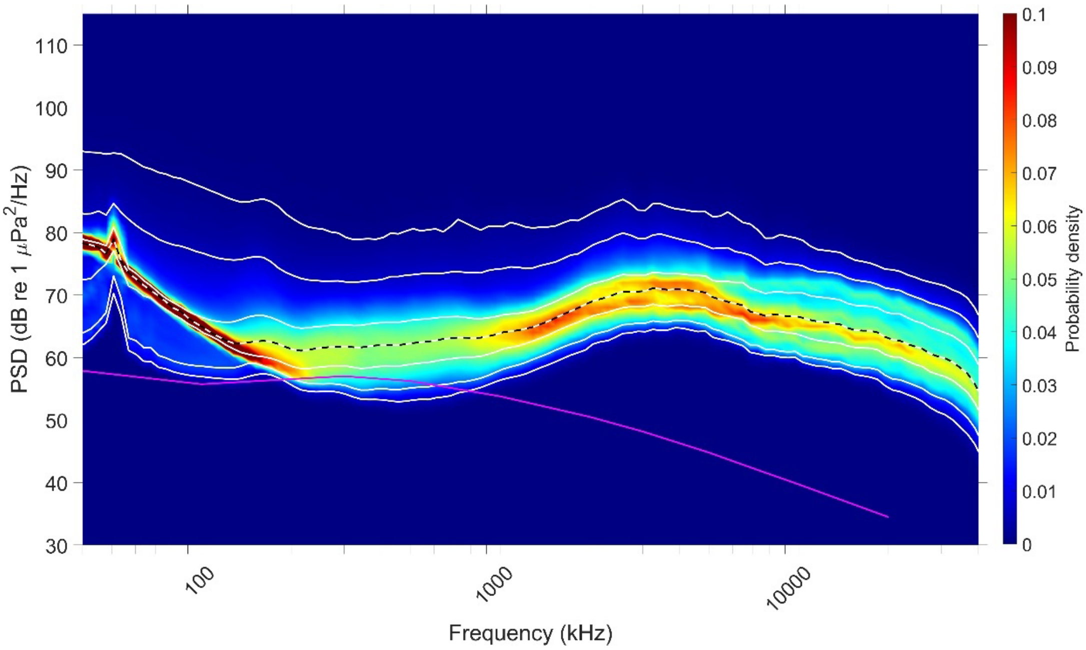

Figure 22. PSD percentiles (1, 5, 25, 75, 95, and 99% shown as white lines; 50% shown as a dashed white-black line) computed over and probability density of PSD levels (shown in colour) for Site 8 (Kwinana Shelf North). Pink line is the Cato model of underwater noise at a wind speed of 5 kn.

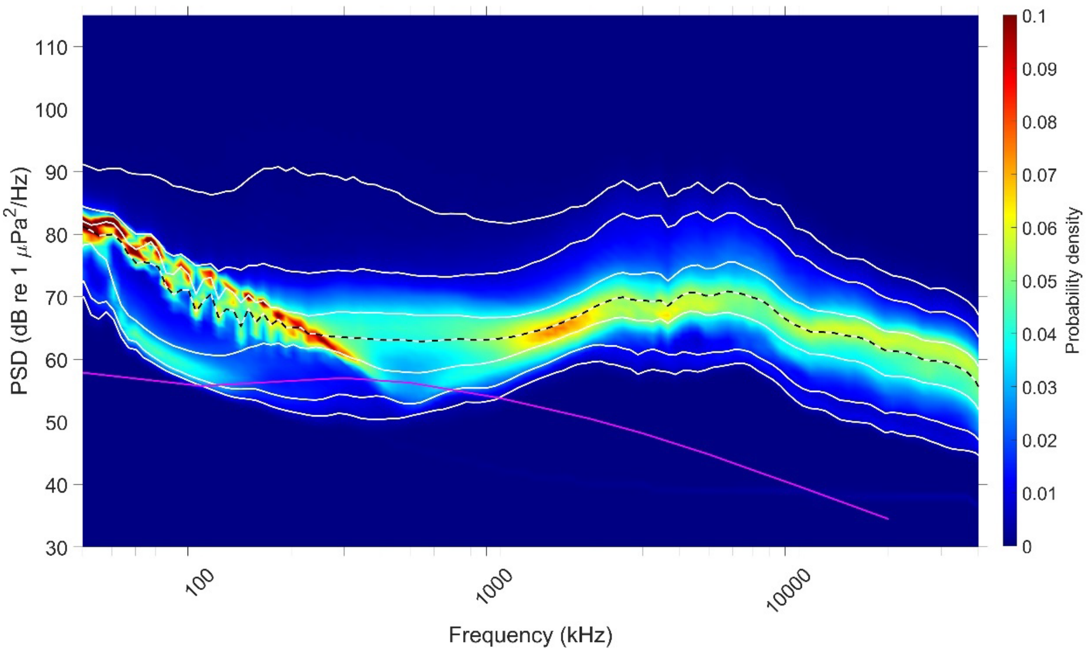

Figure 23. PSD percentiles (1, 5, 25, 75, 95, and 99% shown as white lines; 50% shown as a dashed white-black line) computed over and probability density of PSD levels (shown in colour) for Site 9 (Owen Anchorage). Pink line is the Cato model of underwater noise at a wind speed of 5 kn.

4.1.2 Soundscape spatial variation

Comparison of the PSD between sites at the 5%, 50%, and 95% percentiles is shown in Figure 23. The median level at the South Basin (Site 6) was the highest at frequencies less than 1 kHz, except for a 50 Hz tone at Kwinana South (Site 7, Figure 24). The shallow waters were on average the highest at frequencies greater than 1 kHz, in particular Kwinana Shelf North (Site 8) and Owen Anchorage (Site 9, Figure 25). Even at their quietest (i.e., at 5%), North Channel (Site 1) and Inside Rock (Site 2) were noisier than average/ambient noise across all frequencies, and Mangles Bay (Site 5) and South Basin (Site 6) for frequencies less than 500 Hz. On average, North Basin (Site 3) was the quietest below 100 Hz, Kwinana North (Site 8) between 100 and 500 Hz, and Mangles Bay (Site 5) above 500 Hz. At the 95% level, representing the “loudest” (i.e., highest levels) times, North Channel (Site 1) and Owen Anchorage (Site 9) (outside Cockburn Sound) were the highest for frequencies greater than 2 kHz, and North Channel (Site 1) and Inside Rock (Site 2) both showed a “notch” for frequencies between 200 Hz and 1000 Hz, likely due to propagation effects in the seabed between those recorders and the shipping lanes, which are dominant sources of noise at those frequencies. Below 100 Hz, South Basin (Site 6) was the loudest, possibly due to its proximity to the Kwinana Grain Terminal, with Sites 7, 8, 9 (all in shallower water) among the quietest, except for a 50 Hz tone at Site 7.

Correlation coefficients that were larger than 0.6 between pairs of sites, calculated for each OTO band and for broadband levels, are summarised in Table 34 (Appendix) and visualised in Figure 25. There was no correlation in the daily broadband levels between sites, except a slight negative correlation (-0.59) between Site 5 and 7 during Deployment 3. However, there were correlations greater than 0.6 between sites at various OTO bands, and these correlations were used to create the schematic in Figure 25, depicting the spatial correlation in soundscape in the study area. The shallow water sites (1, 2, 7, 8, and 9) were positively correlated, predominately at frequencies greater than 1 kHz. In addition, Sites 1 and 2 were correlated at 203 Hz (Deployment 1), Sites 2 and 9 were correlated at 100 Hz (Deployment 1), and Sites 7 and 8 were correlated at 50 Hz (Deployment 3). Site 4 was the only deeper-water site where the levels were correlated with other sites, namely, a positive correlation with Site 7 between 4 and 13 kHz (Deployment 2), and negative correlations with Site 1 above 6.5 kHz, and Site 2 above 16 kHz in Deployments 2 and 3.

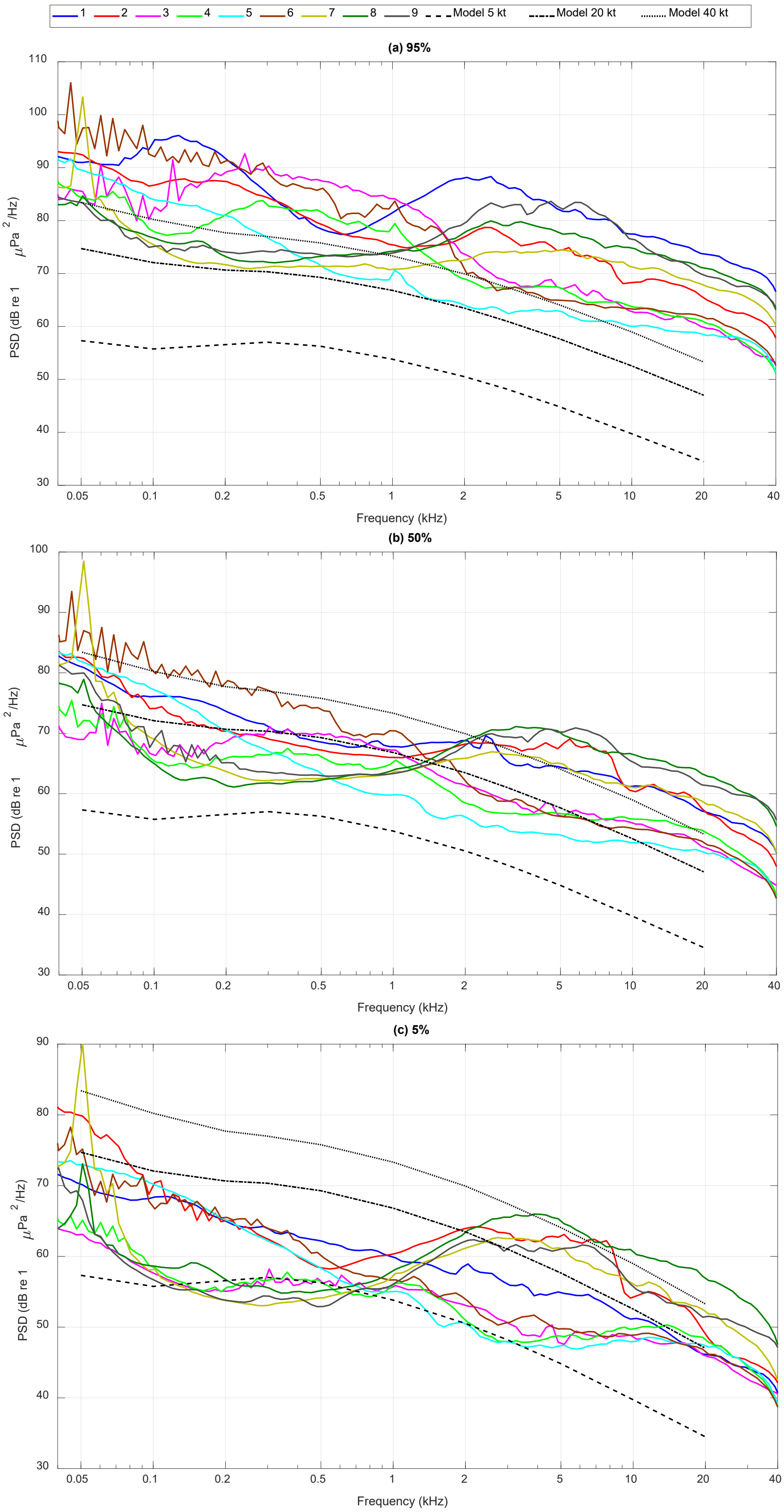

Figure 24. PSD plots at (a) 95%, (b) 50, and (c)5% for all sites with Cato wind model at 5, 20, and 40 knots.

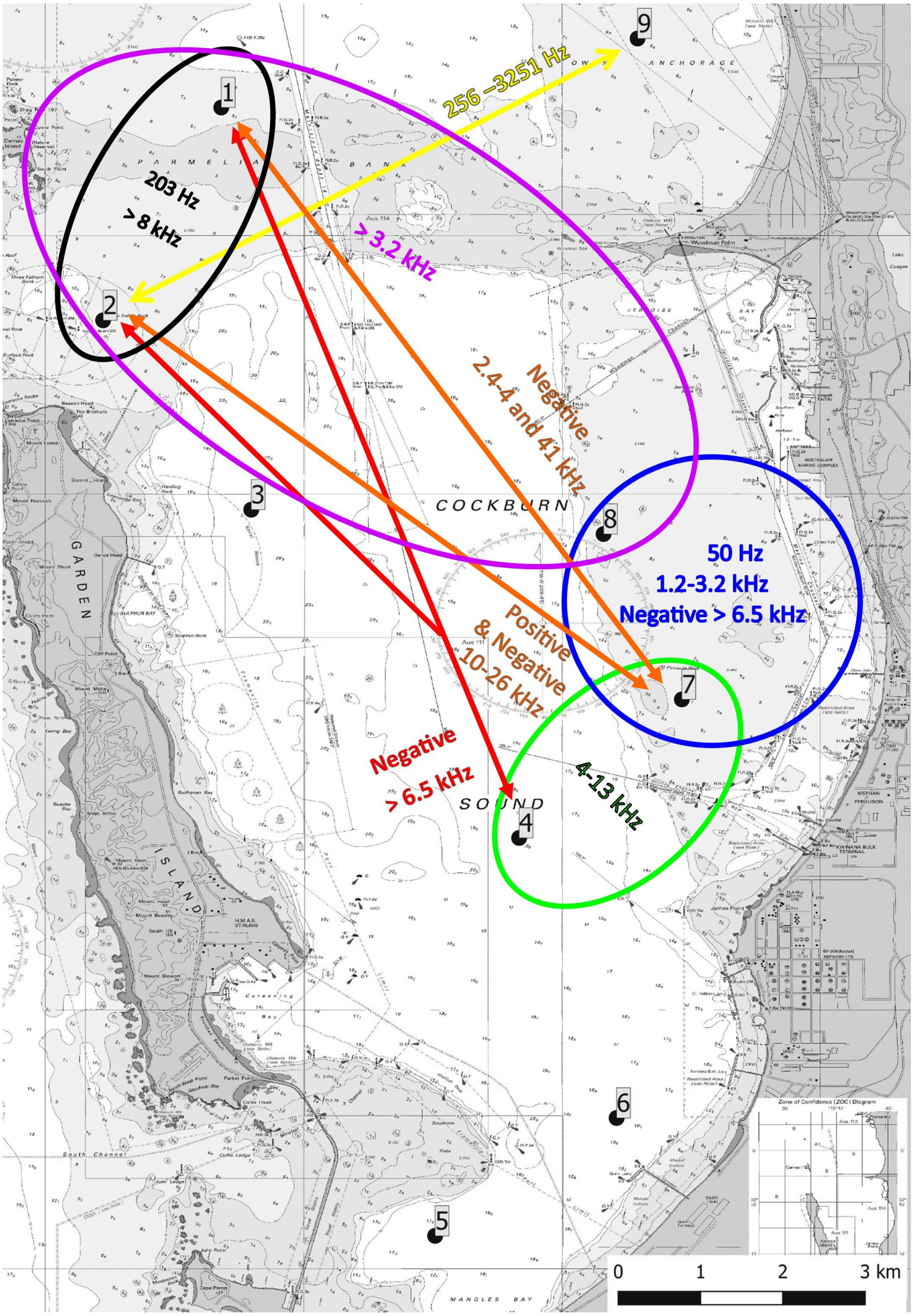

Figure 25. Soundscape spatial correlation between sites overlaid on a chart of Cockburn Sound. Coloured ellipses and arrows connect sites that had strong correlation in daily octave band levels, e.g. Sites 1 and 2 were correlated in sound levels at 203 Hz and above 8 kHz (black ellipse), Site 4 was negatively correlated with Site 1 and 2 at frequencies > 6.5 kHz (red arrows).

4.1.3 Soundscape temporal variation

Temporal variation in soundscape between days was investigated using PCA of the mean daily variations in the OTO band levels. Figure 26 shows the percentage contribution of the different frequency bands to day-by-day variability in the soundscape, which was predominately at frequencies between 100 and 1000 Hz for most sites. Mangles Bay (Site 5) and Owen Anchorage (Site 9) had slightly more contribution to the soundscape temporal variation from frequencies above 2000 Hz than the other sites (Figure 26).

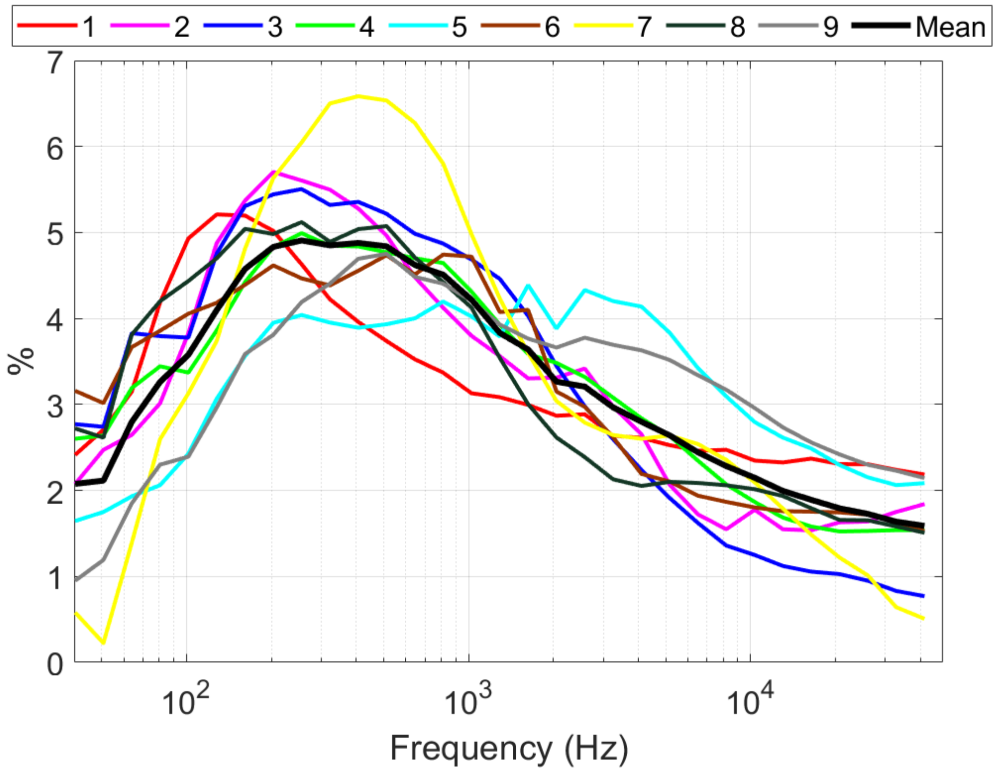

Figure 26. Percentage contribution of the OTO bands to the temporal variation in the soundscape.

Figure 27 is a plot of the difference between OTO band levels between day and night at each site for each deployment. All sites except Mangles Bay (Site 5) and South Basin (Site 6) had significantly higher levels on average during the day than night, predominantly at frequencies between 100 and 1000 Hz (Figure 27). The diurnal effect was likely due to anthropophony sources, e.g., vessels and machinery, which tend to operate at a higher duty cycle during daylight hours, and is explored in detail in Section 4.1.3. Only North Channel (Site 1) and the Kwinana Shelf (Sites 7 and 8) had significantly higher levels at night, and these were predominantly at frequencies greater than 10 kHz, mostly due to increased activity in snapping shrimp noise (Figure 27), which is investigated more in Section 4.1.6.

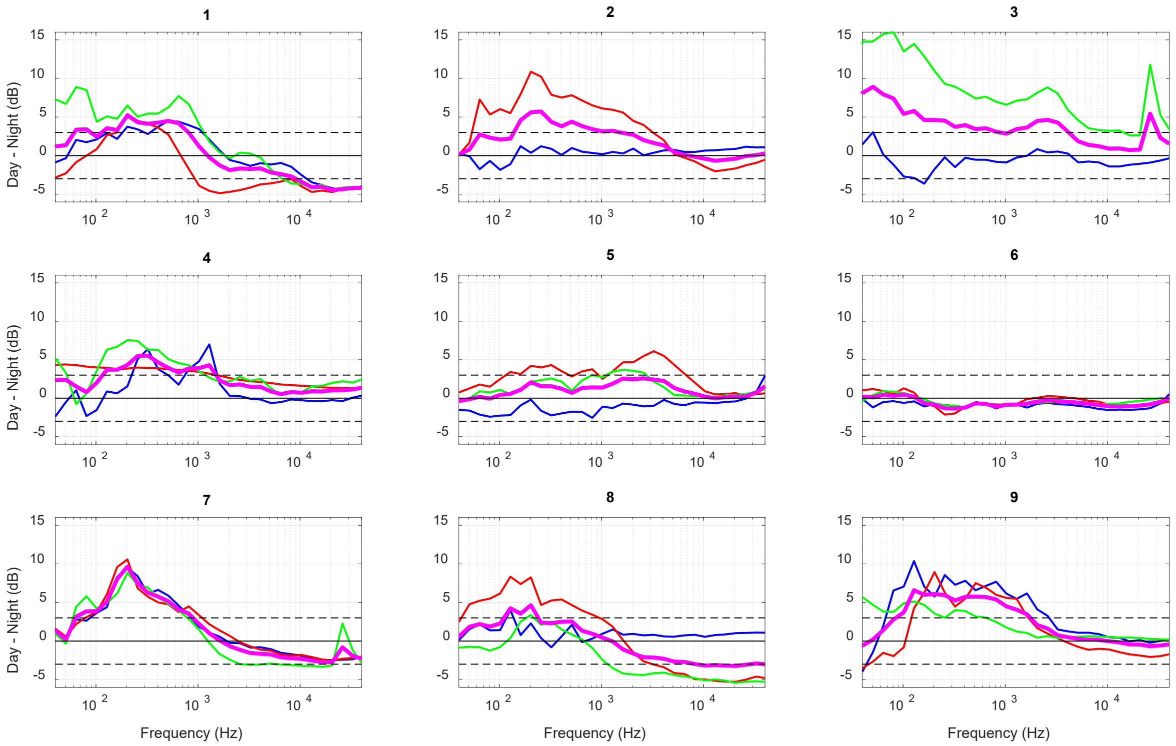

Figure 27. Diurnal variation in soundscape: mean day-time PSD minus night-time PSD for Sites 1-9 for deployments 1 (blue), 2 (red), and 3 (green) and mean (magenta). Dashed black lines are +/- 3 dB.

4.1.4 Geophony

The main contribution of geophony to the underwater soundscape of Cockburn Sound was wind. There was a strong correlation between the hourly wind speed measured at Garden Island and the sound levels recorded at Sites 1, 3, 5, 7, 8, and 9 (Table 7). Example correlations are shown for Mangles Bay (Site 5, Figure 28) and Kwinana Shelf South (Site 7, Figure 29). The correlation of sound levels with wind was typically stronger at night than during the day (Figure 28, Figure 29), most likely due to the reduced noise from vessels in the same band. Correlation was more apparent at wind speeds above 10 kn (Figure 28, Figure 29). Sound levels at all shallow water sites except Inside Rock (Site 2), were correlated with wind speed, and mainly between 323-813 Hz (Table 7), and in some instances the measurements compared well to the Cato wind model (Figure 29). Sites 3 and 5 were correlated with wind speed at a higher frequencies than the shallower sites, predominately 2048-6502 Hz (Table 7), however these data did not compare well with the Cato wind model (Figure 28). Sites 3 and 5 are both significantly sheltered from westerly winds by their locations just east of Garden Island and Mangles Bay.

Rain noise was not a significant component of the underwater soundscape during the deployment period, mainly due to masking by snapping shrimp noise (Section 4.1.6).

Table 7. Sites and the frequency bands that correlated with wind speed data from Garden Island.

Site	Frequency bands (Hz) with a correlation higher than 0.6 with wind speed	Frequency band with max correlation with wind speed (Hz)
1	323-1290	512
2	No correlation	
3	2048-6502	4096
4	No correlation	
5	813, 1290-6502	3251
6	No correlation	
7	323-1024	406
8	40-813	161
9	813	813

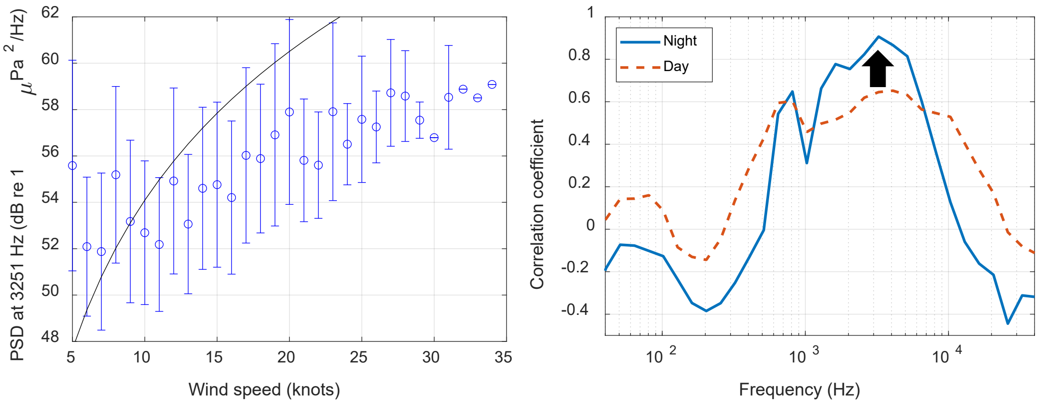

Figure 28. Correlation of sound levels with wind at Site 5 (deployment 2): mean (+/- 1 S.D.) PSD at 3251 Hz (at night) vs wind speed (left), with Cato model plotted in black; and correlation coefficient of wind speed (>5 knots) vs PSD at each octave band (right). The frequency of highest correlation is indicated with a black arrow on the right-hand panel.

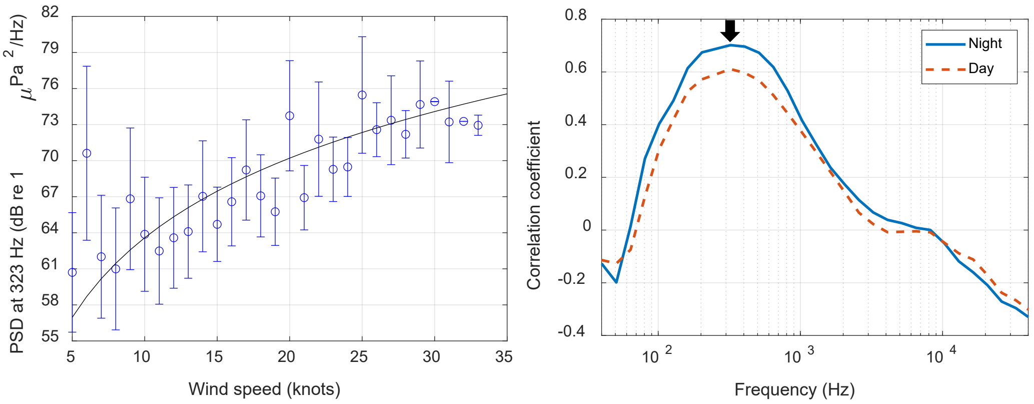

Figure 29. Correlation of sound levels with wind at Site 7 (deployment 2): mean (+/- 1 S.D.) PSD at 323 Hz (at night) vs wind speed (left), with Cato model plotted in black; and correlation coefficient of wind speed (>5 knots) vs PSD at each octave band (right). The frequency of highest correlation is indicated with a black arrow on the right-hand panel.

4.1.5 Anthropophony

Anthropophony was a major contribution to the underwater soundscape in Cockburn Sound, particularly between 40 and 1000 Hz. At most sites, anthropophony was louder during the day than night (Figure 27), except Mangles Bay (Site 5) and South Basin (Site 6) which were relatively uniform between day and night (Figure 27). The main anthropogenic sound source was vessels, which was typically broadband, and when moving close by a recorder would create a “bathtub” interference pattern in the spectrogram (Figure 30). Detailed analysis of frequency signatures and source level are the focus of Section 4.2. In addition to vessels underway, docked or moored vessels, as well as machinery operated on nearby jetties or at anchor, such as at South Basin (Site 6) (Figure 31), were significant sources of noise. Other anthropophony recorded included those made by equipment operated from vessels, such as sound pulses transmitted by echosounders (Figure 32), sub-bottom profilers (Figure 33), and air guns (Figure 12), but due to their short duration these were not significant contributions to the overall soundscape. Occasionally, marine-based pile driving was recorded (Figure 34).

Cockburn Sound is a high-loss environment (Section 4.3), therefore most vessels could not be heard directly through the water column beyond 2 km. Sound pulses from echosounders and sub-bottom profilers had to be even closer to a recorder to be detected above the ambient noise. Consequently, it is important to consider the vessel activity near the recorder locations. Figure 35 is a heatmap of the mean AIS vessel location reports per week in Cockburn Sound during Deployments 2 and 3. Note that AIS is only required by regulated vessels, and not mandatory for recreational and small commercial vessels, so it does not capture all vessel activity. Nevertheless, all sites showed a correlation between the number of AIS vessels and some mean OTO band levels, except at North Basin (Site 3) and Central Basin (Site 4). Example correlations between sound levels and the number of AIS vessels for Sites 1, 5 and 6 are shown in Figure 36 to Figure 38. At these sites, there was a strong correlation of the number of vessels underway and sound from 100 to 2000 Hz. At South Basin (Site 6), the correlation is even stronger and over a wider band width when all vessels are considered, i.e., including ones that are docked.

There was an unidentified anthropophony sound at Kwinana Shelf South (Site 7), which was an almost constant 50 Hz tone. This 50 Hz tone at Site 7 varied in level with time of year (Figure 39). At the start of Deployment 1 (October-November 2022) the daily mean was between 87 to 91 re 1 $\mu Pa^2/Hz$, and then increased over the summer and reached a peak of just over 98 dB re 1 $\mu Pa^2/Hz$ between 8 August and 11 September 2023, before decreasing to below 84 re 1 $\mu Pa^2/Hz$ at the end of 2023. This 50 Hz tone was also seen at a lower sound level at Kwinana Shelf North (Site 8) in Deployment 1 (Figure 21). A well-known source of a 50 Hz tone is a mains power source, but there were no obvious electrical sources close to Sites 7 and/or 8.

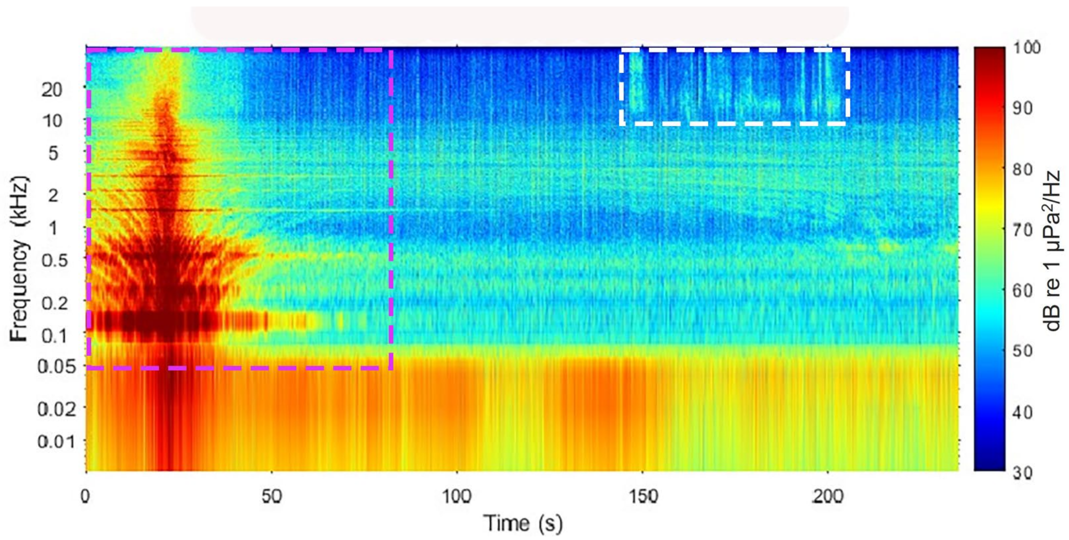

Figure 30. Spectrogram of passing vessel (magenta dashed box) and dolphin echolocation (white dotted box).

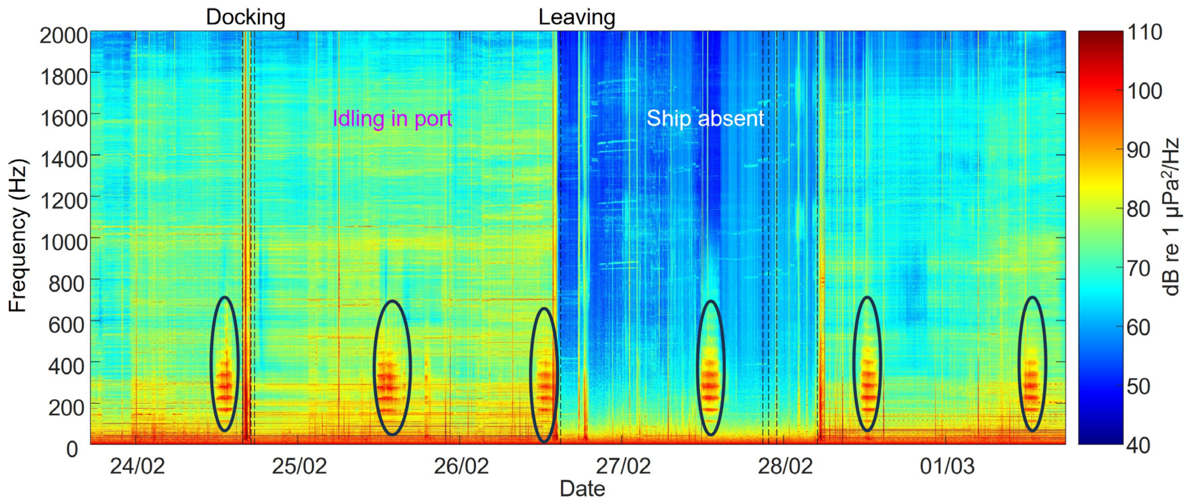

Figure 31. Spectrogram of vessels docking, idling and leaving port, as well as fish choruses (black ellipses) at Site 6 between 24th February and 1st March 2023.

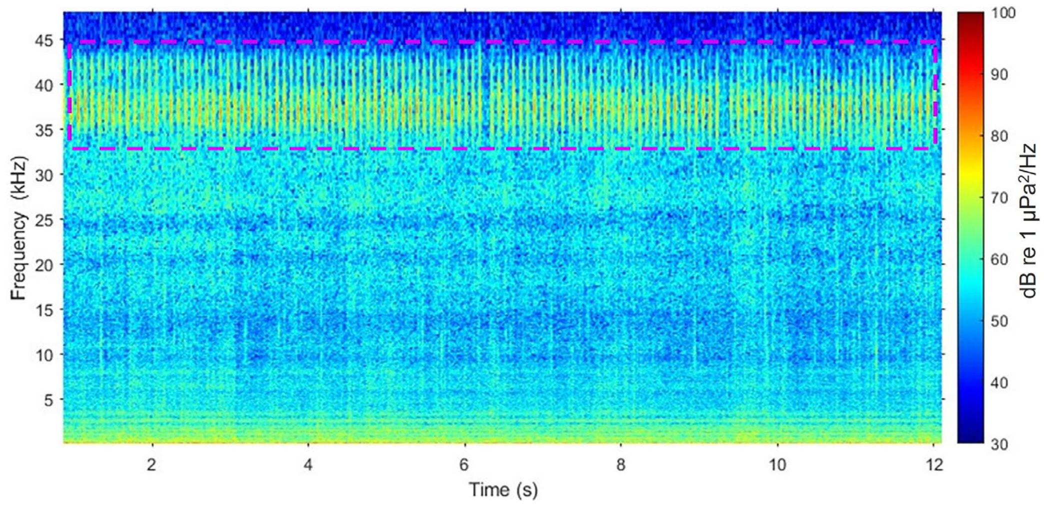

Figure 32. Spectrogram of echosounder pulses (magenta dashed box).

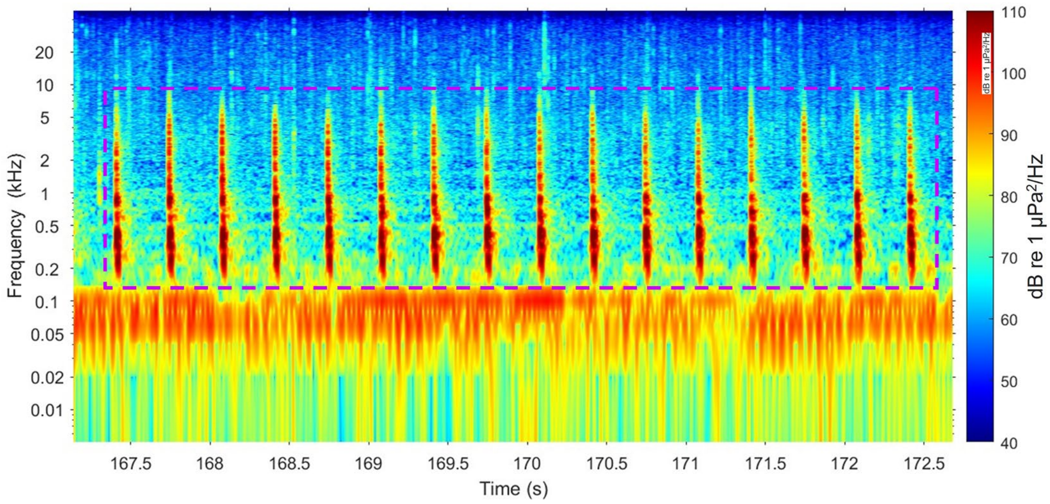

Figure 33. Spectrogram of sub-bottom profiler pulses (magenta dashed box) recorded within 100 m of Site 7.

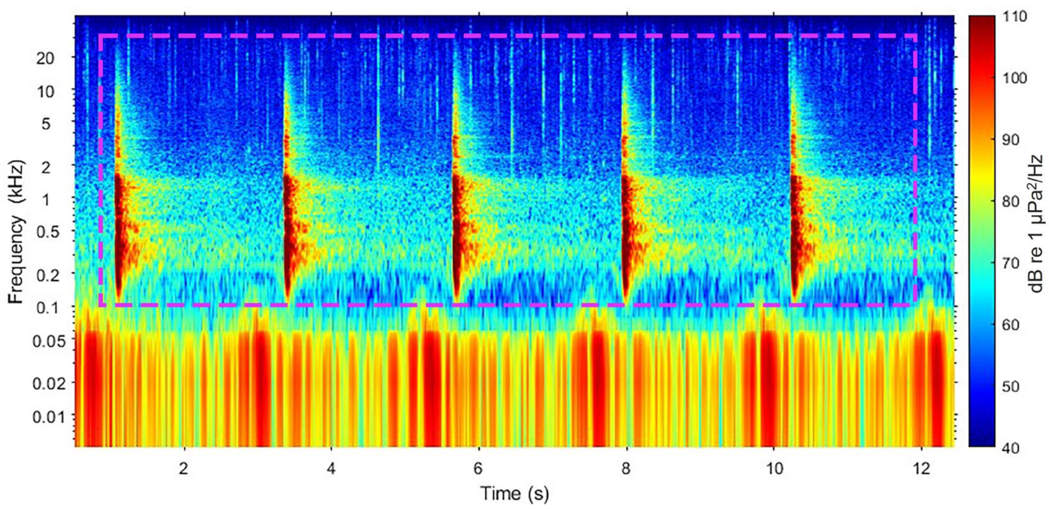

Figure 34. Spectrogram of pulses from impact pile driving (magenta dashed box) carried out off the southeast coast of Garden Island recorded at Site 4.

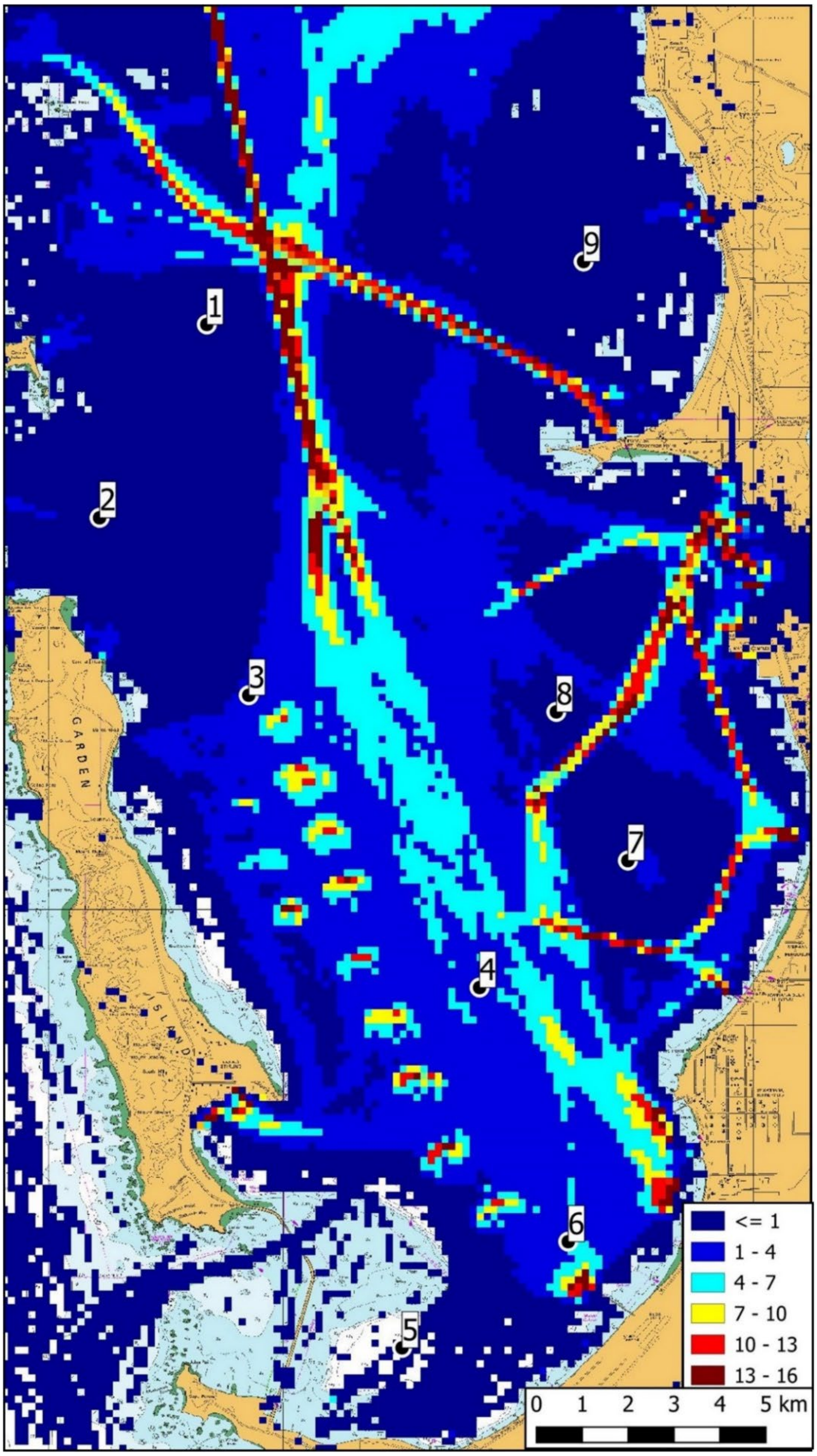

Figure 35. Mean number (colour axis) of all AIS vessels per week 8th February – 31 December 2023 (cell size 94 x 111 m), with the locations of the underwater sound recorders (Sites 1-9), over nautical chart AUS117.

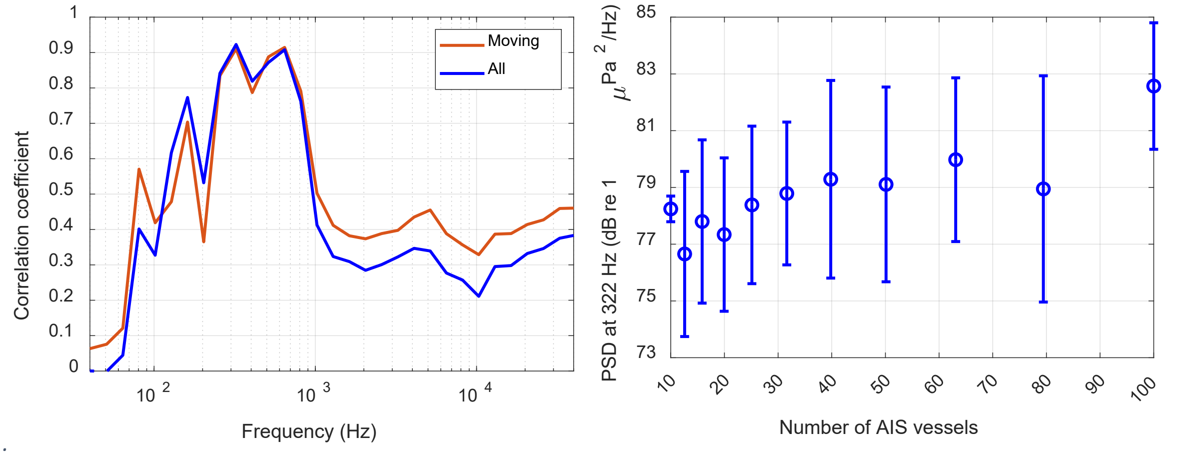

Figure 36. Correlation of number of AIS vessels within 6 km of Site 1 versus mean: OTO band levels (left), and PSD at 322 Hz (+/- 1 S.D.) (right).

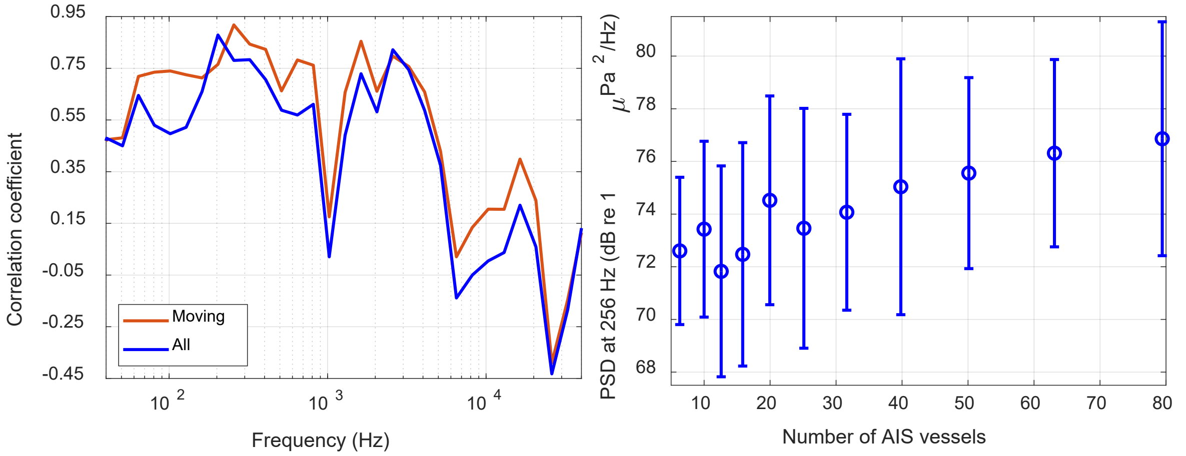

Figure 37. Correlation of number of AIS vessels within 6 km of Site 5 versus mean: OTO band levels (left), and PSD at 256 Hz (+/- 1 S.D.) (right).

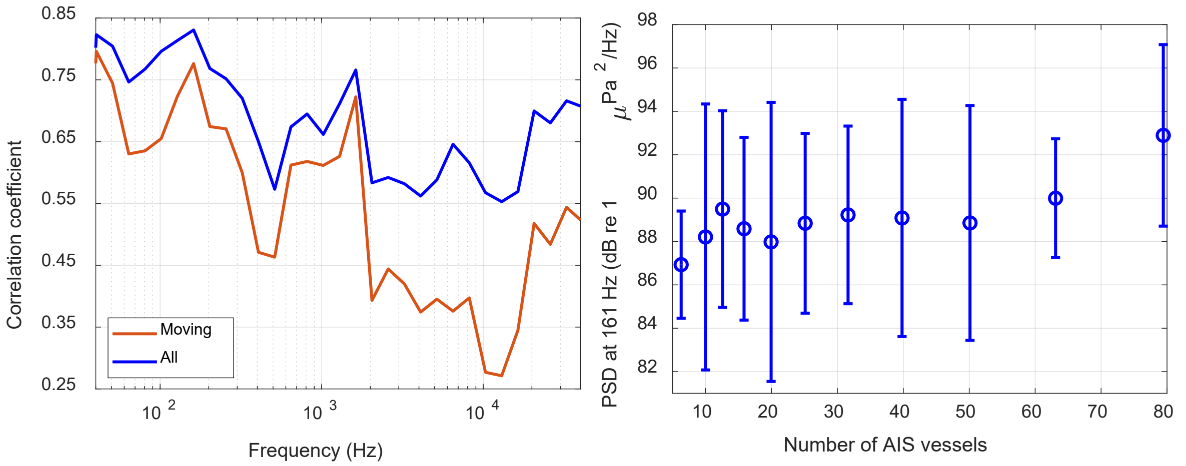

Figure 38. Correlation of number of AIS vessels within 4 km of Site 6 versus mean: OTO band levels (left), and PSD at 161 Hz (+/- 1 S.D.) (right).

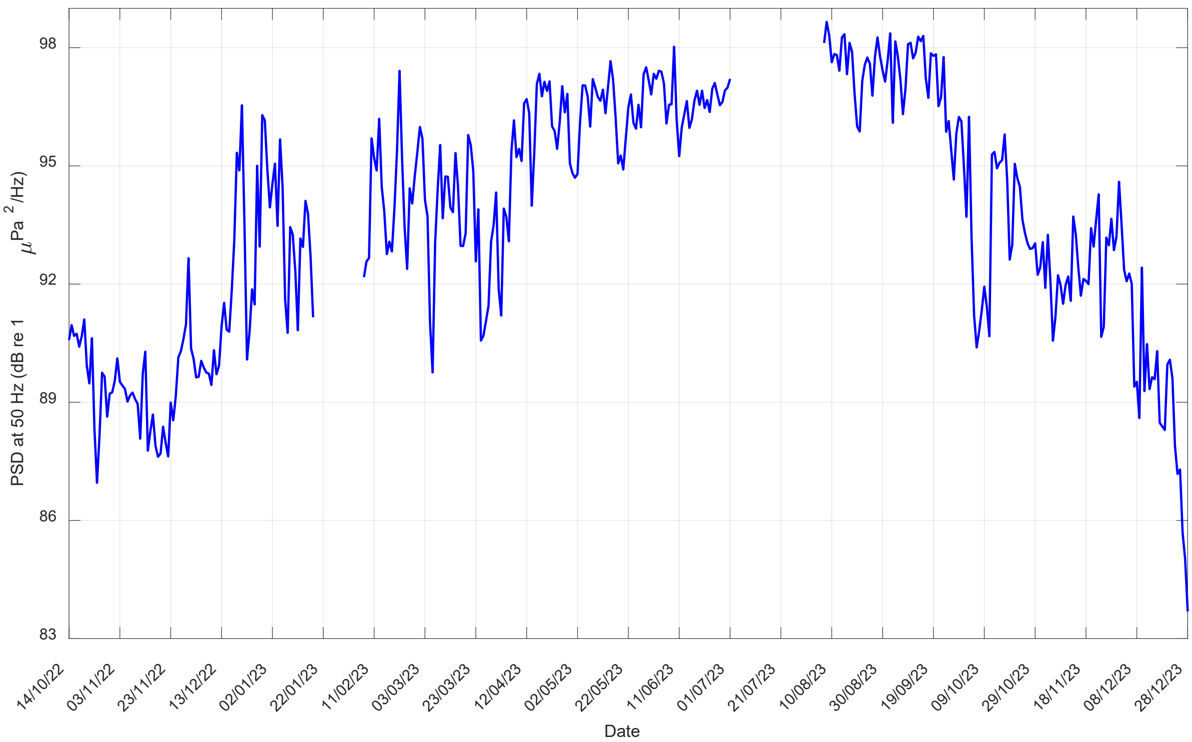

Figure 39. Daily mean PSD 50 Hz at Site 7.

4.1.6 Biophony

There were three main contributions to the biophony that were detected in the underwater soundscape of Cockburn Sound: dolphins, fish, and snapping shrimp.

Dolphins: Dolphin sounds were detected at all sites. Dolphin sounds that were recorded around Cockburn Sound, included echolocation clicks and buzzes (Figure 40), and whistles (Figure 41). The dolphin sounds detected were similar to those recorded from Indo-Pacific bottlenose dolphins (*Tursiops aduncus*) in the nearby Fremantle Inner Harbour (Ward et al. 2016). Finer temporal scale analysis of North Channel (Site 1), Mangles Bay (Site 5), and the Kwinana Shelf (Sites 7 and 8), found that dolphin sounds were detected in every season at these sites, and the sites on the Kwinana Shelf (Sites 7 and 8) were more acoustically active than other site. Whistles were challenging to detect, due to masking by vessels and other anthropogenic sources (between 1 and 20 kHz). Although echolocation clicks overlapped with snapping shrimp clicks, they were easier to detect than whistles as they had some separation in their peak frequencies.

Fish: Fish sounds were detected at all sites, except Kwinana Shelf South (Site 7) and Owen Anchorage (Site 9). Figure 42 shows spectrograms of some the fish sounds recorded. All the fish sounds that were detected sounded alike and looked similar on the spectrograms. Most of the energy was between 100 Hz and 500 Hz, and individual sounds were typically about 1 s in duration (Figure 42). The fish sounds detected in Cockburn Sound have similar characteristics to ones made by mulloway (*Argyrosomus japonicus*), a vocal sciaenid known to frequent the nearby Swan River (Parsons et al. 2013). Fish choruses were recorded in the spring, summer, and autumn months at Inside Rock (Site 3), Central and South Basin (Sites 4 and 6), and none were detected in the winter. Figure 43 shows some examples in long-term spectrogram from these sites, where the chorus can be seen as an increase in levels at 200-500 Hz for a discrete period in the evenings. At Inside Rock (Site 3), a post-sunset fish chorus was detected most nights from 9 October 2022 to 19 January 2023 (after which the recorder was recovered). At Central Basin (Site 4), a post-sunset fish chorus was detected most nights between 27 March 2023 and 24 April 2023. At South Basin (Site 6), a post-sunset fish chorus was detected most nights from the start of Deployment 2 (8 February) to 5 April 2023. Some nights fish choruses were slightly masked by anthropogenic noise, but most of the time choruses were almost as loud as anthropogenic noise heard in those frequency bands (Figure 43).

Snapping shrimp: Snapping shrimp (*Alpheidae* species) were prominent in underwater sound above 1 kHz at most sites, particularly at the shallow-water sites (1, 2, 7, 8, and 9). Some sites had a diurnal pattern with snapping shrimp louder at night, e.g., Sites 1, 7, and 8 (Figure 25). Figure 41 shows long-term spectrograms from spring and summer 2022 and autumn 2023 from North Channel (Site 1). The increase in snapping shrimp noise at night can be seen in Figure 41 (i.e., increased sound at frequencies above 1 kHz), and the level increased from September 2022 to March 2023. Previous studies have found there can be a correlation between snapping shrimp acoustic activity and water temperature (Bohnenstiehl et al. 2016, Monczak et al. 2019). To investigate this possible correlation, the mean sound pressure level between 20 and 48 kHz was calculated for each deployment night (this frequency range was chosen to avoid influence from other sources, e.g., vessels) and plotted as time series with sea surface temperature in Figure 42. At Site 1, there was a slight offset between the dates of the peaks of the two data (21 days), but there was strong correlation between SPL (20-48 kHz) and sea surface temperature (R = 0.81), in particular for the first two deployments (Figure 42). The same correlation was not found at other sites.

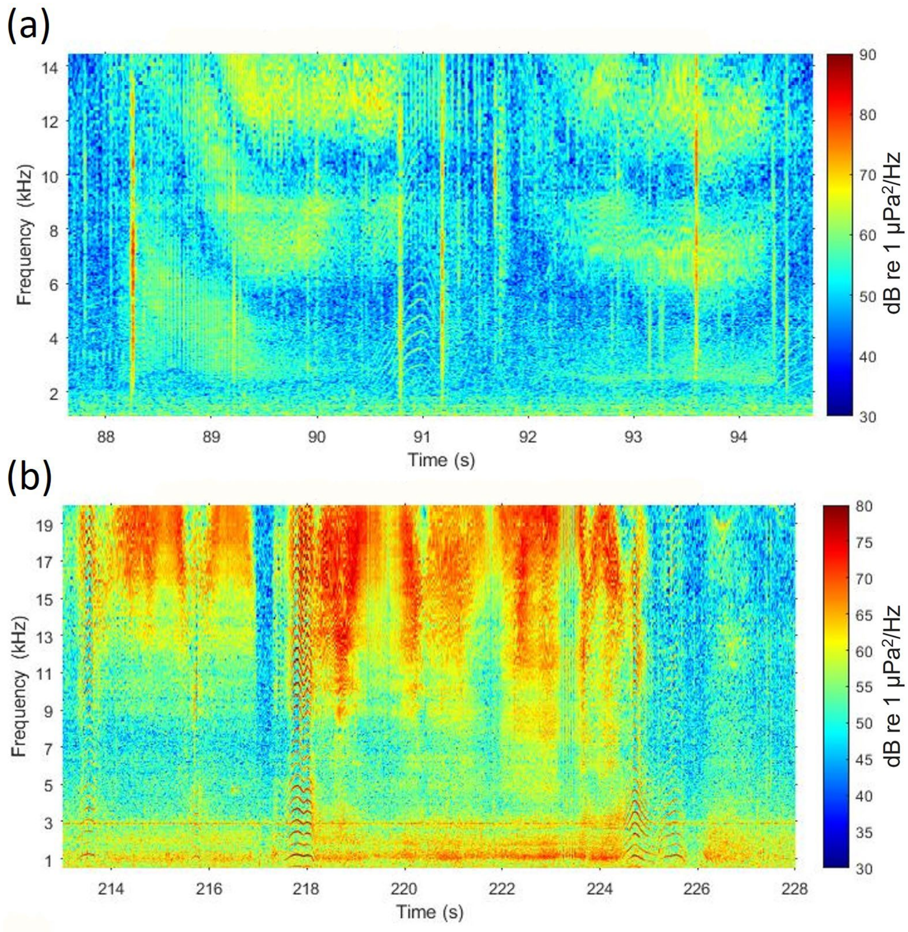

Figure 40. Spectrograms of dolphin clicks and buzzes recorded at (a) Site 4 and (b) Site 5.

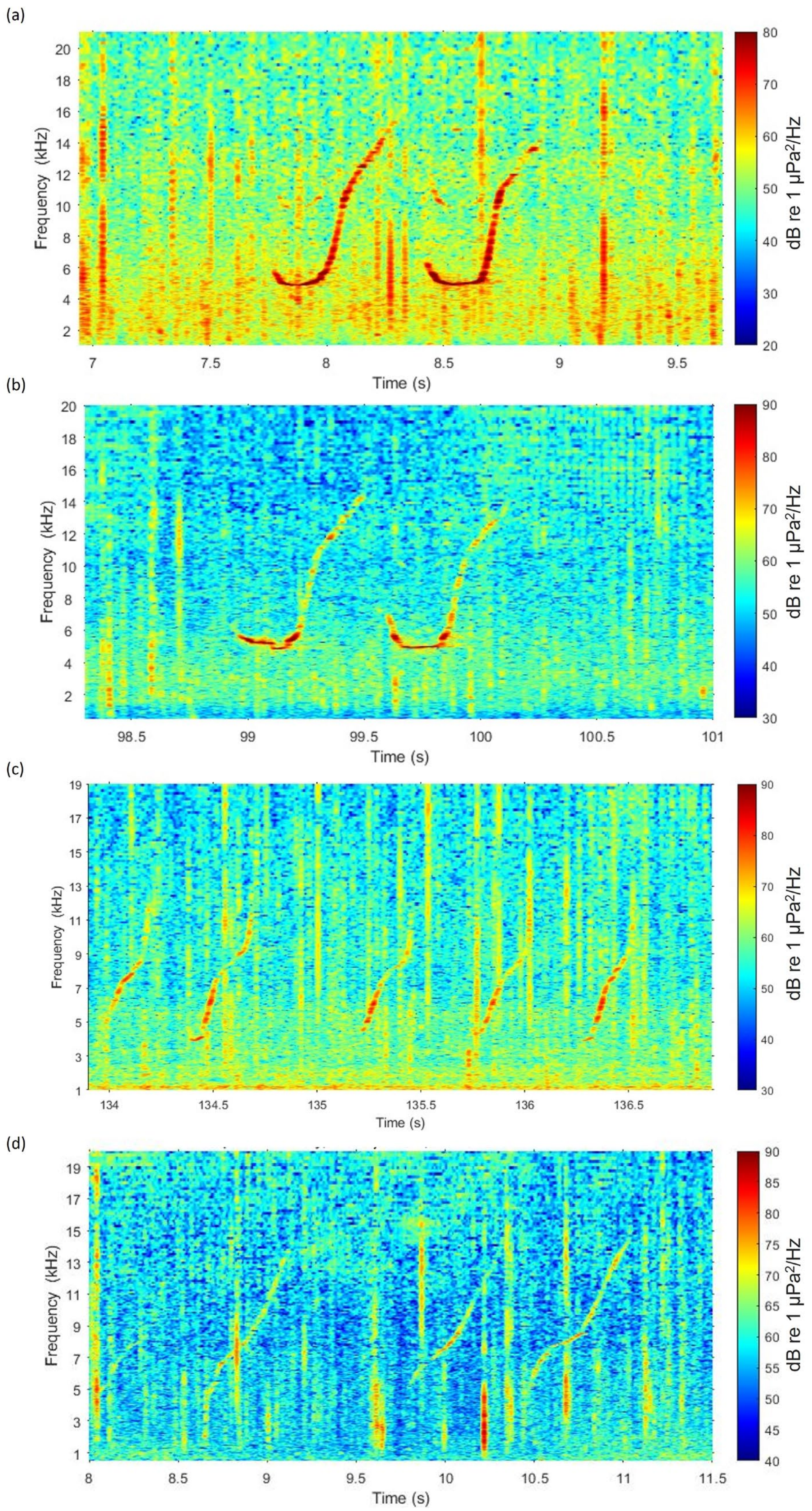

Figure 41. Possible signature whistles from Site 7 (a)-(c) and Site 8 (d).

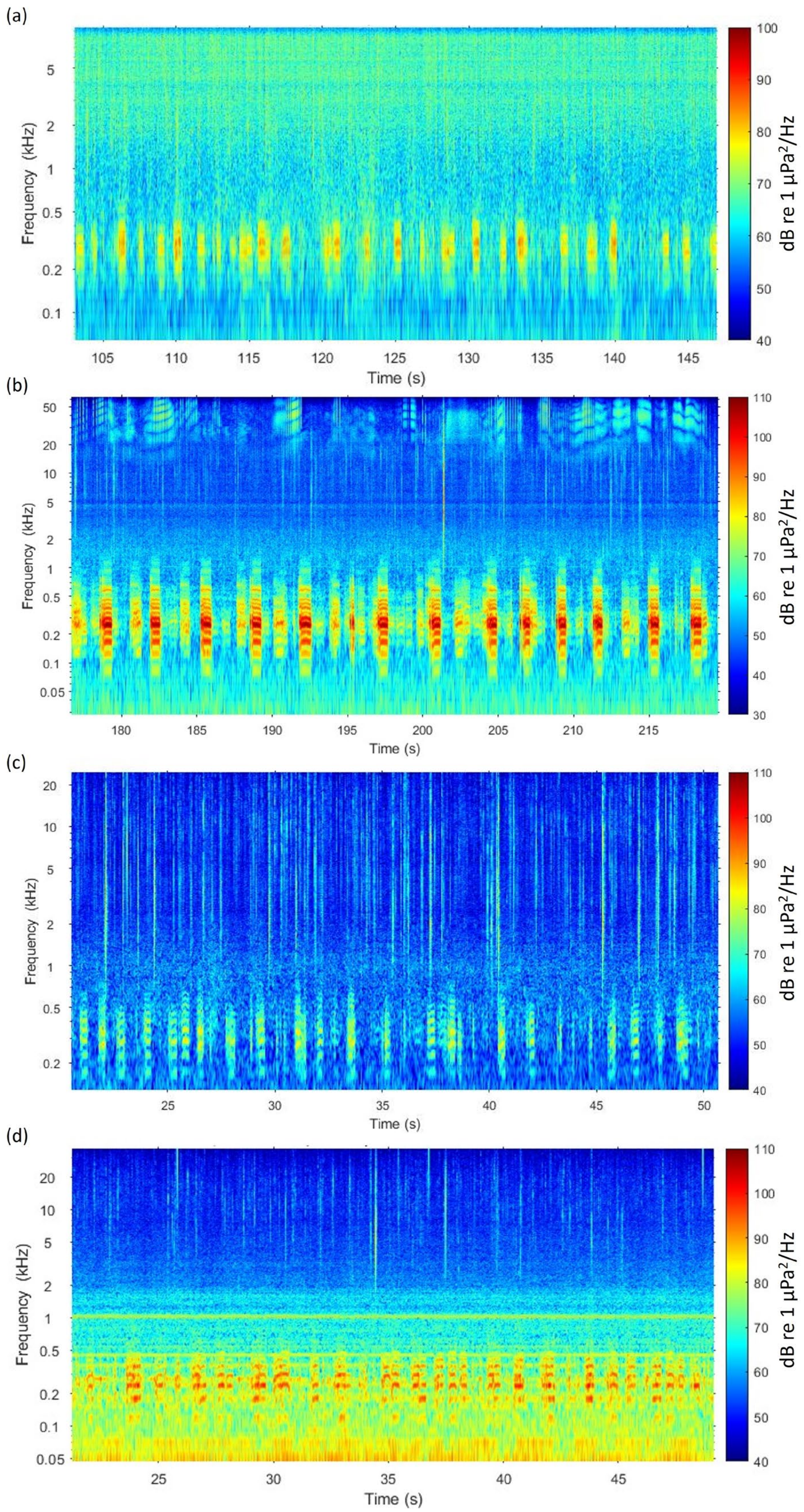

Figure 42. Spectrograms of fish sounds (100-500 Hz) recorded at (a) Site 2, (b) Site 3, (c) Site 4, and (d) Site 6.

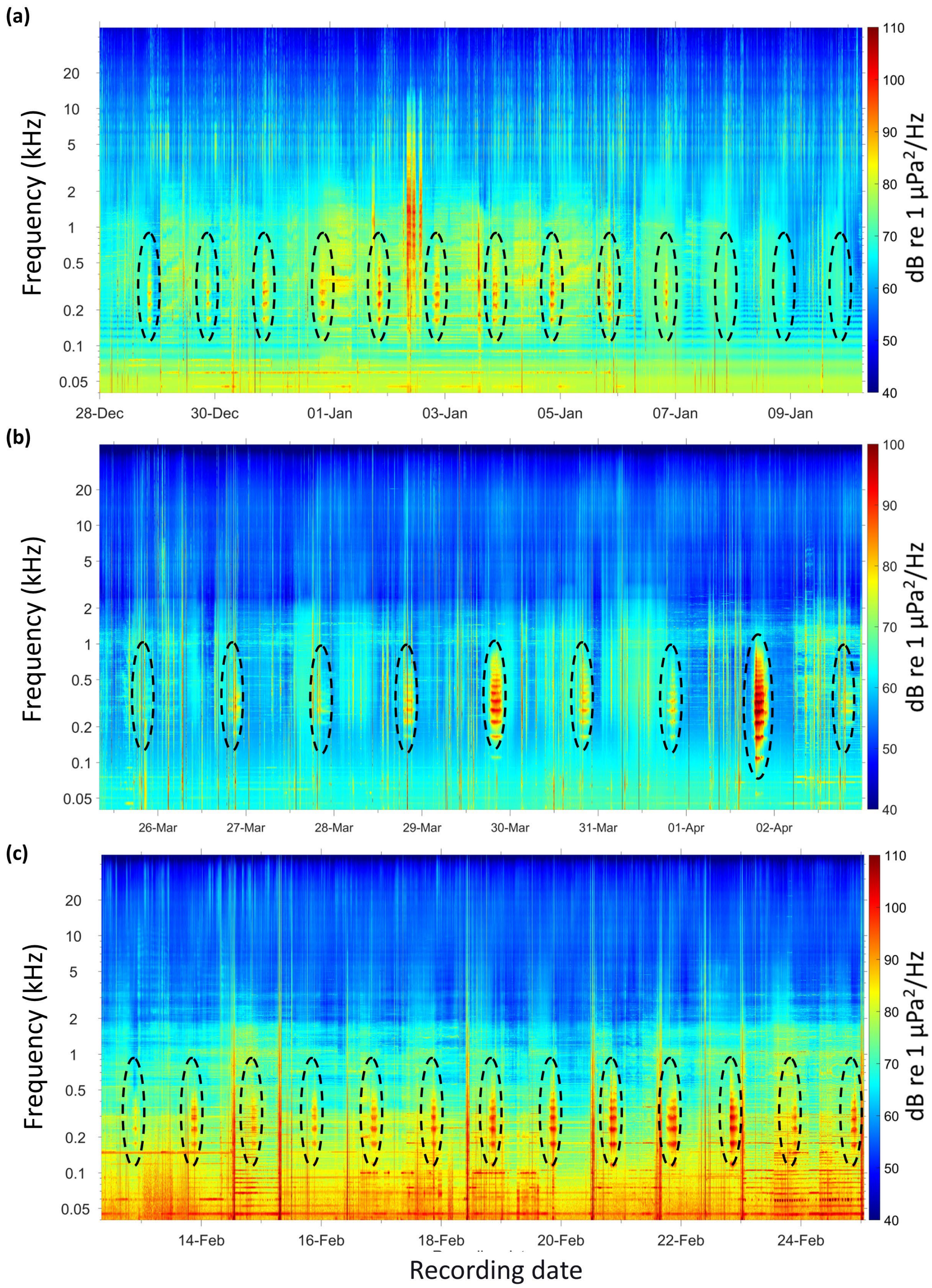

Figure 43. Fish Choruses (black ellipses) seen in long term spectrograms from (a) Site 3, (b) Site 4, and (c) Site 6.

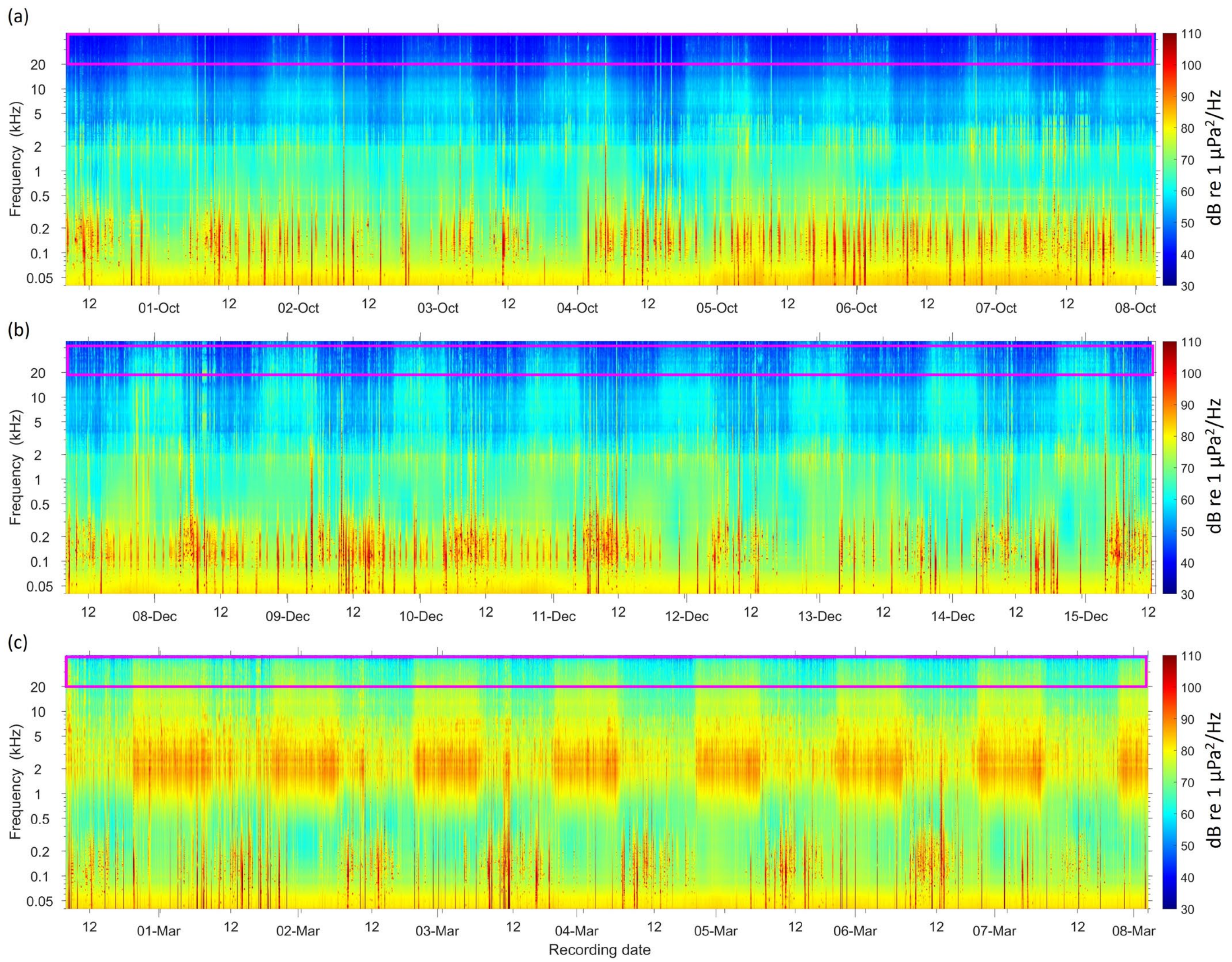

Figure 44. Long-term spectrograms from Site 1 indicating the increase in snapping shrimp noise at night: (a) 1-8 October 2022, (b) 8-15 December 2022, and (c) 1-8 March 2023. Pink rectangle indicating 20-36 kHz frequency band.

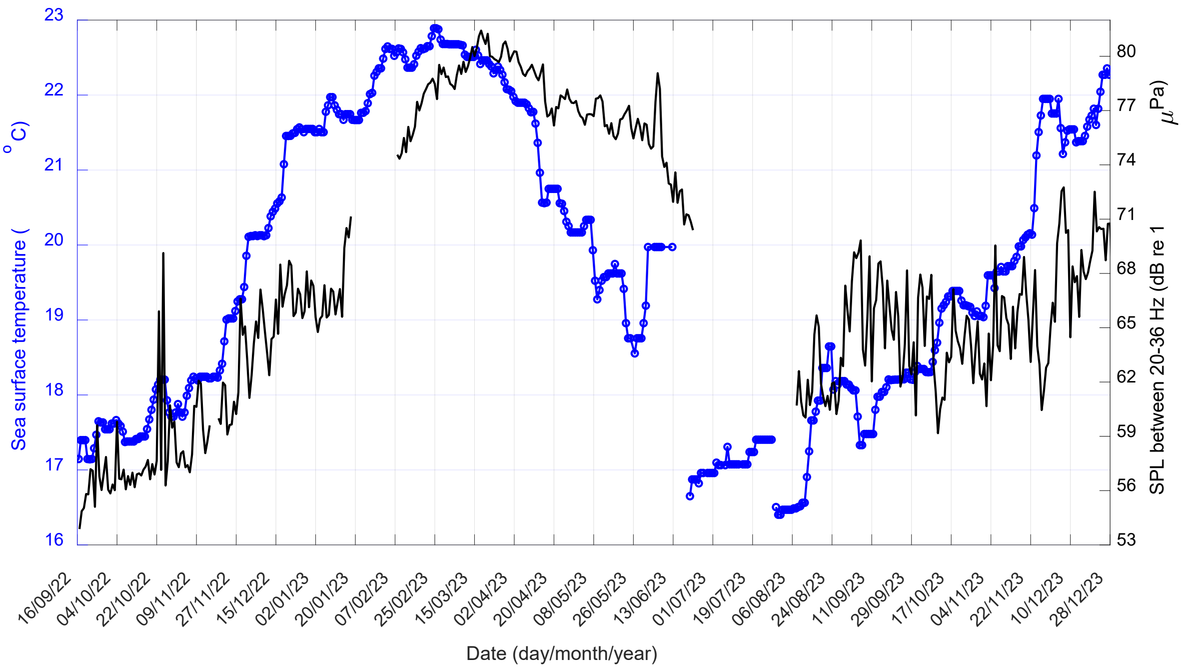

Figure 45. Temporal comparison between mean sound pressure level between 20 and 48 kHz for each night, and sea surface temperature from Cockburn Sound.

4.2 Noise source signatures

Vessels of every class co-exist in Cockburn Sound, ranging in length from a few metres to hundreds of metres, including personal watercraft, small boats including pilot boats, ferries, tugs, navy ships, and the largest ships such as tankers, bulk carriers, and container ships. In order to associate acoustic recordings to a specific vessel, it was necessary to know the vessel's position; however only vessels over a certain size[1] and passenger vessels of any size are legally required to have AIS systems (International Maritime Organization (IMO) 2015). Therefore, the focus of the measurements described in this report is limited to vessels commonly found in Cockburn Sound whose position was recorded on AIS. Measurements of received level for individual ships were converted ship source level for four classes of ship (bulk carriers, tankers, tugs, and pilot boats) that are commonly found in Cockburn Sound. In addition, the combined noise arising from port operations at the Kwinana Grain Terminal was measured and its source level estimated.

4.2.1 New measurements of vessel noise source spectra in Cockburn Sound

Vessel speed distribution

Vessel speed is one of the primary drivers of vessel noise, and "speed over ground" (SOG) is one of the fields included in an AIS report. Depending on currents, SOG may not be a perfect proxy for the engine state which will be determined by the vessel's speed through water; however, being readily available from the AIS reports, it is a useful metric to assess the observed spread in vessel speeds. Figure 46 is a histogram of speeds observed during the measurements made on the four vessel classes. Bulk carriers and tankers had relatively consistent speeds around 10-11 kn, while the tugs were typically moving at 11 kn or less, and often less than 5 kn, and the pilot boat was generally moving faster than 10 kn and most commonly 20-25 kn.

[1] All ships over 300 gross tons engaged on international voyages, cargo ships over 500 gross tons not engaged on international voyages, and all passenger ships irrespective of size.

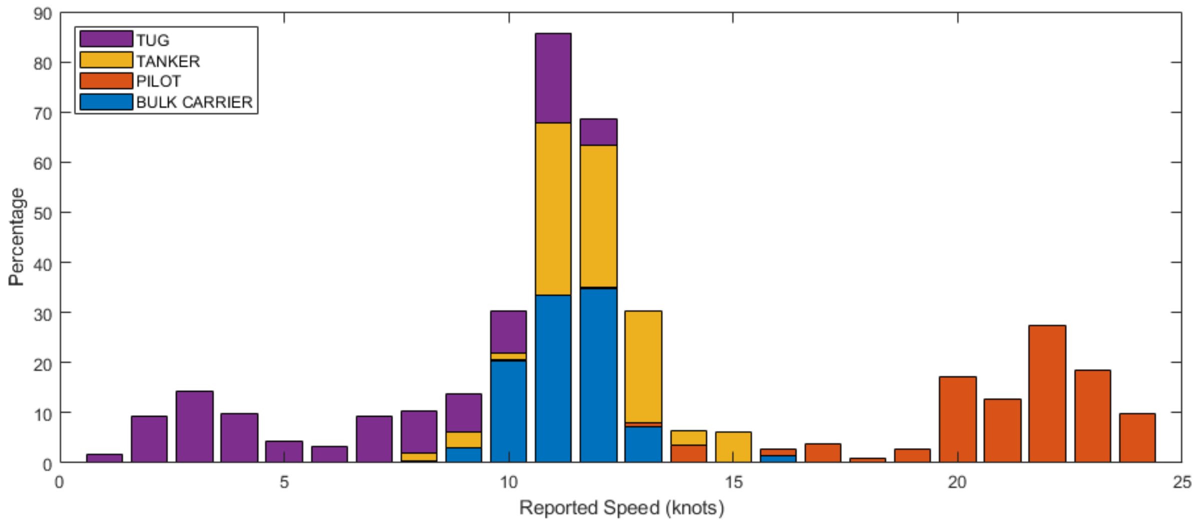

Figure 46. Histogram of speed over ground (SOG) as reported by AIS for four ship classes studied in this report: bulk carriers, pilot boats, tankers, and tugs.

Tankers and Bulk Carriers

Figure 47 is a map of the relative position of the recorders and ships for a representative single ship pass, the southbound bulk carrier RANGAKU on 10 September 2022 at 11:03:01. Colours for the range and bearing/aspect correspond to the plot lines in Figure 48. The bow aspect angle would be 0°, broadside or beam aspect would be 90°, and stern aspect would be 180°. In general, the aspect angle at t_0 is not necessarily the broadside aspect, nor is it necessarily the time of CPA to either recorder, because the ships were generally crossing the line at an angle.

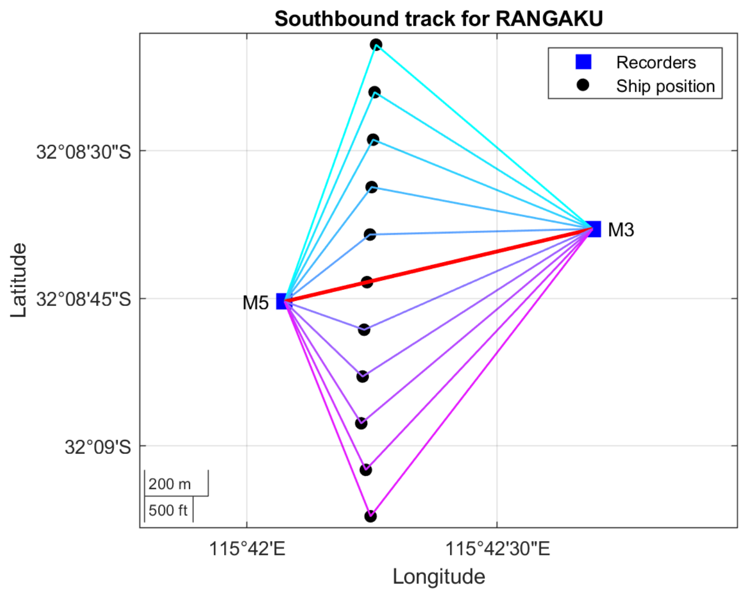

Figure 47. Position of recorders M3 and M5 (blue squares) and southbound bulk carrier RANGAKU (black circles), which crossed the line between M3 and M5 (t_0) on 10 September 2022 at 11:03:01. The straight-line path and relative aspect to each recorder is shown in shades of cyan/blue before t_0 and purple/magenta after t_0. Colours correspond to the plot lines in Figure 48.

Figure 48 is a plot of the OTO band received levels between 10 Hz and 10 kHz for the representative single ship pass that was plotted in Figure 47 (the southbound bulk carrier RANGAKU on 10 September 2022 at 11:03:01). The time and range window resulted in 11 samples at 30-s intervals, with aspect angles ranging from 52° to 136° from the port side at M3 (top plot in Figure 48) and 18° to 164° from the starboard side at M5 (bottom plot in Figure 48). The line colours for the OTO band levels change gradually from cyan at the lowest aspect angle to magenta at the highest aspect angle. The OTO band levels at the time t_0 when the ship crosses the line between M3 and M5 are plotted in red, and the noise floor plotted in black. The range R_0 at time t_0 (729 m to M3 and 266 m to M5) reflects the fact that the traffic separation scheme requires that southbound traffic pass closer to M5, while northbound traffic passes closer to M3.

The received level (Figure 48) is higher than the noise floor at most aspect angles for frequencies above 20 Hz. The highest level at both receivers is at the lowest aspect angle (closest to bow aspect), and the levels decrease with increasing aspect angle. There are minima in the t_0 PSD (red line) observed at M3 at 40-50 Hz and again at 100-200 Hz, while at M5 there is a less pronounced minimum between 100-200 Hz and none at 40-50 Hz, suggesting that there are differences in acoustic propagation in the seabed to the east and west of the traffic lanes (i.e., along the red line in Figure 47).

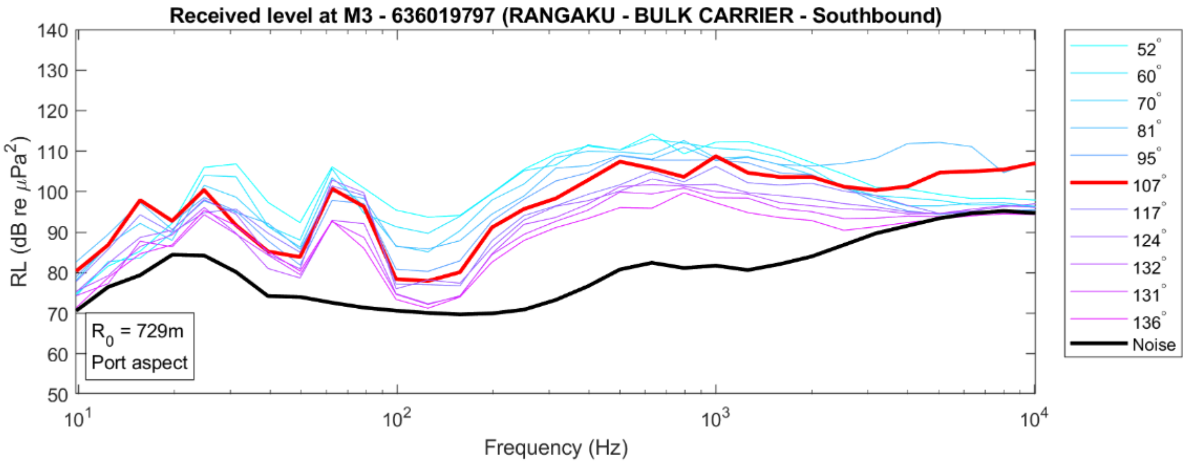

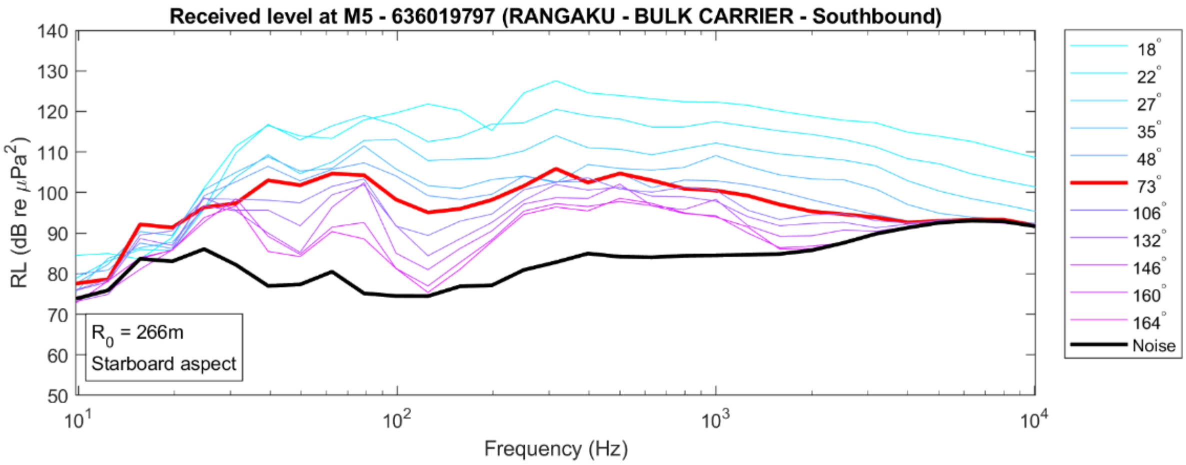

Figure 48. OTO band received level (dB re μPa^2) as a function of frequency (Hz), calculated at 30-s intervals, for a single ship pass at the northern end of Cockburn Sound, at receivers M3 (top) and M5 (bottom). Ship aspect angles are indicated by colour (0° is bow aspect and 180° is stern aspect). The measurement for which the ship crosses the imaginary line between M3 and M5 (Figure 47) is plotted in red and the background noise is plotted in black.

Upon examination of all 28 equivalent plots for the 28 ship passes, it became apparent that there was no "typical" ship pass. Aspect angles ranged between 15° and 170°. Some ships had noise level maxima at broadside aspect, but most did not. Some ships had minima in their spectra, and others did not.

The SL was calculated from the measured RL by interpolating the empirical equations for propagation loss (PL) described in Section 3.2.3 at the specified ranges and frequencies for each time step, resulting in estimates of source level as a function of frequency and aspect (Figure 49). The quality control requirements relating to SNR and range (Section 3.2.1) resulted in some missing values in the OTO SL estimates for this particular ship pass (e.g., below 20 Hz and above 2 kHz).

Figure 50(a) is a plot of the OTO band source level (SL) as a function of aspect angle at selected band centre frequencies. At 20 Hz, the SL does not depend on aspect angle, while at 500 Hz and 4000 Hz, there is a drop of 12-13 dB between 15° (near bow aspect) and 175° (near stern aspect). In contrast, for an intermediate frequency of 99 Hz, the SL drops from 194 dB re μPa^2m^2 at 15° to a minimum of 163 dB re μPa^2m^2 at 125° aspect before rising again to 176 dB re μPa^2m^2 at 175° aspect. The angular dependence is also pronounced for the broadband source level, with a maximum of 205 dB re μPa^2m^2 at 45° aspect and a minimum of 192 dB re μPa^2m^2 at 145° aspect. Since the receiver positions were fixed, the lowest and highest aspect angles were measured at the longest ranges (900-1000 m).

Figure 51 is a plot of all the individual measurements of OTO source level for bulk carriers (top panel) and tankers (bottom panel) observed from M3 and M5, overplotted with median values and 10^{th} and 90^{th} percentiles. Missing values in individual traces are for data points which did not pass the SNR and range quality control tests. There is no systematic difference in OTO SL measured at the two different receivers for each vessel class. There is a ±25 dB spread of individual SL estimates at frequencies above 100 Hz, decreasing gradually to about ±15 dB at 25 Hz, reflecting the variety of aspect angles, machinery states, speeds, and individual ship design differences that are represented in the dataset. However, the median values and percentiles as a function of frequency agree within ±3.65 dB at any given frequency between the two ship classes, reflecting the general similarity of these ships: lengths of about 200m, beam of about 30 m, gross tonnage of 35,000–50,000 tons, similar speeds and propulsion systems.

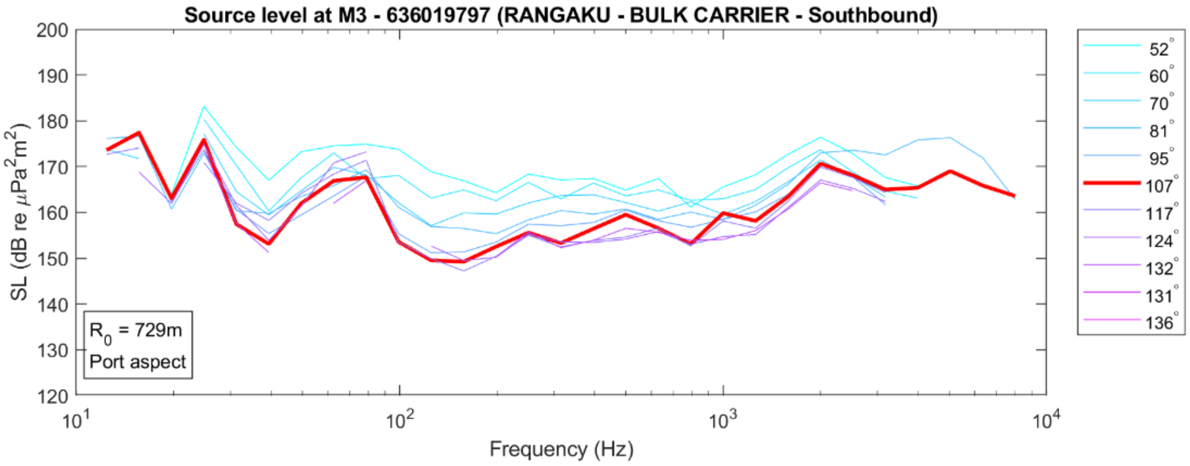

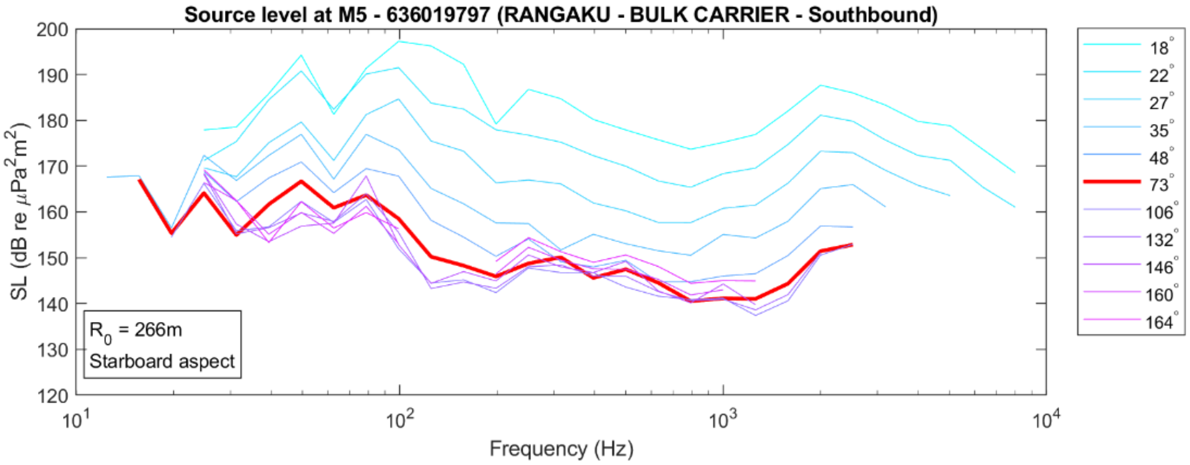

Figure 49. OTO band source level (dB re μPa^{2}m^2) as a function of frequency (Hz), calculated at 30-s intervals, for a single ship pass at the northern end of Cockburn Sound, at receivers M3 (top) and M5 (bottom). Ship aspect angles are indicated by colour (0° is bow aspect and 180° is stern aspect). The measurement for which the ship crosses the imaginary line between M3 and M5 (Figure 47) is plotted in red.

9

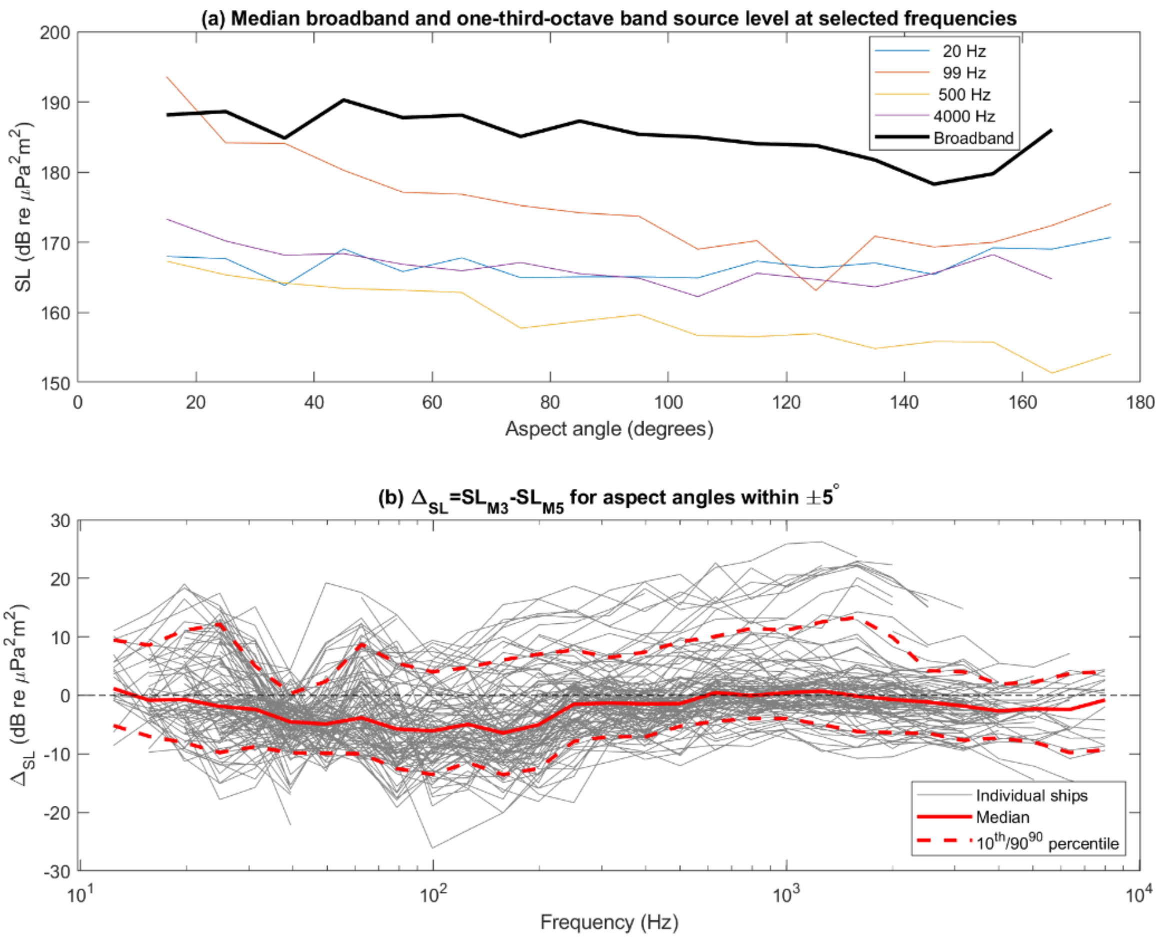

Figure 50. (a) Median OTO band source level at selected frequencies (coloured lines) and broadband source level (black line) as a function of aspect angle; (b) Difference in source level estimated at M3 and M5 for the same aspect angle, as a function of frequency.

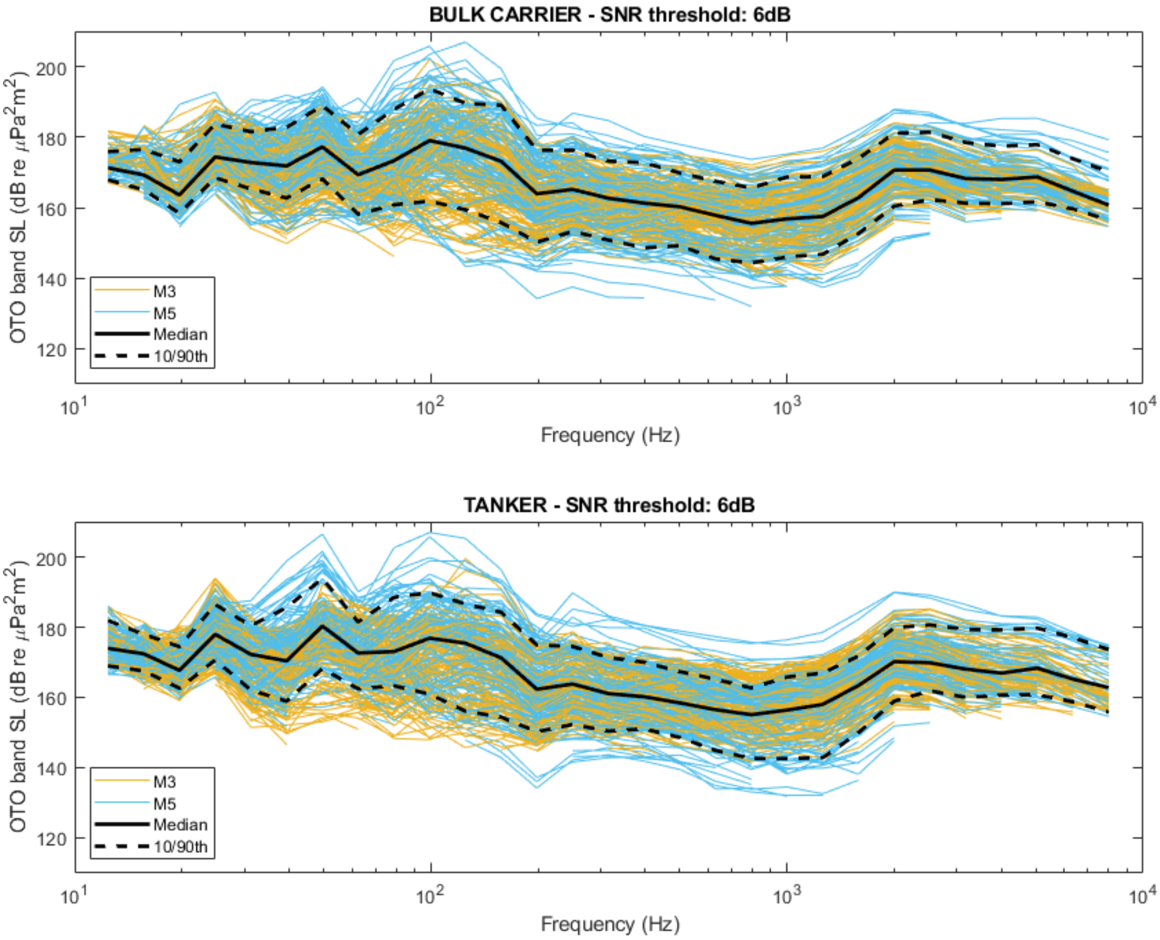

Figure 51. OTO band SL as a function of frequency for all ship noise samples that passed the quality control tests (Section 3.2.1) for observations from M3 (yellow lines) and M5 (blue lines). Median values are plotted as a thick black line and 10th and 90th percentiles are a dashed black line. Top panel: bulk carriers, Bottom panel: tankers.

Tugs and Pilot Boat

For the tug and pilot boats, specific vessels were identified passing Site 6 for analysis during the selected time period of February-March 2023. Two tugs, the SVITZER ALBATROSS and SVITZER HARRIER, made a total of 68 passes with CPAs within 200 m of Site 6 that were suitable for analysis, while the pilot boat GENESIS made a total of 23 passes within 200 m of Site 6. Due to the nature of their role in harbour operations, the passes were not generally the straight-line approaches followed by CPA and departure as they were for tankers and bulk carriers. The variability in their reported speeds (Figure 46) reflects this variability in "pattern-of-life" for working boats in Cockburn Sound. However, each boat pass was processed in the same manner as the tankers and bulk carriers at the northern end of Cockburn Sound, with the same quality control requirements.

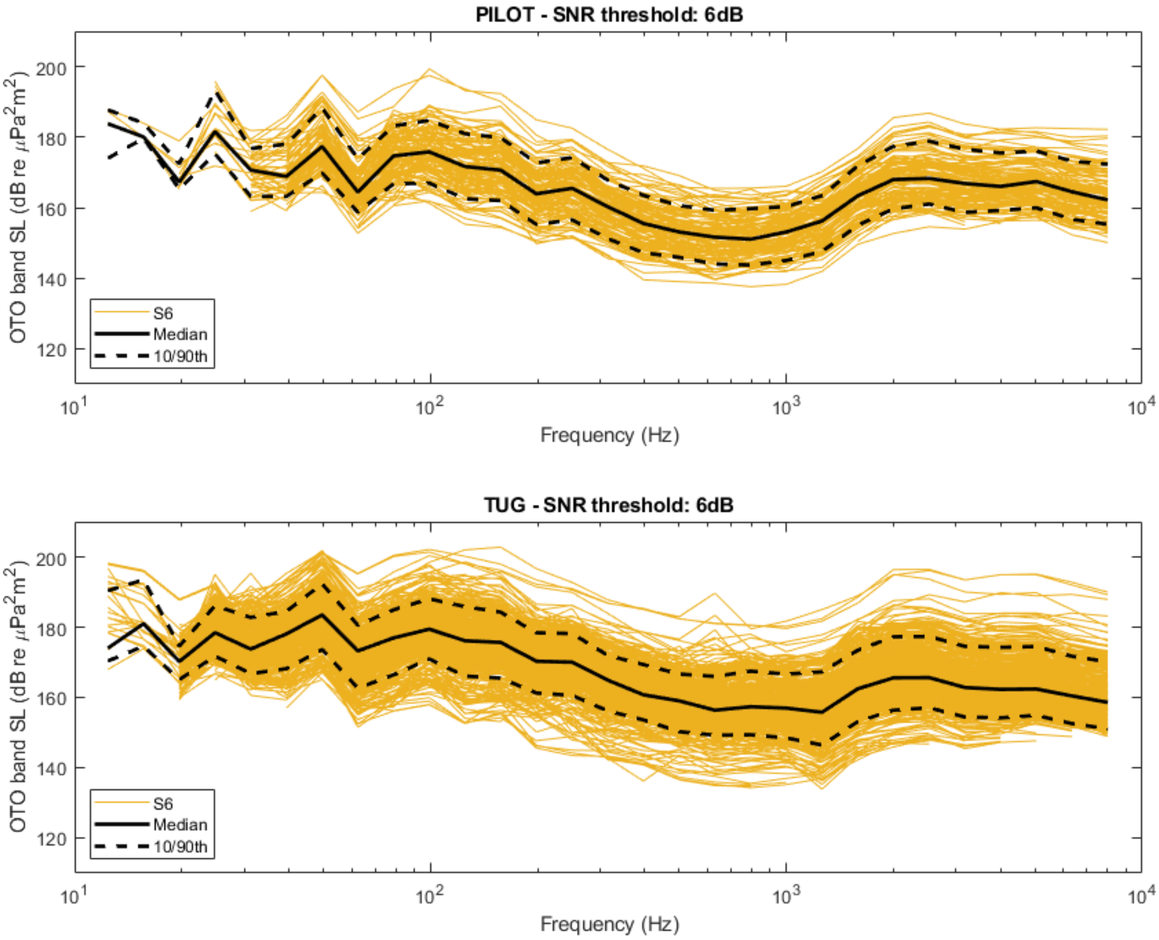

Figure 52. OTO band SL as a function of frequency for all ship noise samples that passed the quality control tests (Section 3.2.1) for observations at Site 6 (blue lines). Median values are plotted as a thick black line and 10th and 90th percentiles are a dashed black line. Top panel: pilot boat (GENESIS), Bottom panel: tugs (SVITZER ALBATROSS and SVITZER HARRIER).

Figure 52 is a plot of individual measurements of OTO band SL for the pilot boat (top panel) and tugs (bottom panel), overplotted with median values and 10th and 90th percentiles. Missing values in individual traces are for data points which did not pass the SNR and range quality control tests. The spread in SL at any given frequency is greater for tugs than for the pilot boat; for example, at 500 Hz there is a 30-dB difference between minimum and maximum SL for the pilot boat, and a 45-dB difference for the tugs. The median values follow the same general pattern, with differences at individual frequencies ranging from 0.7 to 9.3 dB.

Figure 53 is a plot of broadband source level as a function of vessel speed for the two tugs and the pilot boat. The difference in observed speeds as boats passed Site 6 is very clear: the tugs both travelled at speeds less than 11 kn and the pilot boat travelled at speeds of 16-25 kn. Although it may appear that the higher speeds are correlated with slightly lower broadband source levels, there is no way to attribute the difference in SL to speed or vessel type or an interplay of both.

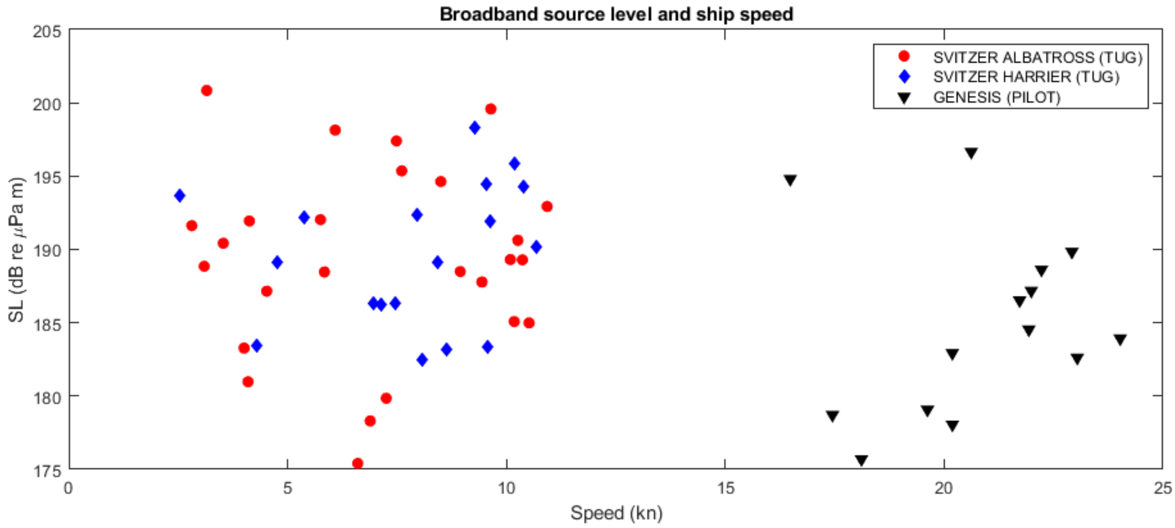

Figure 53. Broadband SL as a function of vessel speed for tugs (red, blue) and pilot (black) boats.

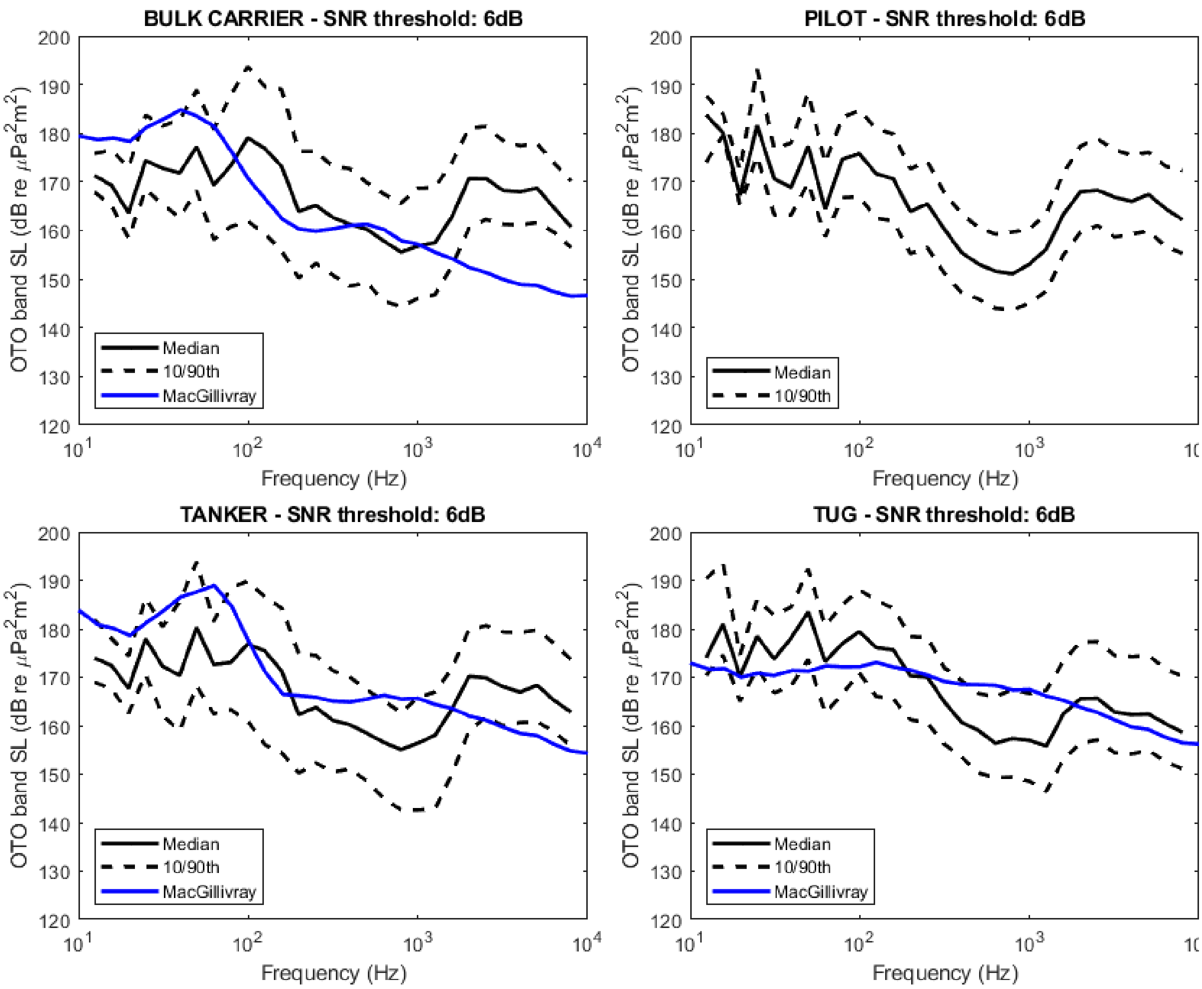

Figure 54. OTO band SL as a function of frequency for four vessel classes: median (black solid line), 10th and 90th percentiles (dashed black line), and prediction from MacGillivray (2022) (blue solid line).

Figure 54 is a plot of median, 10th, and 90th percentile OTO band SL for each of the four vessel classes, along with predicted SL based on the functional regression model developed by MacGillivray et al. (2022). The predicted SL was calculated using representative vessel operation and design parameters (**Table 8**) as inputs to the functional regression model for each vessel class except pilot boats (which were not included in the model). Representative values for draft, speed through water, length overall, main engine revolutions per minute (RPM), main engine power, design speed, and age were estimated either from observations or from the distributions for the same vessel class plotted in MacGillivray et al (MacGillivray et al. 2022), resulting in the blue lines plotted in Figure 54.

Table 8. Summary of vessel design parameters used to estimate SL in Figure 54.

	Bulk carrier	Tanker	Tug
Draft (m)	7	8	4
Speed through water (kn)	12	12	10
Length overall (m)	210	167	31
Main Engine RPM	100	150	1500
Main Engine power (kW)	10000	10000	1000
Design speed (kn)	13	13	11
Vessel age (years)	7	9	12

Port Operations

Figure 55 is a plot of measured port operations noise: the median, 10th, and 90th percentile SL as a function of frequency for the three different activities described in Section 3.2.1 (arrival, loading, and departure). For each activity, the median value (Figure 55a) has similar frequency dependence, with highest levels at the lowest frequencies, and some evidence of high and low loss frequency bands introducing artifacts (maxima and minima) into the SL estimation between 25-125 Hz. SL decreases steadily between 125 Hz and 630 Hz, with a slight peak near 1000 Hz, and decreases further up to 2000 Hz. From 2000 Hz to 8000 Hz there is a slight increase (5-6 dB), which may not be from port operations but is likely due to the presence of snapping shrimp in the area, clearly heard on the audio files. The highest sound levels for frequencies above 31.25 Hz are observed during departure, and the lowest levels occur during loading, with arrival at intermediate values from 125 Hz to 1000 Hz.

The range of values captured by the 10th and 90th percentiles are similar for all three activities (Figure 55b-d), with a maximum range between percentiles of 37.7-42.7 dB at the lowest frequencies, and a minimum range of 5.9 to 9.5 dB. Departure (Figure 55d) has greater variability at frequencies above 1000 Hz than arrival and loading, while the variability is comparable for all three activities at frequencies less than 1000 Hz.

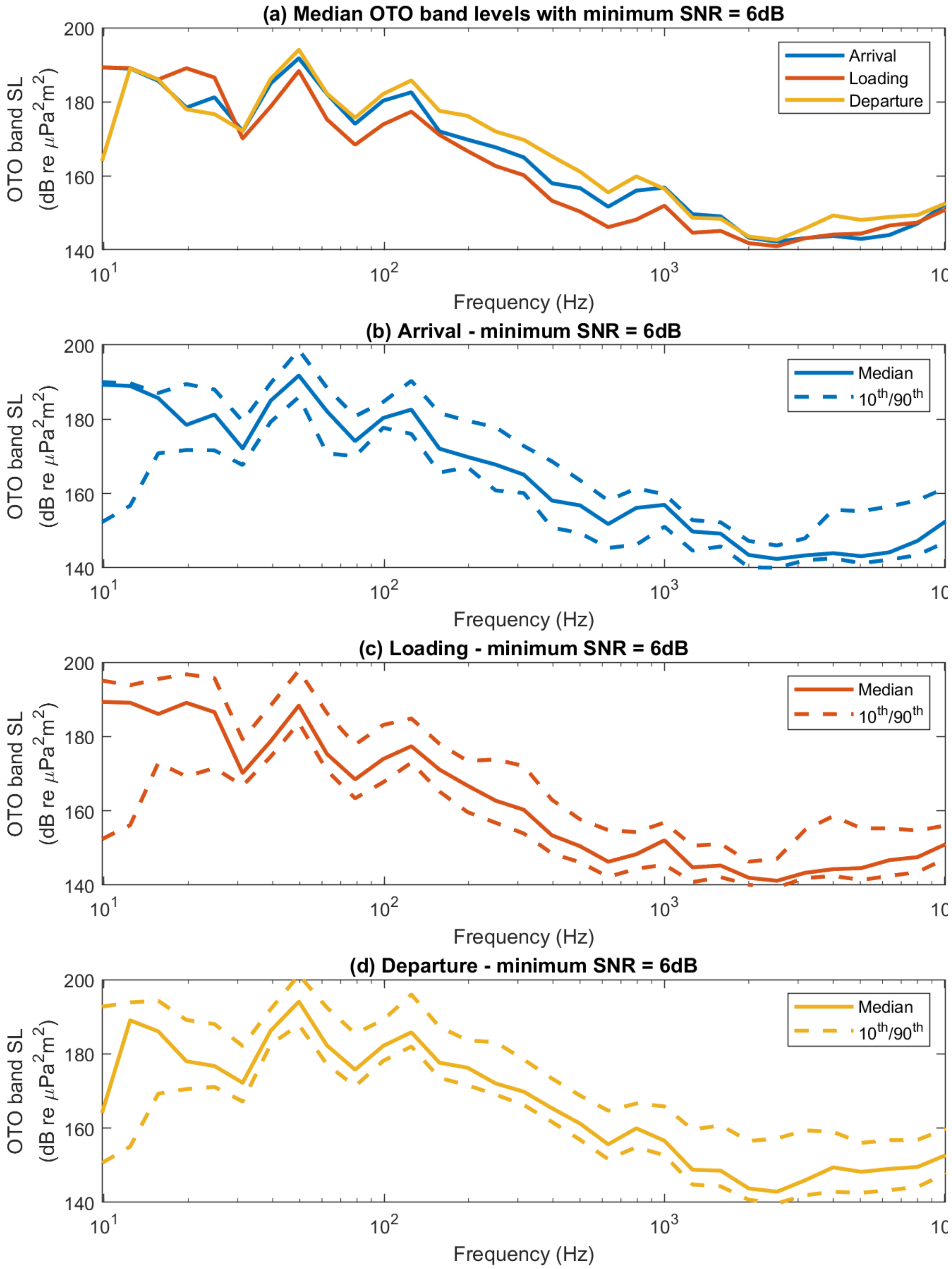

Figure 55. (a) Median OTO band SL as a function of frequency. Median, 10th, and 90th percentile OTO band SL as a function of frequency for three phases of port operations: (b) arrival, (c), loading, (d), departure.

4.3 Sound propagation model input parameters

Acoustic propagation in a shallow water environment such as Cockburn Sound is strongly dependent on the geoacoustic properties of the seabed, so establishing appropriate geoacoustic seabed models was an important goal as an enabler of numerical propagation modelling for this area. In order to develop geoacoustic models for the central basin (Table 9) and eastern (Kwinana) shelf (Table 10), information was synthesised from previously reported seabed geology of Cockburn Sound (Skene et al. 2005, Anning 2023) and the airgun head wave analysis (Section 3.2.3). The thickness of the overlying unconsolidated sediment layer in the resulting geoacoustic model was adjusted to obtain a good match between measured and modelled propagation loss between 500 Hz and 1 kHz.

The models for the two areas are very similar with only minor differences in depths and sound speeds of the deeper layers. The main difference is the thickness of the top sandy mud layer, with a 2 m thick layer giving the best match to measured data in the central basin and a 0.5 m layer giving the best match on the eastern shelf.

These models were then used as input to the wavenumber integration code SCOOTER (Porter 2020), which was used to calculate the propagation loss as a function of range and frequency for a source depth of 3 m and a receiver on the seabed. The model results are plotted and compared to similar plots of the propagation loss measured during the airgun runs in Figure 56 (central basin) and Figure 57 (eastern shelf).

Table 9. Geoacoustic model for the central basin of Cockburn Sound derived from a combination of previous studies of the seabed geology of the sound, airgun headwave analysis, and adjusting the thickness of the sandy mud layer to obtain a good match between measured and modelled propagation loss at frequencies from 500 Hz to 1 kHz.

Layer	Depth range (m below seafloor)	Density (kg/m^3)	Compressional wave speed (m/s)	Compressional wave absorption (dB/wavelength)	Shear wave speed (m/s)	Shear wave absorption (dB/wavelength)
Sandy mud	0 to 2 m	1694	1550	0.41	-	-
Calcarenite	2 to 415	2200	2219	0.1	1100	0.2
Limestone	415 to ∞	2800	3393	0.1	1600	0.2

Table 10. Geoacoustic model for eastern shelf of Cockburn Sound derived from a combination of previous studies of the seabed geology of the sound, airgun headwave analysis, and adjusting the thickness of the sandy mud layer to obtain a good match between measured and modelled propagation loss at frequencies from 500 Hz to 1 kHz.

Layer	Depth range (m below seafloor)	Density (kg/m^3)	Compressional wave speed (m/s)	Compressional wave absorption (dB/wavelength)	Shear wave speed (m/s)	Shear wave absorption (dB/wavelength)
Sandy mud	0 to 0.5 m	1694	1550	0.41	-	-
Calcarenite	0.5 to 416	2200	2128	0.1	1000	0.2
Limestone	416 to ∞	2800	3132	0.1	1500	0.2

A number of points are worthy of note:

- The “blocky” appearance of the measured propagation loss plot in Figure 56 is a result of these measurements being made by a long-term recorder (Figure 3, site 4) that was recording for 4 minutes out of every 5, leading to artificial “steps” in the interference patterns.
- The very high propagation loss at low frequencies is a result of waveguide cut-off effects (the acoustic waves are effectively too long to fit into the water column), which is a typical feature of shallow water propagation in many environments, but is made very obvious in this environment by the very low acoustic reflectivity of calcarenite at low grazing angles.
- The horizontal, low propagation loss bands at low frequencies are a particular feature of acoustic propagation over calcarenite seabeds and are explained in Duncan et al. (2013). They are more prominent and extend to higher frequencies in the model results than in the measurements because the model assumes a perfectly flat interface between the sandy mud and calcarenite, whereas in reality this interface is rough and could also be sloping.
- The low-frequency propagation loss is higher on the eastern shelf than it is in the central basin. This is for two reasons: on the shelf the shallower water depth increases the frequencies below which each mode is cut off, and the thinner sediment provides less “insulation” between the sound in the water column and the extremely lossy calcarenite.
- The diagonally sloping interference pattern at higher frequencies is a result of interference between different propagating acoustic modes, and is again a typical feature of shallow water propagation.

Figure 58 through to Figure 61 compare the measured and modelled propagation loss averaged over OTO bands, and Table 11 quantifies the differences between them by way of the root mean square (RMS) dB difference between the measurements and the model for each band.

As mentioned in Section 3.2.4, range-dependent low-frequency modelling requires equivalent fluid geoacoustic models of the seabed, which were derived from the geoacoustic models given in Table 9 and Table 10 using the method described in Appendix 9.1. The resulting parameters are given in Table 12 (central basin) Table 13 (eastern shelf). Note that these parameters should not be used for modelling at frequencies below the minimum frequency limits stated in the table captions.

Fits of measured OTO band averaged propagation loss to Equation (1) resulted in the coefficients listed in Appendix 9.5 in Table 35 for the central basin and in Table 36 for the eastern shelf. Note that this equation should only be used for the valid range intervals given in the tables, and are specific to a source depth of 3 m and a receiver on the seabed. Plots of the measured data PL as a function of R and of the lines of best fit (Appendix 9.5) are found in Figure 71 and Figure 72 for the central basin and eastern shelf respectively.

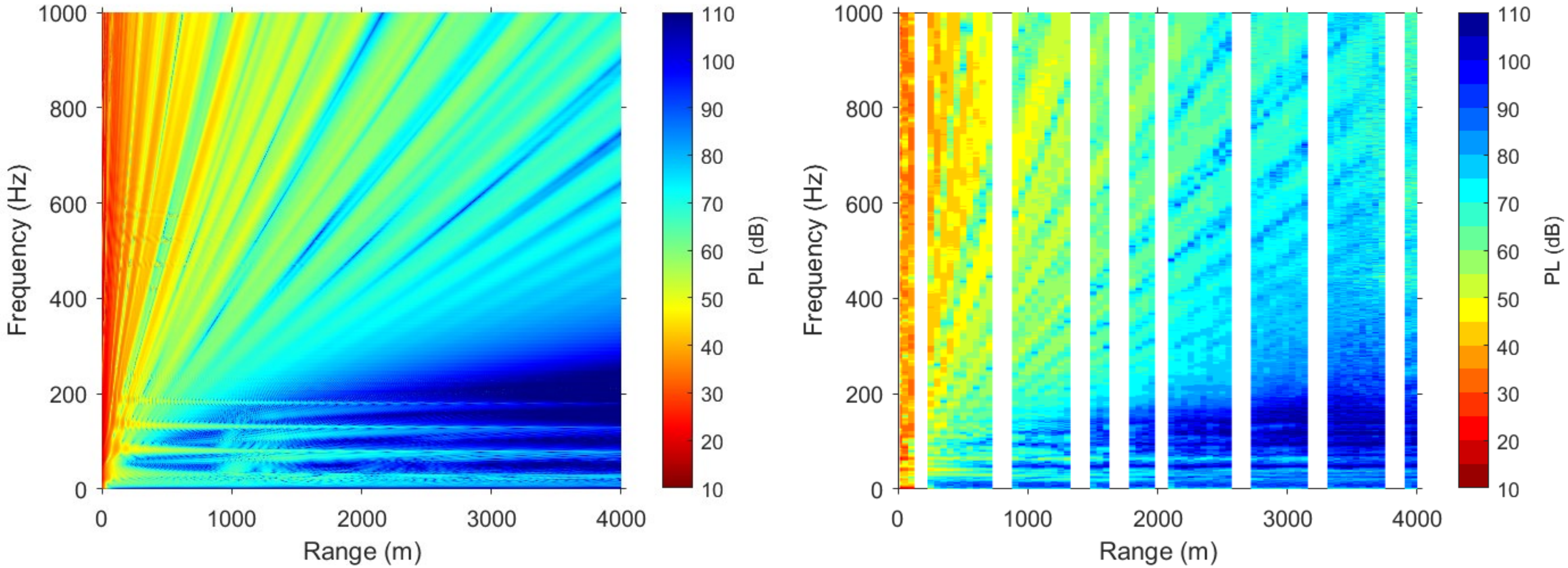

Figure 56. Modelled (left) and measured (right) propagation loss vs. range and frequency for the central basin of Cockburn Sound. Source depth is 3 m, water depth is 19 m and the receiver is on the seabed. The "blocky" appearance is a result of the recorder duty cycle (recording 4 minutes out of every 5).

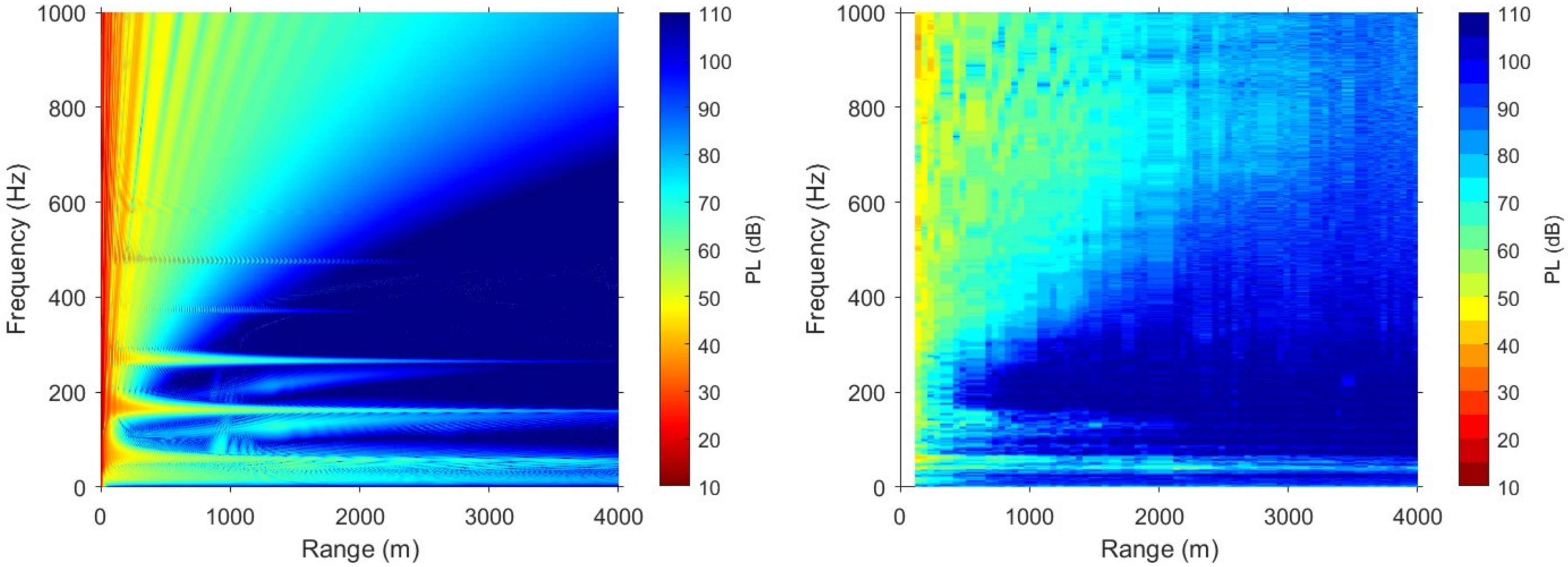

Figure 57. Modelled (left) and measured (right) propagation loss vs. range and frequency for the eastern shelf of Cockburn Sound. Source depth is 3 m, water depth is 10 m and the receiver is on the seabed. The "blocky" appearance is a result of the recorder duty cycle (recording 4 minutes out of every 5).

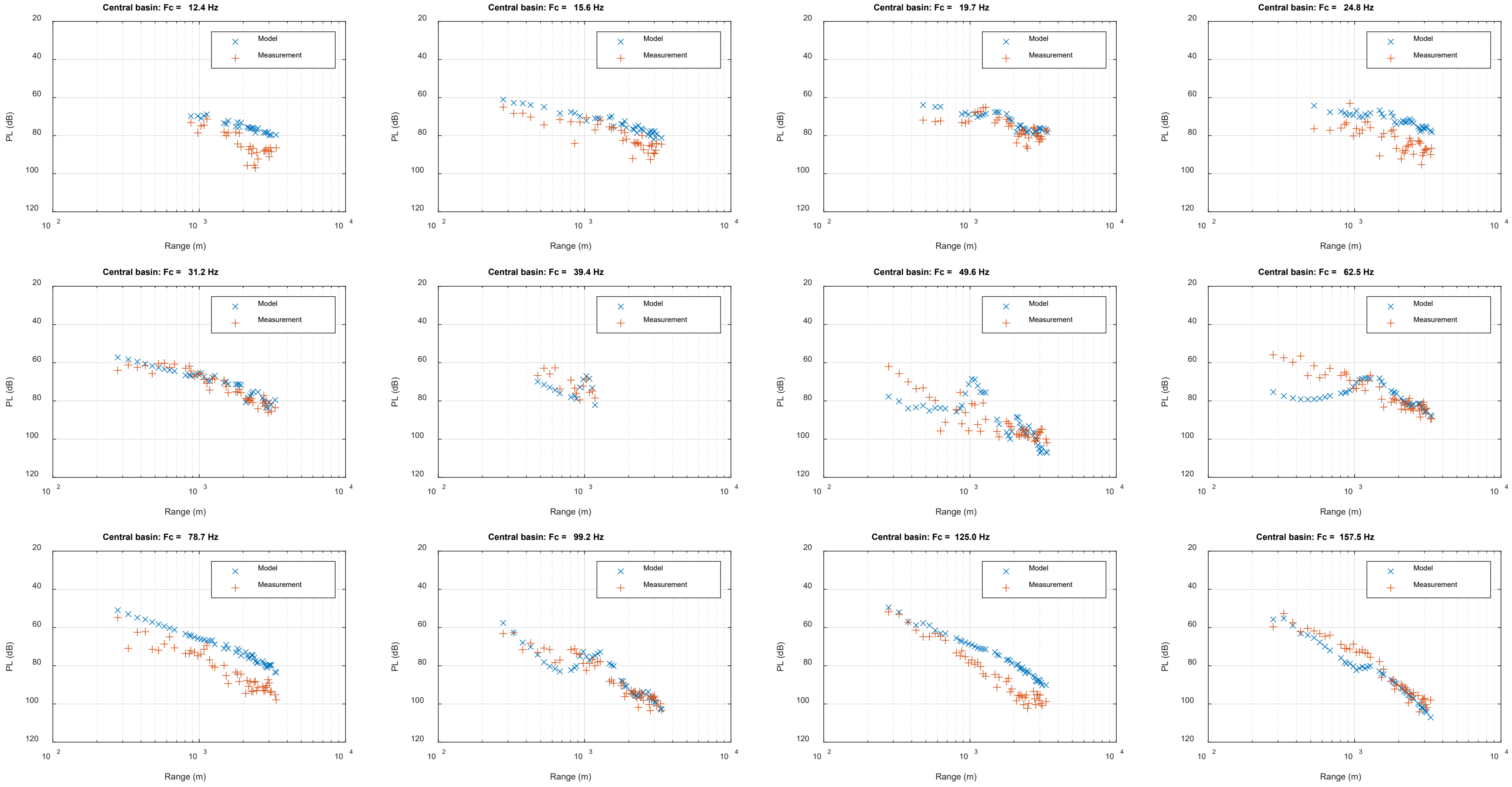

Figure 58. Modelled and measured OTO band averaged propagation loss as a function of range for the central basin and band centre frequencies from 12.4 Hz to 157.5 Hz.

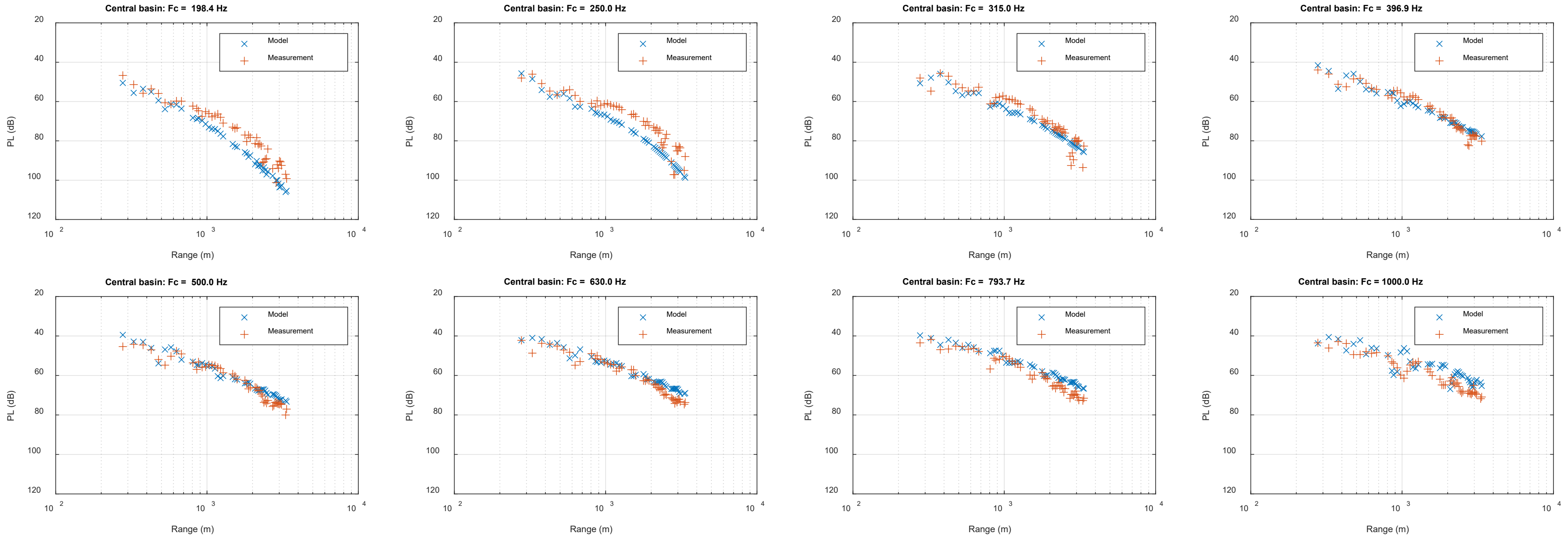

Figure 59. Modelled and measured OTO band averaged propagation loss as a function of range for the central basin and band centre frequencies from 198.4 Hz to 1 kHz.

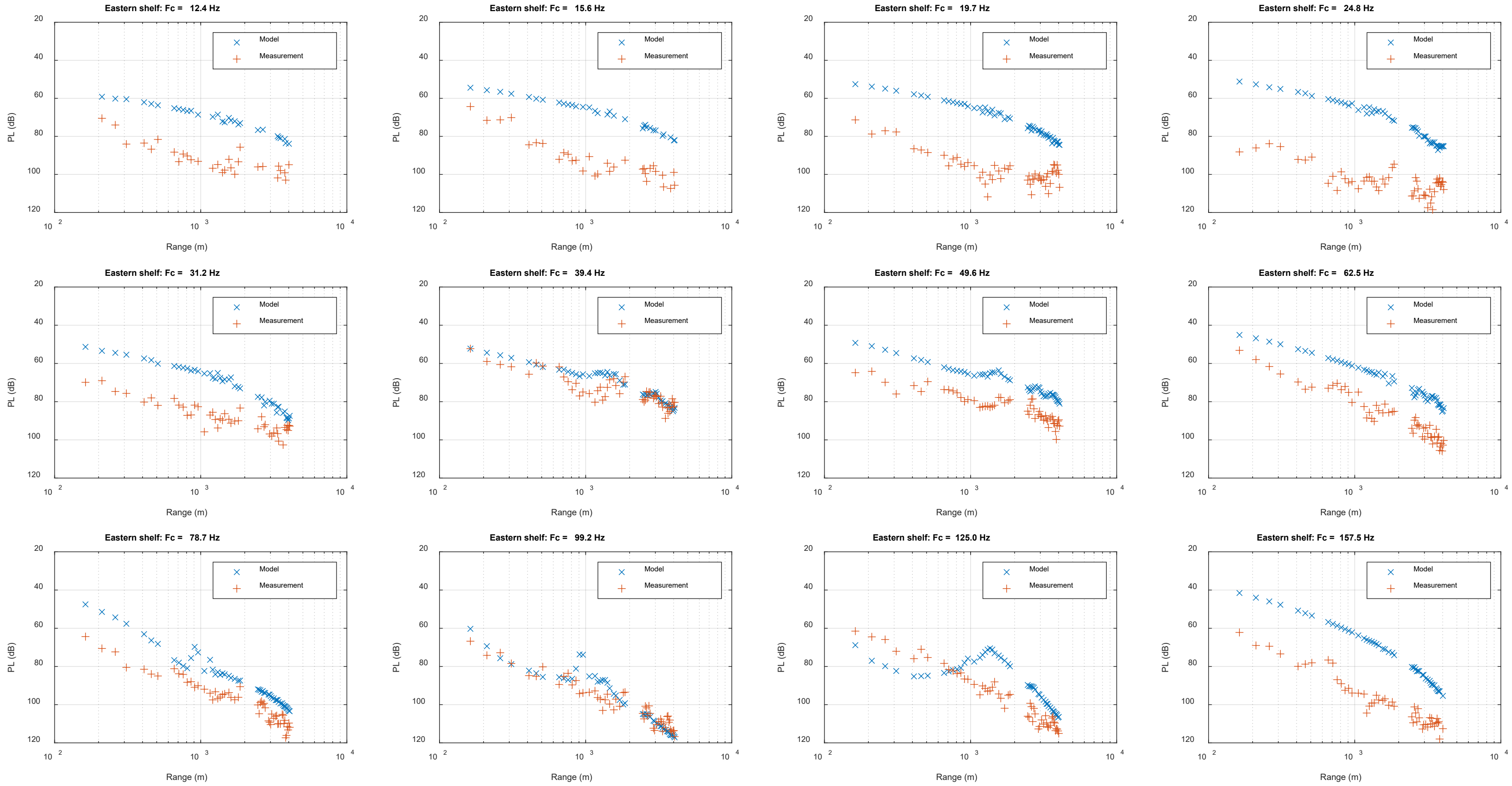

Figure 60. Modelled and measured OTO band averaged propagation loss as a function of range for the eastern shelf and band centre frequencies from 12.4 Hz to 157.5 Hz.

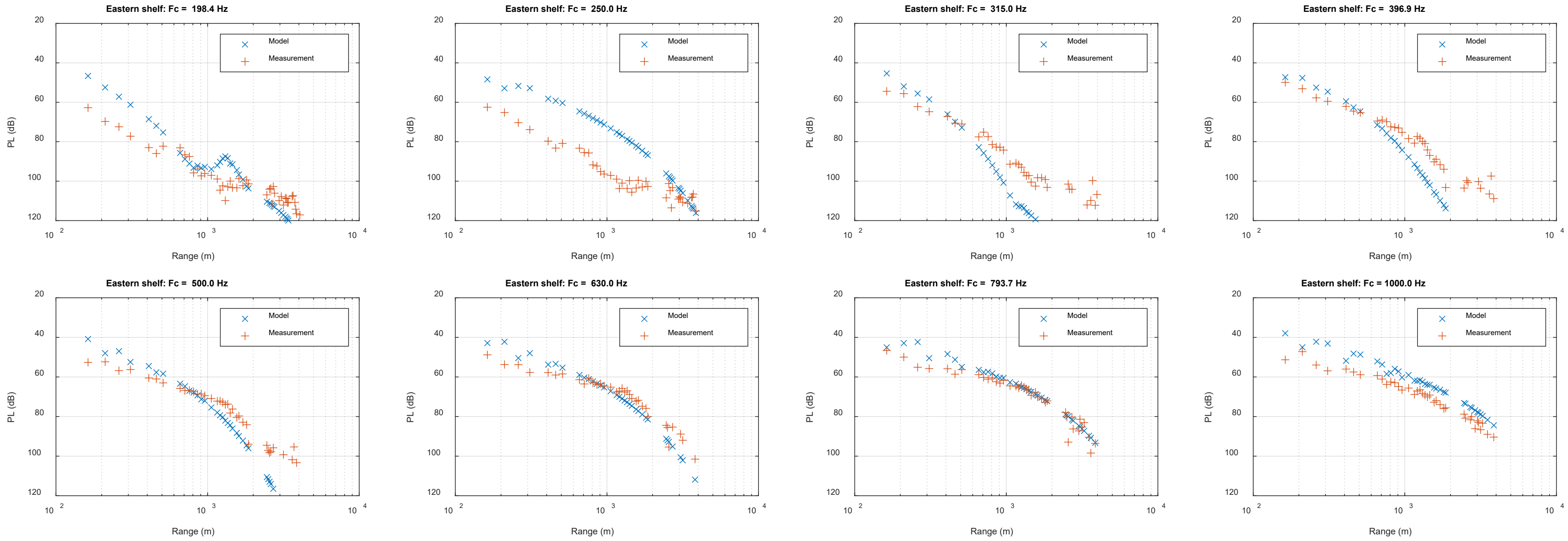

Figure 61. Modelled and measured OTO band averaged propagation loss as a function of range for the eastern shelf and band centre frequencies from 198.4 Hz to 1 kHz.

Table 11. Root mean square (RMS) dB differences between modelled and measured propagation loss averaged over OTO bands.

Centre frequency (Hz)	12.4	15.6	19.7	24.8	31.3	39.4	49.6	62.5	78.7	99.2	125.0	157.5	198.4	250.0	315.0	396.9	500.0	630.0	793.7	1000.0
Central basin (dB)	10.6	7.5	4.4	11.6	3.3	6.0	9.6	8.5	12.3	4.7	11.1	5.1	7.6	7.4	4.4	3.0	3.3	3.7	4.5	6.2
Eastern shelf (dB)	21.7	24.7	27.1	32.4	18.0	5.6	13.9	18.3	12.1	6.6	13.1	25.7	10.1	17.5	22.7	20.5	15.0	5.7	4.3	7.3

Table 12. Equivalent fluid geoacoustic model for the central basin of Cockburn Sound (see Appendix 9.4) suitable for range dependent propagation modelling at frequencies of 200 Hz and above.

Layer	Depth range (m below seafloor)	Density (kg/m^3)	Compressional wave speed (m/s)	Compressional wave absorption (dB/wavelength)	Shear wave speed (m/s)	Shear wave absorption (dB/wavelength)
Sandy mud	0 to 2 m	1694	1550	0.41	-	-
Calcarenite	2 to ∞	2200	1096	0.7	-	-

Table 13. Equivalent fluid geoacoustic model for the eastern shelf of Cockburn Sound (see Appendix 9.4) suitable for range dependent propagation modelling at frequencies of 400 Hz and above.

Layer	Depth range (m below seafloor)	Density (kg/m^3)	Compressional wave speed (m/s)	Compressional wave absorption (dB/wavelength)	Shear wave speed (m/s)	Shear wave absorption (dB/wavelength)
Sandy mud	0 to 0.5 m	1694	1550	0.41	-	-
Calcarenite	0.5 to ∞	2200	975	4.5	-	-

5 Discussion

5.1 Soundscape

Sound levels and noise sources recorded at the Cockburn Sound field sites (Figure 3) were comparable to other nearby measurements, including the Fremantle Inner Harbour, the Swan River, and the Perth Canyon. Salgado-Kent et al. (2012) measured sound levels in the Fremantle Inner Harbour for five months in 2010 and observed anthropophony including vessel traffic, vehicle traffic from nearby roads, machinery noise, and pile driving, as well as biophony that included noise from snapping shrimp, mulloway, and dolphins. Another study that collected a large dataset spanning eight years of data from five sites in the Swan River contained many of the same components of anthropophony, biophony, and geophony, and was dominated by vessel traffic and snapping shrimp (Marley et al. 2017).

Despite being only 60 km from Cockburn Sound, Perth Canyon is a deep-water offshore area with significantly different soundscape components. In a summary of the soundscape in Perth Canyon measured by a long-term mooring in water depth of 430-490 m, Erbe et al. (2015) observed a combination of geophony, biophony, and anthropophony. Whales were dominant seasonally for frequencies below 400 Hz, while fish and invertebrate choruses dominated frequencies between 1800 and 2500 Hz at night throughout the year. In contrast, the significantly shallower water (10-20m) in Cockburn Sound means large baleen whales do not enter Cockburn Sound, and the sounds made while they swim offshore does not propagate into Cockburn Sound. At Perth Canyon, nearby ship passes (heading to or from Cockburn Sound) contribute significantly to the 8-100 Hz band, for a few hours at a time, at all times of the day and year. Rain noise was observed during the winter season while wind noise was significant at 200-3000 Hz.

5.1.1 Baseline levels and statistics

The baseline ambient noise levels measured in this project will be useful in any future environmental impact assessment (EIA). Of all the sites studied in this project, Site 6 (South Basin) was on average the loudest site between 60 and 1000 Hz, with dense traffic and frequent utilisation of the near-by grain terminal. The levels were comparable to those reported for Fremantle Inner Harbour from 10 Hz to 11 kHz by Marley et al. (2017) and from 10 Hz to 5 kHz by Salgado-Kent et al. (2012). The shallow sites experienced the highest average sound levels at frequencies greater than 1 kHz, in particular Kwinana Shelf North (Site 8) and Owen Anchorage (Site 9), which was mainly due to snapping shrimp activity. On average, the quietest site below 100 Hz was North Basin (Site 3), between 100 and 500 Hz it was Kwinana North (Site 8), and above 500 Hz it was Mangles Bay (Site 5), with levels comparable to the quietest parts of the Swan River (Marley et al. 2017).

While positive spatial correlation between nearby sites make sense, e.g., shallow water sites at high frequencies, the negative correlation between some sites needs further investigation to understand if there is a physical explanation or if this is a coincidence. Further investigation could include modelling or experimental measurements to investigate whether there is a physical explanation to negative spatial correlation of underwater sound between sites. Additional future work could include applying weighting curves for penguin hearing, sea lions (such as those from WWMSP Project “Hearing sensitivity of Australian sea lions, little penguins, and fish”), and bottlenose dolphins, in order to determine potential impact of existing and predicted future noise levels.

5.1.2 Sound sources

Anthropophony: Recreational vessels are not required to have AIS therefore it was not possible to quantify their specific contribution to overall sound levels, despite the fact that their sound contributed to the measured sound levels. Additional work could be done to automatically identify ships and small boats in the recordings and compared to AIS records, in order to quantify the relative contributions of recreational and shipping noise to the soundscape. Recordings of echosounders and sub-bottom profilers could be combined with ship positions derived from AIS to determine sound exposure contours for geophysical survey systems, which would better inform impact assessments for geophysical surveys.

Biophony: Dolphins were detected at all sites except Site 6 (South Basin). The lack of observations at Site 6 might be due to other sounds masking their vocalisations, which could be further investigated. Broadscale analysis found dolphins recorded at Sites 1, 5, 7, and 8 year-round. Finer temporal resolution studies of activity would be insightful to assess daily presence and diurnal activity, as well as investigating any relationship to anthropogenic noise and masking of communication (Figure 28). The resulting information could be combined with outputs from projects from WWMSP Theme 8: Apex predators and iconic species, for improved ecological modelling for predicting spatial temporal presence of dolphins in Cockburn Sound. Additionally, photo ID with possible signature whistles (Figure 41), might be a useful way to monitor specific individuals in future. There may also be a relationship between different biophony sources, e.g., fish and dolphins were heard at the same time (Figure 39). Fish species and chorus identification could be used to understand stocks in combination with projects from WWMSP Theme 4: Fisheries and aquatic resources. Snapping shrimp noise could potentially be used as a proxy for marine habitat condition ("health check") and measurable response to climate change (Legg 2010, Bohnenstiehl et al. 2016, Monczak et al. 2019, Hawkins et al. 2023).

Geophony: Due to the relatively sheltered nature of parts of Cockburn Sound, the Cato model (Cato 1997) accurately predicted wind-generated noise in some, but not all, areas of the Sound. The lack of agreement with the Cato model suggests that in sheltered locations the model may not apply due to the limited fetch, and/or due to the fact that the Cato wind model was developed for open ocean, and its suitability in coastal waters is not well established. Winters in Perth are characterised by brief but relatively intense rainfall events, which may have been observable on the underwater recordings. However, the lack of nearby weather data limited the possibility of extracting portions of the recordings with rainfall for further study. In future studies, a more complete picture of environmental conditions would be achievable by locating a weather station closer to recorder locations or the use of rain radar, and in some cases metocean data could be collected with the sound recorders, e.g. water temperature, and current speed and direction.

5.2 Noise source signatures

Determining a suitable PL "correction" for the range between a vessel and recorder in order to derive SL from RL was one of the most challenging parts of this work. The calcarenite bottom and overlying sediments resulted in narrow frequency bands between approximately 100 Hz and 200 Hz that alternated between high and low PL (differences of 30-40 dB). The exact frequencies of the low-loss bands depend strongly on the layer thickness and sound speeds in the layers, which vary in a range-dependent manner not fully captured by range-independent propagation models. In practice, this means that the theoretical sharply defined bands (such as those in Figure 56) are "smeared out" over multiple frequencies in a real-world environment. Due to imperfect knowledge of the spatial dependence of bottom sediments, the PL banding from a model is not likely to align perfectly with the true high-absorption frequencies observed between two points in the real environment of Cockburn Sound. Therefore, SL derived from RL observations in Cockburn Sound, whether corrected by using PL from a model or from in situ airgun observations made nearby (Section 3.2.3), should be viewed with caution for frequencies of 50-200 Hz.

Underwater radiated noise levels from ships depend on vessel speed and aspect. Vessel speeds in Cockburn Sound near the recorders did not vary significantly for some vessel classes. Bulk carriers and tankers moved at 10-12 knots generally, due to navigation requirements, and the pilot boat tended to be either stationary or moving at 20-25 knots. However, there was a large variation in speed for the tugs. The aspect dependent noise level observations were modified by the significant low-frequency losses between source and receiver: unlike other studies in deeper water (e.g., McKenna et al. (2012)), the highest noise levels in Cockburn Sound were not observed at stern aspect, but rather near bow aspect. The highest aspect dependence was observed for intermediate frequencies (100-500 Hz), driving the minimum in median broadband source level at 140° (port/starboard quarter) aspect, 7 dB re μPa·m less than at aspect angles of 15° (port/starboard bow).

The spread in estimated SL for bulk carriers and tankers passing the recorders at M3 and M5 near the north end of Cockburn Sound did not depend on ship type, direction, or recorder location. There was a broad peak in SL centred at 100 Hz and an increase in SL for frequencies greater than 2000 Hz. For tugs and pilot boats, it was not possible to determine whether differences in SL could be attributed to boat design or boat speed, or a combination of both. Comparison of median OTO SLs with predictions from MacGillivray et al. (2022) is qualitatively good for bulk carriers and tankers, especially considering the simplicity of the calculation of SL From RL. However, the predicted OTO SL for tugs is flatter in frequency than the observed SL, possibly due to the tugs in Cockburn Sound being observed at a wider range of speeds than those in the model.

The combined noise from tugboat(s), a pilot boat, and a bulk carrier carrying out routine port operations was measured near Kwinana Grain Terminal. Noise was estimated separately for three phases of operation: arrival, loading, and departure. During the loading period, the bulk carrier was the only vessel near the recorder for most of the time spent loading, and the noise levels were lowest during loading. The highest noise levels were observed during departure, perhaps due to the relative complexity of the actual manoeuvres required by multiple vessels to depart safely. The SL estimates between 50-200 Hz likely suffered from similar problems with the PL correction as they did at the north end of Cockburn Sound. There was a large range between the 10^{th} and 90^{th} percentiles for frequencies less than 30 Hz in the port operations noise measurements. Observations of the raw data files confirmed the presence of strong noise lines of likely electrical origin in the area near the terminal.

Although vessel classes observed in Cockburn Sound included pleasure craft, passenger vessels, bulk carriers, tankers, cargo (container) ships, and tugs, the source level analysis in this report was limited to those vessels that passed on a predictable track near recorders M3 and M5 (Figure 4) and that were sufficiently isolated from other vessels that the noise signature of the passing vessel could reasonably be extracted. As a result, the 28 large ships whose signatures are described in this report were tankers and bulk carriers. No container ships passed near the recorders in a configuration suitable for source level measurement. It is unclear whether this was because operational requirements for container ships resulted in tracks unsuitable for analysis, or merely statistics combined with luck: it was qualitatively observed that tankers and bulk carriers dominated the marine traffic in Cockburn Sound. However due to the fact that container ships, bulk carriers, and tankers are vessel classes of comparable sizes and speeds, with very similar noise signatures (MacGillivray et al. 2022), the conclusions presented here can reasonably extended to container ships, especially at the constrained speeds required of ships manoeuvring in Cockburn Sound. The variability in source level observed from individual ships was far larger than any variability between ship classes. There were insufficient high-quality data at varying ship sizes to support the development of any additional scaling law.

5.3 Sound propagation model input parameters

5.3.1 General features of acoustic propagation in Cockburn Sound

The geoacoustic properties of the Cockburn Sound seabed result in very high propagation loss in broad frequency bands centred on approximately 100 Hz for propagation in the central basin and 200 Hz for propagation over the eastern shelf. The corresponding rates of change of propagation loss are close to

40 dB per factor of ten change in range for the central basin and 60 dB per factor of ten change in range for the eastern shelf. By comparison, spherical spreading corresponds to a 20 dB increase in PL per factor of ten increase in range; in other words, the geoacoustic properties of Cockburn Sound cause much higher attenuation and consequent loss of sound intensity than would be expected from simple spherical spreading.

At frequencies below those corresponding to the maximum propagation loss there are low PL frequency bands and high PL frequency bands in both the measurements and the model predictions, but the low PL frequency bands are much broader in the measured PL than they are in the modelled PL. This is a result of the model treating the interface between the sandy mud and calcarenite as perfectly flat whereas in reality it is rough.

Propagation loss at frequencies higher than about 150 Hz (basin) or 300 Hz (shelf) depends strongly on the thickness of the overlying sandy mud layer, with thicker layers resulting in lower propagation loss. As mentioned previously, coupling of sound into shear waves results in calcarenite having a very low reflectivity at the small grazing angles important for near-horizontal propagation in Cockburn Sound. A mud seabed, which doesn't support shear waves, is more reflective than a calcarenite seabed at these angles. The presence of a mud layer on top of a calcarenite layer therefore has the effect of increasing the seafloor reflectivity, with the reflectivity (and hence received sound levels) increasing as the thickness of the mud increases.

From these frequencies up to 1 kHz the measured propagation loss tends to reduce with increasing frequency. Above 1 kHz the trend in the measured data is less clear due to the poorer signal to noise ratio of the airgun measurements, however the numerical models predict the propagation loss will continue to reduce with increasing frequency until the effects of water column absorption become apparent above about 5 kHz.

5.3.2 Propagation loss modelling recommendations

The physics of acoustic propagation in Cockburn Sound is complicated and depends on both the compressional wave and shear wave properties of the seabed. For range independent situations a wavenumber integration program such as SCOOTER (Porter 2020) or OASES (Schmidt 2020) can capture all of distinctive features of propagation in Cockburn Sound; in particular, the low-loss frequency bands with high-loss bands in between, and the interference pattern at high frequencies. However, the roughness of the sandy mud-calcarenite interface means that this is never a truly range independent environment, with the result that all models will predict much sharper low-loss frequency bands that extend to higher frequencies than those seen in the measured data. As a result, direct comparison between modelled and measured results leads to large discrepancies in OTO band averaged propagation loss seen in Figure 58 to Figure 61 and Table 11 at frequencies below 150 Hz (basin) and 300 Hz (shelf). Neither of these models can deal with range dependent situations in which the water depth, seabed properties and/or water column properties vary with distance from the source.

For the purposes of environmental noise estimation the difficulties of numerical propagation modelling in this environment can to some extent be circumvented by calculating OTO band propagation loss using Equation (1) and the coefficients in Table 35 or Table 36. However, this equation should only be used for calculating the PL in the valid range intervals specified in the tables. Note that this approach is specific to range independent cases with a source depth of 3 m and a receiver on the seabed.

Root mean square (RMS) PL differences between Equation (1) and measured OTO band PL values were up to 4.9 dB for the central basin and up to 4.7 dB for the eastern shelf. The corresponding mean (over frequency bands) RMS differences were 3.2 dB and 3.3 dB respectively. From Figure 71 and Figure 72 it can be seen that these differences are primarily due to variability in the measured data, which is likely due to a combination of noise from other sound sources and random effects in the environment, particularly scattering from waves on the sea surface, seafloor roughness, and rough interfaces between seabed layers.

For calculations outside the range of validity of the empirical OTO band models, including range dependent situations and different source or receiver depths the following recommendations are made:

- For frequencies greater than 300 Hz (shelf) and 150 Hz (basin) fully range-dependent numerical modelling can be carried out using the parabolic equation model, RAMGeo, with an equivalent fluid seabed (see Table 12 and Table 13). Tests indicate this is computationally feasible to a maximum frequency of at least 10 kHz. Note that RAMGeo does not include the effect of water column absorption loss, which is significant for frequencies of 5 kHz and above for ranges of a few km or more. However, the absorption loss can be calculated separately and added to the propagation loss calculated by RAMGeo.
- For frequencies of 2 kHz and above, numerical propagation modelling can be carried out using a ray or beam code, e.g. Bellhop (Porter 2020), with plane-wave seafloor reflection coefficients for the geoacoustic models given in Table 9 and Table 10 calculated numerically, for example using Bounce (Porter 2020). However, this approach proved to be more computationally demanding and produced noisier results than RAMGeo with an equivalent fluid seabed for frequencies up to the maximum tested frequency of 10 kHz, so it is recommended that RAMGeo be used instead wherever computationally practical. (See Appendix 9.5.)
- Range dependent acoustic propagation modelling in this environment at frequencies below 300 Hz (shelf) and 150 Hz (basin) cannot currently be carried out with any readily available acoustic propagation model. An approach involving piecewise use of OTO band fits might be possible but has not been tested.

6 Conclusions and recommendations

A comprehensive study of underwater noise in Cockburn Sound was undertaken with three main aims:

1. To record and quantify the baseline marine soundscape over a 12-month period at multiple sites,
2. To fill the gap in noise data for port operations and ships under specific conditions, and
3. To develop validated models for sound propagation in Cockburn Sound.

The baseline marine soundscape was measured over a 12-month period at nine sites, seven within Cockburn Sound and two just outside of Cockburn Sound to the north. At each site, noise percentiles across a frequency range of 20-48000 Hz were calculated for narrowband, broadband, and OTO band levels. Seasonal variability, diurnal variability, and spatial and temporal correlations among sites were quantified using statistical methods including correlation analysis and principal component analysis. Observed sounds were grouped into three categories: geophony, anthropophony, and biophony. The geophony was dominated by wind-generated noise. Anthropophony was dominated by vessel noise, with industrial noise contributing at the south end of Cockburn Sound and an unknown but strong 50-Hz noise source contributing to the noise measured on the Kwinana Shelf. Biophony was dominated by dolphins, fish, and snapping shrimp, which varied also by location, season, and time of day.

Noise source signatures were observed for large ships (tankers and bulk carriers) entering Cockburn Sound via the channel at its northern end. Due to the peculiarities of underwater acoustic propagation in Cockburn Sound, broadband ship noise at close range was higher from the bow aspect of the ship, dominated by frequencies higher than 1000 Hz, and varied considerably between ships of the same classes. Source signatures for a pilot boat and several tugs were measured at the southern end of the Sound. Broadband noise levels varied up to ±15 dB for both boat classes and did not show a significant dependence on vessel speed over the limited number of observations available. The combined noise from port operations was measured for ships arriving, loading, and departing the Kwinana Grain Terminal at the southern end of Cockburn Sound. Pilot boats and tugs were involved in the arrival and departure, contributing to higher noise levels for a short time, while the loading phase was quieter.

Sound propagation input model parameters, in particular, parameters describing propagation in the sediments, were explored by using a combination of airgun measurements and modelling. The accuracy of an “equivalent fluid layer” model for bottom parameters was compared with a more conventional two or three-layer structure and with in situ propagation measurements. Models were able to qualitatively reproduce the higher propagation losses observed at frequencies of 100-300 Hz, but the detailed pattern of high-loss and low-loss frequencies depends strongly on the assumed layer properties. In practice, the layering between any source and receiver will vary in a range-dependent manner and the high- and low-loss bands be smoothed out across multiple frequencies, resulting in a high-loss “notch” in which sound propagates more efficiently through the bottom than via the water column. Suggested model parameters derived from a combination of airgun experiments and modelling are summarised for future use.

Future work was identified that could be explored with the existing datasets. Additional finer-scale temporal analysis of biophony could include exploration of the behavioural and ecological implications of presence and absence of various species, and examination of the potential impact of masking by anthropophony. Sound exposure levels from geophysical surveys and other types of sonar noise could be measured in a relatively straightforward way by combining AIS tracks during known geophysical surveys with existing measurements of underwater noise. Analysis of port operations noise and noise from individual ships and boats could be expanded from the few dozens of occasions described in this document to the several hundred occasions theoretically available by exploiting the entire dataset, in order to increase the statistical validity of the conclusions.

7 Acknowledgements

The authors would like to thank Malcolm Perry, Paul Nguyen Hong Duc, and Evgeny Sidenko for their assistance with field work, as well as Tony Scarangella and crew at Andro Maritime Services Australia for providing vessels and assistance with the field work. We would also like to thank Renee Schoeman for field support and for collecting the AIS data at Fremantle and Rottnest Island, and personally repaired the system every time it went offline. Thanks also to MMA Offshore Ltd and members of the Royal Australian Navy who recovered one of the sound recorders.

8 References

Amron A, Hidayat R, Sefnianti Y, Sari R (2021) Underwater noise of commercial vessels in Nusakambangan Strait and the relationship with distance. Omni-Akuatika 17:46-59

Anning J (2023) DOT415821 Westport Marine Geophysical Survey Area1 Factual Report. Surrich Hydrographics Pty Ltd

Ansmann IC, Goold JC, Evans PGH, Simmonds M, Keith SG (2007) Variation in the whistle characteristics of short-beaked common dolphins, *Delphinus delphis*, at two locations around the British Isles. Journal of the Marine Biological Association of the United Kingdom 87:19-26

Barclay D, Buckingham M (2013) Depth dependence of wind-driven, broadband ambient noise in the Philippine Sea. The Journal of the Acoustical Society of America 133:62-71

Barlett ML, Wilson GR (2002) Characteristics of small boat signatures. The Journal of the Acoustical Society of America 112:2221-2221

Baumann-Pickering S, Wiggins SM, Hildebrand JA, Roch MA, Schnitzler HU (2010) Discriminating features of echolocation clicks of melon-headed whales (*Peponocephala electra*), bottlenose dolphins (*Tursiops truncatus*), and Gray's spinner dolphins (*Stenella longirostris longirostris*). The Journal of the Acoustical Society of America 128:2212-2224

Baumgartner MF, Van Parijs SM, Wenzel FW, Tremblay CJ, Esch HC, Warde AM (2008) Low frequency vocalizations attributed to sei whales (*Balaenoptera borealis*). The Journal of the Acoustical Society of America 124:1339-1349

Bohnenstiehl DR, Lillis A, Eggleston DB (2016) The Curious Acoustic Behavior of Estuarine Snapping Shrimp: Temporal Patterns of Snapping Shrimp Sound in Sub-Tidal Oyster Reef Habitat. Plos One 11:e0143691

Branstetter BK, Moore PW, Finneran JJ, Tormey MN, Aihara H (2012) Directional properties of bottlenose dolphin (*Tursiops truncatus*) clicks, burst-pulse, and whistle sounds. The Journal of the Acoustical Society of America 131:1613-1621

Cato DH (1978) Marine biological choruses observed in tropical waters near Australia. The Journal of the Acoustical Society of America 64:736-743

Cato DH (1980) Some unusual sounds of apparent biological origin responsible for sustained background noise in the Timor Sea. The Journal of the Acoustical Society of America 68:1056-1060

Cato DH (1997) Ambient sea noise in Australian waters. Proc 5th International Congress on Sound and Vibration

Chion C, Lagrois D, Dupras J (2019) A meta-analysis to understand the variability in reported source levels of noise radiated by ships from opportunistic studies. Frontiers in Marine Science 6:714

Clarke D, Dickerson C, Reine K (2003) Characterization of underwater sounds produced by dredges. Proc Dredging '02: Key Technologies for Global Prosperity. American Society of Civil Engineers

Cockburn Sound Management Council (2018) State of Cockburn Sound Marine Area Report. Department of Water and Environmental Regulation, Government of Western Australia

Collins MD (1993) A split-step Padé solution for the parabolic equation method. The Journal of the Acoustical Society of America 93:1736-1742

Crocker SE, Fratantonio FD, Hart PE, Foster DS, O'Brien TF, Labak S (2019) Measurement of sounds emitted by certain high-resolution geophysical survey systems. IEEE Journal of Oceanic Engineering 44:796-813

Croll DA, Clark CW, Acevedo A, Tershy B, Flores S, Gedamke J, Urban J (2002) Only male fin whales sing loud songs. Nature 417:809

Deane GB (2000) Long time-base observations of surf noise. The Journal of the Acoustical Society of America 107:758-770

Duncan AJ, Gavrilov A, Hu T (2008) Using offshore seismic surveys as acoustic sources of opportunity for geoacoustic inversion. The Journal of the Acoustical Society of America 123:3365-3365

Duncan AJ, Gavrilov AN (2019) The CMST airgun array model—A simple approach to modeling the underwater sound output from seismic airgun arrays. IEEE Journal of Oceanic Engineering

44:589-597
Duncan AJ, Gavrilov AN, McCauley RD, Parnum IM, Collis JM (2013) Characteristics of sound propagation in shallow water over an elastic seabed with a thin cap-rock layer. The Journal of the Acoustical Society of America 134:207-215
Erbe C, Houser D, Bowles A, Porter MB (in press) Marine Mammal Acoustics in a Noisy Ocean. Springer Cham
Erbe C, Verma A, McCauley R, Gavrilov A, Parnum I (2015) The marine soundscape of the Perth Canyon. Progress in Oceanography 137:38-51
Etter PC (2018) Underwater Acoustic Modeling and Simulation. CRC Press, Boca Raton, FL, USA
Gales RS (1982) Effects of noise of offshore oil and gas operations on marine mammals - An introductory assessment. U.S. Naval Ocean Systems Center, San Diego, CA
Gavrilov A (2021) Feasibility and accuracy of multi-component models of ocean ambient noise to predict noise spectra on a short-time scale and assess long-term trends in noise components. Report for Office of Naval Research Global. Centre for Marine Science and Technology, Curtin University, Perth, Western Australia
Gavrilov AN, Parnum IM, Sidenko E, Tollefsen C (2024) Measuring the frequency characteristic of underwater sound recorders ST500 and ST600 from Ocean Instruments. In: Lyons S (ed). Proc Acoustics 2024, Acoustics in the Sun
Gavrilov AN, Parsons MJG (2014) A Matlab tool for the characterisation of recorded underwater sound (CHORUS). Acoustics Australia 42:190-196
Greene CR, Richardson WJ (1988) Characteristics of marine seismic survey sounds in the Beaufort Sea. The Journal of the Acoustical Society of America 83:2246-2254
Guerra M, Thode A, Blackwell S, Macrander M (2011) Quantifying seismic survey reverberation off the Alaskan North Slope. The Journal of the Acoustical Society of America 130:3046-3058
Hall MV (1996) Measurement of seabed sound speeds from head waves in shallow water. IEEE Journal of Oceanic Engineering 21:413-422
Hawkins LA, Saunders BJ, Landero Figueroa MM, McCauley RD, Parnum IM, Parsons MJ, Erbe C (2023) Habitat type drives the spatial distribution of Australian fish chorus diversity. The Journal of the Acoustical Society of America 154:2305-2320
Hiley HM, Perry S, Hartley S, King SL (2017) What's occurring? Ultrasonic signature whistle use in Welsh bottlenose dolphins (*Tursiops truncatus*). Bioacoustics: The International Journal of Animal Sound and its Recording 26:25-35
International Maritime Organization (IMO) (2015) Revised Guidelines For The Onboard Operational Use Of Shipborne Automatic Identification Systems (AIS). Accessed 11 Jun 2024. https://wwwcdn.imo.org/localresources/en/OurWork/Safety/Documents/AIS/Resolution%20A.1106(29).pdf
International Organization for Standardization (2017) Underwater acoustics—Measurement of radiated underwater sound from percussive pile driving (ISO 18406). Geneva, Switzerland
Jensen FB, Kuperman WA, Porter MB, Schmidt H (2011) Computational Ocean Acoustics. Springer-Verlag, New York
Kyhn LA, Sveegaard S, Tougaard J (2014) Underwater noise emissions from a drillship in the Arctic. Marine Pollution Bulletin 86:424-433
Lagrois D, Kowalski C, Sénécal J-F, Martins CCA, Chion C (2023) Low-to-Mid-Frequency Monopole Source Levels of Underwater Noise from Small Recreational Vessels in the St. Lawrence Estuary Beluga Critical Habitat. Sensors 23:1674
Lammers MO, Au WWL, Herzing DL (2003) The broadband social acoustic signaling behavior of spinner and spotted dolphins. The Journal of the Acoustical Society of America 114:1629-1639
Legg MW (2010) Non-Gaussian and non-homogeneous Poisson models of snapping shrimp noise PhD Thesis, Curtin University, Bentley, WA, Australia
Leroy EC, Samaran F, Bonnel J, Royer J-Y (2016) Seasonal and diel vocalization patterns of Antarctic Blue Whale (*Balaenoptera musculus intermedia*) in the southern Indian Ocean: A multi-year and multi-site study. Plos One 11:e0163587

Locascio JV, Mann DA (2011) Localization and source level estimates of black drum (*Pogonias cromis*) calls. The Journal of the Acoustical Society of America 130:1868-1879

MacGillivray AO, Ainsworth LM, Zhao J, Dolman JN, Hannay DE, Frouin-Mouy H, Trounce KB, White DA (2022) A functional regression analysis of vessel source level measurements from the Enhancing Cetacean Habitat and Observation (ECHO) database. The Journal of the Acoustical Society of America 152:1547-1563

Madsen PT, Wahlberg M, Møhl B (2002) Male sperm whale (*Physeter macrocephalus*) acoustics in a high-latitude habitat: implications for echolocation and communication. Behavioral Ecology and Sociobiology 53:31-41

Marley SA, Erbe C, Salgado Kent CP, Parsons MJG, Parnum IM (2017) Spatial and temporal variation in the acoustic habitat of bottlenose dolphins (*Tursiops aduncus*) within a highly urbanised estuary. Frontiers in Marine Science 4:197

Matuschek R, Betke K (2009) Measurements of Construction Noise During Pile Driving of Offshore Research Platforms and Wind Farms. Proc NAG/DAGA Int Conference on Acoustics

McCauley RD, Cato DH (2000) Patterns of fish calling in a nearshore environment in the Great Barrier Reef. Philosophical Transactions of the Royal Society of London B 355:1289-1293

McCauley RD, Gavrilov AN, Jolliffe CD, Ward R, Gill PC (2018) Pygmy blue and Antarctic blue whale presence, distribution and population parameters in southern Australia based on passive acoustics. Deep-Sea Research Part II: Topical Studies in Oceanography

McCauley RD, Thomas F, Parsons MJG, Erbe C, Cato D, Duncan AJ, Gavrilov AN, Parnum IM, Salgado-Kent C (2017) Developing an underwater sound recorder. Acoustics Australia 45:301-311

McKenna MF, Ross D, Wiggins SM, Hildebrand JA (2012) Underwater radiated noise from modern commercial ships. The Journal of the Acoustical Society of America 131:92-103

McKenna MF, Wiggins SM, Hildebrand JA (2013) Relationship between container ship underwater noise levels and ship design, operational and oceanographic conditions. Scientific Reports 3:1-10

Mellen RH (1952) The thermal-noise limit in the detection of underwater acoustic signals. The Journal of the Acoustical Society of America 24:478-480

Minnaert M (1933) On musical air-bubbles and the sounds of running water. The London, Edinburgh, and Dublin Philosophical Magazine and Journal of Science 16

Monczak A, Mueller C, Miller ME, Ji Y, Borgianini SA, Montie EW (2019) Sound patterns of snapping shrimp, fish, and dolphins in an estuarine soundscape of the southeastern USA. Marine Ecology Progress Series 609:49-68

Nedwell JR, Edwards B (2004) A review of measurements of underwater man-made noise carried out by Subacoustech Ltd, 1993–2003. Subacoustech Ltd, Hampshire, UK

Neves S (2013) Acoustic behaviour of Risso’s dolphins, *Grampus griseus*, in the Canary Islands, Spain. Ph.D. Thesis, University of St Andrews, St Andrews, Scotland

Ocean Instruments (2020) SoundTrap ST500 User Guide. Ocean Instruments

Ocean Instruments (2023) SoundTrap ST600 and ST640 User Guide. Ocean Instruments

Parks SE, Clark CW, Tyack PL (2007) Short- and long-term changes in right whale calling behavior: The potential effects of noise on acoustic communication. The Journal of the Acoustical Society of America 122:3725-3731

Parsons MJ, McCauley RD, Mackie MC (2013) Characterisation of mulloway *Argyrosomus japonicus* advertisement sounds. Acoustics Australia 41:196-201

Parsons MJG, Erbe C, Meekan MG, Parsons SK (2021) A review and meta-analysis of underwater noise radiated by small (<25 m length) vessels. Journal of Marine Science and Engineering 9:827

Parsons MJG, Salgado-Kent CP, Marley SA, Gavrilov AN, McCauley RD (2016a) Characterizing diversity and variation in fish choruses in Darwin Harbour. Ices Journal of Marine Science

Parsons MJG, Salgado-Kent CP, Recalde-Salas A, McCauley RD (2016b) Fish choruses off Port Hedland, Western Australia. Bioacoustics 26:135-152

Payne RS, McVay S (1971) Songs of humpback whales. Science 173:585-597

Pijanowski BC, Villanueva-Rivera LJ, Dumyahn SL, Farina A, Krause BL, Napoletano BM, Gage SH,

Pieretti N (2011) Soundscape Ecology: The Science of Sound in the Landscape. Bioscience 61:203-216
Porter M (2020) Acoustics Toolbox. Accessed 18 Mar 2024. http://oalib.hlsresearch.com/AcousticsToolbox/
Press WH, Teukolsky SA, Vetterling WT, Flannery BP (2007) Numerical Recipes: The Art of Scientific Computing. Cambridge University Press, Melbourne
Radford CA, Jeffs AG, Tindle CT, Montgomery JC (2008) Temporal patterns in ambient noise of biological origin from a shallow water temperate reef. Oecologia 156:921-929
Rankin S, Ljungblad D, Clark CW, Kato H (2005) Vocalisations of Antarctic blue whales, *Balaenoptera musculus intermedia*, recorded during the 2001/2002 and 2002/2003 IWC/SOWER circumpolar cruises, Area V, Antarctica. Journal of Cetacean Research and Management 7:13-20
Reinhall PG, Dahl PH (2011) Underwater Mach wave radiation from impact pile driving: Theory and observation. The Journal of the Acoustical Society of America 130:1209-1216
Robinson SP, Theobald PD, Lepper PA (2012) Underwater noise generated from marine piling. Proceedings of Meetings on Acoustics 17:070080
Salgado-Kent C, McCauley RD, Parnum IM, Gavrilov AN (2012) Underwater noise sources in Fremantle Inner Harbour: Dolphins, pile driving and traffic. Conference of the Australian Acoustical Society, 21-23 Nov 2012, Fremantle, Australia
Samarra FIP, Deecke VB, Miller PJO (2016) Low-frequency signals produced by Northeast Atlantic killer whales (*Orcinus orca*). The Journal of the Acoustical Society of America 139:1149–1157
Samarra FIP, Deecke VB, Vinding K, Rasmussen MH, Swift RJ, Miller PJO (2010) Killer whales (*Orcinus orca*) produce ultrasonic whistles. The Journal of the Acoustical Society of America 128:EL205-EL210
Schmidt H (2020) OASES - Ocean Acoustics and Seismic Exploration Synthesis. Accessed 18 Mar 2024. https://oalib-acoustics.org/website_resources/FFP/oases-public.zip
Simard Y, Roy N, Gervaise C, Giard S (2016) Analysis and modeling of 255 source levels of merchant ships from an acoustic observatory along St. Lawrence Seaway. The Journal of the Acoustical Society of America 140:2002-2018
Skene D, Ryan D, Brooke B, Radke L (2005) Report on the Geomorphology and Sediments of Cockburn Sound. Geoscience Australia, Canberra
Slabbekoorn H, Bouton N, van Opzeeland I, Coers A, ten Cate C, Popper AN (2010) A noisy spring: the impact of globally rising underwater sound levels on fish. Trends in Ecology & Evolution 25:419-427
Staaterman E, Clark C, Gallagher A, deVries M, Claverie T, Patek S (2011) Rumbling in the benthos: acoustic ecology of the California mantis shrimp Hemisquilla californiensis. Aquatic Biology 13:97-105
Stafford K, Moore S, Berchok C, Wiig O, Lydersen C, Hansen E, Kalmbach D, Kovacs K (2012) Spitsbergen's endangered bowhead whales sing through the polar night. Endangered Species Research 18:95-103
Thompson PO, Findley LT, Vidal O (1992) 20-Hz pulses and other vocalizations of fin whales, *Balaenoptera physalus*, in the Gulf of California, Mexico. The Journal of the Acoustical Society of America 92:3051-3057
Tindle CT, Zhang ZY (1992) An equivalent fluid approximation for a low shear speed ocean bottom. The Journal of the Acoustical Society of America 91:3248-3256
Todd VLG, Williamson LD, Jiang J, Cox SE, Todd IB, Ruffert M (2020) Proximate underwater soundscape of a North Sea offshore petroleum exploration jack-up drilling rig in the Dogger Bank. The Journal of the Acoustical Society of America 148:3971-3979
van Geel NCF, Risch D, Wittich A (2022) A brief overview of current approaches for underwater sound analysis and reporting. Marine Pollution Bulletin 178:113610
Wahlberg M, Jensen F, Soto N, Beedholm K, Bejder L, Oliveira C, Rasmussen M, Simon M, Villadsgaard A, Madsen P (2011) Source parameters of echolocation clicks from wild bottlenose dolphins

(*Tursiops aduncus* and *Tursiops truncatus*). The Journal of the Acoustical Society of America 130:2263-2274

WAMSI (2022) WAMSI Westport Marine Science Program - Science Plan 2022. Western Australian Marine Science Institution, The University of Western Australia, Crawley, WA

Ward R, Parnum I, Erbe C, Salgado-Kent CP (2016) Whistle characteristics of Indo-Pacific bottlenose dolphins (*Tursiops aduncus*) in the Fremantle Inner Harbour, Western Australia. Acoustics Australia 44:159-169

Wenz GM (1962) Acoustic ambient noise in the ocean: spectra and sources. The Journal of the Acoustical Society of America 34:1936-1956

Zhang Y, Tindle C (1995) Improved equivalent fluid approximations for a low shear speed ocean bottom. The Journal of the Acoustical Society of America 98:3391-3396

9 Appendices

9.1 One-third octave band power spectral density percentiles

Table 14. OTO band power spectral density percentiles (dB re µPa^2/Hz) for Site 1 (North Channel).

Frequency band (Hz)	1%	5%	25%	50%	75%	95%	99%
40	68.5	71.7	80.4	83	84.8	92.2	104.7
51	66.8	70.2	78.7	80.8	83.1	91.4	103.6
64	65.3	68.9	76.9	78.6	81.6	90.9	103.8
81	64.3	68.3	74.2	76.7	81.4	92.8	104.1
102	64.2	68.6	73	76.5	82.6	95.1	105.1
128	64.3	68.1	71.8	76.4	83.4	96	103.1
161	63	66.6	70.8	75.5	82.5	94.7	100.5
203	61.9	64.9	69.3	73.8	80.1	91.9	98.4
256	61.1	64.2	68.4	72.1	77.3	88.2	95.2
323	60.4	63.6	67.7	70.8	74.7	84.3	92.3
406	59.7	62.9	66.9	69.6	72.9	81.1	89.6
512	59.1	62.1	65.8	68.5	71.5	78.4	87.4
645	58.3	61.2	65.1	67.9	71.7	77.6	86.1
813	57.5	60.8	65.2	68.5	73.1	79.3	85.2
1024	56.9	59.8	63.7	67.8	74.3	82	85.7
1290	56.1	59.1	63.3	68.3	76.4	84.3	87.4
1625	54.6	58	62.7	68.6	78.8	86.9	90.1
2048	55	58.6	63.1	68.4	80	87.9	91.2
2580	54	57.4	62.5	68.4	80.1	87.7	91.1
3251	52.9	56.1	60.3	64.9	78.7	86	89.2
4096	50.7	54.6	60	64.5	77.2	83.9	86.9
5161	51.1	54.8	59.5	64.3	75.8	82.1	85.1
6502	51.5	54.3	58.5	63.6	74.3	81	84.5
8192	50.4	52.6	57.3	62.8	72.7	79.7	83.7
10321	48.4	51.1	55.9	61.3	70.8	77.3	80.2
13004	46.7	49.8	54.8	60.7	70	76.6	79.1
16384	44.9	47.6	52.6	58.9	68.5	75.2	77.8
20643	43.8	46.1	51	57	66.6	73.7	76.3
26008	42.4	44.9	49.7	55.6	64.9	72.1	75.3
32768	41.4	43.6	48.2	54	63.2	70.5	73.6
41285	38.4	39.9	43.9	49.4	58.4	65.5	68.8

Table 15. OTO band power spectral density percentiles (dB re µPa^2/Hz) for Site 2 (Inside Rock).

Frequency band (Hz)	1%	5%	25%	50%	75%	95%	99%
40	81.2	81.7	83.4	84.1	85.1	93.4	105.2
51	78.9	79.6	81.1	82	83.7	92.5	103.3
64	76.7	77.3	78.6	79.1	81.3	90.5	101.1
81	73.5	74.3	75.6	76.3	78.8	88.4	98.2
102	70.3	71.4	72.8	73.9	77.2	87.8	97.7
128	68.4	69.5	70.6	72.2	76.7	89.3	98.7
161	66.4	67.3	69	71.2	75.8	88.7	98.4
203	64.1	65.3	67.6	70.4	74.9	88.5	98.6
256	62.4	63.6	66.6	69.8	74	86.2	95.1
323	60.2	61.9	65.4	68.9	72.9	84.3	93
406	57.7	59.8	64.4	68	71.8	81.7	90.6
512	55.6	58.3	63.5	67.2	70.8	79.4	88.1
645	56.3	58.7	63.2	66.6	70	77.5	86.2
813	57.4	59.8	63.4	66.3	69.5	76.7	85.6
1024	58	60.5	63.6	66	68.8	75.5	84.4
1290	59.5	61.7	64.5	66.5	68.6	75.4	84.7
1625	60.9	62.9	65.5	67.3	69	75.8	84.8
2048	62.1	64	66.5	68.3	70.2	77.5	85.8
2580	61.6	63.7	66.4	68.2	70.4	78.6	86.4
3251	60.8	62.6	65.6	67.5	70.1	76.3	83.8
4096	60.8	62.4	65.6	67.9	70.7	76	83
5161	61	62.6	65.8	68.3	70.8	74.5	81
6502	60.6	62	65.7	67.5	70.5	73.1	79
8192	58.7	60.5	63.3	65.4	67.9	71.1	77.2
10321	53	54.5	57.5	60.7	63.6	68.4	72.9
13004	53	54.3	57.5	60.9	64	68.7	71.9
16384	50.8	52.5	56.1	59.9	62.8	67.5	71.4
20643	46.9	48.6	52.7	57	60.3	65.1	69.3
26008	44.7	46	50.1	54.2	58	62.9	67.3
32768	43.3	44.6	48.1	52	56.3	61.6	66.2
41285	40.3	41.5	44	47.1	51.3	56.9	62.7

Table 16. OTO band power spectral density percentiles (dB re µPa^2/Hz) for Site 3 (North Basin) – Deployment 1.

Frequency band (Hz)	1%	5%	25%	50%	75%	95%	99%
40	80.4	80.5	80.8	81	81.8	93	101.4
51	76.8	77.1	78.6	78.9	79.3	86.8	100.5
64	75.1	75.4	75.6	76.3	78.8	89.3	105.5
81	71.9	72	72.3	72.7	74.6	85.5	103.5
102	68.9	69.2	70	70.5	71.9	82.3	99.3
128	65.8	66.1	67	68.7	72.8	85.1	100.6
161	64.5	65	66.3	68.9	74.6	87.1	104.3
203	61.9	62.7	65.9	70	75.9	88.6	104.8
256	59.8	61.5	66	70.4	75.5	89.1	104.3
323	57.6	60.9	66.5	70.7	77.4	89	104.5
406	55.3	60.5	66.6	70.5	76.5	88.5	104.1
512	52.7	60.2	66.1	70	75.9	87	101.5
645	52.7	59.7	66	69.7	75.6	86.8	99.2
813	53	58.7	64.9	68.6	74.1	85.6	96.9
1024	52.4	57.9	63.8	67.6	73.8	85.1	94
1290	52.8	57.1	61.8	65.3	70.8	83.3	92
1625	50.5	55.3	59.7	62.8	67.6	79.4	88.4
2048	50.6	55.1	58.9	62.1	66.1	76	86.2
2580	51.6	54.4	57.9	61.1	64.4	73.5	82.3
3251	48.9	51.7	55.7	59.4	62.6	70.9	77.6
4096	45.4	51.8	55.6	59	62.1	71.4	77.8
5161	42.1	52.1	55.7	58.6	62	71.9	78.1
6502	40.2	51.9	55.4	57.9	61.1	70.6	76.9
8192	39.1	51.1	54.5	57.1	59.6	68.6	75.7
10321	39	49.3	52.6	55.7	57.9	65.8	72.7
13004	38.5	48.5	51.5	54.1	56.2	64	70.6
16384	38.4	47.9	50.7	53	54.9	62.4	68.4
20643	38.3	47	49.5	51.6	53.6	60.5	66.7
26008	38.3	45.8	48.1	50	52	58.8	65.2
32768	38.3	44	46	47.7	49.6	56.9	62.9
41285	38.8	42.4	44	45.6	47.5	55.2	61

Table 17. OTO band power spectral density percentiles (dB re µPa^2/Hz) for Site 3 (North Basin) – Deployment 3.

Frequency band (Hz)	1%	5%	25%	50%	75%	95%	99%
40	63.8	64	64.5	66.6	75.6	87.1	96.6
51	62.6	62.8	63.2	64.7	73.7	84.4	93.3
64	60.9	61.3	62.4	67.9	77.3	89.2	101.1
81	58.8	59.3	60.4	63.9	73.1	83.7	98.2
102	56.6	57.3	58.7	62.4	72	82.4	95.2
128	55.1	55.8	58.3	63.9	76.2	88.6	98.1
161	53.9	55	60	67	78	87.6	100.3
203	52.8	54.6	61.6	68.9	78.6	89.6	100.4
256	52.5	55.2	63	70.1	80.2	91.1	100.5
323	51.9	56.8	64.7	71.4	79.3	89.2	99
406	50.6	55.1	63.5	69.9	78.1	87.9	97.3
512	50.4	55.5	64	70	78.6	88	97.2
645	51	56	63.8	69.5	77	86.3	94.6
813	51	54.7	62.6	67.8	75.3	84.9	92.7
1024	51.2	55.1	61.5	66.7	74.3	83.2	90.6
1290	50.9	54.8	60.3	64.8	71.4	81.5	87
1625	50.3	53.7	58.4	62.7	68.2	77.8	83.5
2048	49.9	52.6	57.2	61	64.8	72.5	80
2580	48.9	51.2	56	59.5	62.6	68.8	78.3
3251	47.2	49.2	54.3	57.9	60.8	66.5	75.7
4096	47.2	48.9	53.5	57.4	60.2	66.1	75.7
5161	46.2	48	52.5	56.2	58.6	64.6	74.4
6502	46.8	48.5	52.6	56.3	58.4	63.9	73.7
8192	46.9	48.3	51.6	55.1	57.2	62.5	71.6
10321	47.1	48.3	51.3	54.8	56.9	61.7	69.9
13004	46.4	47.5	50.3	53.7	55.8	60.9	69.2
16384	46.4	47.4	49.9	53.1	55.3	61.3	69.4
20643	44.6	45.6	47.8	50.6	53	59.5	66.8
26008	42.9	43.8	45.9	48.5	50.9	57.8	66
32768	40.9	41.8	43.7	46.1	48.5	54.6	63.2
41285	39.2	40	42	44.1	46.4	51.9	58.9

Table 18. OTO band power spectral density percentiles (dB re µPa^2/Hz) for Site 4 (Central Basin).

Frequency band (Hz)	1%	5%	25%	50%	75%	95%	99%
40	64.7	66.8	71.1	76.8	83.2	88.3	95.5
51	63.1	64.4	67.7	72	80.2	84.9	96
64	62.9	64.5	67.7	73.7	78.9	85	94.9
81	60.4	61.9	65.2	71.2	76.7	82.7	93.9
102	56.9	58.5	61.5	65.8	73.5	79	93.2
128	55.1	56.6	60.2	65.3	71.5	78.8	92
161	53.9	55.8	59.9	65.6	70.2	80	93
203	53.3	55.9	60.5	66.3	70.2	82.1	95.4
256	54.3	56.8	62	66.5	71.1	83.2	96.2
323	54.9	57.6	63.3	67.2	71.9	83	95.3
406	54	57	62.6	66.8	71.6	82.5	94.1
512	52.8	56.5	62	66.1	70.4	81.6	93
645	51.5	55.2	60.9	65.1	69.6	80.4	90.6
813	51.2	54.7	60.5	64.4	68.7	78.7	90.3
1024	52	56.3	61.5	65.2	69.4	78.2	88.7
1290	52.2	55.9	60.3	63.6	67	74.7	86.2
1625	50.9	53.9	57.9	61.1	64.5	71.7	81.6
2048	48.6	51.1	54.9	58.5	62.4	69.1	79
2580	46.2	48.7	53	57.1	61.6	67.5	78
3251	45.9	47.9	52.7	56.8	61.4	67.4	78.1
4096	46	48.2	52.9	56.8	61.4	67.5	77.8
5161	46.7	48.8	53.2	56.7	60.6	67	77.4
6502	46.5	48.4	52.6	55.8	59.3	65	74.9
8192	47.9	49.5	53.1	55.9	59.6	64.7	74
10321	48.5	49.9	53	55.8	59.3	63.8	71.9
13004	48.1	50	53	55.5	58.5	62.7	70
16384	46.7	49.1	52.3	54.5	57.5	61.7	68.6
20643	46.4	47.9	51.2	53.4	56.6	60.7	67.7
26008	42.9	45.9	49.1	51	53.9	58.4	66.3
32768	39.2	43.1	46.3	48.1	50.7	55.7	64.1
41285	35.5	37.7	40.4	42.3	45	50.3	59.2

Table 19. OTO band power spectral density percentiles (dB re µPa^2/Hz) for Site 5 (Mangles Bay).

Frequency band (Hz)	1%	5%	25%	50%	75%	95%	99%
40	71.3	73.6	78.6	83.9	88.3	92.9	98.3
51	70	73	77.4	81.7	85.9	89.4	94.9
64	69.3	72.2	76.4	80.2	84.1	88	94.2
81	69.1	71.5	75.5	78.9	82.2	86.1	92.4
102	68	70.2	73.7	77.2	79.6	84.2	91.7
128	66.7	68.8	71.9	75.2	77.3	83.7	92
161	65	67	70.1	72.9	75.1	82.8	91.9
203	62.7	65.1	68.1	70.4	72.9	81.3	90.3
256	60.4	63.3	66.3	68.3	70.7	78.8	87.2
323	59.2	61.8	64.8	66.7	69	76.3	84.7
406	57.1	60	63	64.9	67	73.5	82.9
512	55.8	58.2	61.1	63.2	65.4	71.4	81.2
645	53.4	56.3	59.4	61.3	63.8	69.6	79
813	52	55.2	58.2	60.1	63.1	69	77.8
1024	53.1	55.1	57.7	59.9	63	69.6	77
1290	51.4	53.4	56.1	58.4	61	66.5	75.3
1625	48.1	50.8	53.8	56.1	58.9	65	74.1
2048	47.5	50.4	53.6	55.9	58.3	64	73.1
2580	46.1	48.5	51.5	54.6	57.5	63.6	73.2
3251	45.9	47.7	50.7	53.8	56.8	62.9	72.4
4096	46.1	47.3	50.3	53.5	56.7	63.1	72.6
5161	46.2	47.2	50.1	52.9	56	62.6	71.5
6502	46.4	47.3	49.7	52.1	54.9	61.2	69.2
8192	47.1	48	50	52.2	55	61	68.3
10321	47.4	48.2	50	52	54.7	60.2	66.9
13004	47.4	48.3	49.9	51.5	54.2	59.7	66.3
16384	46.9	47.8	49.3	50.7	53.6	59.1	65.2
20643	46.5	47.4	48.9	50.2	53.1	58.6	64.6
26008	45.2	46	47.4	49.2	52	58.1	64.9
32768	42.9	43.7	45.5	47.8	50.8	56.7	63.4
41285	37.4	38.2	39.7	41.7	45.1	50.7	57.5

Table 20. OTO band power spectral density percentiles (dB re µPa^2/Hz) for Site 6 (South Basin).

Frequency band (Hz)	1%	5%	25%	50%	75%	95%	99%
40	77.1	80.7	88.8	92.8	97.4	104.5	110
51	71	74.4	83.3	87.6	91.4	97.2	105
64	65.7	70.8	81.7	86.8	91.4	97.7	104
81	66	71.7	80.4	85.7	90.2	96.3	102.5
102	62.4	68.3	77.2	82.2	86.6	92.7	102.3
128	61.1	69.1	76.4	81.2	85.3	91.4	100.8
161	60.8	67.9	76.2	80.9	85.5	91.6	101.2
203	60.3	66.1	74.1	78.8	83.4	91	100.1
256	60.6	65.4	73.3	77.6	82.1	89.7	99.9
323	59.6	64.2	72.7	77.2	81	88.1	97.9
406	57.7	62.2	70.3	74.8	79.5	86.3	95.5
512	55.2	60.3	69.2	73.9	79.1	85.4	93.2
645	53.4	58.4	66.3	70.6	75.6	81.3	90.3
813	51.8	57.6	65.8	70	75.8	81.9	90.1
1024	52.2	56.9	65.6	70.5	76.5	82.1	88.7
1290	52.5	57.2	63.6	67.4	72.8	78.6	84.9
1625	50.7	55.1	61.4	65.5	71	77.4	83.3
2048	51.2	54.1	58.9	62.1	65.6	70.6	80
2580	48.8	51.2	56.1	59.5	62.8	68	78.2
3251	49.2	51.3	55.7	58.9	61.9	67	77.2
4096	49.6	51.2	54.5	57.3	60.3	65.9	75.9
5161	48.4	49.8	53.4	56.2	59.2	64.9	74.8
6502	48	49.3	52.6	55.5	58.4	64.3	73.7
8192	47.7	48.9	51.8	54.4	57.5	63.6	72.7
10321	47.8	48.9	51.7	54.2	57.1	63.4	72.1
13004	47.2	48.6	51.2	53.7	56.7	63.1	71.4
16384	46	47.5	50.2	52.8	56	62.4	70.3
20643	44.8	46.4	49.1	51.7	55.2	61.7	69.1
26008	43.1	44.8	47.3	49.8	53.5	59.8	67.5
32768	41.1	42.7	45	47.2	51.1	57.3	65
41285	36.5	37.7	39.8	41.7	45.5	51.7	59.6

Table 21. OTO band power spectral density percentiles (dB re µPa^2/Hz) for Site 7 (Kwinana Shelf South).

Frequency band (Hz)	1%	5%	25%	50%	75%	95%	99%
40	68.5	74.4	78.7	82.3	84	86.4	89.7
51	83.1	87.1	90.1	93.6	96.4	98.2	99
64	67.4	70.8	74	77.3	79.1	82.5	88.3
81	60.5	61.3	64	72	74.3	78.3	85
102	57.3	57.8	61.5	69.1	71.5	75.2	82.8
128	55.5	55.9	60.8	66.7	69.1	72.9	81.1
161	53.9	54.5	61.3	65.1	67.5	72.1	81.5
203	52.4	53.8	60.7	63.7	66.6	71.7	81.9
256	51.4	53.3	59.6	62.4	65.9	71.1	80.3
323	50.9	53.4	58.9	62.3	66.3	71.4	79.6
406	50.8	53.8	58.6	62.5	66.4	71.4	79.1
512	52	54.4	58.5	62.6	66.5	71.4	78.7
645	53.4	55.1	59	62.7	66.3	71.5	79
813	54.2	55.9	59.7	63	66.1	71.4	78.9
1024	55.7	57.5	60.9	63.6	66.1	70.9	78.1
1290	57.2	59	62.1	64.3	66.8	71.5	78.1
1625	58.4	60.1	63.1	65.3	67.7	72.2	78.9
2048	59.8	61.2	64	66	68.3	72.8	79.3
2580	59.4	62.3	65	66.8	69.1	74	81.3
3251	59.8	62.4	64.6	66.3	68.5	74.1	81.6
4096	60.1	61.9	63.6	65.8	67.6	74.3	81.6
5161	59.2	60.5	62.3	64.5	66.8	74.5	81.8
6502	57.4	58.7	60.7	62.9	65.5	73.6	79.9
8192	56	57.3	59.6	61.8	65.2	72.6	78.2
10321	54.5	55.9	59	61.1	65.1	71.3	75.8
13004	53.9	55.2	58.2	60.8	64.9	70.8	75
16384	51.3	53	56.6	59.5	63.7	69.1	72.9
20643	49.8	51.9	55.2	58.4	62.3	67.7	71.2
26008	46.8	49.4	53.3	56.7	60.9	66.6	70.3
32768	44	46.8	51.1	54.8	59	64.6	67.9
41285	38.9	41.2	45.6	49.3	53.5	59.2	62.4

Table 22. OTO band power spectral density percentiles (dB re µPa^2/Hz) for Site 8 (Kwinana Shelf North).

Frequency band (Hz)	1%	5%	25%	50%	75%	95%	99%
40	63.1	64.8	73.6	78.7	79.3	83.6	93
51	68.4	70.1	75.8	76.9	78.7	83.5	93
64	59.8	62.1	70.3	71.7	72.5	80.8	91
81	57.9	59.6	67	68.1	68.9	78.5	89.1
102	57	58.7	64.1	64.8	66.5	77	87.3
128	56.7	58.7	61.5	62.5	66.1	76	85.4
161	57.4	58.7	60.1	62.6	66.7	76	85.3
203	55.6	56.7	58.7	61.5	65.2	73.5	82.5
256	54.7	55.9	58.6	61.7	65.2	72.6	80.9
323	53.9	55.3	58.6	61.8	65.3	72.4	79.4
406	53.2	55	58.7	62.1	65.7	73	79.7
512	53.3	55.3	59.1	62.4	66.1	73.6	80.3
645	53.9	55.8	59.7	63	66.6	73.8	81.1
813	55.1	56.6	60.2	63.3	66.4	73.7	81.2
1024	56.6	58.3	61.4	64.1	66.9	74.4	81.3
1290	58	59.8	62.8	65.1	67.7	74.5	80.9
1625	60	61.8	64.8	67	69.6	75.9	81.6
2048	62.1	63.6	66.6	69	71.8	78	83.2
2580	63.3	65	67.9	70.4	73.1	79.6	84.7
3251	63.7	65.6	68.3	70.9	73.4	79.5	84.2
4096	63.8	65.7	68.2	70.8	73.3	78.9	83.6
5161	62.7	64.6	67.4	69.8	72.6	77.9	83
6502	61.2	62.7	65.8	68.1	71.7	76.9	81.9
8192	59.8	61.2	64.2	66.8	70.5	75.2	79.3
10321	59	60.3	63.4	66.3	70.2	74.6	78.4
13004	58	59.3	62.4	65.4	69.4	73.5	76.7
16384	56.4	58.3	61.5	64.3	68.3	72.3	75.1
20643	54.4	56.6	60.3	63	67.2	70.9	73.7
26008	52	54.8	58.4	61.2	65.4	69.3	72.2
32768	48.8	52.2	56.2	59.2	63.4	67.5	70.6
41285	42.8	46.3	50.6	53.6	57.9	62.2	65.7

Table 23. OTO band power spectral density percentiles (dB re µPa^2/Hz) for Site 9 (Owen Anchorage).

Frequency band (Hz)	1%	5%	25%	50%	75%	95%	99%
40	68.8	71.2	77.2	81.3	82.6	84.6	91.2
51	65.9	67.7	73.7	79.4	81	82.9	92.2
64	60.6	61.8	65.4	76	78	80	90.6
81	57.7	58.6	62.3	72.5	74.2	77	89.5
102	55.7	56.6	60.9	70.6	71.9	75.1	88.6
128	54.1	55.4	61.2	68.4	69.9	74.8	89.4
161	53	54.9	62.7	67.1	68.6	75.4	91.6
203	51.6	53.9	62.5	65	67.5	74.4	91.2
256	51.1	53.9	62	63.8	67.3	74.2	90.4
323	51.1	54.2	60.2	63.5	67.6	74.4	89.4
406	50.6	54.1	58.5	63.1	67.4	74	87.8
512	51.3	53.1	58	63	67.2	73.6	85.5
645	52.2	54.7	58.5	63.1	67.1	73.3	83.6
813	53.1	55.4	59.2	63.2	66.8	73.6	83
1024	54.2	56.4	60.2	63.5	66.8	74.2	81.9
1290	56.5	58.6	61.9	64.5	67.6	75.6	82.6
1625	58.2	60.6	63.7	66.1	69.5	77.9	83.9
2048	59.4	62.2	65.5	68.3	72	80.4	85.9
2580	58.5	61.7	66.6	69.7	73.7	82.9	87.9
3251	57.9	61.4	66.3	69.3	73.7	82.9	87.7
4096	57.8	60.9	67.2	70.2	74.5	82.7	86.9
5161	58.5	61	67.3	70.5	75.1	82.9	87.2
6502	59	61.3	66.9	70.5	75.2	82.7	86.8
8192	56.5	59	64.5	68.3	72.6	80.1	84.8
10321	52.8	55.5	61.6	65.2	69	76.3	80.4
13004	51	54.1	60.5	64.3	67.6	73.4	77.1
16384	49.7	52.9	59.3	63.3	66.5	71.9	75.4
20643	48.2	51.5	57.5	61.5	64.6	69.6	73.3
26008	47.2	50.7	56.5	60.3	63.4	68.1	71.6
32768	45.6	49.3	55.3	59.2	62.3	67	70.3
41285	44	46.4	51	54.6	57.8	62.4	65.8

9.2 One-twelfth octave band power spectral density percentiles

Table 24. One-twelfth octave band power spectral density percentiles (dB re µPa^2/Hz) for Site 1 (North Channel).

Frequency band (Hz)	1%	5%	25%	50%	75%	95%	99%
40	68.4	71.5	80.2	82.7	84.6	92.1	104.7
43	67.9	71.1	79.8	82.1	84.2	91.7	104.1
45	67.6	70.9	79.5	81.6	83.9	91.5	103.7
48	67.1	70.4	79.1	81.2	83.4	91	103
51	66.7	70.1	78.8	80.9	83.1	91	102.7
54	66.2	69.6	78.2	80.3	82.6	91.1	103.5
57	65.8	69.2	77.7	79.7	82.1	90.9	103.6
60	65.5	68.9	77.2	79	81.8	90.6	103.8
64	65.2	68.8	76.7	78.5	81.4	90.6	103.3
68	65	68.5	76.2	78	81	90.6	103.3
72	64.7	68.3	75.7	77.4	80.7	90.4	103.1
76	64.4	68.2	74.7	76.8	81	91.9	103.3
81	64.1	67.9	73.8	76.2	80.7	91.6	103.5
85	64.1	68	73.3	76	80.7	92.5	104.2
91	64	68.1	73.3	76.2	81.4	93.8	104.6
96	64	68.2	73	76.1	81.5	93.4	105.3
102	64.1	68.4	72.8	76.1	81.9	95.3	105
108	64.1	68.4	72.6	76.1	82.1	95.2	104.8
114	64.1	68.5	72.3	76.1	82.5	95.3	104.5
121	64.2	68.3	71.9	76	82.7	95.9	103.7
128	64.2	68	71.7	76.1	82.9	96.1	103
136	64.2	67.7	71.5	75.8	82.5	95.4	102.2
144	64	67.5	71.3	75.6	82.3	94.9	101.2
152	63.8	67.2	71.1	75.5	82.2	95	100.9
161	63.3	66.6	70.8	75.2	82	94.2	100
171	62.9	66	70.3	74.8	81.6	93.8	99.8
181	62.7	65.6	70	74.5	81.2	93.3	99.3
192	62.5	65.3	69.6	74	80.5	92.5	98.4
203	62.1	64.9	69.2	73.5	79.7	91.5	98
215	61.8	64.5	68.9	73.1	79.1	90.6	97.3
228	61.6	64.3	68.6	72.7	78.5	89.8	96.5
242	61.4	64.1	68.3	72.2	77.8	88.9	95.7
256	61.3	64	68.2	71.9	77.1	87.7	94.8
271	61.2	64.1	68.2	71.7	76.4	86.9	94.1
287	61.3	64.2	68.4	71.5	75.9	85.9	93.4
304	61	63.8	67.9	71	75.1	84.9	92.7
323	60.4	63.3	67.3	70.4	74.3	83.9	92
342	60.1	63.2	67.2	70.2	73.9	83	91.3
362	60.3	63.4	67.4	70.6	74.6	82.5	90.3
384	60.1	63.1	67.1	70	73.4	81.3	89.4
406	59.8	62.7	66.6	69.2	72.4	80.3	89.1
431	59.7	62.6	66.4	69.1	72.2	80.6	89.4
456	59.6	62.4	66.2	68.8	71.8	79.5	88.3
483	59.5	62.3	66	68.6	71.5	78.8	87.7
512	59.4	62.1	65.8	68.5	71.4	78.3	87.3
542	59.1	61.8	65.5	68.3	71.4	77.9	86.7
575	59	61.7	65.4	68.2	71.5	77.7	86.3
609	58.8	61.5	65.2	68	71.5	77.4	86
645	58.2	61	64.9	67.7	71.6	77.4	85.7
683	58.1	60.9	64.9	67.7	71.8	77.7	85.6
724	58	60.8	64.9	67.8	72.1	78.1	85.4
767	57.9	60.9	65.1	68	72.5	78.5	85.2
813	57.8	60.9	65.4	68.6	73.2	79.2	84.8
861	57.6	60.7	65.2	68.7	73.7	79.8	84.7
912	57.5	60.3	64.4	68	73.3	80.4	84.9
967	57.3	60	63.9	67.8	73.6	81.1	85
1024	57.2	59.8	63.6	67.8	74.1	81.8	85.5
1085	56.8	59.3	63.2	67.7	74.7	82.6	86.1
1149	56.6	59.2	63.2	67.9	75.2	83.1	86.5
1218	56.5	59.1	63.3	68.1	75.7	83.6	86.8
1290	56.4	59.1	63.4	68.3	76.3	84.2	87.2
1367	56.1	58.9	63.3	68.4	76.8	84.7	87.8
1448	55.8	58.7	63.1	68.5	77.5	85.5	88.5
1534	55.4	58.3	62.8	68.5	78.1	86.2	89.3
1625	54.8	57.9	62.6	68.5	78.7	86.8	89.9
1722	54.5	57.6	62.4	68.5	79.4	87.4	90.6
1825	54.3	57.5	62.3	68.4	79.8	87.8	91
1933	55	58.4	63.1	68.8	80	87.9	91.2
2048	55.8	58.9	63.5	68.7	80.3	88.2	91.6
2170	55.1	58.1	62.7	67.8	79.9	87.8	91.1
2299	54.7	57.8	62.5	67.5	79.9	87.7	91
2435	54.2	57.7	63.3	69.6	80.3	88	91.5
2580	54.5	57.6	62.7	69	80.5	88.3	91.9
2734	53.9	56.9	61.6	67.2	79.7	87.2	90.4
2896	53.4	56.4	60.8	65.9	79.3	86.8	89.9
3069	53.2	55.9	60	65	78.6	86.1	89.2
3251	53.3	55.9	59.9	64.7	78.6	86.2	89.6
3444	53.1	56.1	60.2	64.6	78.5	85.8	89.4
3649	51.9	55.5	60.4	64.9	77.9	84.7	88
3866	50.7	54.4	59.9	64.4	77.2	84	87.2
4096	51	54.7	59.8	64.3	77.1	84	87.2
4340	50.9	54.5	60	64.6	77	83.7	86.8
4598	51.2	54.8	60	64.6	76.6	83.1	86.2
4871	51.5	55	59.9	64.5	75.8	82.2	85.3
5161	51.4	54.8	59.5	64.3	75.5	81.7	84.8
5468	51.4	54.6	59.1	64.1	75.4	81.7	85.2
5793	51.6	54.5	58.6	63.6	75.3	82.1	86.1
6137	51.7	54.5	58.6	63.7	74.8	81.6	85.5
6502	52.1	54.6	58.8	63.7	73.9	80.4	83.7
6889	51.7	54.1	58.3	63.4	73.6	80.2	84.2
7298	51.6	53.7	58	63.2	73.4	80.2	84.5
7732	51.1	53.2	57.6	63	73.2	80.3	84.5
8192	50.6	52.7	57.3	62.8	72.8	80	84.2
8679	50	52.1	56.8	62.4	72	79	83
9195	49.3	51.5	56.2	61.4	70.9	77.7	81.4
9742	48.8	51.1	55.8	61.2	70.8	77.5	80.6
10321	48.8	51.2	55.9	61.3	70.9	77.4	80.5
10935	48.5	51.1	55.9	61.2	70.5	77.1	80
11585	48.1	50.8	55.8	61.3	70.3	76.9	79.7
12274	47.6	50.4	55.4	61.1	70.3	77	79.7
13004	47.2	49.9	54.8	60.6	69.9	76.7	79.3
13777	46.6	49.3	54.2	60.3	69.6	76.3	78.9
14596	45.9	48.7	53.6	59.7	68.9	75.7	78.3
15464	45.2	48.1	53	59.3	68.7	75.5	78.2
16384	45.2	47.6	52.6	58.9	68.5	75.2	78.1
17358	45	47.2	52	58.4	68.2	74.9	77.8
18390	44.5	46.6	51.4	57.7	67.5	74.3	77.1
19484	44.2	46.2	51	57.2	66.7	73.8	76.6
20643	44.2	46.1	50.9	56.9	66.5	73.6	76.6
21870	43.9	46	50.7	56.5	66	73.5	76.2
23170	43.7	45.8	50.6	56.3	65.7	73.3	76.4
24548	43.2	45.3	50.1	55.8	65.2	72.5	75.9
26008	42.5	44.7	49.5	55.2	64.6	71.9	75.4
27554	42	44.4	49.3	55.1	64.3	71.6	75
29193	41.9	44.3	49.2	55	64	71.1	74.4
30929	41.8	44	48.6	54.4	63.6	70.9	74.3
32768	41.6	43.6	48.1	53.9	63.1	70.5	73.9
34716	41.4	43.4	47.7	53.5	62.6	70	73.4
36781	41	42.7	46.9	52.6	61.9	69.2	72.5
38968	40.4	41.6	45.5	51.3	60.4	67.7	71
41285	38.4	39.7	43.5	49	58.1	65.3	68.8
43740	35	36.2	40.7	45.9	54.4	61.4	65
46341	31.1	31.8	35.5	41.9	49	55.8	59.8

Table 25. One-twelfth octave band power spectral density percentiles (dB re µPa^2/Hz) for Site 2 (Inside Rock).

Frequency band (Hz)	1%	5%	25%	50%	75%	95%	99%
40	80.5	80.9	82.7	83.3	84.5	93	104.4
43	80.2	80.4	82.1	82.6	84.1	92.8	103.9
45	79.3	80.4	81.4	82.6	84.3	92.8	103.5
48	78.7	80	81.6	82.6	84.3	92.7	103.6
51	79.1	79.8	81.5	82.4	84	92.4	103.1
54	77.9	79	80.4	81.7	83.1	91.6	102.6
57	76.1	77.3	78.8	80.8	82.1	91	101.6
60	75.8	76.7	78	79.4	81.3	90.5	101.2
64	76.5	77.2	78.2	79.2	81.2	90	100.4
68	75.7	76.4	78.3	79.6	81.3	89.7	99.5
72	74.2	75.5	77.8	78.9	80.5	89	99
76	72.5	73.8	75.4	77.2	78.9	88.2	97.9
81	71.9	72.8	74.6	75.9	78.2	87.6	97.5
85	70.9	71.8	74.8	76.5	78.6	87.4	97
91	69.9	71.5	74.1	75.5	77.9	87.2	97.1
96	68	68.8	71.4	74.1	76.6	86.5	96.3
102	69.4	70.4	72.7	74.1	76.8	86.7	96.6
108	69.2	70.7	73.1	74.4	77.2	87	97
114	66.6	67.5	70.5	73.4	76.3	87.4	97.6
121	67.4	68.8	71.6	73	76.5	87.6	97.9
128	66.1	68.4	71	72.8	76.4	87.8	97.8
136	65	66.5	69	71.7	75.7	87.9	97.9
144	65.1	67.4	70.2	71.9	75.8	87.4	97.4
152	63.5	65.1	69.2	71.3	75.4	87.2	96.8
161	64.8	66.7	69.3	71.4	75.4	87.3	96.8
171	63.5	65	68.6	70.9	75.1	87.5	97
181	64.2	66.1	68.5	70.9	75	87.6	97.3
192	63.6	64.9	67.8	70.4	74.7	87.5	97.8
203	63.8	65.1	67.7	70.4	74.6	87.4	97.9
215	63.7	65	67.4	70.1	74.3	86.9	96.8
228	62.6	63.8	66.8	69.8	74.1	86.6	96
242	63	64.2	66.9	69.9	74	85.9	95.1
256	62.7	63.8	66.7	69.8	73.9	85.4	94.4
271	62	63.2	66.3	69.6	73.6	84.9	93.8
287	61.4	62.7	66	69.3	73.3	84.6	93.6
304	61	62.4	65.7	69	73	84.3	92.9
323	60.6	61.9	65.4	68.8	72.8	83.7	92.8
342	60.1	61.5	65.2	68.6	72.6	83.4	92.1
362	59.4	61	64.9	68.4	72.3	82.8	91.6
384	58.7	60.4	64.6	68.1	72	82.1	90.9
406	57.9	59.8	64.3	67.9	71.8	81.3	90.2
431	57.2	59.3	64.2	67.8	71.5	80.7	89.8
456	56.7	58.9	63.9	67.5	71.2	80.3	89.3
483	56.1	58.5	63.6	67.3	71	79.6	88.5
512	55.9	58.3	63.5	67.1	70.7	79.2	87.8
542	55.7	58.2	63.3	66.9	70.5	78.7	87.3
575	56	58.3	63.2	66.8	70.3	78.1	86.8
609	56.2	58.5	63.2	66.6	70.1	77.6	86.5
645	56.5	58.8	63.2	66.6	69.9	77.2	86
683	56.8	59	63.2	66.5	69.8	77	85.7
724	57.1	59.3	63.3	66.5	69.7	76.9	85.6
767	57.5	59.6	63.4	66.4	69.6	76.7	85.5
813	57.7	59.9	63.4	66.3	69.4	76.6	85.5
861	57.8	60	63.5	66.2	69.3	76.4	85.6
912	57.9	60.1	63.4	66.1	69	76	84.8
967	58.1	60.2	63.4	66	68.9	75.5	84.3
1024	58.2	60.4	63.6	66	68.7	75.4	84.3
1085	58.4	60.7	63.7	66	68.6	75	84
1149	58.9	61	63.9	66.1	68.5	74.9	84.1
1218	59.4	61.4	64.2	66.3	68.6	75	84.1
1290	59.8	61.7	64.5	66.4	68.6	75.2	84.4
1367	59.9	61.9	64.7	66.6	68.6	75.2	84.4
1448	60.3	62.2	64.9	66.8	68.7	75.3	84.5
1534	60.6	62.5	65.1	67	68.8	75.3	84.5
1625	61	62.8	65.4	67.2	69	75.5	84.6
1722	61.5	63.2	65.7	67.5	69.2	75.7	84.7
1825	61.9	63.5	66.1	67.8	69.6	76.1	84.8
1933	62.1	63.8	66.4	68.1	70	76.6	85
2048	62.4	64	66.5	68.3	70.2	77.2	85.3
2170	62.4	64.2	66.6	68.4	70.4	77.8	85.9
2299	62.5	64.1	66.6	68.3	70.4	78.4	86.3
2435	62.3	64	66.6	68.4	70.5	78.7	86.5
2580	61.8	63.8	66.5	68.4	70.4	78.7	86.4
2734	61.4	63.4	66.3	68.1	70.4	78.2	85.9
2896	61.5	63.4	66.2	68	70.4	77.4	85.2
3069	61.4	63.2	66.1	67.9	70.4	76.8	84.5
3251	60.5	62.3	65.6	67.6	70.1	76	83.6
3444	60.6	62.2	65.1	67.1	69.6	75.2	82.4
3649	61	62.4	65.1	67.4	70.1	75.4	82.5
3866	60.6	62.1	65	67.4	70.1	75.6	82.8
4096	60.6	62.1	65.5	67.9	70.6	76	83.4
4340	61.2	62.7	66.1	68.4	71.3	76	83.2
4598	61.6	62.8	65.9	67.9	70.7	75.2	82.4
4871	61.3	62.7	65.3	67.4	70	74.4	81.4
5161	61.7	63.1	65.8	68.3	70.7	74.5	80.6
5468	60.7	62.3	65.8	69	71.3	74.9	80.5
5793	60.3	62.1	66	68	70.7	73.5	79.7
6137	60.5	61.9	65.8	67.7	70.6	73.2	79
6502	60.9	62.3	65.8	67.9	70.7	73.4	79.1
6889	61.2	62.4	65.7	67.6	70.4	73.1	79
7298	60.7	62	65.2	67	69.8	72.3	78.5
7732	60.7	62.2	65.2	67	69.7	72.3	78.5
8192	59.6	61	63.7	65.9	68.2	71.6	77.6
8679	56.2	58.1	60.6	63.1	65.4	69.4	75.6
9195	53	54.9	58.1	61.4	63.8	68.1	74
9742	52.6	54.1	57.2	60.6	63.5	68.2	73.4
10321	53.2	54.4	57.4	60.3	63.6	68.4	72.6
10935	53.4	54.7	57.7	60.8	63.6	68.4	72.2
11585	53.8	55	58.1	61.3	64.2	68.9	72.3
12274	53.5	54.8	58.1	61.5	64.3	69	72.1
13004	53.2	54.5	57.5	60.9	64.1	68.8	71.8
13777	52.8	54	57.1	60.4	63.7	68.5	71.8
14596	52.2	53.5	56.7	60.2	63.3	68.1	71.5
15464	51.5	53	56.3	60	63	67.9	71.5
16384	51.3	52.9	56.4	60.3	63	67.6	71.6
17358	50.5	52.1	55.8	59.8	62.7	67.1	71.2
18390	49.2	50.9	54.7	58.8	61.9	66.6	70.5
19484	47.9	49.6	53.4	57.6	60.9	65.7	69.5
20643	46.8	48.4	52.4	56.7	60.1	65	69.2
21870	46.1	47.4	52	56.4	59.6	64.5	68.8
23170	46	47.3	51.5	55.8	59.1	64	68.1
24548	45.5	46.6	50.7	54.8	58.3	63.2	67.7
26008	44.6	45.8	49.8	54	57.7	62.8	67.3
27554	44.4	45.6	49.5	53.5	57.4	62.5	66.9
29193	44.1	45.5	49.2	53.2	57.3	62.5	66.8
30929	43.8	45	48.6	52.5	56.9	62.1	66.7
32768	43.5	44.7	48.1	52	56.3	61.6	66.3
34716	43.1	44.2	47.6	51.5	55.8	61.1	65.9
36781	42.6	43.7	46.8	50.6	55	60.3	65.1
38968	41.9	42.8	45.6	49	53.5	58.9	64
41285	40.3	41.4	43.7	46.7	50.9	56.6	62.6
43740	36.9	38	41.2	43.9	47.5	53.9	61.1
46341	32.6	33.3	36	40.4	43.9	51.4	60

Table 26. One-twelfth octave band power spectral density percentiles (dB re µPa^2/Hz) for Site 3 (North Basin) – Deployment 1.

Frequency band (Hz)	1%	5%	25%	50%	75%	95%	99%
40	79.5	79.6	79.8	80	80.7	84.7	99.1
43	78.7	78.8	78.9	79	79.3	83.6	96.3
45	77.4	77.5	78.6	78.9	79.5	88.1	96.2
48	76.1	76.3	79.1	79.2	79.4	82.7	95.1
51	76.2	76.6	79.2	79.4	79.7	85.6	97.8
54	77.1	77.5	78.4	78.8	79.2	86.9	101.1
57	76.2	76.4	77	77.8	78.6	87.5	105.8
60	74.6	74.8	75.2	76.9	79.7	90.6	107.5
64	73.9	74.2	74.9	75.3	76	86.8	105.5
68	72.6	73	75.7	76.3	78.3	88.9	103.2
72	70.9	71.4	75.7	76	76.4	87.1	105.5
76	71.9	72.3	73.1	74.1	75.4	86.8	105.6
81	68.6	68.7	69.2	70.4	73.5	82.7	103.6
85	67.5	68.5	70.3	71.5	72.4	81.4	99.5
91	66.3	67.5	72.1	72.5	73.6	84.4	99
96	65.4	66.7	69.1	70.7	72	81.1	100.1
102	65.7	66	66.9	68.3	70.9	79.1	99.2
108	66.4	68.5	70.4	71.1	72.4	82.1	98.9
114	64	65.1	69.2	70.7	71.8	83.3	100
121	63.4	64	65.7	68	71.2	84.1	101.1
128	63.8	66.5	68.8	69.4	71.6	84.7	100.9
136	62	63.5	66.4	68.7	73.9	85.6	100
144	61	62	65	67.1	71	86.2	100.2
152	64.7	66.2	67.7	69.2	73.1	85.2	101.4
161	60.3	61.6	64.3	67.2	71.9	86	103.2
171	63.6	65.2	66.6	68.7	72.8	87.5	104.1
181	60.5	61.8	65	68.7	74.5	88.6	105.3
192	62.1	63.7	66	68.9	74	87.7	106.6
203	60.7	62.2	65.5	69.4	75.5	88.1	104.1
215	60.2	62.2	65.9	70.2	76.1	88.9	104.1
228	60.2	62.1	65.7	69.9	75.6	89.6	104.6
242	60.5	61.9	65.8	69.7	75	88.5	104.1
256	59.6	61.4	65.7	70.4	76	88.6	105.1
271	59.5	61.3	65.9	69.9	75.3	89.6	106.1
287	59.3	61.3	65.9	69.8	75.7	89.1	103.9
304	58.5	61.2	66.1	70	75.9	88.4	105.4
323	58	60.9	66.1	70.4	77	89.2	104.2
342	57.5	60.9	66.2	70.4	76.5	88.9	105.2
362	57.5	61.2	66.7	71	77.5	89.1	103.9
384	56.6	60.8	66.4	70.5	76.5	88.7	103.9
406	56.4	61	66.6	70.6	75.8	89	104.8
431	56.1	60.7	66.5	70.4	75.6	88.3	103.1
456	55.2	60.5	66.2	70	75.5	87.6	103.7
483	55.4	60.4	66.1	70	75.4	87	103.4
512	54.1	60.4	65.8	69.9	75.6	87	101.8
542	55.2	60.4	65.9	69.8	75.5	86.4	100.3
575	54.3	59.7	65.8	69.5	75.2	86.5	100
609	54.2	59.6	65.7	69.4	75	86.6	100.3
645	54.9	59.9	65.7	69.4	75.7	86.9	99.4
683	55.3	59.9	65.6	69.6	75.4	86.5	98.9
724	55.2	60	65.7	69.4	75.2	86.2	98.5
767	54.7	59.4	65.1	68.9	74.1	85.7	97.1
813	54.5	59.2	65	68.7	73.7	86	97
861	54.1	58.9	64.7	68.2	73.4	85.5	96.6
912	54.2	58.7	64.2	67.7	73	84.9	95.5
967	54	58.4	63.9	67.7	73.3	85.5	94
1024	54.3	58.4	63.9	68	74.1	86.2	94.4
1085	54.5	58	63.3	67.1	73.6	84.5	94
1149	54.5	57.7	62.6	66.3	72.6	84.4	93.2
1218	54.6	57.5	62.2	65.8	71.2	84.1	93
1290	54.8	57.5	61.8	65.3	70.4	83.7	92.1
1367	54.7	57.2	61.3	64.6	69.7	81.4	91.1

Frequency band (Hz)	1%	5%	25%	50%	75%	95%	99%
1448	54.2	56.7	60.7	64	69.1	81.7	90.1
1534	53.3	55.9	60	63.2	68.2	80.8	89.4
1625	52.6	55.3	59.4	62.6	67.3	78.9	88.5
1722	52.6	55.3	59.4	62.5	66.8	77.6	87.2
1825	52.8	55.3	59.1	62.3	66.4	76.6	87
1933	52.9	55.1	59	62.2	66.4	76.5	87
2048	53.2	55.2	58.9	62	65.9	76	86.2
2170	53.6	55.5	59	62.1	65.8	75.8	85.1
2299	53.7	55.4	58.7	61.8	65.4	74.7	85.2
2435	53.5	55.2	58.5	61.4	64.8	74	83.6
2580	52.9	54.5	57.9	61	64.2	73.4	81.7
2734	52.6	54	57.5	60.8	63.9	72.7	80.9
2896	52	53.4	57	60.5	63.8	72.2	79.8
3069	50.9	52.4	56.3	59.9	63.1	71.3	78.3
3251	50.2	51.6	55.6	59.4	62.6	70.7	77.4
3444	49.9	51.3	55.1	58.8	62	69.7	76.9
3649	50.1	51.4	55	58.5	61.6	70	77.3
3866	50.1	51.4	54.9	58.3	61.4	70.7	77.2
4096	50.7	52	55.6	58.9	62.1	71.3	77.8
4340	51.2	52.5	56.1	59.4	62.5	71.7	78.4
4598	51	52.3	56	59.5	62.6	72	78.6
4871	50.9	52.1	55.5	58.6	61.8	71.9	78.5
5161	51	52.2	55.6	58.4	61.8	71.8	78.7
5468	51.1	52.4	55.9	58.6	61.9	71.3	77.4
5793	51.1	52.5	55.9	58.7	62	71.4	77.7
6137	51.3	52.6	55.9	58.2	61	70	76.6
6502	50.4	51.8	55.1	57.4	60.2	69.1	75.3
6889	50.5	51.8	55.2	57.9	61.1	70.9	77.3
7298	50.8	52	55.2	57.6	60.8	70.5	77.7
7732	50.4	51.7	54.9	57.2	59.9	68.9	76.7
8192	49.9	51.2	54.4	56.9	59.2	68.3	75.5
8679	49.8	51.1	54.4	57.1	59.3	68.1	75.2
9195	49	50.3	53.6	56.5	58.6	66.6	73.6
9742	48	49.2	52.4	55.6	57.7	65.2	72.6
10321	48	49.2	52.5	55.5	57.7	65.1	72.9
10935	48.5	49.6	52.8	55.8	57.9	65.7	73.2
11585	48.3	49.4	52.4	55.2	57.4	65.3	72
12274	47.9	48.9	52	54.8	56.9	64.8	71.7
13004	47.7	48.7	51.6	54.1	56.1	63.8	70.8
13777	47.4	48.4	51.2	53.5	55.4	62.8	69.5
14596	47.1	48.1	50.8	53.1	55	62.3	68.9
15464	47.3	48.3	50.9	53.1	55.1	62.6	68.9
16384	47.3	48.3	51	53.1	54.9	62.3	68.7
17358	47.1	48	50.7	52.9	54.8	61.8	68
18390	46.7	47.7	50.2	52.4	54.2	61	67.3
19484	46.4	47.3	49.8	51.9	53.9	60.5	66.4
20643	46.3	47.1	49.5	51.4	53.2	60.2	66.1
21870	46.1	47	49.3	51.3	53.5	60.3	67
23170	45.9	46.9	49.2	51.2	53	60.1	67.1
24548	45.7	46.6	48.8	50.6	52.7	59.5	66.4
26008	45	45.9	48	49.8	51.7	58.4	65.4
27554	44.8	45.6	47.6	49.3	51.4	57.9	64.2
29193	44.2	45	47	48.7	50.8	57.1	63
30929	44	44.8	46.6	48.3	50.2	57.1	63.5
32768	43.3	44.1	45.9	47.5	49.4	56.4	63
34716	42.9	43.7	45.4	47.1	49.2	56.5	62.9
36781	42.6	43.3	45	46.6	48.6	55.9	61.9
38968	42.3	43	44.6	46.2	48.2	55.4	61.5
41285	42	42.7	44.2	45.7	47.6	55.3	61.4
43740	41.4	42.1	43.5	44.9	46.9	54.5	60.9
46341	40.9	41.5	42.8	44.1	45.9	53.3	59.7

Table 27. One-twelfth octave band power spectral density percentiles (dB re µPa2/Hz) for Site 3 (North Basin) – Deployment 3.

Frequency band (Hz)	1%	5%	25%	50%	75%	95%	99%
40	63.6	63.8	64.2	65.3	72.3	83.7	96.2
43	63.4	63.6	64	64.8	71.2	84.3	94.7
45	63.2	63.4	63.8	64.9	71	85.1	94.3
48	62.8	63	63.3	64.1	71.2	86.3	91.2
51	62.8	63	63.5	64.6	70.9	85.5	92
54	62	62.3	62.8	64.3	72.4	82.7	93.9
57	61.6	61.9	62.6	64.7	71.8	81.6	97.1
60	61.4	61.8	62.9	67.9	79.7	90.5	102.6
64	60.7	61.1	61.9	64.1	69.4	83.6	101.4
68	60.3	60.8	61.9	66.3	74.3	85.7	100.5
72	59.7	60.2	61.1	64.1	71.6	88.5	100.9
76	59.3	59.8	60.9	64.1	72.4	85.8	100.7
81	58.5	59.1	60	62.3	71.3	83.2	98
85	58.1	58.7	59.6	61.7	68	79.6	96.2
91	57.5	58.2	59.4	62.9	72.3	84.8	94.7
96	57.1	57.7	58.9	61.7	69.3	80	94.4
102	56.6	57.3	58.5	61.8	69.8	83	94.6
108	56.2	56.9	58.4	62	69.7	81.6	96.1
114	55.7	56.5	58	61.9	70.2	82.7	95.6
121	55.3	56.1	58.2	63.6	76	92.1	99
128	55	55.7	57.8	63.1	72.4	83.5	98.1
136	54.7	55.5	58.2	63.9	72.8	86.4	98.5
144	54.4	55.2	58.2	64.4	74.1	87.1	99.4
152	54.1	55	58.9	65.4	74.8	86.3	100.2
161	53.7	54.8	59	65.9	75.3	87.5	101.4
171	53.5	54.6	59.6	66.3	75.2	87.7	99.6
181	53.4	54.7	61	68.2	79.7	89	99.9
192	53	54.4	60.7	67.7	76.6	88.7	100
203	52.6	54.4	61.1	68.3	77.7	89.4	101.2
215	52.6	54.4	61.5	68.8	78.8	89.7	99.8
228	52.5	54.5	62.2	69.1	78.6	89.9	100.3
242	52.6	55.1	63	70.1	81.2	93.3	100.1
256	52.2	54.4	62.2	69.2	77.7	89.2	98.8
271	52.3	55.3	63.1	69.9	77.8	89.9	100.5
287	51.9	54.7	62.7	69.6	77.7	89.6	100.9
304	52.2	56.9	65.1	72	79.1	90.6	99
323	51.4	55	63.1	69.7	78.1	88.7	98.3
342	51.1	55	63.2	69.6	77.6	88.3	98.5
362	50.9	55.6	63.8	70.5	78.3	88.6	98.1
384	50.6	54.6	62.9	69.2	76.2	87.6	98.7
406	50.4	54.6	63.1	69.4	77.2	88.1	96.9
431	50.4	55.2	63.5	69.6	77.4	87.9	97.1
456	50.2	54.9	63.5	69.6	77.8	87.7	97.1
483	50.5	55.8	64.1	70	78.6	88	97.1
512	50.1	55	63.7	69.6	78.3	87.6	97.2
542	50.3	55.4	63.9	70	78.4	87.5	96.6
575	50.3	54.7	63.3	69.1	77.4	87	95.7
609	51.1	56.4	64.3	69.5	77.1	86.1	95
645	50.8	55.4	63.6	69.3	76.3	86.5	94.5
683	50.6	54.6	63	68.5	76.2	85.5	95
724	51	55.1	63.3	68.7	75.4	85.4	94.8
767	50.8	54.6	62.9	68.1	75.2	84.9	93.2
813	50.7	54.4	62.3	67.5	74.8	84.1	92.6
861	50.4	54.2	61.9	67.1	74.2	84.3	92.3
912	51.1	54.8	61.9	67.1	76.1	84.7	91.8
967	51	54.9	61.6	66.9	74.6	83.9	91.2
1024	51.4	55.3	61.5	66.7	74.4	83.2	91.2
1085	51.1	55	61.2	66.1	73	82.6	90.5
1149	50.9	54.8	60.7	65.6	72.7	82.2	89
1218	50.9	54.7	60.5	65.2	71.5	81.8	88.1
1290	50.8	54.6	60.2	64.6	71.3	81.5	87.6
1367	50.8	54.7	59.8	64.1	70.3	80.7	86.2

Frequency band (Hz)	1%	5%	25%	50%	75%	95%	99%
1448	50.8	54.6	59.5	63.8	70	79.9	86.1
1534	50.5	54	58.8	63.1	68.7	78.8	84.6
1625	50.1	53.5	58.3	62.7	68.4	77.4	83.4
1722	50.1	53.2	57.9	62	66.7	75.7	82.6
1825	49.9	53	57.5	61.4	65.7	75.4	81.8
1933	49.8	52.8	57.3	61.3	65.2	73.1	81.1
2048	49.8	52.5	57.1	60.8	64.4	72.4	80.1
2170	49.8	52.3	57	60.6	64.2	71.5	79.2
2299	49.6	52.1	56.7	60.2	63.6	70.7	79.4
2435	49.3	51.7	56.4	59.8	62.9	69.6	78.9
2580	48.7	51.1	55.9	59.3	62.5	68.5	77.6
2734	48.3	50.5	55.4	58.9	62	67.5	76.9
2896	48.1	50.3	55.1	58.5	61.3	67.1	76.1
3069	47.7	49.8	54.8	58.3	61.2	66.7	75.8
3251	47.5	49.5	54.6	58.2	61	66.7	75.8
3444	46.3	48.3	53.4	57.2	60.1	65.9	75.4
3649	46.3	48.2	53.1	57.1	60	65.9	75.4
3866	46.7	48.4	52.7	56.4	59.1	65	74.6
4096	46.3	48.1	52.7	56.8	59.8	65.3	74.8
4340	47.6	49.4	54	58.1	60.9	66.7	76.1
4598	47.9	49.8	54.3	57.9	60.2	66.5	76.5
4871	45.2	47.2	52.1	55.8	58.2	64.2	74.2
5161	45.2	47	51.4	55.4	57.8	63.5	73.2
5468	46.6	48.2	52.4	56.2	58.7	64.5	74
5793	47.2	48.9	53.1	56.7	59	65	74.8
6137	46.9	48.6	52.7	56.2	58.4	64	73.8
6502	46.7	48.4	52.5	56.2	58.4	63.5	73.2
6889	46.6	48.2	52.3	56.1	58.3	63.4	72.8
7298	46.8	48.3	52.1	55.4	57.3	62.7	72.4
7732	46.5	48	51.5	55	57.1	62.3	71.9
8192	47.2	48.6	51.9	55.3	57.3	62.6	71.9
8679	47	48.3	51.4	54.9	57	62.2	70.8
9195	47.1	48.5	51.6	55.1	57.3	62.1	70.3
9742	47.5	48.8	51.8	55.2	57.3	61.9	70
10321	46.8	48.1	51.1	54.7	56.8	61.3	69.5
10935	46.9	48.1	51.1	54.6	56.6	61	69.2
11585	46.7	47.8	50.7	54.2	56.2	61.2	69.6
12274	46.4	47.5	50.4	53.8	56	60.9	69.2
13004	46.2	47.4	50.2	53.5	55.6	60.7	68.8
13777	46.3	47.4	50.1	53.4	55.6	60.5	68.6
14596	46.5	47.6	50.1	53.5	55.7	61.1	69
15464	46.6	47.7	50.2	53.5	55.8	61.8	69.8
16384	46.5	47.6	50.2	53.4	55.6	61.6	69.7
17358	46.1	47.2	49.7	52.7	54.9	60.7	68.4
18390	45.5	46.6	49	51.8	54.1	60.4	67.6
19484	44.8	45.8	48.1	50.9	53.3	59.8	67.1
20643	44.6	45.5	47.8	50.6	52.9	59.4	66.7
21870	44.4	45.4	47.5	50.1	52.4	59.1	66.2
23170	43.9	44.9	47	49.8	52.1	58.7	65.8
24548	43.5	44.4	46.6	49.2	51.5	57.8	66.2
26008	42.7	43.6	45.8	48.4	50.7	57	66.2
27554	42.2	43.1	45.2	47.7	50.1	57.4	66.7
29193	41.7	42.6	44.6	47.1	49.5	56.2	64.9
30929	41.2	42.1	44.1	46.5	48.9	55.4	63.6
32768	41	41.8	43.8	46	48.4	54.1	61.8
34716	40.5	41.4	43.3	45.5	47.8	53.4	60.8
36781	40	40.9	42.9	45.3	47.7	53.7	60.2
38968	39.6	40.6	42.5	44.5	46.8	52.4	59.9
41285	39.2	40	41.9	43.9	46.1	51.8	58.7
43740	38.8	39.5	41.4	43.3	45.5	51	58.1
46341	38.2	38.9	40.7	42.6	44.7	50.1	57.2

Table 28. One-twelfth octave band power spectral density percentiles (dB re µPa2/Hz) for Site 4 (Central Basin).

Frequency band (Hz)	1%	5%	25%	50%	75%	95%	99%
40	63.4	65	68.6	73.8	82.1	87	94.8
43	62.9	64.4	67.6	72.8	81.4	86.3	94.3
45	63.5	65.8	69.8	75.4	81.5	86	93.8
48	62.6	63.9	66.5	71	80.2	84.7	93
51	63.8	65.1	68.5	72.1	79.9	84.2	92.2
54	62.3	63.5	67	72	79.7	84.1	91.9
57	62.2	63.2	65.8	70.8	78.9	83.8	92.5
60	63.3	64.8	68.2	73.3	79.2	84.6	94.1
64	61.9	62.8	65.5	70.8	78.2	84.4	94.4
68	62.7	64.3	67.9	74.4	78.8	85.5	95.2
72	61.1	62.1	65	70.9	77.3	84.3	95.3
76	61.2	62.6	66.5	72.9	77.8	84.4	94.4
81	59.4	61.1	63.8	69	75.9	82.1	92.9
85	58.7	60.4	63.1	67.9	75.3	80.6	92
91	58.5	60	62.7	67.1	74.8	79.9	90.9
96	57.1	58.8	61.7	65.9	73.9	78.5	89.9
102	56.8	58.4	61.2	65.2	73.3	77.8	89.6
108	56.2	57.7	61	65.1	72.7	77.5	90.3
114	55.7	57.1	60.5	64.6	72.2	77.2	90.7
121	55.4	56.9	60.3	64.7	71.8	77.4	91.5
128	54.9	56.5	60.2	65	71.4	77.5	91.6
136	54.7	56.2	60	64.9	71	77.6	91.7
144	54.1	55.6	59.4	64.2	70.5	77.6	91.8
152	53.7	55.4	59.3	64.3	70.2	78.5	91.8
161	53.3	55.1	59.3	64.6	69.9	79.1	92.5
171	53.3	55.4	59.3	64.9	69.6	79.3	93.1
181	53.6	55.7	60.2	66	69.8	80.2	93.1
192	52.9	55	59.7	65.5	69.5	80.5	93
203	53.2	55.6	60.1	66	69.9	81.2	93.1
215	52.8	55.7	60.5	66.2	70.2	81.9	94.3
228	53.1	56.2	61.1	66.1	70.4	82.2	95.6
242	53.8	56.3	61.2	66.1	70.7	82.3	95.7
256	53.2	56.1	61.3	66.1	70.7	82.9	95.8
271	54.2	56.9	62.3	66.5	71.2	83.6	96.2
287	53.8	56.5	62.4	66.4	71.1	83.8	95.8
304	54	56.7	62.3	66.4	71.1	82.7	95.1
323	53.9	56.9	62.7	66.8	71.4	82.6	95.2
342	53.8	56.8	62.6	66.7	71.4	82.5	94.7
362	54.8	57.8	63.2	67.5	72.2	82.3	94.5
384	54	56.7	62.4	66.6	71.5	81.9	94.5
406	53.9	56.7	62.3	66.5	71.4	81.8	93.5
431	53.2	56.8	62.4	66.6	71.3	82	93.4
456	52.8	56.5	62.1	66.4	70.8	81.8	92.7
483	53.2	56.7	62.2	66.4	70.8	82	93.2
512	52.5	56.1	61.8	65.9	70.2	81.5	92.9
542	52.2	55.7	61.3	65.4	69.7	80.6	92.7
575	51.7	55.1	60.7	64.9	69.4	80.3	91.2
609	51.3	54.8	60.3	64.8	69.3	79.8	90.6
645	51.1	55	60.6	64.9	69.4	79.3	89.8
683	51	54.6	60.5	64.8	69.4	79.6	90.4
724	50.8	54.6	60.7	64.9	69.2	79.8	91.4
767	50.3	54.3	60.2	64.1	68.7	79.2	91
813	50.5	54.3	60.1	64	68.5	78.5	90.3
861	50.9	54.7	60.3	64.2	68.4	78	89.8
912	50.8	54.9	60.5	64.4	68.7	78	89.6
967	51.6	55.5	60.9	64.8	69	77.9	89
1024	51.9	56.2	61.8	65.6	70	79.4	88.9
1085	52.1	56.2	61.3	64.9	68.9	77.7	88.2
1149	52.3	56	60.9	64.3	68	76.4	87.7
1218	52.4	55.9	60.7	64	67.5	75.3	86.9
1290	52.4	55.8	60.3	63.5	66.8	74.5	86.1
1367	52.1	55.1	59.4	62.8	66.2	73.6	85.3

Frequency band (Hz)	1%	5%	25%	50%	75%	95%	99%
1448	51.8	54.7	58.9	62.3	65.7	72.8	84
1534	51.5	54.1	58.4	61.5	64.8	72	82.4
1625	51.2	53.8	57.8	60.9	64.2	71.3	81.2
1722	50.7	53.1	57.1	60.3	63.8	70.7	80.3
1825	50.1	52.4	56.3	59.6	63.1	69.8	79.6
1933	49.2	51.5	55.3	58.7	62.5	69.2	79.3
2048	48.5	50.7	54.6	58.3	62.2	68.8	78.8
2170	48	50.2	54.4	58.1	61.9	68.3	78.6
2299	47.2	49.5	53.8	57.6	61.6	67.8	78.7
2435	46.4	48.8	53.2	57.1	61.3	67.2	77.8
2580	46.3	48.6	52.8	56.9	61.5	67.3	77.7
2734	45.9	48	52.6	56.8	61.4	67.4	77.7
2896	46	48	52.6	56.7	61.4	67.3	77.5
3069	45.9	47.9	52.6	56.7	61.3	67.3	77.8
3251	46.1	48.1	52.7	56.7	61.2	67.4	78.2
3444	46	47.9	52.6	56.5	61.2	67.3	77.9
3649	45.9	47.9	52.6	56.5	61.2	67.4	77.7
3866	46	48	52.7	56.6	61.2	67.4	77.9
4096	46.2	48.1	52.8	56.7	61.4	67.6	78
4340	46.4	48.3	53	56.8	61.4	67.5	77.5
4598	46.7	48.7	53.2	56.9	61.2	67.5	77.5
4871	46.9	48.8	53.1	56.7	61.1	67.5	77.5
5161	46.8	48.7	53.1	56.6	60.8	67.1	77.4
5468	47	48.9	53.2	56.6	60.1	66.4	77.1
5793	46.9	48.8	53.1	56.3	59.9	65.9	76
6137	46.3	48.3	52.6	55.8	59.4	65.2	74.8
6502	46.3	48.2	52.4	55.6	59	64.5	74.6
6889	46.8	48.6	52.5	55.6	59.1	64.5	74.6
7298	47.3	48.9	52.7	55.7	59.3	64.6	74.2
7732	47.9	49.4	52.9	55.8	59.4	64.6	73.9
8192	48	49.4	53	55.9	59.5	64.6	73.8
8679	48.4	49.8	53.2	56.1	59.7	64.7	73.7
9195	48.5	50	53.3	56.1	59.5	64.3	72.9
9742	48.3	49.7	53	55.8	59.3	63.9	72.4
10321	48.6	49.8	53.1	55.8	59.2	63.6	71.7
10935	48.9	50	53.1	55.8	59.2	63.6	71.4
11585	49	50.1	53	55.7	59	63.3	70.6
12274	48.9	49.9	52.9	55.5	58.7	63	70.3
13004	49	50.1	53	55.5	58.4	62.7	70
13777	49.3	50.3	53.3	55.6	58.2	62.3	69.3
14596	49.1	50.1	53	55.1	57.7	62	69.2
15464	48.7	49.7	52.6	54.8	57.5	61.8	68.8
16384	48.3	49.2	52.4	54.5	57.5	61.8	68.5
17358	47.8	48.8	52.1	54.3	57.3	61.6	68.3
18390	47.7	48.7	52	54.2	57.2	61.4	68.1
19484	47.6	48.6	51.8	54	57.1	61.1	67.7
20643	46.8	47.9	51.3	53.4	56.4	60.6	67.5
21870	46.4	47.5	50.8	52.9	56.1	60.3	67.3
23170	46.2	47.3	50.4	52.4	55.6	59.8	67.2
24548	45.6	46.7	49.7	51.6	54.6	59	66.8
26008	44.7	45.8	49.1	50.9	53.8	58.3	66.3
27554	44.5	45.6	48.6	50.3	53.1	57.7	65.6
29193	43.8	44.8	47.9	49.6	52.3	57	65.2
30929	42.9	43.9	47.1	48.9	51.5	56.3	64.7
32768	42.3	43.3	46.4	48.2	50.7	55.6	64.2
34716	41.6	42.6	45.4	47.2	49.8	54.8	63.5
36781	40.3	41.3	44.2	46	48.6	53.9	62.6
38968	39	39.9	42.6	44.4	47	52.3	61.2
41285	36.5	37.5	40.1	41.9	44.6	49.9	58.9
43740	33.6	34.5	36.9	38.6	41.3	46.4	55.5
46341	30.3	31	33	34.5	37.2	41.9	51.2

Table 29. One-twelfth octave band power spectral density percentiles (dB re µPa2/Hz) for Site 5 (Mangles Bay).

Frequency band (Hz)	1%	5%	25%	50%	75%	95%	99%
40	70.7	73.4	78.1	83.3	87.7	91.4	96.6
43	70.5	73.3	77.9	82.9	87.2	90.9	95.9
45	71.4	73.5	78.3	83.2	87.3	91.7	96.5
48	69.9	73	77.5	82.1	86.2	89.8	95.1
51	69.5	73	77.4	81.7	85.8	89.5	95
54	69	72.7	77.2	81.3	85.4	89.1	94.8
57	69.1	72.5	76.8	80.8	84.8	88.7	94.7
60	69.8	72.4	76.7	80.7	84.6	88.6	94.7
64	68.4	72.1	76.3	80	83.8	87.9	94.4
68	68.6	72.1	76.2	79.8	83.6	87.6	93.8
72	67.9	71.7	75.8	79.3	83	86.9	93.3
76	69.5	71.7	75.8	79.3	82.7	86.7	92.8
81	68.5	71.3	75.3	78.6	81.9	85.9	92.2
85	68	71	74.8	78.2	81.4	85.4	92.1
91	68.5	70.9	74.9	78.2	81	85.1	91.8
96	68.2	70.5	74	77.5	80.1	84.3	91.4
102	67.7	70.1	73.5	77.1	79.4	83.9	91.5
108	67.3	69.8	73.1	76.7	78.9	83.7	91.6
114	66.2	69.4	72.6	76.2	78.3	83.7	91.8
121	67.3	69.1	72.3	75.7	77.7	83.4	92
128	65.6	68.7	71.7	75	77.1	83.1	91.8
136	66	68.4	71.5	74.6	76.7	82.9	92
144	66.3	67.9	71	74	76.1	82.8	91.9
152	65.4	67.6	70.6	73.6	75.7	82.8	91.9
161	64.6	67	70	72.7	74.8	82.2	91.8
171	63.6	66.5	69.4	71.9	74.2	81.9	91.7
181	62.8	66	68.9	71.4	73.6	81.4	91.1
192	62.5	65.4	68.3	70.7	73	81.1	90.5
203	62.6	65.1	68.1	70.3	72.7	80.9	90.2
215	62.5	64.7	67.7	69.9	72.3	80.6	89.4
228	61.6	64.2	67.1	69.2	71.7	79.8	88.8
242	60.5	63.7	66.6	68.6	71	78.9	87.5
256	59.8	63.2	66.1	68.1	70.5	78.3	87
271	60.3	62.9	65.8	67.8	70.2	77.8	86.3
287	60	62.5	65.5	67.4	69.7	77.3	85.8
304	58.6	62.1	65.1	66.9	69.2	76.6	85.1
323	58.6	61.7	64.7	66.6	68.8	76	84.5
342	58.6	61.4	64.4	66.4	68.6	75.6	84.1
362	58.8	61	64.1	66	68.1	74.7	83.5
384	57.4	60.4	63.4	65.2	67.3	73.8	82.9
406	56.6	60	62.9	64.8	66.9	73.3	82.6
431	56.5	59.5	62.5	64.4	66.5	72.9	82.4
456	56.1	59.1	62	64.1	66.4	72.5	82.1
483	56.3	58.6	61.5	63.8	66	72	81.5
512	55.8	58.1	61	63	65.3	71.2	81.3
542	55.5	57.7	60.6	62.6	64.8	70.7	80.8
575	53.9	57.1	60.2	62	64.3	70.1	80.1
609	53.2	56.5	59.7	61.6	64.1	69.8	79.3
645	53.2	56.2	59.4	61.4	63.8	69.5	78.7
683	53	56	59	60.9	63.4	69.3	78.2
724	52.6	55.6	58.7	60.5	63.2	69.1	77.9
767	51.7	55.1	58.3	60.2	63	68.9	77.7
813	51.6	55	58.1	60	62.9	68.8	77.6
861	51.9	55	57.9	59.9	63	69	77.5
912	52.2	55	57.7	59.8	62.8	68.8	77.5
967	52.4	55	57.6	59.8	62.5	68.8	77.3
1024	52.8	55.1	57.6	59.8	63.1	70.6	77.5
1085	53	55	57.6	59.8	62.8	69.8	76.5
1149	52.8	54.7	57.4	59.6	62.5	68	75.8
1218	52	54	56.8	59.1	61.9	67.4	75.4
1290	51.2	53.3	56.1	58.3	61	66.4	75.1
1367	50	52.4	54.9	57	59.7	65.6	74.8

Frequency band (Hz)	1%	5%	25%	50%	75%	95%	99%
1448	49	51.4	54.2	56.4	59.2	65.2	74.6
1534	48	50.4	53.7	56	58.9	65	74.3
1625	47.5	50	53.3	55.8	58.8	64.9	74
1722	47.8	50.4	53.5	56.1	58.9	64.9	73.7
1825	48.2	50.6	53.7	56.4	58.9	64.6	73.3
1933	48	50.7	53.9	56.4	58.8	64.3	72.9
2048	47.4	50.3	53.5	56	58.4	63.8	72.9
2170	46.7	49.7	53.1	55.4	57.8	63.5	72.9
2299	46	48.7	52.3	54.7	57.3	63.3	72.9
2435	45.3	48.4	51.6	54.4	57.3	63.4	73
2580	45.7	48.1	51.2	54.6	57.6	63.7	73.1
2734	46.4	47.8	51.2	54.7	57.5	63.5	72.9
2896	46.3	48	51.2	54.4	57	62.9	72.3
3069	45.9	47.8	50.8	53.8	56.6	62.4	71.8
3251	45.6	47.6	50.6	53.7	56.8	62.8	72.1
3444	45.6	47.3	50.3	53.5	56.7	62.9	72.5
3649	45.8	47.2	50.3	53.6	56.7	62.9	72.4
3866	46	47.3	50.4	53.6	56.7	63.1	72.6
4096	46.1	47.5	50.4	53.5	56.7	63.2	72.8
4340	46.1	47.3	50.1	53.3	56.6	62.9	72.2
4598	46	47.1	50.1	53.3	56.4	62.9	72
4871	46.2	47.3	50.3	53.3	56.4	63	72.1
5161	46.4	47.4	50.2	53	56	62.7	71.6
5468	46	47	49.8	52.6	55.5	62	70.7
5793	45.9	46.9	49.6	52.3	55.2	61.6	70
6137	46.1	47	49.5	52.1	54.9	61.2	69.2
6502	46.4	47.3	49.7	52.2	54.8	61	69.1
6889	46.5	47.4	49.6	51.9	54.7	61	68.8
7298	46.7	47.6	49.7	52	54.7	61	68.8
7732	46.8	47.6	49.8	52.1	54.9	61	68.5
8192	47.2	48	50	52.3	55.1	61.1	68.2
8679	47.3	48.2	50.1	52.3	55	60.9	68
9195	47.2	48.1	50	52.2	54.9	60.4	67.4
9742	47.1	47.9	49.8	51.9	54.7	60.1	67
10321	47.2	48	49.8	51.9	54.6	60	66.8
10935	47.6	48.4	50.1	51.9	54.7	60.2	66.7
11585	47.7	48.6	50.2	51.9	54.7	60.2	66.7
12274	47.6	48.5	50.1	51.7	54.4	59.9	66.5
13004	47.4	48.4	49.9	51.5	54.2	59.7	66.3
13777	47.1	48	49.6	51.2	53.9	59.3	66.1
14596	46.9	47.9	49.4	50.9	53.7	59.1	65.6
15464	46.9	47.8	49.3	50.8	53.6	59.1	65.3
16384	46.8	47.6	49.1	50.6	53.5	58.9	65.1
17358	46.8	47.7	49.2	50.7	53.6	58.9	65
18390	46.8	47.7	49.3	50.8	53.7	58.9	64.8
19484	46.6	47.5	49	50.4	53.3	58.6	64.6
20643	46.2	47.2	48.7	50.1	52.8	58.3	64.4
21870	46.4	47.3	48.7	50.1	52.9	58.4	64.5
23170	45.9	46.8	48.3	49.8	52.5	58.2	64.5
24548	45.3	46.2	47.7	49.3	52	58	64.7
26008	45.1	45.9	47.3	49.2	52.1	58.2	65.1
27554	44.9	45.6	47.2	49.2	52	58	65.1
29193	44.2	44.9	46.6	48.8	51.6	57.6	64.6
30929	43.6	44.3	46	48.4	51.4	57.3	64.2
32768	43	43.8	45.6	48	50.9	56.7	63.5
34716	42.1	42.9	44.7	47	50.2	55.9	62.6
36781	41.1	41.9	43.7	45.8	49.2	54.7	61.5
38968	39.4	40.2	41.7	43.7	47	52.6	59.5
41285	37.1	37.8	39.3	41.2	44.6	50.1	57.2
43740	33.7	34.3	35.6	37.6	41.2	46.7	54
46341	30.2	30.6	31.7	33.3	36.8	42.3	49.6

Table 30. One-twelfth octave band power spectral density percentiles (dB re µPa2/Hz) for Site 6 (South Basin)

Frequency band (Hz)	1%	5%	25%	50%	75%	95%	99%
40	71.9	75	81.8	85.1	89.6	97.6	107.2
43	73	75.8	82.1	85.3	89.4	96.4	106.2
45	72.4	78.3	87.8	93.5	99.1	106	111.4
48	72	74.4	80.4	83.7	87.9	94.5	103.8
51	72.7	75.2	82.5	87	91.2	97.5	103.6
54	66	71.7	81.8	86.6	91	97.6	104.4
57	63.8	68.6	78.4	82.2	86.6	93.6	103.6
60	65.9	70.6	82.5	87.5	92.4	99.8	105.8
64	63.7	67.7	76.5	80.2	84.8	92.2	103.1
68	65	71.6	80.8	86.3	91.5	99.3	104.8
72	65.2	69.6	76.4	80.1	84.3	93.2	105.9
76	65.4	70.7	80	85	89.9	97.2	103.6
81	64.3	69.9	78.4	83.1	87.5	95.3	102.6
85	63.8	70	77.7	82.3	86.6	93.6	101.8
91	64.7	71.4	79.9	85.2	90.4	98	104.3
96	62	67.8	76.3	80.9	85.6	92.6	101.6
102	61.2	66.7	75.1	79.9	84.3	92.1	101.2
108	60.7	67.5	76.3	81.4	86.4	93.9	101.5
114	61.5	67.5	74.6	79.1	83.9	91.2	100.5
121	61.1	68.7	76.3	80.5	84.8	92.1	100.8
128	60.7	67.7	75.3	79.6	83.7	90.9	100.8
136	60.5	68	75.8	81.1	86.2	93.4	100.8
144	60.3	67.1	74.4	79.6	84.3	91.1	100.9
152	60.4	67.8	75.1	80.5	85.4	92.9	101.6
161	59.9	66.9	74.4	78.8	83	90.6	100.8
171	60	65.8	73.1	77.7	81.6	90.2	101
181	61.3	67	75.4	80.3	85.6	93	100.4
192	59.9	65.4	72.3	77.7	83.1	90.8	100.2
203	60.3	65.5	73.7	78.7	83.6	91.3	99.8
215	59.7	65.1	73.8	78.4	82.7	91	100.4
228	60	65.3	73.1	77.3	81.1	90	100.5
242	60	65.3	73.2	77.5	81.3	89.5	99.8
256	59.9	64.4	71.5	76.3	81	88.8	99.9
271	60.6	65.2	72.9	77.7	82.8	90.3	100.2
287	59.9	64.3	72.5	77.4	82.7	90.9	99.4
304	59.4	63.9	72.4	77	81.2	88.8	97.8
323	59	63.6	71.7	76.6	80.5	87.7	98.1
342	58.8	63.3	70.3	74.4	78	86.8	97.5
362	59.2	63.7	71	75.2	79.5	86.4	96.7
384	58	62.4	69.6	74.1	79	87	95.9
406	57.5	62.1	70.1	74.6	79.4	86.6	95.3
431	57	61.4	70	74.6	79.6	86.2	95.1
456	56.3	60.5	69.5	74.2	78.5	86.1	94.8
483	55.5	60.6	69.6	74.2	79.2	85.7	94.4
512	54.7	59.8	68.7	73.7	79.2	86.1	93.4
542	54.2	59.3	68.5	73.6	78.8	84.9	92
575	53.7	58.8	67	71.8	76.6	83.1	91.4
609	53.4	58.3	65.9	70.3	74.6	80.4	89.9
645	53.1	58.1	65.7	70.1	75.1	81.2	89.3
683	52.8	57.7	65.2	69.6	74.6	81.4	90.2
724	52.6	57.5	65.6	69.8	74.9	81.4	90.5
767	51.5	57.2	65.1	69.3	74.3	80.6	90.7
813	51	57.2	65.6	69.9	75.3	81.7	90.9
861	51.5	57.1	65.6	69.9	76.2	83.1	89.6
912	52	56.8	65.2	69.8	76.2	82.3	89.1
967	52.2	56.7	65.3	70.4	76.5	82.2	88.5
1024	51.9	56.7	65.4	70.4	76.3	83.7	90
1085	51.6	56.4	65	69.9	75.3	81.4	87.6
1149	51.6	56.7	64.6	69	74	79.7	86.3
1218	52.6	57.2	63.9	68.2	73.2	79.1	86
1290	52.5	56.7	63	67	72.3	78.8	85.4
1367	51.4	55.9	62.3	65.9	71.5	78.1	84.6

Frequency band (Hz)	1%	5%	25%	50%	75%	95%	99%
1448	50.2	54.8	62	65.7	71.4	79	85.4
1534	49.4	54.2	61.1	65.3	71.1	78.6	84.3
1625	49.8	54.5	61.2	65.7	71.2	77.5	83.6
1722	50.7	54.7	61.3	65.4	70.1	75.9	82.9
1825	51.1	54.8	60.5	64	67.7	73.1	81.9
1933	51.3	54.3	59.4	62.8	66.2	72.1	80.6
2048	51	53.7	58.4	61.6	64.9	70	79.7
2170	50.3	52.9	57.7	60.9	64.6	70.2	79.2
2299	49.1	51.8	56.7	60.1	63.3	69.3	78.8
2435	48.3	51.2	56.3	59.7	63.2	68.9	78.4
2580	48.3	50.8	56	59.5	62.9	68	78.1
2734	48.3	50.3	55.2	58.8	61.7	66.7	77.6
2896	48.4	50.5	55.3	58.8	61.8	67.1	77.6
3069	48.6	50.7	55.6	58.8	61.9	67.1	77.5
3251	48.8	51.1	55.9	59.1	62.2	67.4	77.3
3444	49.2	51.4	55.5	58.8	61.7	67.1	76.8
3649	49.6	51.5	55.1	58.1	60.9	66.4	76.5
3866	49.9	51.7	55.1	57.8	60.7	66.4	76.3
4096	49.4	51.1	54.4	57.2	60.4	66	75.8
4340	49.2	50.6	53.9	56.8	59.8	65.3	75.5
4598	48.8	50	53.5	56.5	59.5	65	75
4871	48.5	49.7	53.4	56.3	59.4	65	74.8
5161	48.3	49.8	53.4	56.2	59.2	64.9	74.9
5468	48.1	49.7	53.3	56.1	58.9	64.9	74.7
5793	47.7	49.3	52.9	56	58.9	64.8	74.4
6137	47.8	49.2	52.7	55.9	58.7	64.4	73.8
6502	48	49.4	52.7	55.6	58.5	64.1	73.6
6889	48.1	49.3	52.5	55.1	58	64.2	73.5
7298	47.6	48.8	51.9	54.6	57.8	63.8	73.1
7732	47.5	48.7	51.7	54.4	57.5	63.5	72.6
8192	47.5	48.7	51.6	54.3	57.5	63.7	72.8
8679	47.9	49.1	51.9	54.5	57.5	63.7	72.6
9195	47.8	49	51.9	54.5	57.4	63.5	72.3
9742	47.7	48.8	51.7	54.4	57.3	63.4	72.2
10321	47.8	48.9	51.6	54.1	57.1	63.3	72
10935	47.9	49.1	51.7	54.1	57	63.4	72.1
11585	48	49.1	51.7	54.1	57	63.4	71.9
12274	47.8	49	51.5	53.9	56.9	63.3	71.5
13004	47.5	48.7	51.2	53.6	56.8	62.9	71.3
13777	47.2	48.5	51	53.5	56.6	62.8	71.2
14596	46.8	48.1	50.7	53.2	56.3	62.6	70.9
15464	46.4	47.7	50.4	52.9	56.1	62.4	70.4
16384	46.2	47.5	50.2	52.8	56.1	62.4	70.3
17358	46	47.3	50	52.6	56	62.4	70
18390	45.9	47.2	49.9	52.5	56	62.3	69.9
19484	45.4	46.9	49.6	52.1	55.6	61.9	69.4
20643	44.7	46.2	48.9	51.5	55	61.5	68.9
21870	44.6	46.1	48.8	51.3	55	61.5	68.9
23170	44.2	45.7	48.3	50.9	54.5	60.9	68.6
24548	43.6	45	47.7	50.3	53.9	60.2	67.8
26008	43.5	44.8	47.2	49.7	53.5	59.9	67.5
27554	43.2	44.5	46.9	49.3	53.2	59.4	67.1
29193	42.6	43.9	46.3	48.6	52.5	58.6	66.4
30929	42.1	43.3	45.6	47.9	51.9	58	65.8
32768	41.6	42.8	45.1	47.3	51.2	57.3	65.1
34716	40.8	42	44.3	46.4	50.3	56.3	64
36781	40	41.1	43.3	45.4	49.3	55.4	63.2
38968	38.5	39.6	41.8	43.7	47.6	53.7	61.7
41285	36.6	37.6	39.6	41.4	45.2	51.3	59.4
43740	34	34.8	36.6	38.2	41.6	47.7	56
46341	31.5	32	33.3	34.6	37.4	43.1	51.9

Table 31. One-twelfth octave band power spectral density percentiles (dB re µPa2/Hz) for Site 7 (Kwinana Shelf South).

Frequency band (Hz)	1%	5%	25%	50%	75%	95%	99%
40	67.3	72.7	77.4	81.3	83.2	86.3	89.9
43	67.7	73.2	77.8	81.6	83.3	86.2	89.9
45	69.6	74.9	79.6	82.4	84.2	86.6	90.1
48	80	83.6	86.8	90.5	93.5	95.3	96.2
51	87.6	90.1	94.6	98.5	101.5	103.3	104.1
54	77.6	80.1	84	89.4	91.1	92.5	93.6
57	68.5	72.3	75.9	78.6	80.5	84.4	90.1
60	68.3	72.1	75.9	78.6	80.3	83.9	89.3
64	65.5	68.9	72	75.9	78.1	82	87.8
68	67.7	70.3	73.5	76.8	78.6	82	86.9
72	63.2	64.7	67.5	73.7	76	80.1	85.6
76	61.6	62.7	65.1	72.6	75	79.1	84.9
81	59.7	60.4	63.3	71.5	74.1	78.3	83.9
85	58.9	59.6	62.6	70.8	73.4	77.5	83.3
91	58	58.7	61.9	70.2	72.6	76.6	82.6
96	57.5	58.1	61.5	69.3	71.9	75.9	81.9
102	57.6	58.2	61.7	68.9	71.5	75.3	81.7
108	56.5	57	60.9	68.1	70.6	74.6	81.2
114	56.1	56.6	60.6	67.5	70	74	80.4
121	55.8	56.2	60.6	66.9	69.4	73.4	80
128	55.4	55.8	60.6	66.4	68.9	73	79.9
136	55.2	55.6	60.6	65.9	68.5	72.5	79.5
144	54.6	55	60.6	65.5	68	72.2	79.7
152	54.3	54.8	60.8	65.1	67.7	72	79.7
161	53.9	54.4	61	64.8	67.4	71.9	79.9
171	53.5	54.2	61.1	64.6	67.3	72	80.3
181	53.1	54.1	61.1	64.3	67.1	72	80.7
192	52.7	53.9	60.8	63.9	66.8	71.8	80.6
203	52.4	53.7	60.6	63.6	66.6	71.6	80.7
215	52.2	53.6	60.2	63.2	66.3	71.4	80.5
228	51.9	53.4	59.9	62.8	66	71.2	79.7
242	51.6	53.3	59.6	62.5	65.8	71	79.3
256	51.5	53.2	59.4	62.3	65.7	70.9	79.4
271	51.1	53.1	59.2	62.2	65.8	71.1	79.6
287	50.9	53	59.1	62.2	65.9	71.1	79.6
304	50.9	53.1	59	62.2	66	71.3	79.4
323	51	53.3	58.9	62.3	66.2	71.4	79.2
342	50.9	53.4	58.7	62.3	66.2	71.3	79.1
362	50.7	53.5	58.6	62.2	66.2	71.2	79.1
384	50.7	53.6	58.6	62.2	66.2	71.2	78.7
406	50.8	53.7	58.6	62.4	66.4	71.4	78.7
431	50.8	53.8	58.6	62.5	66.4	71.4	78.7
456	51	54	58.5	62.5	66.4	71.3	78.6
483	51.5	54.1	58.5	62.5	66.4	71.4	78.7
512	51.8	54.1	58.4	62.5	66.4	71.4	78.6
542	52.3	54.4	58.5	62.5	66.3	71.3	78.4
575	52.7	54.5	58.5	62.4	66.3	71.4	78.5
609	53	54.7	58.6	62.5	66.2	71.4	78.6
645	53.3	55	58.9	62.5	66.1	71.3	78.4
683	53.6	55.2	59.2	62.7	66.2	71.4	78.9
724	53.7	55.3	59.3	62.8	66.2	71.5	79.3
767	53.9	55.5	59.4	62.8	66.1	71.8	79.1
813	54.1	55.8	59.7	62.9	66	71.5	78.8
861	54.3	56.1	59.8	63	65.9	71.1	78.2
912	54.6	56.3	60	63.1	65.8	71	78.2
967	55	56.8	60.4	63.3	65.8	70.7	78.1
1024	55.7	57.6	61.1	63.7	66.2	70.8	78.1
1085	55.9	57.7	61	63.6	66.1	70.9	78
1149	56.3	58	61.2	63.8	66.3	71	78
1218	56.8	58.5	61.6	64	66.5	71.2	78.1
1290	57.1	58.9	62	64.3	66.8	71.4	78.1
1367	57.4	59.2	62.4	64.6	67	71.7	78.1
1448	57.7	59.6	62.7	64.9	67.2	71.9	78.2
1534	58	59.8	62.9	65.1	67.4	71.9	78.4
1625	58.3	60	63.1	65.3	67.7	72.2	78.8
1722	58.6	60.3	63.4	65.6	68	72.4	79.2
1825	58.9	60.6	63.6	65.7	68.1	72.5	79.4
1933	59.3	61	63.8	65.8	68.2	72.4	79
2048	59.7	61.3	64	65.9	68.2	72.7	79.1
2170	60.2	61.5	64.2	66.2	68.5	73	79.2
2299	60.5	61.8	64.6	66.5	68.8	73.6	80.1
2435	60.8	62.1	64.8	66.7	69	73.9	80.9
2580	61.2	62.5	65.1	66.9	69.3	74.1	81.3
2734	61.4	62.7	65.2	66.9	69.2	74.1	81.7
2896	61.4	62.5	65	66.6	68.8	74	81.7
3069	61.4	62.5	64.8	66.5	68.7	74.1	82.1
3251	61.5	62.5	64.8	66.4	68.6	74.2	81.6
3444	61.6	62.5	64.5	66.2	68.3	73.9	81.1
3649	61.4	62.4	64.2	66.2	68.1	74.1	81
3866	61.2	62.3	64	66	67.9	74	81.4
4096	61.1	62.2	63.8	66	67.8	74.1	81.5
4340	60.6	61.6	63.3	65.4	67.4	74.4	81.6
4598	60.2	61.1	62.8	65	67	74.1	81.7
4871	60.3	61.2	62.9	65.1	67.2	74.4	81.6
5161	60.2	61.1	62.6	64.9	67	74.5	81.8
5468	59.2	60	61.8	63.9	66.4	74.2	81.8
5793	58.3	59.4	61.4	63.5	66.1	74.3	81.9
6137	58.4	59.3	61.1	63.3	65.7	73.4	80.4
6502	58.1	59	60.7	63	65.4	72.8	79.4
6889	57.3	58.3	60.3	62.4	65.4	73.2	79.6
7298	57.4	58.1	60	62.3	65.3	73	79.1
7732	56.9	57.6	59.6	61.8	65.2	72.5	78.5
8192	56.4	57.4	59.6	61.8	65.2	72.3	78.1
8679	56.2	57.3	59.7	61.8	65.3	72.2	77.6
9195	55.6	56.7	59.3	61.4	65.1	72.2	77.7
9742	55.3	56.3	59.1	61.1	65	71.4	76.3
10321	54.7	55.8	58.9	61	65	71.1	75.9
10935	54.7	55.9	58.9	61.2	65.2	70.8	75.4
11585	55.3	56.4	59	61.4	65.3	71	75.4
12274	55	56.1	58.7	61.3	65.3	71.1	75.5
13004	54.6	55.6	58.4	61	65	70.9	75.3
13777	53.8	54.8	57.9	60.5	64.6	70.4	74.8
14596	52.5	53.5	57.1	59.8	64.1	69.8	74.3
15464	52.2	53.5	56.8	59.6	63.8	69.3	73.5
16384	52.1	53.4	56.7	59.6	63.7	69	72.8
17358	51.7	53.1	56.4	59.4	63.5	68.8	72.6
18390	51.4	52.9	56.2	59.2	63.2	68.4	72.2
19484	51.1	52.5	55.7	58.8	62.8	68	71.8
20643	50.5	51.9	55	58.2	62.1	67.5	71.3
21870	50.2	51.8	54.9	58.2	61.9	67.2	71
23170	49.3	51.1	54.5	57.7	61.6	66.8	70.9
24548	48.5	50.2	53.7	57.1	61.1	66.7	70.8
26008	47.8	49.8	53.4	56.8	60.9	66.6	70.6
27554	47.1	49.2	53	56.5	60.6	66.3	70.2
29193	46.4	48.5	52.4	55.9	60	65.9	69.7
30929	45.7	47.9	51.9	55.5	59.6	65.2	68.9
32768	45.2	47.3	51.4	55.1	59.1	64.6	68.1
34716	44.3	46.3	50.4	54.1	58.3	63.8	67.2
36781	43.2	45.1	49.4	53.1	57.3	62.8	66.1
38968	41.6	43.5	47.7	51.4	55.6	61.2	64.6
41285	39.4	41.2	45.4	49	53.2	59	62.5
43740	36.3	37.8	41.9	45.4	49.6	55.6	59.3
46341	32.5	33.7	37.4	40.7	45	51.2	55.3

Table 32. One-twelfth octave band power spectral density percentiles (dB re µPa2/Hz) for Site 8 (Kwinana Shelf North).

Frequency band (Hz)	1%	5%	25%	50%	75%	95%	99%
40	62.1	64	72.4	78.2	78.9	83	93
43	63	64.6	72.7	78	78.6	83	92.8
45	64.2	65.8	73.9	77.6	78.3	83.4	92.8
48	65.6	67.2	75	76.7	77.9	82.8	92.5
51	70.3	73.1	77.1	78.9	80.9	84.7	92.7
54	66.8	69.5	74.5	75.5	78	83.2	92.6
57	61.1	63.1	71.4	73.6	74.3	82.1	91.9
60	60.5	62.7	70.8	72.6	73.5	81.2	91.2
64	59.4	61.6	69.9	71.6	72.4	80.3	90.5
68	59.4	61.6	69.5	70.7	71.5	79.7	90.2
72	58.5	60.3	68.5	69.9	70.4	78.9	89.6
76	58.2	59.9	67.7	68.9	69.5	78.4	89.4
81	57.7	59.4	66.9	67.9	68.8	78	88.9
85	57.4	59.1	66.2	67.4	68.1	77.8	88.7
91	57.2	58.8	65.4	66.3	67.4	77.4	88.1
96	57	58.7	64.7	65.5	66.8	77	87.7
102	56.9	58.6	63.9	64.8	66.3	76.7	87.2
108	56.8	58.5	63.4	64	66	76.2	86.7
114	56.7	58.4	62.8	63.4	65.8	75.9	86.2
121	56.6	58.3	62	62.7	65.6	75.7	85.7
128	56.5	58.4	61.4	62.3	65.7	75.6	85.2
136	56.7	58.7	60.8	62.2	66.1	75.7	84.9
144	57	59.1	60.5	62.4	66.5	76	84.9
152	57.3	59	60.3	62.6	66.7	76.2	85.2
161	57.4	58.7	60.1	62.7	66.7	76	85.4
171	57.2	58.3	59.9	62.5	66.4	75.3	85
181	56.8	57.7	59.5	62.2	65.9	74.3	84.2
192	56.2	57.2	59	61.7	65.4	73.6	83
203	55.4	56.6	58.5	61.3	64.9	73.1	82.2
215	54.8	56.1	58.3	61.1	64.7	72.7	81.4
228	54.6	55.9	58.2	61.2	64.8	72.4	80.9
242	54.5	55.8	58.4	61.5	65	72.3	80.7
256	54.6	55.8	58.5	61.6	65	72.2	80.5
271	54.6	55.8	58.7	61.7	65.2	72.3	80.1
287	54.5	55.7	58.7	61.8	65.2	72.3	79.9
304	54.1	55.5	58.7	61.8	65.2	72.1	79.2
323	53.7	55.1	58.4	61.7	65.2	72	78.9
342	53.4	54.8	58.3	61.6	65.2	72.2	79
362	53.3	54.8	58.3	61.8	65.4	72.3	79
384	53.3	55	58.5	61.9	65.5	72.4	78.9
406	53.2	55	58.6	62	65.6	72.6	79.2
431	53.1	54.9	58.6	62	65.7	73	79.9
456	52.9	54.9	58.6	62	65.7	73	79.8
483	53	55.1	58.8	62.2	65.8	73.2	80.2
512	53.2	55.2	59	62.3	66	73.3	80.6
542	53.3	55.3	59.1	62.5	66.1	73.4	80.3
575	53.3	55.3	59.2	62.6	66.2	73.5	80.4
609	53.6	55.5	59.5	62.8	66.4	73.5	80.6
645	53.7	55.7	59.7	63	66.5	73.5	80.1
683	53.9	55.8	59.8	63.1	66.5	73.7	81
724	54.4	56.1	60	63.2	66.6	73.7	82.1
767	54.6	56.2	60	63.2	66.4	73.6	81.5
813	54.9	56.4	60.1	63.1	66.3	73.6	80.9
861	55.2	56.7	60.2	63.2	66.2	73.6	80.4
912	55.7	57.1	60.5	63.4	66.4	73.9	81
967	56.1	57.7	60.9	63.7	66.6	74.1	81
1024	56.5	58.2	61.4	64.1	66.8	74.2	81
1085	56.8	58.5	61.6	64.2	67	74.5	81.6
1149	57.1	58.8	61.9	64.4	67.1	74.5	81.3
1218	57.4	59.2	62.2	64.6	67.3	74.3	80.9
1290	57.9	59.7	62.7	64.9	67.5	74.4	80.7
1367	58.4	60.2	63.1	65.3	68	74.7	80.9

Frequency band (Hz)	1%	5%	25%	50%	75%	95%	99%
1448	58.8	60.7	63.6	65.8	68.5	75	80.9
1534	59.3	61.2	64.2	66.3	69	75.3	81.1
1625	59.9	61.7	64.7	66.9	69.6	75.8	81.6
1722	60.4	62.2	65.2	67.4	70.1	76.4	82
1825	60.8	62.5	65.7	67.9	70.7	76.6	81.9
1933	61.2	62.9	66.2	68.5	71.4	77.3	82.5
2048	62.2	63.7	66.7	69	71.8	78	83.2
2170	62.5	64	67	69.4	72.1	78.5	83.8
2299	62.7	64.3	67.3	69.7	72.5	78.9	84.2
2435	63.3	64.8	67.7	70.2	72.9	79.5	84.9
2580	63.9	65.3	68	70.6	73.3	79.9	85.3
2734	63.9	65.3	68.1	70.5	73.2	79.6	84.6
2896	64.2	65.5	68.2	70.6	73.2	79.1	83.6
3069	64.2	65.5	68.2	70.6	73.2	79.1	83.6
3251	64.5	65.9	68.5	71.1	73.6	79.6	84.6
3444	64.3	65.7	68.3	71	73.5	79.8	84.6
3649	64.4	65.7	68.2	70.8	73.4	79.4	84.2
3866	64.8	66	68.4	70.9	73.5	79.1	83.8
4096	64.7	65.9	68.4	70.9	73.4	78.8	83.7
4340	64.4	65.8	68.2	70.7	73.2	78.6	83.5
4598	64.2	65.5	68.1	70.6	73.2	78.4	83.3
4871	64.3	65.3	68	70.4	73.1	77.9	83.3
5161	63.2	64.6	67.3	69.7	72.3	77.4	82.5
5468	62.9	64.3	66.9	69.3	72.2	77.5	82.7
5793	62.7	63.7	66.7	68.9	72.2	77.6	83.3
6137	62.3	63.3	66.4	68.6	72	77	82.5
6502	61.9	62.8	66.1	68.4	72	76.7	81.6
6889	60.8	62	65.2	67.4	71.1	76.4	81.4
7298	60.6	61.9	64.8	67.1	70.7	75.7	80.4
7732	60.3	61.4	64.2	66.7	70.3	74.8	79.1
8192	60.4	61.4	64.2	66.9	70.5	75.1	79.1
8679	60.1	61	64.2	66.8	70.6	75.3	79.7
9195	60	60.9	64	66.6	70.3	75	79.4
9742	60	61	63.8	66.7	70.4	74.9	79.2
10321	59.3	60.2	63.4	66.4	70.3	74.7	78.8
10935	58.9	60.1	63	66	69.9	74.1	77.8
11585	58.6	59.8	62.8	65.8	69.7	73.8	77.3
12274	58.6	59.6	62.6	65.7	69.6	73.7	77.1
13004	58.3	59.3	62.4	65.5	69.4	73.6	77
13777	58.3	59.3	62.3	65.3	69.2	73.3	76.8
14596	57.8	58.8	61.9	64.8	68.7	72.7	76.1
15464	57.3	58.5	61.6	64.4	68.4	72.4	75.6
16384	57.1	58.4	61.6	64.3	68.3	72.2	75.4
17358	56.9	58.3	61.5	64.3	68.2	72.1	75.1
18390	56.5	58.1	61.3	64	68	71.7	74.7
19484	55.5	57.2	60.5	63.3	67.3	71.1	74.1
20643	54.8	56.6	60.1	62.9	67	70.9	74.1
21870	54.6	56.4	60	62.7	67	70.7	73.8
23170	54.1	56	59.4	62.2	66.4	70.1	73.2
24548	53.6	55.5	58.9	61.8	65.8	69.7	72.9
26008	53	55.1	58.6	61.4	65.5	69.3	72.4
27554	52	54.2	57.7	60.6	64.8	68.7	72.1
29193	51.3	53.7	57.3	60.2	64.4	68.4	71.8
30929	50.9	53.3	57	59.9	64	68	71.5
32768	50.1	52.5	56.4	59.3	63.5	67.5	70.8
34716	48.9	51.5	55.4	58.4	62.7	66.9	70.4
36781	47.8	50.4	54.5	57.4	61.7	65.9	69.5
38968	46.1	48.7	52.7	55.7	60	64.3	67.9
41285	43.6	46.2	50.3	53.3	57.5	61.8	65.5
43740	39.9	42.6	46.7	49.6	54	58.3	62.2
46341	35.5	37.9	42.1	45	49.4	54	58.2

Table 33. One-twelfth octave band power spectral density percentiles (dB re µPa2/Hz) for Site 9 (Owen Anchorage).

Frequency band (Hz)	1%	5%	25%	50%	75%	95%	99%
40	70	72.5	78.3	81.2	82	84.4	91.1
43	67.1	69.8	78.5	80.6	81.5	84	90.7
45	66.5	68.9	76.9	79.8	81.6	83.8	90.2
48	67.6	69.3	75.9	79.9	82	83.6	90.4
51	66.4	67.9	72	80	81.7	83.3	90.5
54	63.5	65	68.7	78.7	80.3	82.2	90.5
57	61.8	63.1	67	76.7	78.5	81	89.8
60	61.6	62.8	66.2	75.4	77.6	80	89.6
64	60.3	61.5	65.1	75.6	78.1	80.1	89.6
68	59.6	60.6	64.2	75.3	78.8	80	89.5
72	58.9	59.9	63.4	74.7	77.1	78.8	89.1
76	58.2	59.1	62.8	71.7	73.8	77.2	88.5
81	57.6	58.5	62.2	70.3	73.6	76.5	87.7
85	57.1	58	61.8	71.1	74.8	76.8	87.6
91	56.6	57.5	61.4	71.1	73.6	75.9	87.2
96	56.1	57	61.1	67.6	70.4	75	86.8
102	55.7	56.6	60.8	69.3	72.8	75.1	86.7
108	55.2	56.2	60.7	70.5	73.1	75.3	86.3
114	54.8	55.8	60.6	66.7	69.6	74.1	86.5
121	54.3	55.5	60.7	68	71.5	74.7	86.9
128	54	55.3	61	67.9	70.6	74.6	87
136	53.8	55.3	61.3	65.3	69.1	74.3	87.8
144	53.7	55.3	61.9	68.1	70.3	75	88.8
152	53.5	55.3	62.2	65.9	69.1	75	89.7
161	53	54.9	62.6	67.4	69.4	75.3	90.5
171	52.5	54.5	62.3	65.5	68.3	74.9	90.5
181	52.1	54.2	62.6	66.4	68.2	74.6	90.8
192	51.8	53.9	62	65.1	67.7	74.2	90.1
203	51.6	53.8	62.4	65.1	67.5	74	90.6
215	51.3	53.7	61.8	65.1	67.3	73.9	89.8
228	51.1	53.6	61.8	64.1	66.9	73.8	89.4
242	51	53.5	62	64.1	67.1	73.9	89.6
256	50.9	53.7	61.8	63.8	67.2	74	89.7
271	51.1	54.1	61.5	63.6	67.4	74.2	89.4
287	51.4	54.4	61.1	63.6	67.6	74.3	89.2
304	51.3	54.4	60.6	63.5	67.6	74.1	88.6
323	51	54.1	60.1	63.4	67.5	74.1	89.2
342	50.6	53.9	59.8	63.5	67.5	74.5	88.4
362	50.5	54	59.2	63.3	67.5	74.3	88
384	50.4	54.1	58.7	63.2	67.5	74.1	87.9
406	50.4	54.1	58.3	63.1	67.4	73.9	87.4
431	50.6	53.7	58.2	63.1	67.3	73.8	87.1
456	50.6	53.2	58.1	63.1	67.3	73.8	86.6
483	50.8	52.9	57.9	63.1	67.3	73.7	85.7
512	51.1	52.9	57.9	62.9	67.1	73.4	85
542	51.3	53.1	57.9	62.9	67	73.3	84.5
575	51.6	53.6	58	62.9	67	73.4	83.9
609	51.9	54.1	58.3	63	67	73.3	83.4
645	52	54.6	58.5	63.1	67.1	73.2	83.3
683	52.4	55	58.7	63.2	67.1	73.2	83.3
724	52.7	55.3	59	63.2	67.1	73.4	83.3
767	53.2	55.5	59.1	63.2	66.9	73.5	83.3
813	53.1	55.4	59.1	63.1	66.8	73.5	82.6
861	53.1	55.4	59.3	63.1	66.7	73.6	82.3
912	53.3	55.5	59.5	63.2	66.7	73.7	82
967	53.6	55.8	59.8	63.3	66.7	73.7	81.9
1024	54.2	56.3	60.1	63.4	66.7	73.9	81.8
1085	54.8	56.8	60.5	63.6	66.8	74.2	81.7
1149	55.5	57.4	60.9	63.8	67	74.4	81.9
1218	56	58	61.4	64.1	67.3	74.9	82.1
1290	56.5	58.5	61.8	64.4	67.6	75.5	82.4
1367	57	58.9	62.2	64.7	67.9	75.8	82.6

Frequency band (Hz)	1%	5%	25%	50%	75%	95%	99%
1448	57.4	59.4	62.6	65	68.3	76.3	82.9
1534	57.9	60	63.1	65.5	68.8	76.9	83.2
1625	58.2	60.5	63.6	65.9	69.4	77.6	83.6
1722	58.8	61.1	64.1	66.5	70	78.5	84.3
1825	59.2	61.5	64.5	66.9	70.5	78.8	84.4
1933	59.4	61.9	65	67.6	71.1	79.1	84.6
2048	59.6	62.3	65.6	68.3	71.9	79.8	85.5
2170	59.7	62.4	65.9	68.8	72.5	81	86.4
2299	59.3	62.1	66.3	69.3	73.1	82	87.4
2435	59.1	62.2	66.6	69.8	73.6	82.7	87.8
2580	58.8	61.8	66.7	69.9	73.9	83.3	88.6
2734	58.5	61.5	66.5	69.6	73.6	82.9	87.9
2896	57.6	60.7	66.2	69.4	73.6	82.5	87.1
3069	58.1	61.3	66.2	69.4	73.8	82.8	87.5
3251	58.4	61.6	66.1	69.3	73.9	83	88.1
3444	58.1	61.2	66.5	69.4	73.6	83	88.3
3649	58	60.8	65.8	68.6	72.5	81.1	86
3866	57.6	60.7	66.6	69.5	73.6	81.5	86.3
4096	58.2	61.2	67.3	70.3	74.5	82.8	87.2
4340	58.2	61	67.7	70.7	75	83.2	87.5
4598	58	60.7	67.6	70.6	75.1	83.6	88.3
4871	58.3	60.9	67.1	70.2	74.5	82.7	87.4
5161	58.7	61.1	67.1	70.2	74.5	82.1	86.6
5468	58.9	61.2	67.4	70.6	75	82.8	87.6
5793	59.1	61.3	67.5	70.9	75.6	83.4	88.2
6137	59.3	61.6	67.2	70.7	75.5	83.4	88
6502	59.4	61.5	66.9	70.4	75	82.8	87.3
6889	59	61.2	66.5	70	74.5	81.9	86.1
7298	58.2	60.4	66	69.7	74	81.2	85.7
7732	57.5	59.8	65.3	69	73.3	80.8	85.6
8192	56.8	59.1	64.4	68.1	72.4	79.9	84.8
8679	55.8	58.2	63.4	67	71.3	79.2	84.6
9195	54.6	57.1	62.6	66.2	70.2	78	83.1
9742	53.5	56.1	61.9	65.5	69.3	76.6	81
10321	52.6	55.3	61.5	65	68.8	76.4	80.7
10935	52.2	54.9	60.9	64.4	68.1	75.6	80.1
11585	52.1	54.9	60.8	64.4	67.8	74.6	79
12274	51.8	54.7	60.7	64.3	67.6	74	78.1
13004	51.1	54.1	60.5	64.3	67.5	73.4	77.1
13777	50.4	53.5	60.1	64	67.2	72.9	76.7
14596	50.1	53.4	59.8	63.8	66.9	72.4	76.1
15464	50	53.1	59.8	63.7	66.9	72.4	76.1
16384	49.9	53	59.4	63.3	66.4	72	76
17358	49.7	52.8	58.8	62.8	65.9	71.4	75.3
18390	49	52.1	58.1	62.1	65.1	70.5	74.5
19484	48.3	51.4	57.4	61.5	64.5	69.9	74
20643	48.5	51.5	57.3	61.3	64.4	69.5	73.4
21870	48.1	51.4	57.3	61.2	64.3	69.3	73.2
23170	47.8	51.1	57.1	61	64.1	69.1	72.9
24548	47.7	51.1	56.8	60.6	63.7	68.6	72.5
26008	47.4	50.8	56.3	60	63.1	68	71.9
27554	46.9	50.4	56.1	59.8	62.9	67.5	71.3
29193	46.5	50.1	56	59.7	62.8	67.6	71.4
30929	46	49.6	55.7	59.5	62.7	67.6	71.3
32768	45.7	49.2	55.3	59.2	62.3	67.1	70.7
34716	45.5	48.9	54.8	58.6	61.7	66.5	70.1
36781	45.4	48.6	54.1	57.9	61	65.8	69.3
38968	45.1	47.8	52.9	56.7	59.8	64.6	68.1
41285	44.2	46.3	50.8	54.4	57.6	62.4	66
43740	40.8	43.5	47.4	50.8	53.9	58.9	62.8
46341	35.4	37.8	42	45.2	48.1	53.8	58.5

9.3 Correlation in sound levels between sites

Table 34. Correlation coefficients greater than 0.6 between sites (i.e., Site A x Site B) for mean, daily OTO bands, for each deployment. Site Values >= 0.7 in bold.

Frequency (Hz)	Deployment		
	1	2	3
50	-	-	**7x8 (0.70)**
203	1x2 (0.63)	-	-
256	2x9 (0.60)	-	-
406	2x9 (0.65)	-	-
512	2x9 (0.60)	-	-
1024	2x9 (0.61)	-	-
1290	2x9 (0.64)	-	7x8 (0.61)
1625	-	-	**7x8 (0.77)**
2048	**2x9 (0.70)**	-	**7x8 (0.79)**
2580	2x9 (0.67)	-	**7x8 (0.77)**
3251	**2x9 (0.75)**	1x7 (-0.63)	**7x8 (0.72)**
	2x8 (0.63)		5x7 (0.62)
4096	2x8 (0.66)	4x7 (0.61)	-
	2x5 (0.60)	1x7 (-0.68)	-
5161	2x8 (0.62)	4x7 (0.61)	-
	1x8 (0.60)		-
6502	2x8 (0.66)	7x8 (-0.64)	-
		1x4 (-0.61)	-
		1x8 (0.60)	-
		4x7 (0.60)	-
8192	1x8 (0.60)	**7x8 (-0.72)**	1x2 (0.65)
	2x8 (0.68)	1x2 (0.65)	
		4x7 (0.61)	
10321	2x8 (0.68)	**2x8 (0.73)**	**2x8 (0.73)**
		1x2 (0.69)	1x2 (0.69)
		4x7 (0.64)	**2x7 (-0.77)**
	1x8 (0.61)	**2x7 (-0.77)**	-
		7x8 (-0.75)	
		4x7 (-0.62)	
13004	**2x8 (0.72)**	**2x8 (0.77)**	**2x8 (0.77)**
	1x8 (0.66)	**1x2 (0.71)**	
	1x3 (0.63)	4x7 (0.60)	**1x2 (0.71)**
		2x7 (-0.78)	
	2x7 (0.60)	**7x8 (-0.73)**	**2x7 (-0.78)**
		4x8 (-0.65)	
16384	**2x8 (0.73)**	**2x8 (0.76)**	**2x8 (0.76)**
		1x2 (0.71)	**1x2 (0.71)**
	1x8 (0.66)	1x4 (-0.63)	2x7 (-0.68)
		2x7 (-0.68)	
	2x7 (0.65)	4x8 (-0.64)	2x4 (-0.60)
		7x8 (-0.67)	
20643	2x8 (0.68)	**1x2 (0.75)**	**1x2 (0.75)**
	1x8 (0.62)	**1x8 (0.74)**	**2x8 (0.73)**
	2x7 (0.63)	1x4 (-0.64)	2x7 (-0.65)
		2x7 (-0.65)	2x4 (-0.62)
26008	1x8 (0.66)	**1x2 (0.76)**	**1x2 (0.76)**
	2x8 (0.67)	**1x8 (0.71)**	
		1x4 (-0.64)	2x8 (0.67)
	2x7 (0.63)	7x8 (-0.60)	
		4x8 (-0.62)	
32768	1x8 (0.62)	**1x2 (0.77)**	**1x2 (0.77)**
		1x8 (0.70)	
		1x4 (-0.66)	1x8 (0.66)
		2x4 (-0.61)	2x4 (-0.61)
		4x7 (0.63)	
41285	-	**1x2 (0.76)**	**1x2 (0.76)**
		1x8 (0.73)	
		1x4 (-0.67)	2x8 (0.62)
		2x4 (-0.60)	
		1x7 (-0.66)	2x4 (-0.60)
		4x8 (-0.64)	

9.4 Equivalent fluid seabeds and propagation model comparisons

As described in Section 5.3, there are no readily available numerical acoustic propagation models that can efficiently model low-frequency, range-dependent underwater sound propagation over seabeds with the relatively high shear speeds (close to 1000 m/s) such as those seen in Cockburn Sound. Conversely, there are many numerical propagation codes that can model low-frequency range-dependent propagation over fluid seabeds. This leads to the idea of using a fluid seabed propagation code with an "equivalent fluid" seabed that matches the reflectivity of the true seabed as closely as possible. This approach was developed using a complex density approach by (Tindle & Zhang 1992, Zhang & Tindle 1995), however their method is only applicable to seabeds with lower shear speeds than those found in Cockburn Sound. Instead, an "equivalent fluid" to the calcarenite layer has been obtained by choosing a fluid with the same density as the calcarenite, and then adjusting its compressional wave sound speed and absorption to obtain the best match to the reflectivity of the true seabed at the low grazing angles that are responsible for acoustic propagation to ranges that are many times the water depth.

The results of this process are shown in Figure 62 (central basin calcarenite) and Figure 63 (eastern shelf) and show excellent agreement between both the magnitudes and phases of the elastic and fluid reflection coefficients for grazing angles up to about 25°. It is impossible for a fluid reflection coefficient to replicate the peak in the magnitude of the calcarenite reflection coefficient that occurs at about 45°, so this method will give poor results at short ranges and for very low frequencies where reflections at this angle are an important contributor to the sound field.

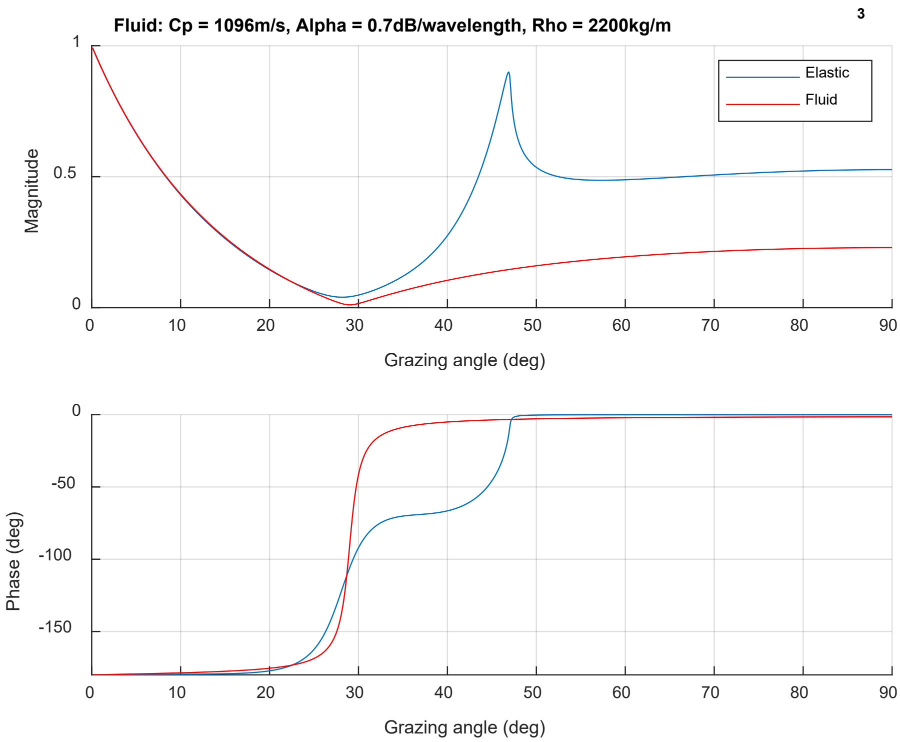

Figure 62. Magnitude (top) and phase (bottom) of the plane-wave pressure reflection coefficient for a water-calcarenite interface (blue) and a water-equivalent fluid interface (red) for the central basin environment. Parameters are: compressional wave velocity *Cp*, compressional wave absorption α, density ρ.

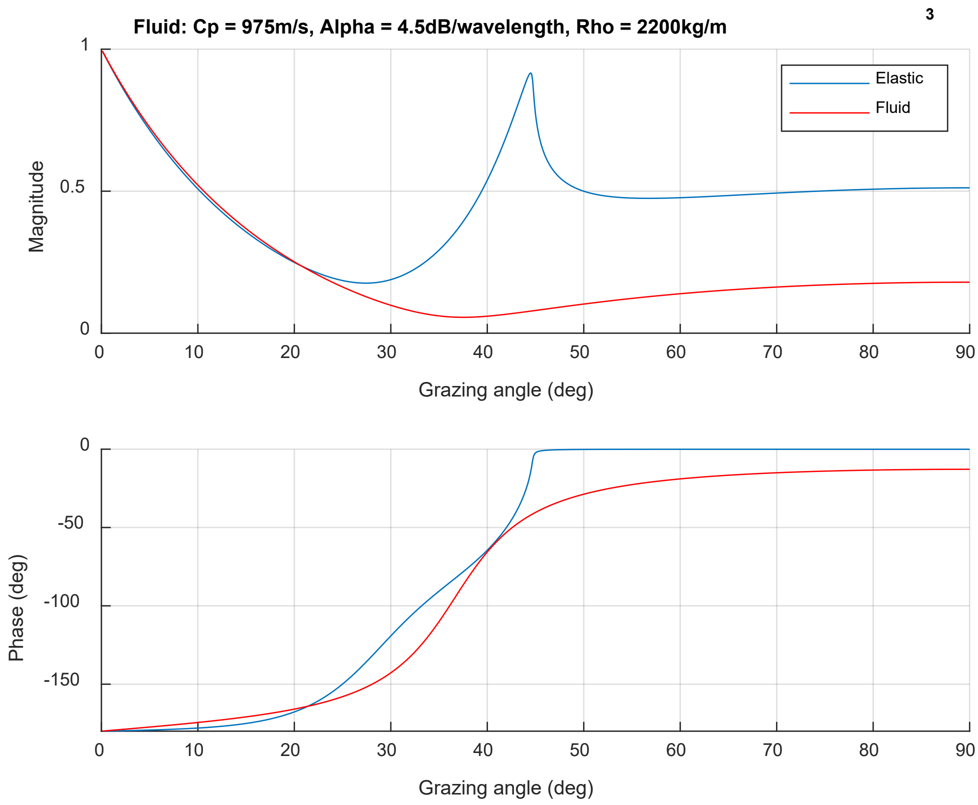

Figure 63. Magnitude (top) and phase (bottom) of the plane-wave pressure reflection coefficient for a water-calcarenite interface (blue) and a water-equivalent fluid interface (red) for the shelf environment. Parameters are: compressional wave velocity *Cp*, compressional wave absorption α, density ρ.

Figure 64 and Figure 65 compare the modelled propagation loss as a function of range and frequency for the eastern shelf computed using three different propagation models: SCOOTER (wavenumber integration) using the full geoacoustic model in Table 10, RAMGeo (parabolic equation) using the equivalent fluid geoacoustic model in Table 13 and Bellhop (Gaussian bean tracing) with Bounce used to calculate the bottom reflection coefficient using the full geoacoustic model. In all cases the water depth was 10 m, the source was at a depth of 3 m, and the receiver at a depth of 9.5 m. Figure 64 covers frequencies from 1 Hz to 1 kHz at a resolution of 1 Hz whereas Figure 65 covers the frequency range 100 Hz to 10 kHz at 100 Hz resolution. Quantitative comparisons between models can be made using the line plots of propagation loss vs range at selected frequencies in Figure 66 through to Figure 70.

The following observations can be made from these results:

- The horizontal bands of low propagation loss clearly visible in the SCOOTER result (top panel of Figure 64) are a result of modal interaction with the sharp peak in the reflection coefficient magnitude visible in Figure 65 at a grazing angle of about 45°, and are not captured by either of the other models.
- At low frequencies RAMGeo grossly overpredicts the propagation loss. This is partly because the equivalent fluid seabed model it uses is unable to replicate the part of the reflection coefficient curve responsible for the low-loss bands and partly because fluid models don't capture a type of interface wave called a Scholte wave that is responsible for the lower propagation loss in the SCOOTER result at frequencies up to about 50 Hz.

- At frequencies from about 300 Hz up to the maximum comparison frequency of 10 kHz there is excellent agreement between SCOOTER and RAMGeo, which is a result of the propagation at these frequencies being dominated by sound travelling at small grazing angles, and the excellent agreement between the full and equivalent fluid reflection coefficients at these small grazing angles.
- As expected for what is effectively a ray code, Bellhop is unable to reproduce the low-frequency cut-off effects seen in the results from the other two models and in the measured data (see Section 4.3). It is also much "noisier" than the other two models, particularly in regions of relatively high propagation loss. It does, however, agree reasonably well with the other two models for frequencies above about 2 kHz.
- RAMGeo proved to be very computationally efficient for this environment, and produced much cleaner results than Bellhop considerably faster, even at 10 kHz.

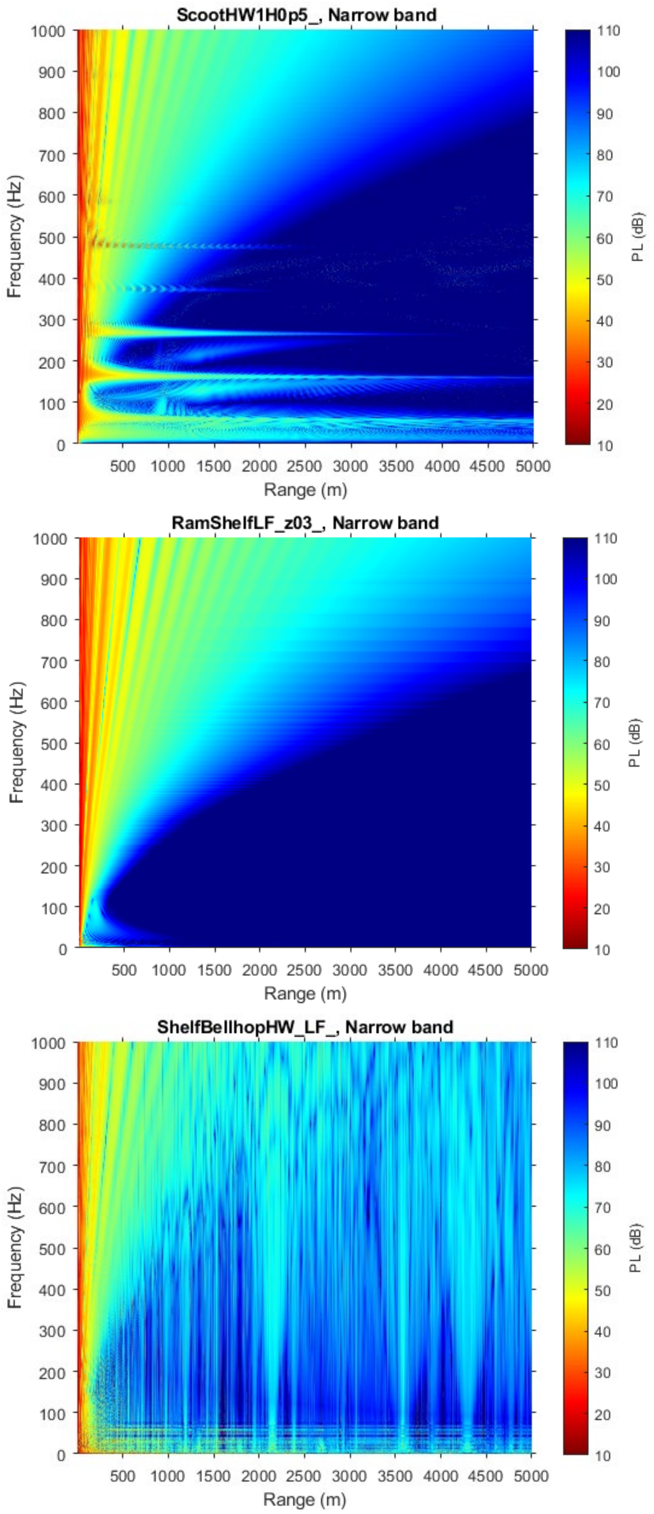

Figure 64. Modelled propagation loss for the eastern shelf as a function of range and frequency for frequencies up to 1 kHz. Top panel: SCOOTER (wavenumber integration) using the full geoacoustic model in Table 10. Middle panel: RAMGeo (parabolic equation) using the equivalent fluid geoacoustic model in Table 13. Bottom panel: Bellhop (Gaussian bean tracing) and Bounce (reflection coefficient calculation) using the full geoacoustic model in Table 10.

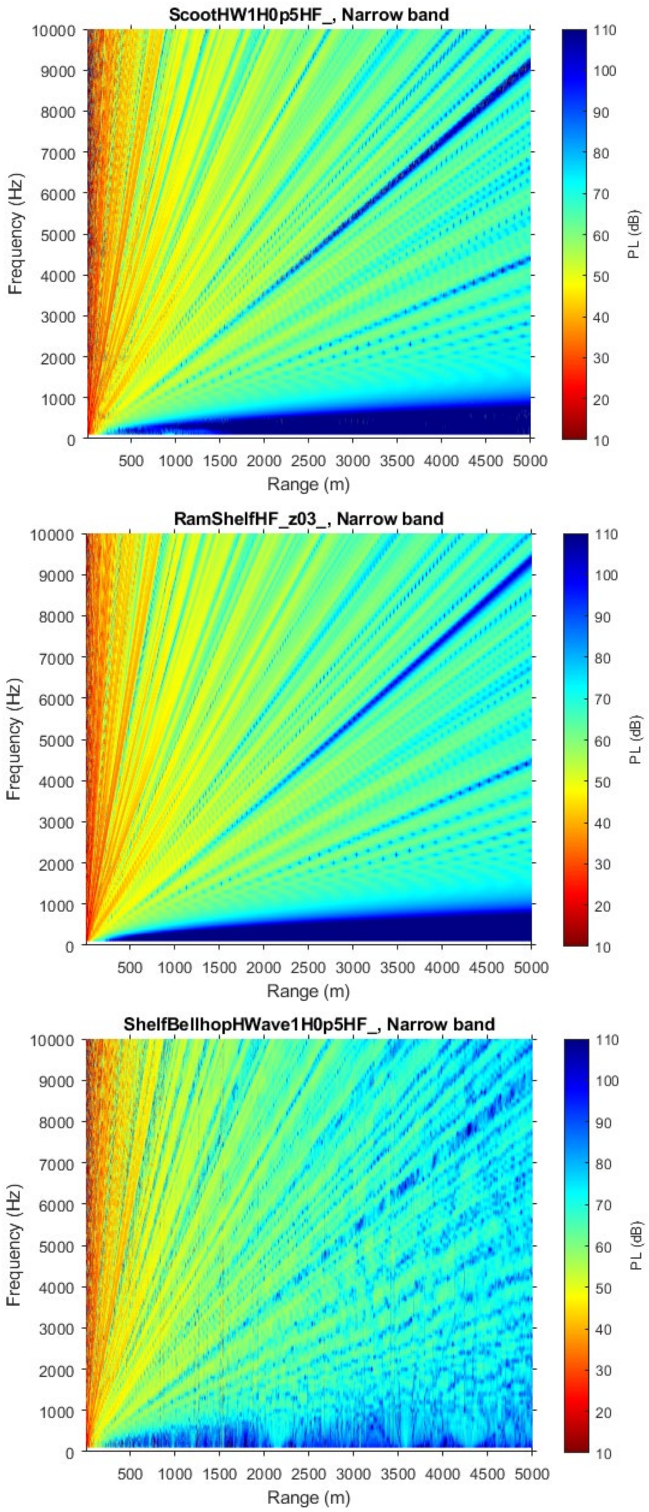

Figure 65. Modelled propagation loss for the eastern shelf as a function of range and frequency for frequencies up to 10 kHz. Top panel: SCOOTER (wavenumber integration) using the full geoacoustic model in Table 10. Middle panel: RAMGeo (parabolic equation) using the equivalent fluid geoacoustic model in Table 13. Bottom panel: Bellhop (Gaussian bean tracing) and Bounce (reflection coefficient calculation) using the full geoacoustic model in Table 10.

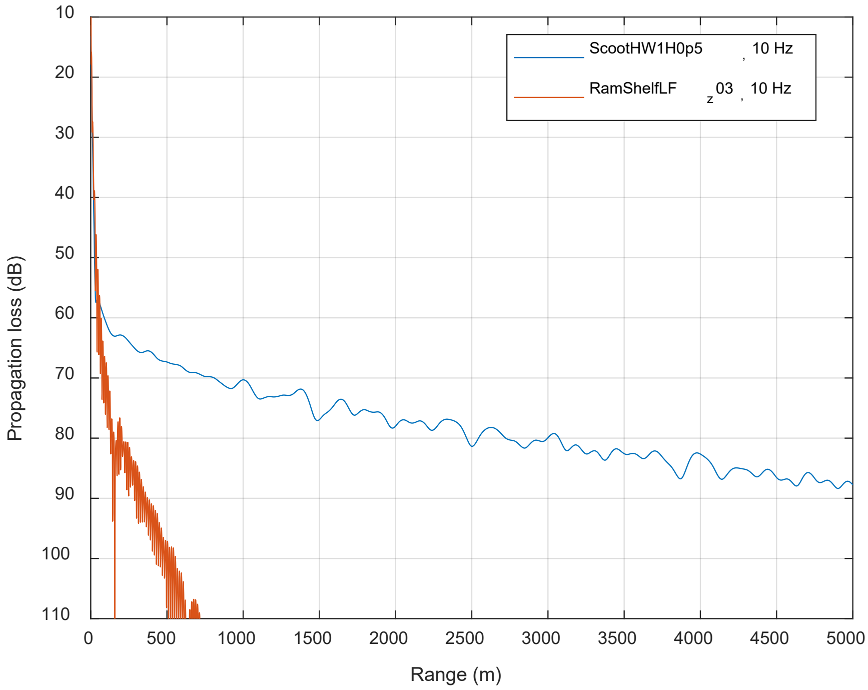

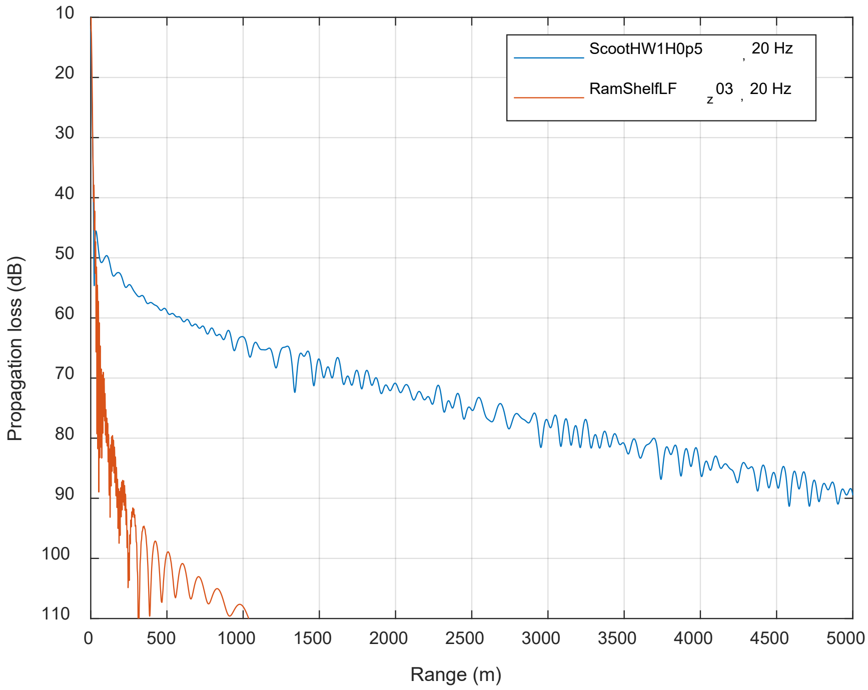

Figure 66. Propagation loss vs. range for the eastern shelf modelled by SCOOTER (blue) with the full geoacoustic model and RAMGeo (red) with the equivalent fluid model for frequencies of 10 Hz (top) and 20 Hz (bottom).

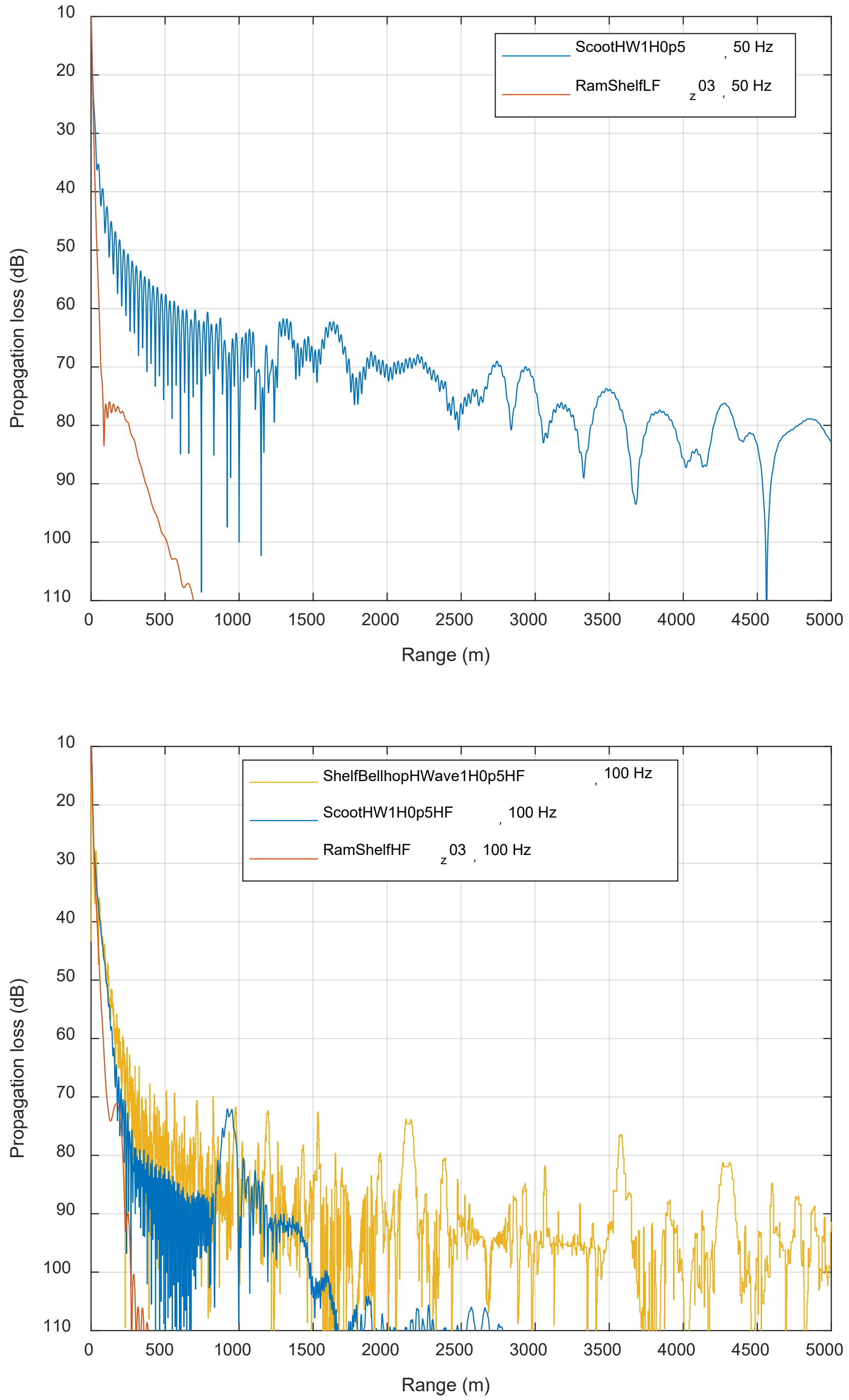

Figure 67. Propagation loss vs. range for the eastern shelf modelled by SCOOTER (blue) with the full geoacoustic model, RAMGeo (red) with the equivalent fluid model, and Bellhop (yellow) with the full geoacoustic model for frequencies of 50 Hz (top) and 100 Hz (bottom).

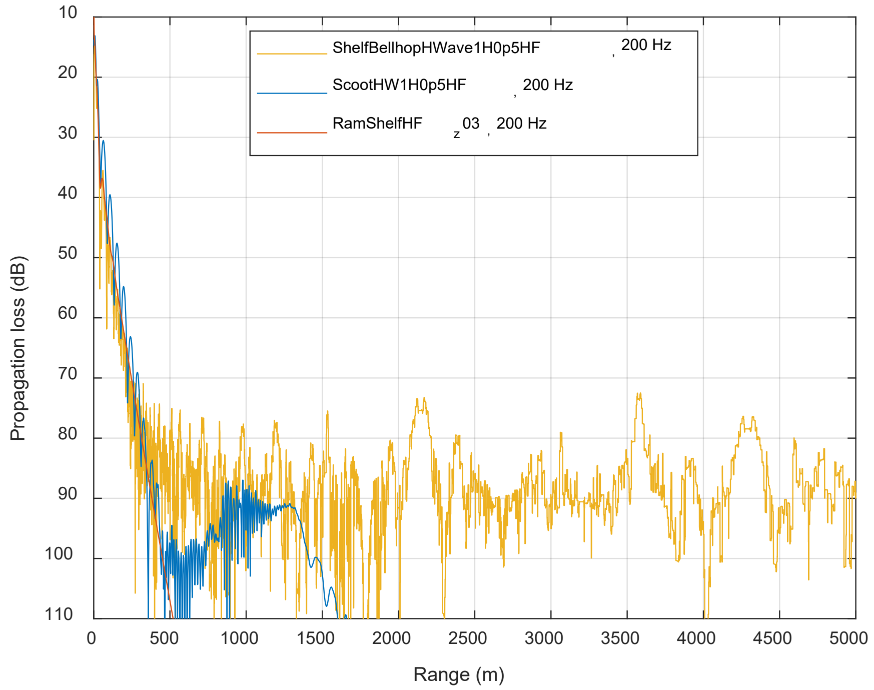

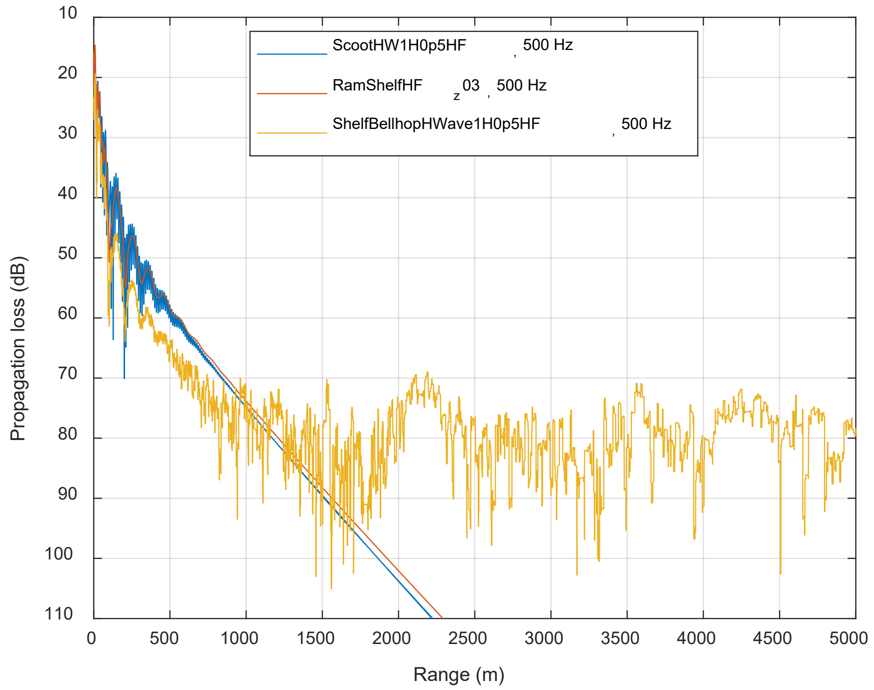

Figure 68. Propagation loss vs. range for the eastern shelf modelled by SCOOTER (blue) with the full geoacoustic model, RAMGeo (red) with the equivalent fluid model, and Bellhop (yellow) with the full geoacoustic model for frequencies of 200 Hz (top) and 500 Hz (bottom).

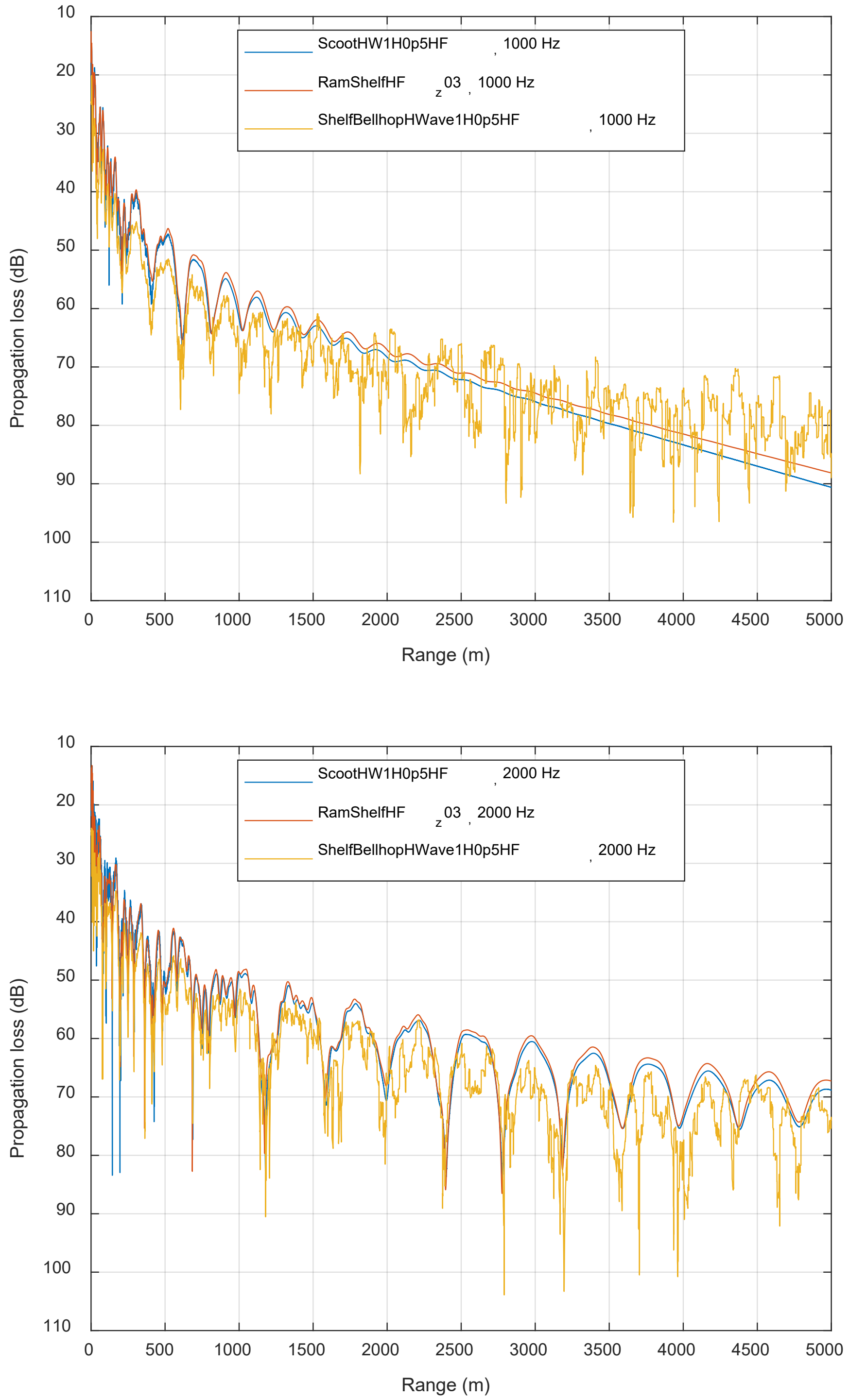

Figure 69. Propagation loss vs. range for the eastern shelf modelled by SCOOTER (blue) with the full geoacoustic model, RAMGeo (red) with the equivalent fluid model, and Bellhop (yellow) with the full geoacoustic model for frequencies of 1000 Hz (top) and 2000 Hz (bottom).

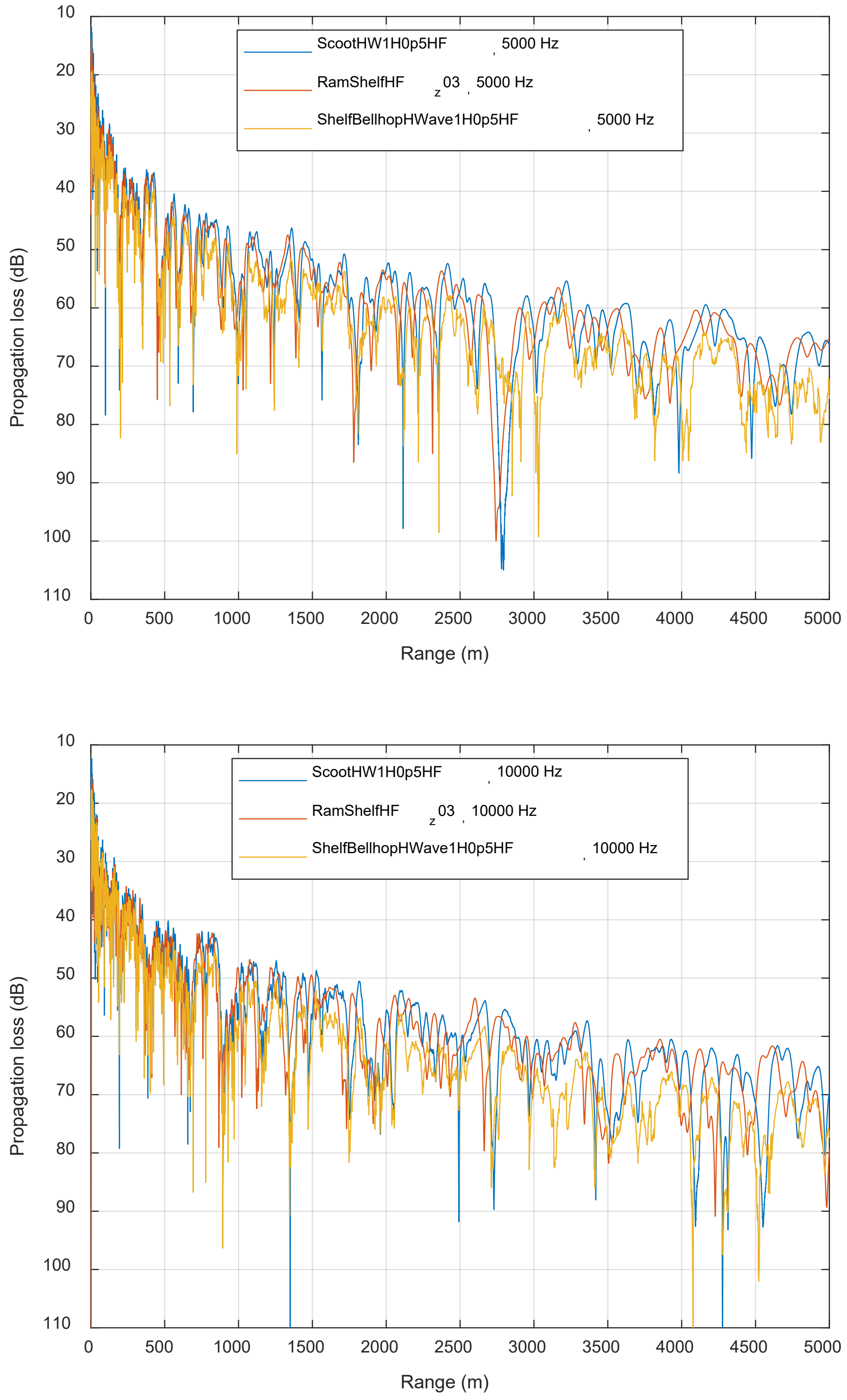

Figure 70. Propagation loss vs. range for the eastern shelf modelled by SCOOTER (blue) with the full geoacoustic model, RAMGeo (red) with the equivalent fluid model, and Bellhop (yellow) with the full geoacoustic model for frequencies of 5000 Hz (top) and 10000 Hz (bottom).

9.5 One-third octave band propagation loss fits

Table 35. Fitted parameter values for the equation $PL = C + B_0 \log_{10}\left(\frac{r}{r_0}\right) + B_1 \log_{10}\left(1 + \frac{r}{R_1}\right)$ giving the OTO band averaged acoustic propagation loss in the central basin of Cockburn Sound for a source depth of 3 m and a receiver on the seafloor. At each frequency the equation is valid for horizontal ranges, r, between R_min and R_max. The last column is the root mean square of the difference between the measured PL and that predicted by the equation for all ranges for which valid measurements were available.

OTO band centre frequency (Hz)	C (dB)	B_0 (dB per decade change in range)	B_1 (dB per decade change in range)	R_1 (m)	R_{min} (m)	R_{max} (m)	Root mean square (RMS) residual (dB)
12.4	3.024	20.261	14.154	200	879	3357	4.1
15.6	14.799	20.123	6.916	3000	278	3357	3.7
19.7	49.167	5.95	40.708	3000	478	3357	4.1
24.8	12.73	20.839	9.32	3000	528	3357	4.3
31.2	8.926	18.741	29.344	3000	278	3307	2.9
39.4	2.269	20.484	16.361	280.745	478	1179	3.4
49.6	12.552	22.221	8.545	200	278	3357	4.9
62.5	7.458	18.776	19.943	859.235	278	3357	2.8
78.7	8.013	20.273	28.888	1268.622	278	3357	3.4
99.2	29.598	12.269	60	1602.61	278	3357	3.1
125	-7.01	19.25	33.76	200	278	3307	2.8
157.5	0.835	19.346	60	1313.542	278	3307	2.8
198.4	-4.732	19.962	60	1669.197	278	3357	3.1
250	7.739	14.368	60	1692.349	278	3357	4.2
315	12.243	11.938	60	1625.763	278	3357	3.9
396.9	6.249	14.18	60	2303.318	278	3357	2.3
500	17.236	9.02	60	1796.07	278	3357	2.1
630	16.941	8.804	60	1971.139	278	3357	1.8
793.7	10.37	11.518	60	2667.203	278	3357	1.8
1000	15.226	10.072	34.348	1166.877	278	3357	2.2
1259.9	-4.791	18.683	13.173	390.435	278	1930	2.6
1587.4	-9.357	19.065	19.654	200	278	1930	1.8
2000	-5.451	19.253	22.373	200	278	1930	3.5
2519.8	-4.863	19.33	21.934	200.323	278	1780	4.3

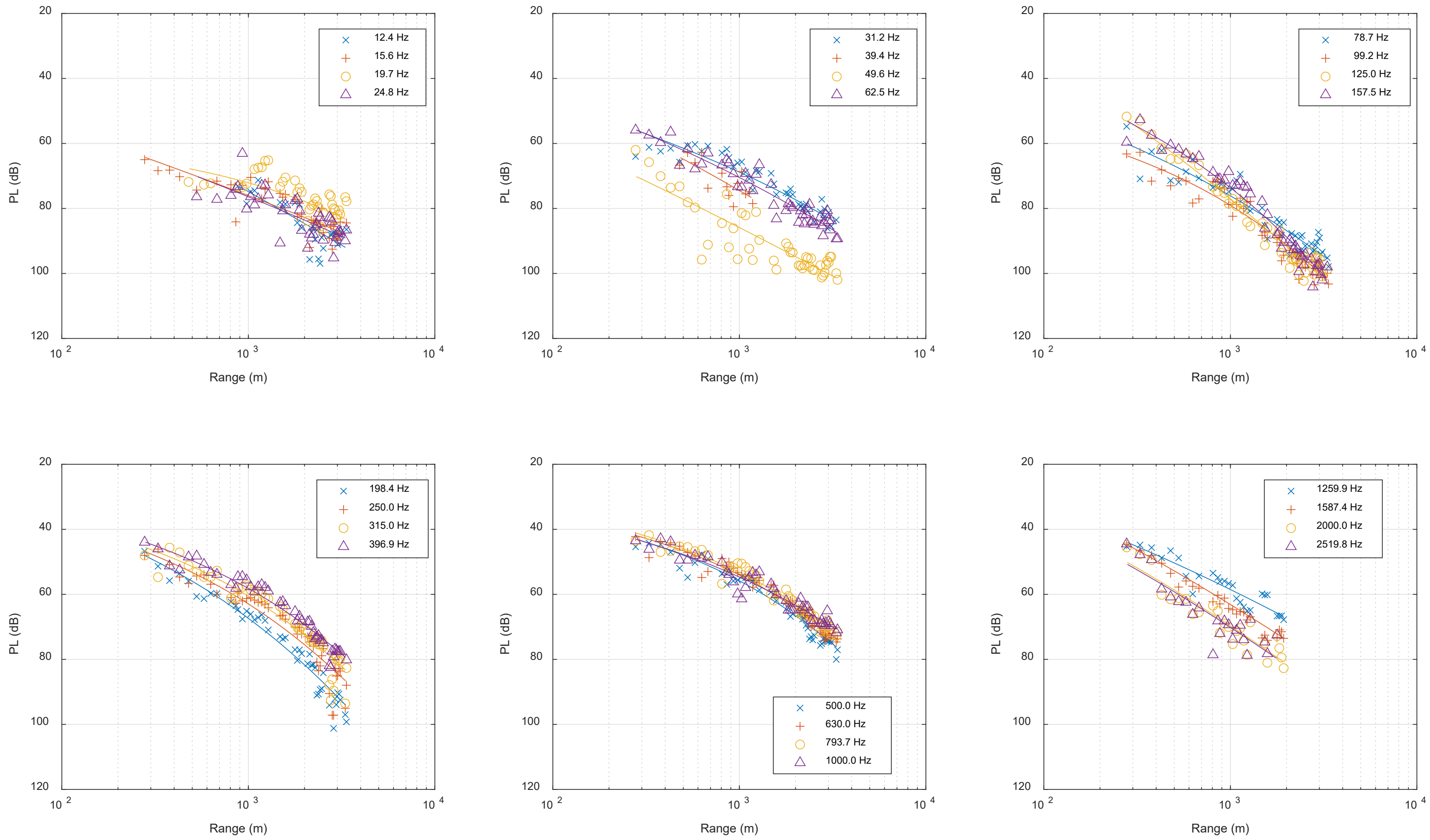

Figure 71. Lines are least squares fits of measured propagation loss (symbols) averaged over OTO bands for the central basin of Cockburn Sound. Band centre frequencies are shown in the legend of each plot.

Table 36. Fitted parameter values for the equation $PL = C + B_0 \log_{10}\left(\frac{r}{r_0}\right) + B_1 \log_{10}\left(1 + \frac{r}{R_1}\right)$ giving the OTO band averaged acoustic propagation loss on the eastern shelf of Cockburn Sound for a source depth of 3 m and a receiver on the seafloor. At each frequency the equation is valid for horizontal ranges, r, between R_min and R_max. The last column is the root mean square of the difference between the measured PL and that predicted by the equation for all ranges for which valid measurements were available.

OTO band centre frequency (Hz)	C (dB)	B_0 (dB per decade change in range)	B_1 (dB per decade change in range)	R_1 (m)	R_{min} (m)	R_{max} (m)	Root mean square (RMS) residual (dB)
12.4	10.21	28.879	-40	2913.413	211	4013	3.5
15.6	-12.615	37.152	-40	2289.27	163	4063	3.8
19.7	23.861	24.924	-29.436	3000	163	4063	4.5
24.8	30.495	25.161	-31.289	2590.505	163	4063	4.7
31.2	16.477	24.029	-21.473	3000	163	4063	3.2
39.4	7.917	21.67	-5.41	737.716	163	4063	3.7
49.6	19.435	19.718	1.449	3000	163	4063	3.3
62.5	3.601	23.557	34.945	2963.989	163	4063	3.2
78.7	14.991	23.984	24.876	2959.097	163	4063	3.1
99.2	14.802	24.509	13.316	1009.652	163	4063	3.3
125	12.446	20.702	28.938	581.535	163	4013	2.7
157.5	-18.795	37.027	-12.058	3000	163	4013	3.7
198.4	15.114	23.408	10.251	200	163	4063	3.9
250	11.773	23.345	12.994	200	163	3863	3.9
315	0.882	21.391	26.141	200	163	3963	4
396.9	10.254	15.545	48.517	595.852	163	3863	3.5
500	3.444	18.956	60	1662.415	163	3863	3.3
630	3.881	18.435	60	2703.701	163	3813	3.7
793.7	4.836	17.522	60	2963.022	163	3863	3.7
1000	5.125	18.416	47.386	3000	163	3863	1.8
1259.9	3.122	20.616	14.283	3000	163	1860	1.5
1587.4	9.707	19.777	14.697	3000	163	1860	1.9
2000	5.473	22.556	-4.16	1467.79	163	1860	2
2519.8	2.42	20.586	8.738	253.433	163	1860	2.5

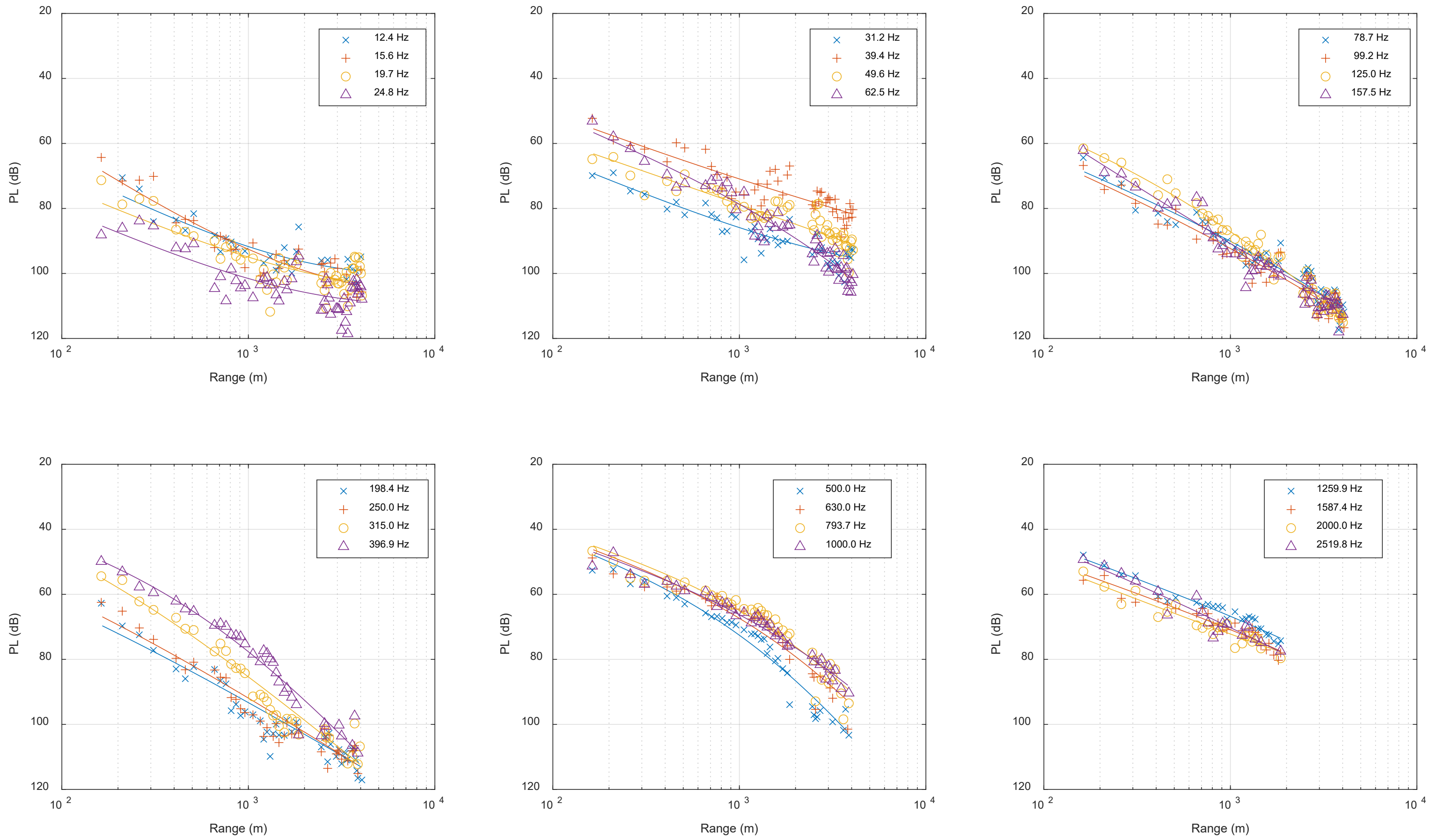

Figure 72. Lines are least squares fits of measured propagation loss (symbols) averaged over OTO bands for the eastern shelf of Cockburn Sound. Band centre frequencies are shown in the legend of each plot.

Submitted as draft	17/06/2024
Review completed	12/09/2024
Submitted as revised draft	13/12/2024
Approved by Science Program Leadership Team	06/03/2025
Approved by WAMSI CEO	26/03/2025
Final report	26/03/2025

WESTERN AUSTRALIAN
MARINE SCIENCE
INSTITUTION